

University of Southampton Research Repository
ePrints Soton

Copyright © and Moral Rights for this thesis are retained by the author and/or other copyright owners. A copy can be downloaded for personal non-commercial research or study, without prior permission or charge. This thesis cannot be reproduced or quoted extensively from without first obtaining permission in writing from the copyright holder/s. The content must not be changed in any way or sold commercially in any format or medium without the formal permission of the copyright holders.

When referring to this work, full bibliographic details including the author, title, awarding institution and date of the thesis must be given e.g.

AUTHOR (year of submission) "Full thesis title", University of Southampton, name of the University School or Department, PhD Thesis, pagination

UNIVERSITY OF SOUTHAMPTON

**Are changes in the lesser flamingo
population a natural consequence of
soda lake dynamics?**

by

Sarah A. Ward

A thesis submitted in partial fulfillment for the
degree of Doctor of Philosophy

in the
Faculty of Social and Human Sciences
Geography and Environment

June 2015

UNIVERSITY OF SOUTHAMPTON

ABSTRACT

FACULTY OF SOCIAL AND HUMAN SCIENCES
GEOGRAPHY AND ENVIRONMENT

Doctor of Philosophy

by Sarah A. Ward

Soda lakes in East Africa are relatively simple ecosystems as a result of extreme saline-alkaline conditions. These shallow lakes undergo rapid fluctuations in response to rainfall, which can cause sudden changes in the phytoplankton community. The lesser flamingo (*Phoeniconaias minor*) population inhabits these lakes and can gather in congregations of over one million birds when the phytoplankton community of a lake is dominated by *Arthrosphaera fusiformis*, their primary food source. The population is thought to be declining, and as a result the lesser flamingo is now considered to be a “near-threatened” species (IUCN, 2006). To investigate the significance of this decline both palaeolimnological techniques and modelling were used in an attempt to gain a deeper insight into the long-term ecosystem dynamics of these lakes and the impact of this upon lesser flamingo populations. The palaeolimnological work undertaken identified interesting pigment changes in sediment cores from Lake Bogoria, the most stable soda lake, which suggested that it has experienced changes in the phytoplankton community more often during lower lake water levels. Differential preservation of some pigments caused some difficulties in bringing together the empirical work and the hydrological and *Arthrosphaera* models. However, a model that coupled rainfall, lake dynamics, and *Arthrosphaera* and flamingo population dynamics was successfully constructed and was capable of generating dynamics that are characteristic of the target ecosystem. The model output suggested that the observed decline in flamingo population is part of the natural fluctuation that occurs as a result of the highly dynamic environment in which they live, and also that population size and flamingo breeding success is limited by the food availability at Lake Natron, their only breeding lake, rather than the availability of breeding islands. In using both empirical data and modelling techniques, a deeper understanding of the changes in these soda lake ecosystems was found as a result of this combined approach, which highlighted the importance of putting the flamingo population changes in the context of longer term fluctuations in lake water levels in East Africa.

Contents

Acknowledgements	vii
0.1 Approach	1
1 The soda lake network	3
1.1 Introduction	3
1.2 Modelling	16
1.3 Model objectives	17
1.4 Hypotheses	18
2 Fieldwork	21
2.1 March 2011	21
2.2 July 2012	23
3 Palaeolimnology	29
3.1 Outline of sample analysis	29
3.2 Dating	31
3.3 LOI and TOC:TN	40
3.4 Pigments	45
3.5 Nitrogen Isotopes	67
3.6 Geochemistry	69
3.7 Discussion	84
3.8 Future work	94
4 Hydrological model	97
4.1 Literature review	97
4.2 Overview	99
4.3 Results	113
5 Arthrospira abundance model	121
5.1 Literature review	121
5.2 Overview	129
5.3 Results	137
6 The lesser flamingo model	163
6.1 Literature review	163
6.2 Overview	176
7 Flamingo hypotheses exploration	205
7.1 Flamingo mortality events	205
7.2 Hypotheses	208
7.3 Starvation	209

7.4 Disease	212
7.5 Low replacement rate	216
7.6 Discussion	220
8 Modelling Discussion	223
9 Synthesis of empirical and modelling work	229
10 Conclusions	237
Appendix	241
Bibliography	265

Acknowledgements

I would like to thank the University of Southampton for the opportunity and funding to undertake this project, the Quaternary Research Association for funding to date my sediments, and BBC Earth for the funding to buy my rainfall data. I am also grateful to Nature Kenya, the National Museums of Kenya, and the Kenya Wildlife Service for monitoring flamingo populations and allowing me to use their flamingo census data.

I am deeply indebted to Dr Jonathan Grey and Phillip Sanders at Queen Mary University of London for the opportunity to return to Lake Bogoria a second time, allowing me to re-core Lake Bogoria and rectify the mistakes made during my first field trip. I thank the Lake Bogoria National Reserve for access to Lake Bogoria and their support on field expeditions, particularly William Kimosop and Jackson Komen.

I am very grateful to Prof. David Harper for introducing me to the East African soda lakes and inspiring me to start this amazing journey. I would like to thank my supervisors Prof. Pete Langdon and Prof. Seth Bullock, who allowed me to explore different ideas, but also knew when to rein me back in the interests of ever completing this project. They have been understanding and supported me many challenges and changes, including marriage, part time work, and moving onto a fishing trawler.

I would like to thank Dr Emma Tebbs for allowing me to use her lake surface area data, Melissa Tompkins for her help with NPZ modelling, Dr Robin Wilson for his help in gathering the TRMM rainfall data, Tom Stephans from BBC Earth for the continuous updates on flamingo populations in 2012, and Reuben Ndolo for his sharp eyes on fieldwork expeditions and flamingo counts.

Finally, I want to thank my husband Sam Ward for his patience, support and encouragement throughout in what turns out to be the hardest thing I have ever done.

0.1 Approach

The aim of this project is to improve understanding about the reduction in lesser flamingo population in the East African Rift Valley in response to changes in the soda lakes that they inhabit. In order to do this a literature review was undertaken to outline the data available about flamingos and their environment, and identify missing data that could be obtained by a field expedition to some of these lakes. The necessity of a two-pronged approach in exploring the research question arose from the literature review, due to the lack of data about the availability of *Arthrosphaera* for flamingos, which required a palaeolimnological approach, and the need for a model to explore flamingo behaviour. By grounding a model with empirical data it was hoped that more insights could be made into the interaction between lesser flamingos and their environment than could be achieved using either of these approaches in isolation.

Field trips were undertaken to core three of the soda lakes visited by flamingos to learn more about the distribution *Arthrosphaera*, their primary food source. Lakes Bogoria, Elmentaita and Oloidien were cored using a Uwitec gravity corer. Palaeolimnological techniques including loss-on-ignition and carbon/nitrogen ratios were used to identify the abundance of organic material in the lake sediment over the last ca. 150 years. Pigment analysis and elemental analysis were used to identify the source of the organic material, with pigment analysis being particularly useful in terms of identifying relative increases in cyanobacteria and in some cases could be used as a proxy for *Arthrosphaera*.

The main driver of changes in the dynamic soda lake ecosystem was identified as rainfall. Changes in rainfall cause large fluctuations in the shallow soda lakes, including the availability of *Arthrosphaera*, which causes flamingos to move in large numbers between the soda lakes in response. To model flamingo populations it was decided that a simple hydrological model driven by rainfall would be required as the foundation, which would then drive an *Arthrosphaera* model, again as simplified as possible whilst still capturing the fluctuations in food abundance observed in the soda lakes. The flamingo energy budget model was then implemented, with flamingo behaviour being driven using the outputs from the hydrological and *Arthrosphaera* model. In order to explore flamingo behaviour, thresholds for different behaviours were included which meant that a flamingo was increasingly likely to change its behaviour in response to an increased environmental pressure. This allowed for flamingo behaviour to vary in response to the same pressures rather than be pre-determined. The model is a highly simplified version of the soda lake ecosystem, and therefore it was used as a tool for exploring hypotheses about flamingo population changes rather than as a predictive model that could reproduce events in real time.

The palaeolimnological data, observed data and model were compared using the frequency of observed flamingo breeding and mortality events, and by comparing qualitative characteristics of each lake with the model outputs. Using the output of the model

and palaeolimnological approaches new hypotheses were formed about the cause of mortality events and recent population changes, and new questions were raised about how flamingos survive longer term fluctuations in rainfall as well as the significance of the more recent observed population changes.

Chapter 1

The soda lake network

1.1 Introduction

The Great Rift Valley is a network of faults and rifts that stretches from the Middle East down through East Africa. The Rift Valley splits into two branches, which together make up the East African Rift system. The Eastern branch bisects Kenya from North to South. The dramatic landscape is semi-arid, characterised by volcanic craters and high escarpments bordering flat plains that are interspersed by a string of shallow lakes. There are freshwater lakes such as Lakes Baringo and Naivasha, mesosaline lakes such as Lake Turkana, and hypersaline lakes which include Lakes Logipi, Bogoria, Nakuru, Elmentaita, Oloidien, Natron, and Magadi. These hypersaline lakes are endorheic, which means that the only outlet is by evaporation rather than overland outflows, causing the concentration of salts in the lake. They are very shallow and strongly dependent upon precipitation. Soda lakes undergo large fluctuations in water level in response to rainfall, which causes rapid changes in their physical and chemical characteristics.

The lakes of the East African Rift are unique ecosystems which are an important resource for wildlife, particularly for the huge number of bird species which live at or visit these sites. At Lake Bogoria alone 373 species have been identified, along with 50 migratory bird species (LBNR Integrated Management Plan, 2007). One bird species which has drawn attention is the lesser flamingo (*Phoeniconaias minor*). The extraordinary spectacle of tens to hundreds of thousands of these birds on the soda lakes of the Eastern Rift has attracted many tourists to Kenya and Tanzania. Flamingos are nomadic, moving between soda lakes unpredictably, in flocks that are highly variable in size (Childress et al., 2007). Their unpredictable movements have given the species an air of mystery that inspired the first scientific study (Brown, 1955).

Lesser flamingos are highly specialised filter feeders. They feed primarily upon blooms of cyanobacteria in congregations that can exceed one million individuals. There is concern regarding the decline in lesser flamingo population, since it is widely regarded

to have halved from two million in the 1950's (Brown, 1955) to around one million today and is now considered to be a "near-threatened" species (IUCN, 2006). This concern for the flamingo population was based on visual estimates that are now regarded as highly inaccurate by the scientific community. The only reliable estimate was made using aerial photography counts over many lakes in East Africa by Simmons (2000), which found a decline of 21% from 5,057,000 to 4,000,000 birds between 1975 and 1997. Flamingos breed at one lake, Lake Natron, under very particular conditions (see Section 6.1.2). There is concern that this makes the flamingos vulnerable to any impact on their breeding lake caused by climate changes and human impact. Proposals for a soda ash plant at Lake Natron have been made which conservationists fear will cause disturbance to the breeding populations.

The network of lakes visited by the lesser flamingo includes lakes Bogoria, Nakuru and Elmenteita, which are important feeding grounds (Owino et al., 2001). Other lakes are not usually visited in such large numbers, but include lakes Oloidien, Manyara, Abijata, Shalla, Eyasi and Magadi (Matagi, 2004). Fluctuations in rainfall cause shifts in phytoplankton abundance and community structure in the Rift Valley soda lakes, which affects the abundance of their primary food source *Arthrospira* (*Arthrospira fusiformis*) available to lesser flamingos using their filter feeding mechanism. Changes in food availability affects the distribution and density of lesser flamingos across the East African soda lakes, and is likely to be an important factor in the mortality events observed at some locations. The largest mortality event occurred at Lake Bogoria in 1999-2000 where 200,000 lesser flamingos died (Harper et al., 2003).

Many hypotheses have been postulated about the causes of lesser flamingo mortality events, including death by starvation, heavy metal poisoning, ingestion of cyanobacterial toxins, and disease. The lack of any continuous data about these lakes or monitoring of flamingo populations has made the evaluation of these hypotheses very difficult.

Field expeditions were undertaken in March 2011 and July 2012 to collect lake sediment cores from Lakes Bogoria, Elmentaita and Oloidien. The variability of these lakes in response to changes in rainfall was investigated using palaeolimnological techniques, including the investigation of phytoplankton abundance and community structure using pigment analysis. Novel methods of flamingo population reconstruction were considered and attempted for Lake Bogoria for the first time, as there are no current data on long term populations in East Africa.

After the reconstruction of these parameters, the modelling work was undertaken to investigate the thresholds that cause changes in *Arthrospira* abundance, the affect of these changes on lesser flamingo movements, and how this might contribute to declines in population. These results would be important for the conservation of lesser flamingos and their habitats.

1.1.1 East African Climate

The temporal dynamics of the East African climate are highly variable (Schagerl & Oduor, 2008), and so the lakes are subject to rapid and unpredictable fluctuations in physical and chemical conditions which affect their ecological state.

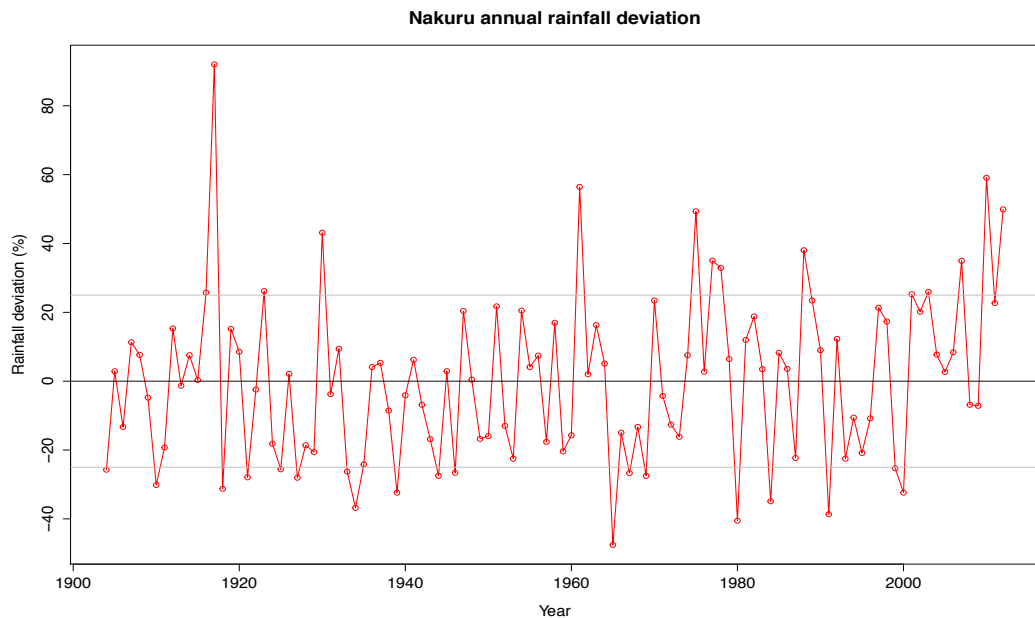


FIGURE 1.1: Lake Nakuru rainfall deviation as a percentage of the average annual rainfall, compiled from data from the Kenyan Meteorology Office and TRMM remote sensing data.

The main driver of changes to the hydrological budget of the soda lakes is variation in rainfall. The amount of rainfall has been attributed to the movement of the Inter Tropical Convergence Zone (ITCZ), a region of low pressure formed as a result of solar heating. More recently however, it has been thought that the stability of the northeasterly and southerly trade winds may also have a significant role in the variation in climate (Nicholson, 2000). The location of the ITCZ in East Africa moves above and below the equator with the seasons, as the latitude closest to the sun changes. By looking at Figure 1.1, which shows the annual rainfall for Lake Nakuru. Distinct flood and drought years can be seen by extreme deviations from the average rainfall.

In an average year Kenya experiences a dry period from December to March which is largely due to the dry winds coming in from the Sahara to the West (Ojany & Ogendo, 1988). The April monsoon follows the dry season, and then by a consistently wet season from May to August, when the ITCZ is directly above the Kenyan Rift Valley (Bergner et al., 2003). September is a dry month, then the second wet season occurs in October and November.

The East African climate has fluctuated between wet and dry periods in the last 1,100 years. Verschuren et al. (2000) reconstructed lake water levels for Lake Naivasha, a fresh

water lake in Kenya, which can be seen in Figure 1.2. During the Medieval Warm Period (years 1000-1270) the East African climate was much drier than it is presently, with Lake Naivasha depths estimated to be ca. 4 m, compared with 16 m in 1993, whilst during the Little Ice Age (years 1270-1850) the climate was much wetter, particularly between 1700 and 1800, where depths may have been more than twice current levels.

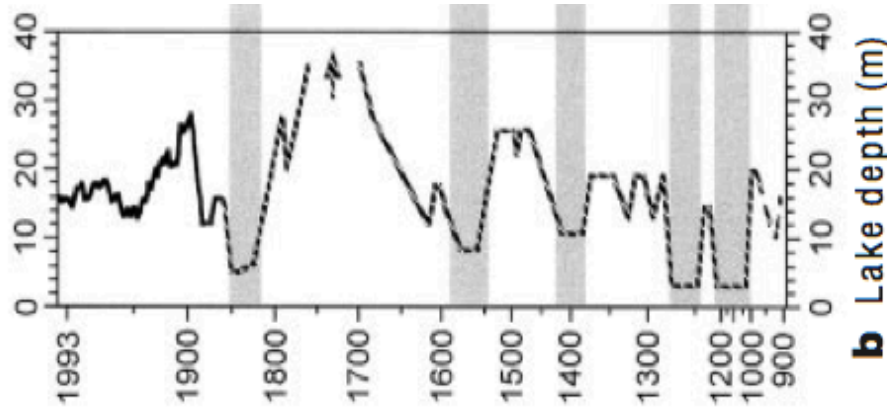


FIGURE 1.2: Lake Naivasha depth between the years 900 and 1993. Figure adapted from Verschuren et al. (2000).

1.1.2 An overview of the key soda lakes

The lakes most often visited by lesser flamingos can be seen in Figure 1.3.

Paleoclimate reconstructions from East African lakes have largely been focused on the identification of longer-term cycles in climate parameters over timescales of the order of thousands of years at low temporal resolution (e.g., Verschuren et al., 2000; Kiage & Liu, 2009). A 1500 year cycle has been identified between drier and wetter climates (Gasse, 2000), as well as evidence of fluctuations corresponding with variations in Earth's orbit around the sun which consist of the 20 ka precession cycle, the 41 ka obliquity and 100 ka eccentricity cycles. There has been far less investigation into the more recent history of the region and the changes that have occurred as a result of human impact on the landscape.

1.1.3 Lake Logipi

Lake Logipi is the northernmost and one of the least studied of the soda lakes in the Kenyan Rift Valley due to its remote location. Average rainfall is only 300 mm per year, with most runoff reaching the lake through the Suguta river (Castanier et al., 1993). The basin is a shallow pan, and the lake surface area varies between 5 km^2 and 200 km^2 during dry and wet years. In dry periods smaller groundwater-fed lagoons remain. Flamingos have been observed at Lake Logipi, a few hundred were seen in 1988

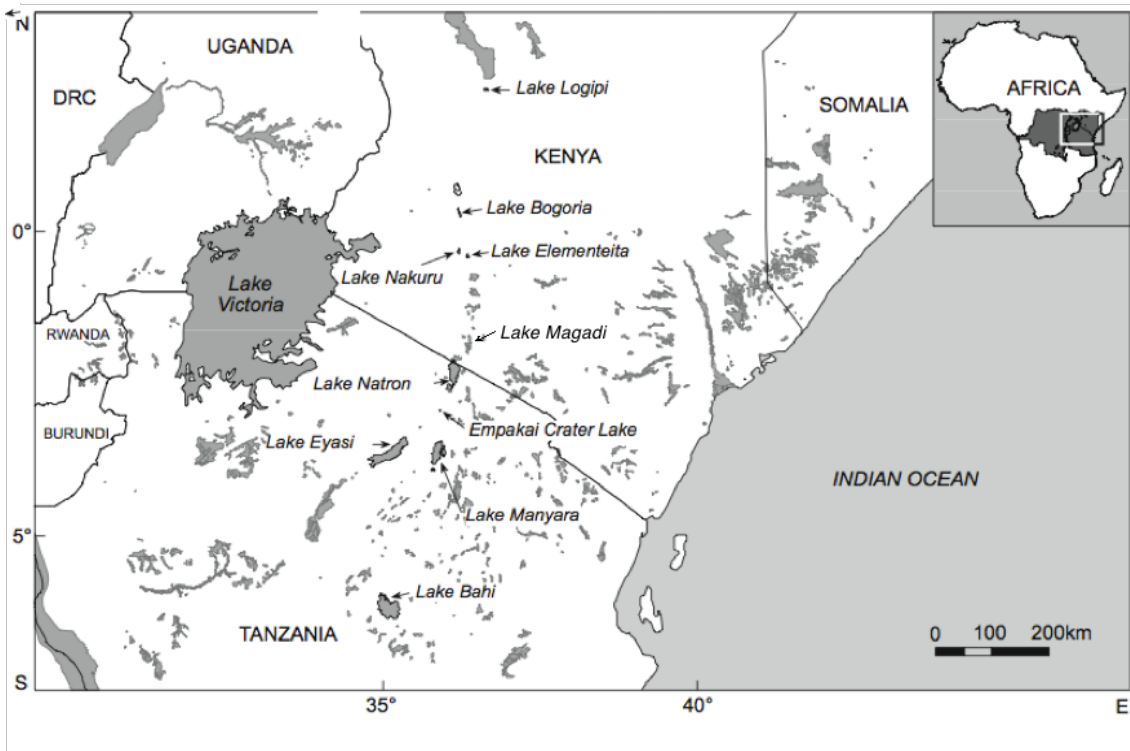


FIGURE 1.3: A map of the soda lakes in Kenya and Tanzania, modified from (Childress et al., 2007)

(Castanier et al., 1993), and in 2012 unto 800,000 are seen there (BBC Earth, pers com.).

1.1.4 Lake Bogoria

Lake Bogoria was designated as part of a national reserve in 1974, and was also designated a wetland of international importance under the Convention on Wetlands, the Ramsar Convention, in 2001. The shape of this basin is unlike the shallow pans of most other soda lakes, being approximately 16 km long, and ranges from 1 km to 4 km wide (see Figure 1.4). It is the most physically and chemically stable soda lake visited by the lesser flamingos, since it is relatively deep with a maximum depth of 12 m recorded in the southern basin (pers. obs., March 2011).

The inflows to Lake Bogoria include two permanent freshwater streams that flow into the southern basin, and the Ndolaita-Loboi river (also permanent) which flows into the northern basin. The seasonal inflows are the Waseges and Sandai rivers, which enter at the northern basin, and the Kipsiraria and Parkirichai rivers which enter at the western shore of the central basin. There are also numerous hot springs along the west and south-eastern shoreline, and an estimated groundwater inflow of 28 million m^3 per year which probably originates from lakes Naivasha and Nakuru, which are at higher elevations (Onyando et al., 2005).

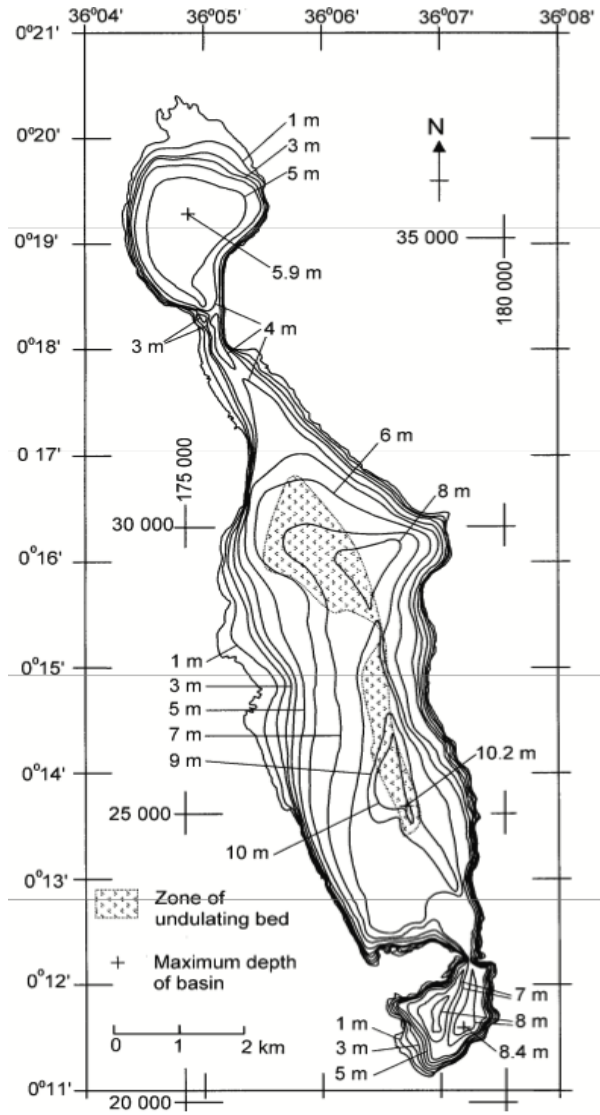


FIGURE 1.4: A bathymetric map of Lake Bogoria. Lake Bogoria consists of three basins joined by narrow necks, and is the deepest and most stable lake visited by lesser flamingos. This image is from Hikley et al. (2003).

Krienitz et al. (2003) found that in 2001 Lake Bogoria nutrient concentrations were very high, with 5.4 mg L^{-1} total phosphorus and 1.4 mg L^{-1} total nitrogen, and salinity was at 45 ppt.

There is usually a high abundance of cyanobacteria, often dominated by *Arthospira* (*Arthospira fusiformis*) (Harper et al., 2003). Despite the comparative stability of Lake Bogoria, *Arthospira* collapse events have occurred here stochastically in the past. These events are associated with a temporary increase in phytoplankton diversity until the recovery of the *Arthospira* population. The earliest known decline in biomass occurred in 1978 (Vareschi, 1987). Other collapses in *Arthospira* population have been recorded more recently during October 2001 (Harper et al., 2003) and from July to September 2004 (Schagerl & Oduor, 2008). However, a study by Krienitz and Kotut (2010)

which periodically sampled Lake Bogoria recorded the cyanobacteria community to be “a nearly monospecific dominance of *A. fusiformis*”, which contradicts other records for the same time. The frequency of visits to Lake Bogoria during this study is unknown, and it may be that fluctuations occurred more rapidly than the observations made during this study. In 2006 there was a change in cyanobacteria community structure to domination by green picoplankton *P. salinarum*. *Arthospira* had recovered to make up one third of the cyanobacteria population by 2008, and the remaining cyanobacteria consisted of lumps of *Anabaenopsis* sp., which disappeared by 2009, allowing *Arthospira* to dominate once more (Krienitz & Kotut, 2010).

Lesser flamingos often congregate at Lake Bogoria in large flocks since it often has very high densities of *Arthospira*. Annual flamingo census data from the National Museums of Kenya, Nature Kenya, and the Kenya Wildlife Service showed that Lake Bogoria was inhabited by an average of 610,000 lesser flamingos during the 1990s, and 252,000 lesser flamingo in the 2000s.

1.1.5 Lake Nakuru

Lake Nakuru was the first Ramsar site in Kenya, and is part of Nakuru National Park. This park is famous for having large numbers of flamingos and a popular tourist destination. The average water depth is 2 m (Moreau et al., 2001). However, the basin is a shallow pan, and the variable rainfall causes large fluctuations in lake surface area and salinity (see Figure 1.5). Lake Nakuru has been known to dry up completely during times of drought, whilst reaching a maximum depth of 4.5 m in 1964 (Vareschi, 1982). There are four seasonal streams or rivers that supply the lake, the Njoro, Makalia, Lamuriak, and Enderit, as well as small inflows from the springs in the northern basin, and the municipality sewage (Schagerl & Oduor, 2008). An influx of groundwater into the lake is speculated to originate from Lakes Naivasha and Elmentaita, or the rift valley escarpment (Becht et al., 2006).

Rapid changes at Lake Nakuru have caused frequent changes in phytoplankton composition, and affected the bird species at the lake (Burgis & Symoens, 1987). A 75% decline in *Arthospira* in 1974 resulted in the emigration of hundreds of thousands of flamingos (Tuite, 2000). There have also been periods where conditions have been fresh enough for fish to be introduced, which happened in 1953, 1959 and 1962 (Trewavas, 1983).

Burian et al. (2014) found *Arthospira* to be the dominant at Lake Nakuru in 2009 when maximum depth was at 1.2m, there were high nutrient concentrations (1.45 mg L^{-1} of soluble reactive phosphorus, 0.711 mg L^{-1} ammonium-N, 0.705 mg L^{-1} nitrate-N, and 0.77 mg L^{-1} nitrite-N) and salinity was 35 ppt.

The lesser flamingo population at Lake Nakuru averaged 232,000 in the 1990s less than half the number at Lake Bogoria. Annual flamingo census data is collected by Nature

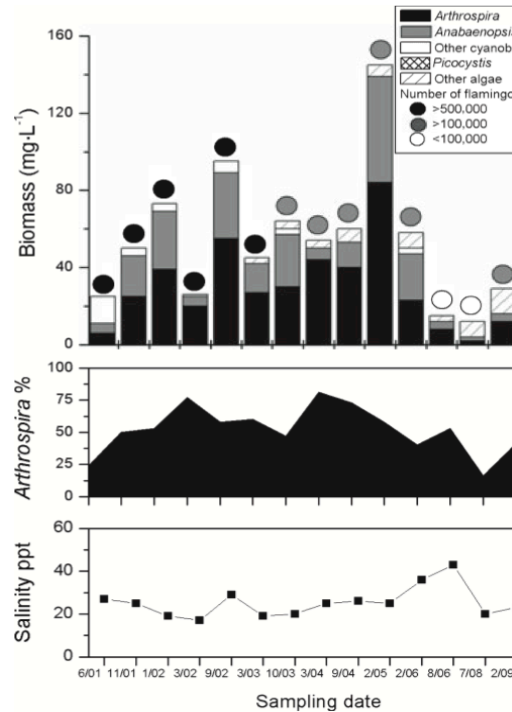


FIGURE 1.5: Lake Nakuru flamingo population, salinity, and algae composition and abundance (Krienitz & Kotut, 2010).

Kenya, the National Museums of Kenya (NMK), and the Kenya Wildlife Service (KWS). Krienitz and Kotut (2010) monitored flamingo population density at Nakuru from 2001 to 2010 and found that numbers were high at half a million birds until March 2003, after which numbers varied between 200,000 to 400,000 (see Figure 1.5). In 2006, 30,000 birds were lost at Nakuru and Bogoria to starvation and disease in response to low food concentrations, and in 2007 the lake was nearly dry before it was filled by the rains, during which time flamingo numbers were less than 100,000.

1.1.6 Lake Elmentaita

Lake Elmentaita is a very shallow saline basin to the Southeast of Lake Nakuru, and was designated as a Ramsar site in 2005. The western side of the lake lies within a private wildlife sanctuary but the rest is unprotected (Bennun & Njoroge, 1999). The average depth is 0.7m, with 0.9 mg L^{-1} total phosphorus and 2.2 mg L^{-1} total nitrogen (Adeka et al., 2008). The shallow basin causes large lake surface area changes in response to rainfall change, and is prone to completely drying up during times of drought. The Mereroni, Mbaruk, and Kariandusi rivers supply Lake Elmentaita, but have dried up in the past (Murimi et al., 1993). Springs continually flow into the lake from the southern end of the basin, an estimated 30% of this spring water originated from Lake Naivasha (Darling et al., 1996), and the remaining subsurface flow diffusing into the Elmentaita basin is estimated at 4.8 million cubic meters per year. This diffuse inflow is also from

Lake Naivasha; water flows underground along a fault, falling 200 m before it reaches Elmentaita (Becht et al., 2006).

Lake Elmentaita is visited by lesser flamingos in smaller numbers than Lakes Bogoria and Nakuru, with numbers averaging at 104,000 in the 1990's and only 9,400 in the 2000's (Nature Kenya, NMK, KWS). *Arthospira* was found to dominate the cyanobacteria population in 2007, but at other times benthic diatoms have been the primary food source at this lake, which flamingos graze during periods of low *Arthospira* abundance (Adeka et al., 2008; Jenkin, 1957; Tuite, 1979). There have been no macrophytes observed at Lake Elmentaita, but like Lake Nakuru, there have been increases in numbers of fish on some occasions (Owino et al., 2001). Fish were observed in March 2011 during high water levels, when water depth was measured at 1.3 m, but observation of salt deposits at the shoreline found that that water levels had been at least 40 cm higher in the months before this (pers. obs., March 2011).

1.1.7 Lake Oloidien

Lake Oloidien was formerly part of the freshwater Lake Naivasha. Pressures from an increasing human population and the flower industry have contributed to a decline in lake water level that resulted in the isolation of Lake Oloidien from Lake Naivasha in 1979. It is a small lake, with the only inputs being rainfall, runoff from the small catchment, and water seeping through the ground from Lake Naivasha (Verschuren et al., 2000). Since this separation the physical conditions and chemical composition of Lake Oloidien has changed, becoming increasingly saline and alkaline (Ballot et al., 2009). This has coincided with a reduction in the number of species found at Lake Oloidien, which is much reduced compared with the high biodiversity still found at Lake Naivasha. There has also been a shift in phytoplankton community (Ballot et al., 2009). The high density of *Arthospira* in the years 2001 to 2011 attracted flocks of lesser flamingos to the lake for the first time in living memory, in numbers of up to 20,000 birds between the years 2006-2010 (Krienitz & Kotut, 2010).

1.1.8 Lake Magadi

Lake Magadi is the most southern soda lake in Kenya. It is extremely hyper-saline, with the total dissolved salts at approximately 30% w/v saturation, which is much higher than the other Kenyan soda lakes which are around 5% w/v saturated (Grant et al., 1990). Little research has been undertaken at Lake Magadi due to the extreme environment and difficulty in accessing this lake.

Water from lakes at higher altitude drains underground along the fault lines to emerge from springs and diffuse into lakes at lower altitudes. Lake Magadi is at the lowest point of the Rift Valley at 580 meters above sea level, and as such it is the final sink for

water from the other Rift Valley lakes. Water emerging at Lake Magadi from springs and other groundwater sources is estimated to total 71 million cubic meters per year (Becht et al., 2006). Groundwater is the main influx of water to Lake Magadi (Executive Summary - Lake Natron Soda Ash ESIA, 2007), since the Ewaso Ngiro river and some small streams reach the lake, but are not significant contributors to the Lake water balance. The salts reach saturation and precipitate out of the lake water onto the lake bed, which has formed a 40 m thick layer of sodium carbonate and bicarbonate (trona) in places (Eugster & Hardie, 1978). A soda crust also forms across the lake surface, restricting the amount of light available within the lake (Executive Summary - Lake Natron Soda Ash ESIA, 2007).

The hyper-saline-alkaline waters of Lake Magadi are usually dominated by red halo-alkaliphilic bacteria (Grant, 2003). *Arthrosphaera* has been identified at Lake Magadi (Grant, 2003). However, *Arthrosphaera* is unlikely to reach significant numbers unless extensive rainfall causes a large influx of rainwater to dilute the salts. Matagi (2004) also noted a lack of cyanobacteria, and found that purple sulphur bacteria (*Ectothiorhodospira sp.*) was the primary producer during that particular time. Hot springs feed lagoons in the northern and southern ends of the basin which are small, more habitable pockets, occupied by fish tolerant of high temperatures and saline conditions (Matagi, 2004).

Despite the lack of cyanobacteria at Lake Magadi, lesser flamingos are known to visit this lake. In 1994, 7765 flamingos were counted here despite water levels being less than 10% of average levels, which would be expected to correlate with low abundances of cyanobacteria (Woodworth et al., 1997). This is a small number of flamingos however in comparison with the number at Lake Natron at that time, which was estimated to be 500,000.

During 1962 when water levels were high, one million pairs attempted to breed at Lake Magadi. There are different reports as to the success of this attempt; it appears to have been successful in the sense that some flamingo chicks did fledge. However, the proportion of flamingo pairs that actually succeeded in rearing a chick was not as high as it would normally be at Lake Natron. It was documented as a “disastrous attempt” by Koenig (2006), who suggested that the low success rate was a result of the high concentration of salts and trona which sticks to the legs of the chicks and hampers them until they eventually die (Koenig, 2006).

1.1.9 Lake Natron

Lake Natron is a shallow, endorheic lake which lies on the Kenyan-Tanzanian border. It is large in comparison with other soda lakes at 22-35 km wide and 75 km long. This is an inhospitable place, with highly caustic water concentrated by the high evaporation rate. The main body of water is only habitable to extremophile bacteria, which give the

water a red colour during blooms. Four rivers and a number of springs supply water to the lake, the springs are particularly important sites for drinking and feeding. The lagoons surrounding these springs have each been found to support different epipelagic and planktonic microbial communities (Tebbs, 2013), and are also inhabited by fish.

The topography and hydrology of the basin offers flamingos the unique opportunity to breed without being disturbed by predators (Childress et al., 2007). This only occurs when the lake water level is high enough to isolate nesting sites and salt islands from the shore, but not so high that it covers these islands or the mud needed to build the nests. When water levels are low mammals can reach nesting sites across the dried salt crust to disturb the flamingos. This breeding site was discovered by Leslie Brown, who documented breeding events in the late 50's and early 60's (Brown, 1973).

Apart from the research by Leslie Brown (Brown, 1973; Brown & Root, 1971) and recent work by Tebbs (Tebbs et al., 2013a) very little is known about Lake Natron. Lakes Natron and Magadi are both in inaccessible locations, and too shallow to launch a boat away from the shoreline. The alternative of wading through the sediment is also difficult and quite hazardous. There is potential for direct measurements and observations to be made at Lake Natron during years of higher than average rainfall. The high rainfall in 2010 did cause a rise in lake water levels at the other Rift Valley Lakes, and it is possible that during such years the water level may increase enough to launch a small boat. The best way to observe these very shallow and caustic lakes so far has been from the air by light aircraft. However, as a result of the recent free availability of Landsat images it is likely that more can be learned about Lake Natron from satellite images than from direct observations in the near future (Tebbs et al., 2013a).

1.1.10 Lake water level

Lake water level is very important to this study since it is a direct response to the amount of rainfall in each lake catchment. Because rainfall is the driver of these lake systems, any available information about past lake water levels must be collated, and used to compare with reconstructions of past lake water level.

Soda lakes are endorheic basins and so lake processes are strongly linked to the hydrology of the catchment and the amount of rainfall. The last four flamingo mortality events at Lake Bogoria have appeared to coincide with La Niña droughts. However, there have been conflicting reports of water level conditions during mortality events and so the link between rainfall and mortality events requires further investigation.

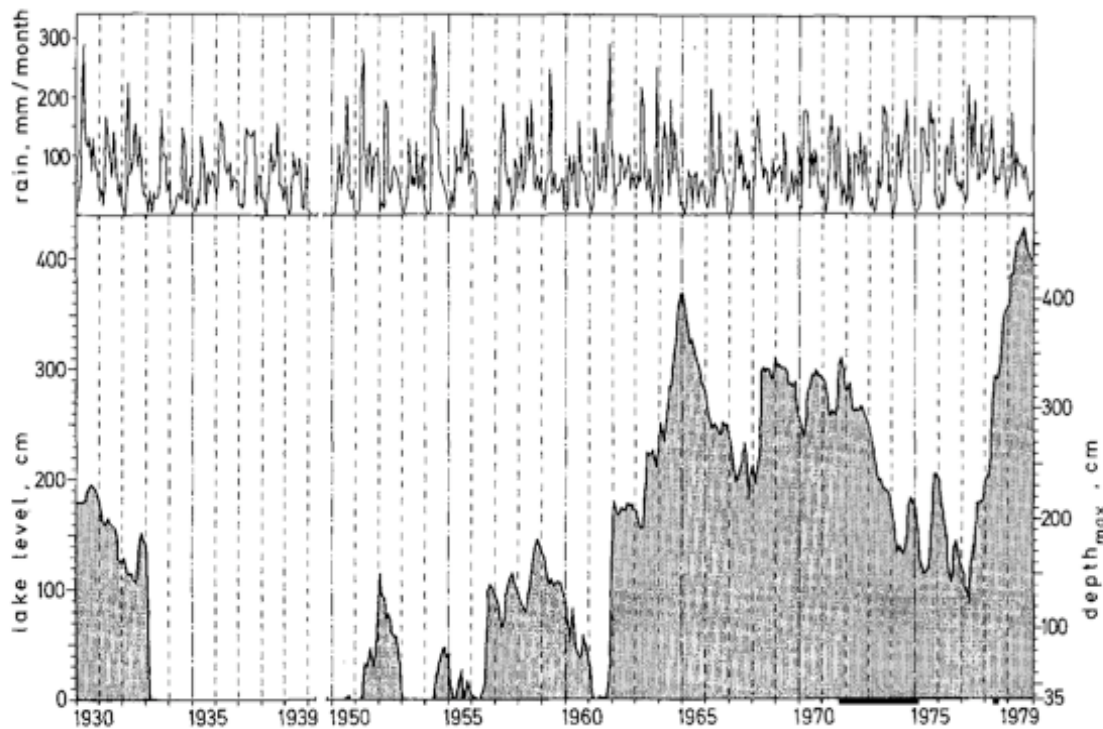


FIGURE 1.6: Rainfall and lake level changes at Lake Nakuru from 1930 to 1979 (Vareschi, 1982). No data was available for 1940-1949.

1.1.11 Dynamical regimes

The rapid changes observed in many shallow lakes since the 1970s has sparked interest in the management of lakes and their sustainability, and during this time modelling of lakes became widespread. Modelling lake ecosystems allows for the hypotheses to be tested, such as the impact of increasing the use of fertilisers in a lake catchment on the lake ecosystem. It has often been assumed that changes in ecosystems occur gradually and linearly with changes, such as nutrient loading, water abstraction or over-fishing, but this is often not the case (Tilman et al., 2001). Some ecosystems can switch between different stable dynamical regimes in response to gradual changes in external parameters (Scheffer et al., 2001). Others may exhibit limit cycle behaviour (Jørgensen & Bendoricchio, 2001), which means that the system is oscillating around a particular point in the phase space. In the case where the behaviour is attractive and so moving towards a particular point, or is stable, a small disturbance will cause the system to return to its limit cycle behaviour. For the case where a system is oscillating about an unstable point in the phase space, a small perturbation in the system can cause an abrupt shift in dynamical regime. Abrupt change may be observed in response to the accumulation of small incremental changes in external parameters over time that reach some threshold where the system shifts to a different dynamical regime. One example of a dynamical regime is a lake is dominated by macrophytes and fish. This regime may remain constant when the concentration of nitrogen and phosphorus is low. Where

nutrient loading occurs, the concentration of these nutrients increases until a threshold is reached where a bloom of algae occurs. The decomposition of the algae causes hypoxia in the lake which kills fish and other organisms, and the lake ecosystem changes to a dynamical regime of eutrophication. Concern about eutrophication drove the development of nutrient-phytoplankton-zooplankton-detritus (NPZD) models. More robust ecosystems are stable across wider ranges of external parameters, and so shallower lakes are less robust than deep lakes, since they will shift to a regime of eutrophication under weaker external forcing. An ecosystem is said to be stable as long as the important parameters to ecosystem functioning are within a particular range. In order to obtain the information how a given system would behave when acted upon by external disturbances, it is necessary to know the structure of the basin boundaries of coexisting attractors.

When an ecosystem changes from one dynamical regime to another as a result of one parameter passing a threshold, simply returning the parameter to a value below the threshold in some cases will not return the ecosystem to its original state. When the structure of the new dynamical regime is different to the previous regime, the feedbacks in the system are different. In a eutrophic lake for example, reducing the phosphorus concentration of the water to the value just below the threshold will have a minimal impact on the turbidity of the water. In the Lake Oloidien basin of Lake Naivasha, Krienitz et al. (2013) noted that once *Arthospira* was established in a lake as the dominant producer, *Arthospira* continued to dominate even when salinity is then reduced below levels that were previously too fresh. Another example of a feedback in the soda lake ecosystem is the lesser flamingos use of their filtering mechanism to graze, creating selective pressure for the growth of cyanobacteria that is inedible to them.

It is in the nature of biological systems that there are many interacting processes with feedbacks that produce non-linear responses to small changes in the system parameters. In the East African soda lakes there are dramatic fluctuations in cyanobacteria and changes in phytoplankton species composition. The lake water level changes continually, causing changes in the lake environment that allow different phytoplankton to dominate the lake ecosystem.

Further research is needed to investigate whether changes in these soda lakes are abrupt or linear, and whether there were any early warning signs that this change was likely to occur. Modelling is one tool that can be used to improve our understanding of the Kenyan soda lake dynamics, and could also give insights into flamingo population changes.

1.2 Modelling

Studying the lakes by using palaeolimnological techniques can improve our understanding of how they function and can reveal past conditions and changes. However, the availability of material and funding limitations on any project restrict the number of proxies that can realistically be considered. It is possible to further explore the East African Rift Valley soda lakes using ecological models, which can be used to explore the complex interactions of the ecosystems of the lesser flamingos and investigate the different hypotheses that have been proposed for the flamingo population decline, as well as directing further empirical work.

A model is a highly simplified version of the real ecosystem, that has the minimum complexity required to capture the behaviour of interest. In an ecological context a model uses the key components and parameters of the target ecosystem. Models are useful for identifying gaps in knowledge about an ecosystem, and can be used to guide experimentation, as well as for giving an insight into the actual relationships that are thought to underly behaviour. There is great potential for models to provide insights into the mechanisms that cause changes to ecosystem behaviour in the East African soda lakes.

It may seem that a very complex model is required to capture the way that an ecosystem functions, where every process must be explicitly understood and may be expressed as a differential equation. If this were the case a very cumbersome model would be produced that takes a prohibitively long time to run. It would also be difficult to fathom the behaviour produced by such a complicated model, since the fundamental physical processes can be obscured (Ermentrout & Edelstein-Keshet, 1993). In order for a model to be useful it must contain enough information about the system of interest to actually represent it, but be as simple as possible. When considering a particular lake for example, is the model specific to that lake or could it be representative of any lake? What are the key parameters that are important to the research question? It is important to have as much data about the environmental and ecological parameters of interest as possible so that informed decisions can be made about how best to model the system, to judge what the important interactions are and what parameters can be assumed to be constant or ignored.

Observational data from the lakes found in the literature, or proxy data obtained from sediment cores (section 3) could be compared with model outputs its response to changes that have occurred in the real system. Using a carefully designed model of the East African soda lakes will allow further insights into their ecosystem dynamics, allow current hypotheses about the ecosystems to be tested, and new hypotheses to be formed which can then be further investigated in the field.

1.3 Model objectives

The literature reviews (chapters 4.1, 5.1 and 6.1), site visits and discussions with other researchers identified five emergent properties that are the result of the dynamic soda lake environments in this study:

1. Blooms of *Arthrospira*.
2. Crashes in *Arthrospira* abundance.
3. Flamingo mortality events.
4. Flamingo breeding events.
5. Flamingo population distribution patterns

The model was constructed with the aim of understanding the mechanisms underlying these emergent properties. The modelling objectives were therefore to:

1. Construct a hydrological model of each flamingo lake that captures the changes in lake surface area and depth in response to rainfall.
2. Model the growth of the primary producers in these lakes, specifically for the cyanobacteria *Arthrospira*, and how this changes in response to different lake conditions.
3. Model the energetics of the lesser flamingo on an individual level.
4. Model the relocation and breeding behaviour of lesser flamingos in response to fluctuations in food abundance and distribution, considering their movements between different soda lakes.

A model designed to investigate the East African soda lakes needs to include the lakes in the Rift Valley that are most important to the lesser flamingos. It is also useful to know what data are available about these lakes from which to construct meaningful representations of the lakes in a model. From the soda lake environment literature review and discussion with park rangers and other researchers (see section 1.1.2), Lakes Logipi, Bogoria, Nakuru, Elmentaita, Oloidien, Magadi and Natron, lie in a ‘chain’ along the Kenyan Rift Valley floor in a north-south direction. These lakes have been identified as ‘flamingo’ lakes since flamingo populations have been observed at each of these lakes in different studies, e.g., Childress et al. (2007), Tuite (2000), and in flamingo census data. Lakes Bogoria, Nakuru and Natron are particularly well known for flamingos. Lakes Bogoria and Nakuru are historically the two most stable lakes and as a result have regularly provided feeding grounds for the lesser flamingos, whilst Lake Natron is essential as the breeding lake. Less is known about the relative significance of most of the other lakes to the survival of the lesser flamingos, other than that flamingos do visit them when there is less food available at lake Bogoria and Nakuru.

A systems dynamics diagram (Figure 1.7) has been used to develop hypotheses relating to cyanobacteria, specifically *Arthrosphaera fusiformis* abundance and flamingo population change that can be further investigated. A systems dynamics approach considers stocks and flows of materials in a system. It was used to show the links between stocks and variables in the soda lake ecosystems, to identify feedback loops, flows of material and information, and the main processes affecting these soda lake ecosystems.

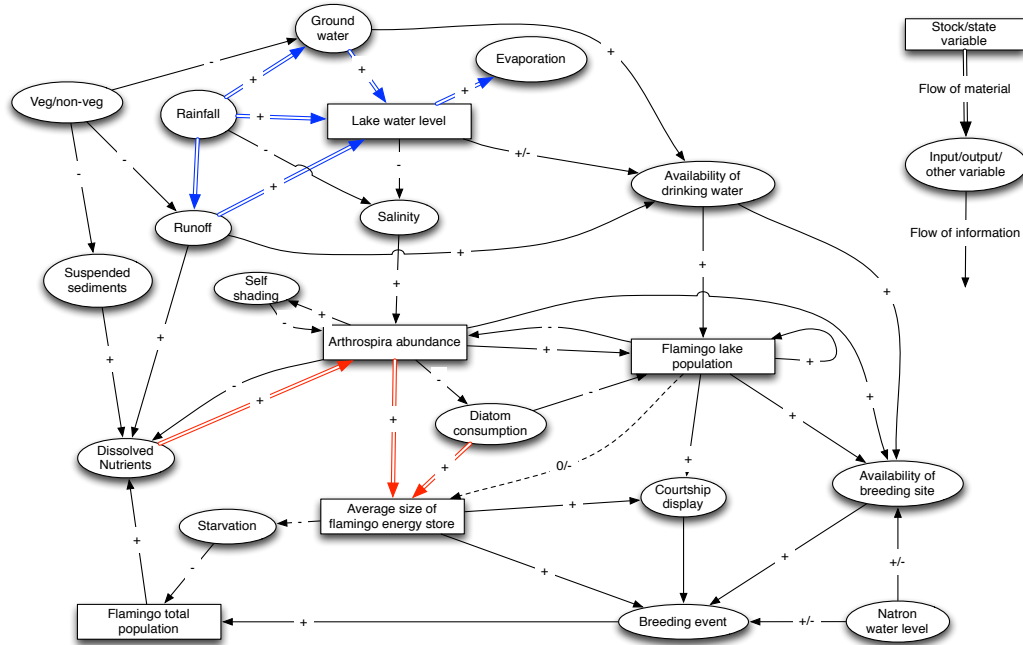


FIGURE 1.7: A systems dynamics diagram of the lesser flamingos and their environment. The important hydrological interactions are highlighted in blue, and the important interactions to flamingo populations are highlighted in red. The '+' or '-' symbol denotes a positive or negative correlation between stocks and variables.

1.4 Hypotheses

The *Arthrosphaera* hypotheses are:

1. Changes in phytoplankton abundance and community structure occur in response to changes in lake water level and direct rainfall.
2. Lesser flamingos can limit *Arthrosphaera* abundance at smaller lakes.

The flamingo hypotheses are:

1. Lesser flamingos increase the rate of nutrient cycling in soda lakes.
2. A reduction in food abundance across all soda lakes leads to malnutrition and death by starvation.
3. Malnutrition increases susceptibility of lesser flamingos to disease.

4. When the cyanobacteria population is dominated by toxic species increased levels of cyanotoxins are ingested by flamingos which leads to death by toxicosis.
5. When low water levels force lesser flamingos to drink exclusively from the hot springs, the toxins produced by cyanobacteria in the hot springs accumulate in flamingo tissues causing death by toxicosis.
6. The flamingo replacement rate is low as a result of a reduction in frequency of suitable breeding conditions.

These hypotheses are driven by changes in lake water level, and so require a past record of lake water level to be investigated. Five of the hypotheses are concerned with cyanobacteria abundance and composition. To consider these hypotheses it is necessary to model cyanobacteria growth and reproduction in response to changing environmental conditions, particularly rainfall, given that changes in phytoplankton composition have often been observed at low or high lake water levels. It is not necessarily possible to create a model to address all of these hypotheses. However, the model is likely to give insights into some of the hypotheses about *Arthrospira* abundance and flamingo population

There is no continuous record of phytoplankton composition and abundance in relation to water level, so the use of palaeolimnological techniques to reconstruct past environmental conditions and cyanobacteria abundance using lake sediment cores is essential to begin to understand soda lake ecosystem dynamics. With reconstructions of past abundance and species composition of phytoplankton, as well as reconstructions of lake water level, it will be possible to validate models of the Rift Valley soda lake dynamics. Using these models the movements of lesser flamingo, their population decline and mortality events can be explored.

The model needs to consider how hydrological parameters will be estimated for each lake, how the growth of *Arthrospira* will be calculated, whether nutrient limitation will need to be included, and what changes in lake salinity or water level can be tolerated by *Arthrospira*. The flamingo model must consider how flamingos decide to change from one behaviour to another, such as deciding to breed or feed on diatoms, or how disease transmission could be implemented.

Chapter 2

Fieldwork

2.1 March 2011

A fieldwork expedition was undertaken from the 5th-12th of March 2011 to obtain sediment cores. This was a collaborative effort between the University of Southampton, Queen Mary University of London and the Natural History Museum. Cores were to be used to gain insight into the past conditions at Lakes Bogoria, Elmentaita and Oloidien, so that the suitability of these lakes as feeding locations for lesser flamingos could be investigated.

The best coring locations in each lake basin are in the deepest parts of the basin, where disturbance to the sediment by bioturbation or changes in lake water level are minimised. The deepest parts of these lakes were cored where possible depending upon accessibility of these locations and permissions. The weather conditions at the coring site also need to be relatively calm, since choppy waters can unsteady the coring platform or small boats. It was therefore advisable to visit the site during the dry season to minimise the chance of unfavourable weather conditions. The wind strength in Kenya usually varies in the same way throughout the day in the Kenyan Rift Valley, being calm in the early part of the day, with wind speeds picking up after midday which can cause the lake surface to become very rough.

For the purpose of this research project, sediment cores of approximately up to metre was required. A Uwitec gravity corer with transparent coring tubes was used for this expedition. A gravity corer consists of a cylindrical tube which is driven into the sediment using only its mass, or with additional weights if required. The top of the tube is sealed to keep the sediment in the tube, allowing the core to be pulled out of the lake bed. Before the bottom of the core leaves the water this end is capped, and the core can then be brought out to the surface. The core can either be transported to the lab for analysis, or extruded and subsampled on site. Before analysis the core should be stored at a constant low temperature of around 4°C. The advantages of using a Uwitec

gravity corer are that it is a relatively simple way to collect short cores, is quick and it also allows for the extrusion of core samples on site.

Sediment cores were collected from Lakes Bogoria, Elmentaita and Olloidien. Most time was spent at Lake Bogoria which has three basins, and so cores were taken from the northern, central, and southern basin (Table 2.1). Five cores were taken from Lake Bogoria in 2011, three of these cores were extruded in the field, two of which were sampled at 1 *cm* intervals, and one from the South basin sampled at 0.5 *cm* intervals due to the fine laminations that were observed in the sediment.

Lakes Elmentaita and Olloidien are single basin lakes, and only one core was taken from each of these due to time constraints and equipment limitations. These cores, as well as the two remaining cores from Lake Bogoria were kept intact. These intact core tubes were cut a few centimetres above the sediment surface-water interface to drain the water above the core surface. The surface sediment was unconsolidated and easily unsettled. It is very likely that simply capping them without stabilising these cores would have resulted in the complete mixing of the sediment during transportation. To stabilise the surface sediment, zorbitrol powder was used to crystallise the water into a gel. Caps or bungs were then fitted and taped to the ends of the tube. The zorbitrol gel was observed to cause some disturbance to the sediment at the surface water interface. However, this was preferable to more extensive mixing of the core. Other difficulties were encountered at Lake Bogoria due to the unconsolidated nature of the sediment including the difficulty in detecting the water-surface interface. The interface was captured by pulling up the corer as soon as the corer was felt to hit the sediment. At lakes Elmentaita and Olloidien, the sediment was more compacted and it was difficult to obtain cores longer than 50 *cm*, and so core lengths were shorter at these lakes (Table 2.2).

Once the cores had been either extruded and put into labeled clear plastic bags or stabilised and capped, the cores and samples were kept dark and either frozen or cold at around 5°C, apart from BGA-G4, which was too long to fit into the fridge-freezer available, and was simply kept dark and at room temperature, the highest recorded temperature at Lake Bogoria during this time was 39°C.

Cores BGA-G4 and BGA-G5 were noted to have laminations, and smell of sulphur, which indicated anoxic conditions where they were obtained in the southern basin at Lake Bogoria. The depths at which these cores were collected exceeded previous measured depths by 2m. The water levels were high and covered the hot springs along the eastern shore of the main basin, which are usually out of the water away from the shore. Lesser flamingos were present at Lake Bogoria at numbers in the order of hundreds of thousands of birds.

At Lake Elmentaita small fish were seen along the eastern shore, which is unusual, since fish in this lake are normally found close to the springs in the southern basin. The observation of these fish in the main body of Lake Elmentaita along with higher than

Date	Core ID	Lake location	N/S \pm 7m	E \pm 7m	Depth(m)
5/3/11	BGC-G1	Bogoria, N. basin	00 19' 41.4"N	36 04' 39.9"E	4
5/3/11	BGC-G2	Bogoria, N. basin	00 19' 41.4"N	36 04' 39.9"E	4
7/3/11	BGB-G3	Bogoria, M. basin	00 16' 16.2"N	36 06' 13.9"E	7
9/3/11	BGA-G4	Bogoria, S. basin	00 11' 35.8"N	36 06' 55.7"E	10
9/5/11	BGA-G5	Bogoria, S. basin	00 11' 33.8"N	36 06' 55.4"E	10.5
3/5/11	ELM-G6	Elmentaita	00 26' 23.6"S	36 14' 54.9"E	1.3
3/5/11	OLO-G7	Oloidien	00 48' 51.3"S	36 16' 22.7"E	4
14/7/12	Sb1	Bogoria, S. basin	00 11' 35.1"N	36 06' 58.6"E	11.9
14/7/12	Sb2	Bogoria, S. basin	00 11' 35.1"N	36 06' 58.6"E	11.9

TABLE 2.1: Core locations are detailed here with the depth of the lake where the core was taken. A map of the core locations can also be seen in Figure 2.1 for Lake Bogoria, Figure 2.2 for Lake Elmentaita and Figure 2.3 for Lake Oloidien.

average water levels suggests that the salinity of Lake Elmentaita was relatively low. A small group of flamingos could be seen at the southern end of the lake. The core collected at Lake Elmentaita, ELM-G6, changed suddenly in colour from pale to dark near the bottom of the core. Darker sediment is likely to be enriched with organic matter, and suggests that lake productivity was higher at the time of deposition of this layer.

At Lake Oloidien flamingos were observed in small numbers. The core retrieved from this lake, OLO-G7, had a marked change in sediment colour from pale to dark was identified 40 *cm* from the surface, and was approximately 3 *cm* thick. Copepods were found in the water above the sediment-water interface of the retrieved core.

The cores and other samples were returned by air and were still frozen when they were stored in a fridge in the University of Southampton's School of Geography. It was later discovered that the intact core BGB-G3 contained a large proportion of water as it had thawed and completely mixed along the length of the core. Core BGA-G4 had partially mixed through during transportation, leaving the top half of the core unusable. The final problem involved core BGA-G5, which part way through the extrusion process was mislabelled, causing the duplication of label names for approximately 20 *cm* of the core. Fortunately, the opportunity arose to replace the south basin Bogoria cores on a second field trip in July 2012.

2.2 July 2012

The second field trip was in July 2012 for two weeks at Lake Bogoria with Queen Mary University of London in the wet season. The lake water levels in Kenya were very high during this time, the highest since the 1960's, with the Loburu geyser KL19 completely inundated. The Wasages river was flowing into the north basin, which had overflowed to the north where a new swamp had grown up around the mouth of the river. A lens of silty, fresh water overlaid the saline lake water in the first half of the basin before

Core ID	Length (cm)	Intact/extruded	Storage before travel
BGC-G1	90	Extruded, 1 <i>cm</i> intervals	Frozen
BGC-G2	75	Extruded, 1 <i>cm</i> intervals	Frozen
BGB-G3	47	Intact	Frozen
BGA-G4	90	Intact	Room temp
BGA-G5	90	Extruded, 0.5 <i>cm</i> intervals	Frozen
ELM-G6	40	Intact	Frozen
OLO-G7	53	Intact	Room temp
SB-1	69	Extruded, 1 <i>cm</i> intervals	Room temp
SB-2	75.5	Extruded, 0.5 <i>cm</i> intervals	Room temp

TABLE 2.2: Information about how the cores were transported.

mixing. There were no flamingos in the north basin but an abundance of other species including egrets, Egyptian geese and pelicans which are usually seen in the freshwater lakes. There was still a high density of *Arthrospera* in the main and southern basins. There were approximately 500,000 flamingos present in the main basin, two small groups a few thousand strong were of young flamingos that probably fledged in January 2012. The adult flamingos appeared to be in good condition, very pink and were displaying in large numbers in the early mornings. Nests and deserted eggs were found on the eastern side of the lake from January or February 2012 (Philip Sanders, pers. comm.). The high water levels had created a small island at the eastern side of the neck of the south basin by August where greater flamingos, *Phoenicopterus roseus*, attempted to breed. The outcome of this attempt is unknown since the birds were not monitored. These observations are the first recorded of flamingos attempting to breed rather than simply building practice nests at Lake Bogoria. Two cores, SB-1 and SB-2, were taken in the south basin using a Uwitec gravity corer (Table 2.1). Core SB-1 was immediately subsampled in 1 *cm* intervals, and the other transported back to camp due to adverse weather conditions and then subsampled in 0.5 *cm* intervals. The sample bags were written out in advance and the labelling was double checked before extrusion. Both cores contained laminations and were not mixed. The samples were then kept in a fridge near our accommodation and in the dark until their transport back to the UK in September 2012 where they were refrigerated at the University of Southampton to reduce pigment degradation.

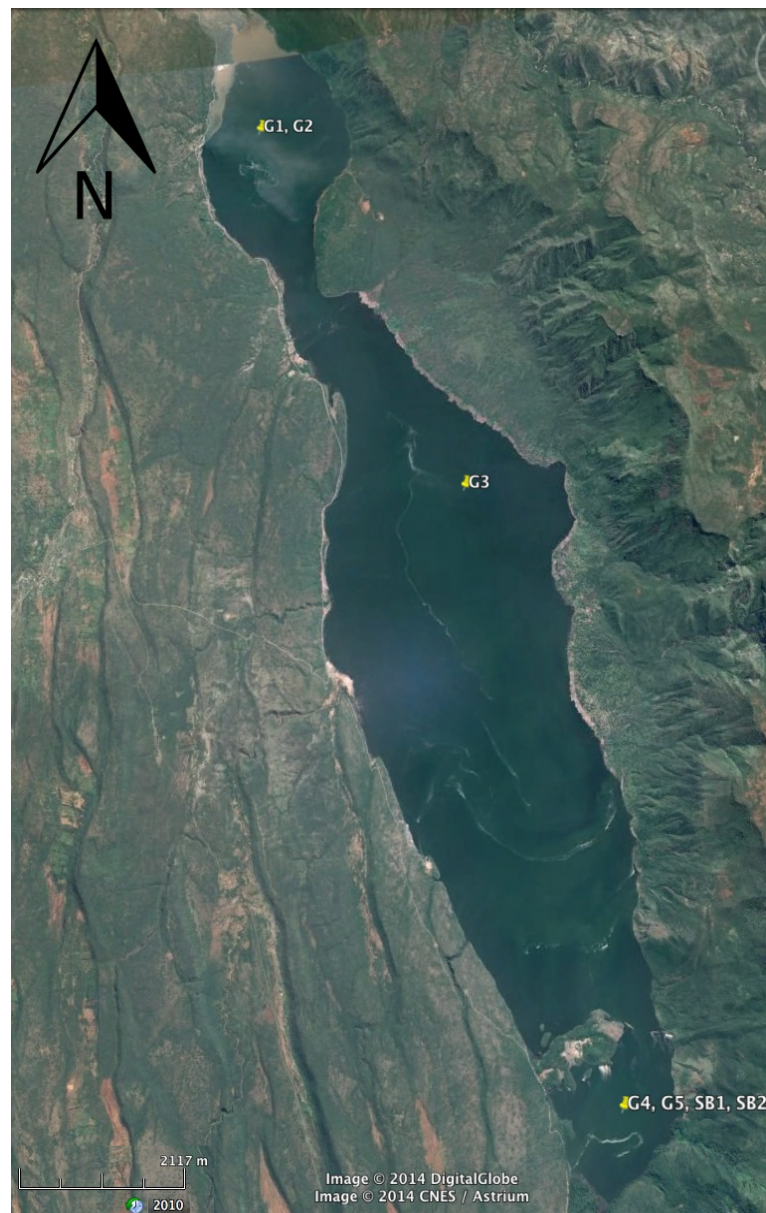


FIGURE 2.1: Lake Bogoria core locations.



FIGURE 2.2: Lake Elmentaita core location.



FIGURE 2.3: Lake Oloidien core location.

Chapter 3

Palaeolimnology

3.1 Outline of sample analysis

To gain insight into changing flamingo populations it is useful to explore the state of the soda lake ecosystems in the past to identify the stability of these lakes and the availability of food during different environmental conditions. To do this the lake sediments of three soda lakes were analysed using palaeolimnological techniques to identify past environmental conditions and biota in these lakes.

A multi-proxy approach is desirable when reconstructing past environmental conditions to help understand as much about the ecosystem as possible, and increase the robustness of the interpretation. The same analyses could not be undertaken for every core due to various logistical constraints, such as time, the cost of different analyses, and availability of sample material with which to undertake these analyses. The analyses that was undertaken is summaries in Table 3.1.

The particular elements that need to be reconstructed for the soda lakes in this study are phytoplankton community structure and abundance, and flamingo population. To date the Lake Bogoria core gamma ray spectroscopy was used. The organic matter content of lake sediments is composed of the lipids, carbohydrates, proteins and any

Analysis	Bogoria core G1	Bogoria core SB1/SB2	Oloidien core G7	Elmentaita core G6
Gamma ray spectroscopy	-	Y	-	-
Loss On Ignition	Y	Y	Y	Y
Total Organic Carbon/Nitrogen	Y	-	Y	Y
Pigment analysis	Y	Y	Y	Y
Nitrogen isotopes	Y	-	-	-
Bulk X-Ray Flourescence	-	Y	-	-
ITRAX core scanning	-	-	Y	Y

TABLE 3.1: A summary of the palaeolimnological analyses undertaken.

other remains of living organisms produced within the lake or washed into the lake from the surroundings. A high proportion of the sediment in the very productive soda lakes such as Lake Bogoria is organic matter (e.g. Verschuren et al., 1999). Total Organic Carbon/Nitrogen (TOC/N) and Loss On Ignition (LOI) (Dean, 1974) were both be used to measure the organic matter content of lake sediments. TOC values tend to be about half of LOI values for the same samples because organic compounds constitute about 50% carbon. These measurements give a bulk value which are be used to identify changes in lake productivity. The TOC/N analysis is also used to help understand whether the organic material originated within or outside of the lake. Pigment analysis was then undertaken to gain more insight into what was growing in the lake more specifically, since some pigments are associated with particular taxa (Proteau et al., 1993). Bulk XRF and ITRAX core scanning were used to identify the elemental composition of the cores. Ratios of different element abundances were used to find changes in environmental and sedimentological conditions.

The study of diatoms were considered to identify changes in salinity at Lakes Bogoria and Elmentaita. However, at Lake Bogoria a preliminary investigation into diatom species found the diatom remains to be low in concentration and significantly damaged by dissolution, and at Lake Elmentaita diatoms were in low abundance, fragmented and also obscured by clay particles (M. Leeson, pers. comm.).

Conservationists are concerned with the decline in population of many species. The cause for population decline is often difficult to determine due to the absence of long term population data (Norris et al., 2007). It is usually the case that population sizes are monitored only after concern about population decline has arisen. Records of population size from direct observations are therefore often only available over very short timescales, which are not sufficient for resolving long term trends or the causes of these changes. Since records of past flamingo abundance are sporadic and highly subjective (see section 6.1.1.) there are very few data before 1990 that can be used as anything more than an estimate of magnitude of flamingo population numbers. If it is possible to reconstruct flamingo abundance at individual lakes using lake sediments, the response of flamingos to climate changes could be investigated, and population changes could be compared with proxies for *Arthrosphaera* abundance at these particular lakes over time. The nomadic nature of flamingo movements may make it difficult to determine the frequency of movement as the birds within different lakes may be interchanging. It may still be possible to distinguish between periods when flamingos are widely dispersed and periods when they are concentrated in large numbers at a particular lake. This superposition is based on observations in recent decades that a large proportion total East African lesser flamingo population has been found at Lake Bogoria during blooms of *Arthrosphaera* (Tuite, 2000). Nitrogen isotope analysis was undertaken to explore the hypothesis that large flamingo populations cause a measurable change in nitrogen isotope ratios by excreting material into the Lake that is enriched with the ^{15}N isotope.

By combining palaeolimnological data with meteorological data, past observations (e.g., Krienitz & Kotut, 2010; Kaggwa et al., 2012) and ecological models (Chapters 4 5 6), the sensitivity of the ecosystem state to fluctuations in rainfall were investigated, and the affect of changes on lesser flamingo populations were explored. Models allow different hypotheses to be investigated in a way that is not achievable by making direct observations alone.

3.2 Dating

Radioactive isotopes of elements such as lead and carbon can be used to date sediments. Radioactive decay is the process by which an unstable ‘parent’ atomic nucleus loses energy and mass by emitting a particle. This changes the properties of the remaining ‘daughter’ atomic nucleus so that it either has a different state, or becomes a different chemical element. Lead-210 (^{210}Pb) is a radioactive isotope created near the end of the decay chain of uranium-238, and was first described by Goldberg (1963). After the creation of ^{210}Pb in the atmosphere it becomes quickly incorporated in ^{210}Pb to soils and lakes, and is deposited in lake sediments. ^{210}Pb has a half life of 22.2 years (Walling et al., 2003), and after a few intermediate stages, decays into lead-206, which is stable. The abundance of ^{210}Pb at different depths in lake sediments can be measured to get a time-depth profile of the sediment. It takes about seven half lives, or 150 years before ^{210}Pb completely decays, after which point there would be no ^{210}Pb remaining in the lake sediments. The total ^{210}Pb in the sediment is the sum of the ^{210}Pb ‘supported’ which is formed within the sediment, and the ^{210}Pb ‘excess’ formed in the atmosphere and washed into the sediment by rain. It is this unsupported or excess ^{210}Pb that is used to calculate the age of the sediments using one of three models, as outlined below.

The constant initial concentration (CIC) model assumes that there is a constant flux of unsupported ^{210}Pb into the sediments, but that an increase in sediment accumulation rate causes an increase in the fraction of unsupported ^{210}Pb incorporated into the sediment. The constant rate of supply (CRS) model assumes a constant flux of excess ^{210}Pb into the lake, and that higher rates of sedimentation cause a dilution of the available unsupported ^{210}Pb (Appleby, 1978). A large scale comparison the CIS and CRS models has been made for lake cores, and the CRS model was found to be more accurate when compared with markers of historical events (Blais et al., 1995). The third model is called the simple model (Krishnaswami et al., 1971), or constant flux constant sedimentation model (CF:CS). The simple model assumes a constant flux of excess ^{210}Pb into the lake, and a constant sediment accumulation rate (Robins, 1978). Erosion rates have been found to increase in Kenya since 1900 (Fleitman et al., 2007) and it is likely that there has been variation in rates of sediment accumulation rate which would make the CRS model the better choice. However, in the absence of sediment density and porosity data, it is the simple model which must be used to estimate the age of the sediments.

Another method used when dating recent sediment deposits is to measure caesium-137 (^{137}Cs) isotope activity. ^{137}Cs is a radioactive isotope formed as a by-product of nuclear fission. Nuclear weapons testing happened on a large scale from 1952, until a treaty in 1963 limited nuclear weapons testing in the atmosphere, and testing has been reduced since this time. As a result there is a peak in ^{137}Cs concentration in 1963-4, which can be detected in lake sediments. There is another small peak corresponding with the Chernobyl disaster in 1986 resulting from the explosion at the Chernobyl nuclear power plant in Ukraine.

Dating lake sediments using ^{210}Pb is common in palaeolimnological analyses. Relatively little ^{210}Pb dating has been done for East African lakes. However, some work has been done at Lake Sonachi, a small shallow soda lake near Lake Naivasha, with a surface area 0.14 km^2 and the deepest point of 4.25 m in 1993 (Verschuren et al., 1999). A 33 cm core was dated using the constant rate of supply (CRS) model. The ^{210}Pb profile can be seen in Figure 3.1. The ^{210}Pb activity fluctuates in the first $15\text{-}20\text{ cm}$ of the core and then follows an exponential decay profile. The deviations from the typical decay profile was assumed to reflect changes in the rate of sediment deposition in the lake (Verschuren et al., 1999).

Svengren (2002) dated cores from Lake Nakuru using the CRS model and estimated the accumulation rate to be 1.26 mm/year , and ^{210}Pb to be 150 Bq kg^{-1} . The top 15 cm of sediment was found to be mixed, and this was assumed to be a consequence of wave action since Lake Nakuru is very shallow. Cesium-137 was found in very low abundance in the sediment, a maximum of 0.35 Bq kg^{-1} was found at a depth of 10 cm . However, the cesium data did not follow the expected profile but fluctuated widely between $0.05\text{-}0.35\text{ Bq kg}^{-1}$ in the top 20 cm of the core (Svengren, 2002).

Stoof-Leichsenring et al. (2011) dated cores from Lake Naivasha using for ^{210}Pb (the CRS model), radon-226 and cesium-137 using the direct gamma assay method. They found that unsupported ^{210}Pb fluctuated around 164 Bq kg^{-1} from 0 to 15 cm from the surface. There was then a slow decrease in activity to a depth of 22 cm , and then a faster decrease in activity to the bottom of the core (35.4 to 37.8 cm). ^{137}Cs activity showed a clear peak between 20 to 25 cm at a maximum activity of 12 Bq kg^{-1} , and ^{210}Pb placed the year 1963 at 20 cm . The sediment accumulation rate calculated using corrected ^{210}Pb activity in the last 15 cm of the core, and the bottom of the core was dated at 1820AD (Stoof-Leichsenring et al., 2011).

3.2.1 Lake Bogoria

^{210}Pb and ^{137}Cs were both used to date the sediments from the south basin core SB1 from Lake Bogoria because this project is concerned with recent changes in the surface sediments. The south basin cores were taken from the deepest part of Lake Bogoria, which contained dark coloured, organic rich, laminated sediments. The cores also

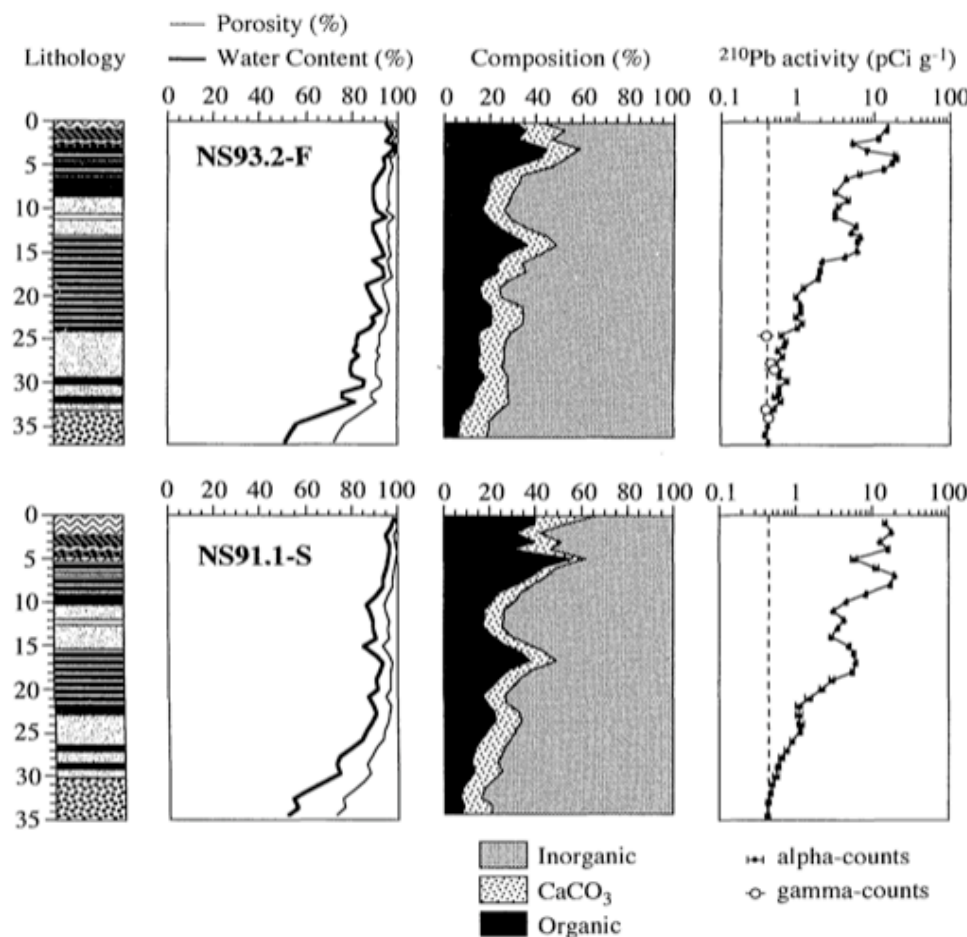


FIGURE 3.1: Lake Sonachi sediments were dated using ^{210}Pb by Verschuren et al. (1999).

smelled strongly of sulphur which indicates that these sediments likely formed in anoxic conditions. These observations suggested that the south basin cores were undisturbed, and as a result, dating of these sediments rather than of the north basin cores was more likely to be successful.

Radioisotope activity from 20 samples was measured using a Canberra well-type HPGe gamma-ray spectrometer (Murray et al., 1987). The samples had been previously freeze dried and lightly ground. The sample preparation was performed by Sarah Ward, and were run on the spectrometer under the direction of Prof. Ian Croudace at the National Oceanography Centre, University of Southampton. Low-background gamma radiation counting was used to measure the activity of ^{210}Pb and ^{137}Cs , to give two independent measures of accumulation rate. Table 3.2 shows the activity of the ^{137}Cs , ^{210}Pb and ^{226}Ra isotopes measured by the gamma ray spectrometer. The ^{210}Pb excess was calculated by subtracting the ^{226}Ra activity from the ^{210}Pb for each sample. The error associated with the activity of each isotope is increased for smaller samples, and

Depth (cm)	^{137}Cs Error	^{137}Cs Error	^{210}Pb Error	^{210}Pb Error	^{226}Ra Error	^{226}Ra Error	^{210}Pb Excess	^{210}Pb Excess error
1	0	0	289	40	48	16	241	56
3	0	0	383	53	37	19	346	72
5	0	0	331	45	36	17	295	62
7	0	0	299	39	40	17	259	56
11	0	0	246	43	70	31	176	74
13	0	0	186	30	41	15	145	45
15	0	0	84	24	0	0	84	24
17	0	0	185	27	42	13	143	40
19	0	0	134	22	49	18	85	40
22	2.9	1.1	118	18	50	13	68	31
24	2.9	1.1	139	24	44	14	95	38
26	4.8	1.3	124	21	41	17	83	38
27	4.6	1.2	118	20	57	13	61	33
27.5	8.4	2.6	95	30	0	0	95	30
29	3.9	1	87	16	41	13	46	29
32	2.7	1.1	89	19	39	15	50	34
34	1.6	0.8	54	12	33	13	21	25
36	0	0	56	14	35	11	21	25
39	0	0	81	15	43	11	38	26
50.5	0	0	60	19	37	17	23	36

TABLE 3.2: The ^{137}Cs and ^{210}Pb gamma ray spectrometer data. All isotope values and errors are measured in $Bq\ kg^{-1}$.

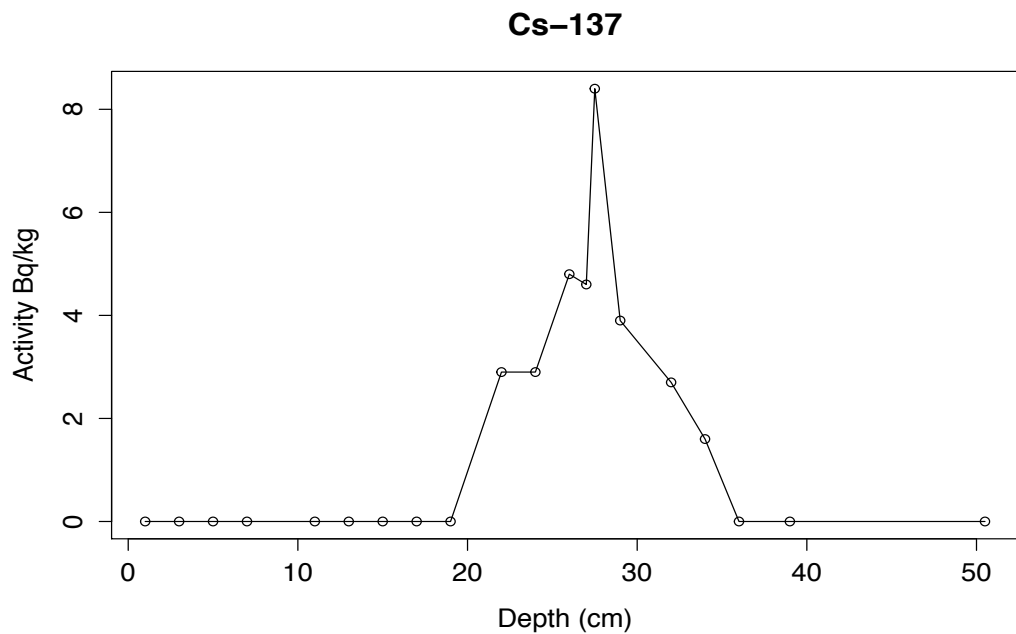
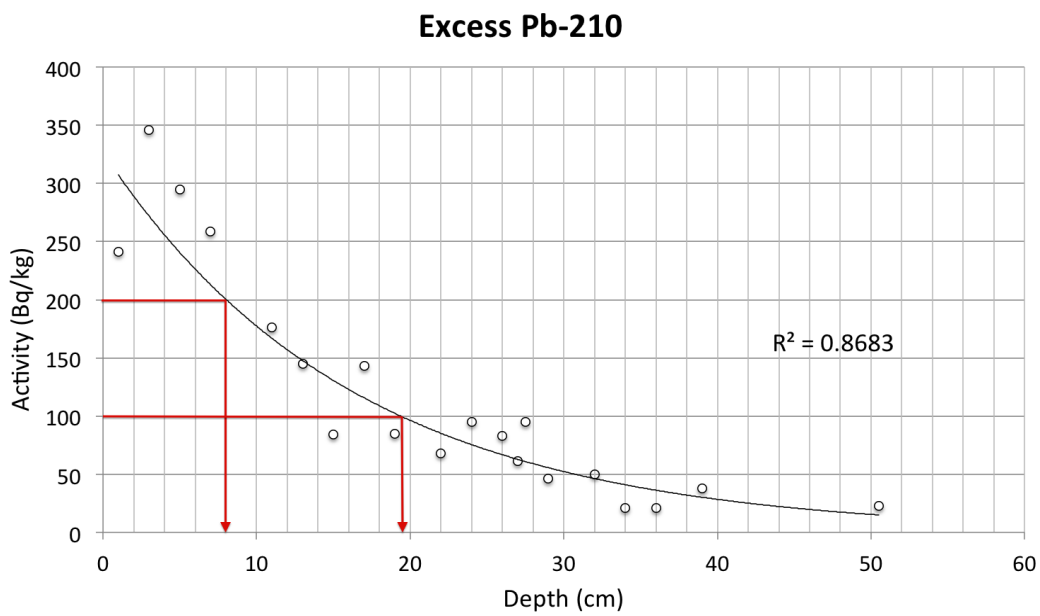
shorter count times. The count times for these samples were relatively short, at approximately 24 hours, which may account for the relatively large error in activity for some samples.

Figures 3.2 and 3.3 show the decay profiles for ^{210}Pb and ^{137}Cs . The ^{210}Pb activity shows a relatively smooth decay curve, that gives a sediment accumulation rate of $0.518\ cm\ yr^{-1}$. The accumulation rate (in $cm\ yr^{-1}$) was calculated by from the difference in depth for a halving of isotope activity and divided by the half life of ^{210}Pb in years:

$$\frac{19.5 - 8.0}{22.2} = 0.518 \quad (3.1)$$

The ^{137}Cs peak is well defined at $27.5\ cm$. This gives an an independent measure of accumulation rate of $0.561\ cm\ yr^{-1}$, in good agreement with the ^{210}Pb output. This was calculated by dividing the peak depth by the number of years between the core extrusion year and 1963:

$$\frac{27.5}{2012 - 1963} = 0.561 \quad (3.2)$$

FIGURE 3.2: ^{137}Cs output from gamma dating of Lake Bogoria sedimentsFIGURE 3.3: ^{210}Pb output from gamma dating of Lake Bogoria sediments

The error in the dates calculated using ^{210}Pb were estimated from the error in the best-fit of the decay profile. The range in the accumulation rate according to the error in the best-fit line was 0.47 cm yr^{-1} to 0.56 cm yr^{-1} . The error in the depth of the ^{137}Cs peak was estimated using the spread of ^{137}Cs activity as $\pm 3 \text{ cm}$, which gave a range in accumulation rate of 0.51 cm yr^{-1} to 0.61 cm yr^{-1} .

Because ^{210}Pb and ^{137}Cs give very similar accumulation rates this allows us to have

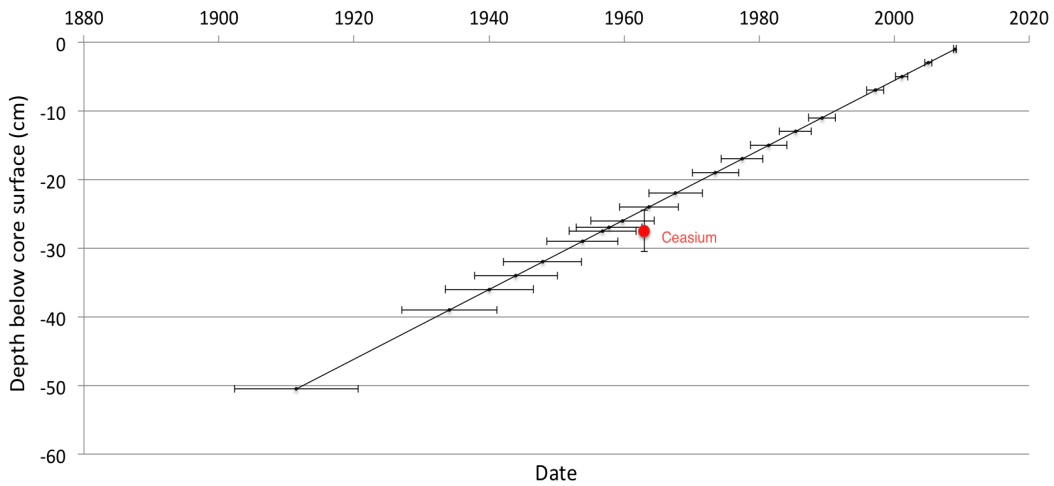


FIGURE 3.4: ^{210}Pb error calculated for the simple model from the best-fit line, and the 1963 depths suggested from the ^{137}Cs activity.

Accumulation rate (cm yr $^{-1}$)	R^2
0.67	0.30
0.65	0.39
0.63	0.52
0.61	0.55
0.60	0.71
0.59*	0.74
0.58	0.64
0.57	0.58
0.56	0.57
0.54	0.42
0.53	0.45

TABLE 3.3: The R^2 values output for comparisons of organic matter content between cores SB1 and G1 for different accumulation rates in the north basin. *When the north basin core was dated according to an accumulation rate of 0.59 cm yr^{-1} , the north and south basin organic matter contents gave the best correlation, with an R^2 value of 0.74. The organic matter profiles can be seen in Figure 3.5 for a north basin accumulation rate of 0.59 cm yr^{-1} .

confidence in the results. By taking the average accumulation rate (0.54 cm yr^{-1}) the deepest sample in this south basin core (SB1) was dated at ca.1872.

To date the north basin core (G1), the organic matter profiles of cores SB1 and G1 were compared. To do this, core G1 age data was estimated for a range of different accumulation rates (see Table 3.3), and the organic matter abundance (found by Loss On Ignition analysis, see section 3.3) of the cores were compared at 27 different years for each accumulation rate. The similarity of these abundances were plotted against each other and the R^2 values calculated to find the accumulation rate that gave the most similar changes in organic matter abundance. It can be seen in Table 3.3 that an accumulation rate of 0.59 cm yr^{-1} produced the most similar output, with an R^2

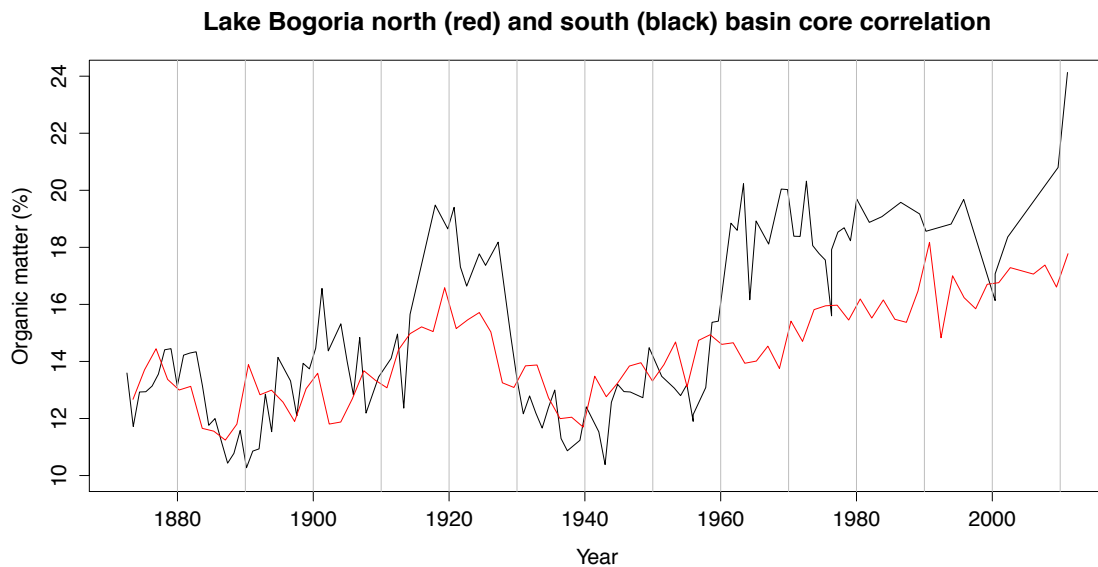


FIGURE 3.5: The organic matter profiles of the north and south basins of Lake Bogoria, where the south basin accumulation rate is 0.54 cm yr^{-1} , and the north basin accumulation rate is 0.59 cm yr^{-1} .

value of 0.74. The R^2 value for the same accumulation rate as the south basin (0.54) is low, at only 0.42. The organic matter profiles can be seen in Figure 3.5, and on visual inspection the organic matter profiles appear to be similar, particularly before 1960, after which the fluctuations in the north basin organic matter abundance (core G1) are less pronounced compared with the south basin organic matter profile. The north basin therefore has a slightly higher accumulation rate (0.05 cm yr^{-1} more) than the south basin. This is not unlikely, since Lake Bogoria is a long narrow lake made up of three distinct basins (see Figures 1.4 and 2.1). The difference in accumulation rate is likely to be a result of the Wasegus river inflow into the north basin of Lake Bogoria, which brings in large volumes of eroded material from the catchment (pers. obs.).

3.2.2 Lake Olloidien

The Lake Olloidien sediments were dated by comparing the organic matter profile (found by Loss On Ignition analysis, see section 3.3) with the Verschuren et al. (1999) core data seen in Figure 3.6. Due to the distinctive shape of the organic matter profile, it was straight forward to date the bottom of the 49 cm long Lake Olloidien core at ca.1860. The average accumulation rate was 0.44 cm yr^{-1} , apart from between years 1870 and 1940, where the average accumulation rate was much lower at 0.22 cm yr^{-1} . The organic matter profile can be seen in Figure 3.10.

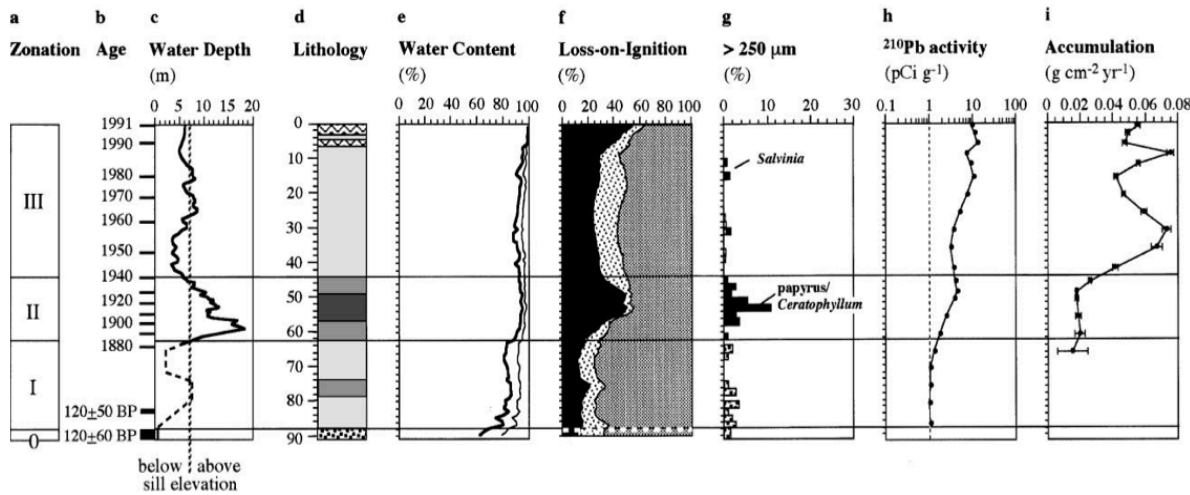


FIGURE 3.6: Lake Oloidien core data by Verschuren et al. (1999).

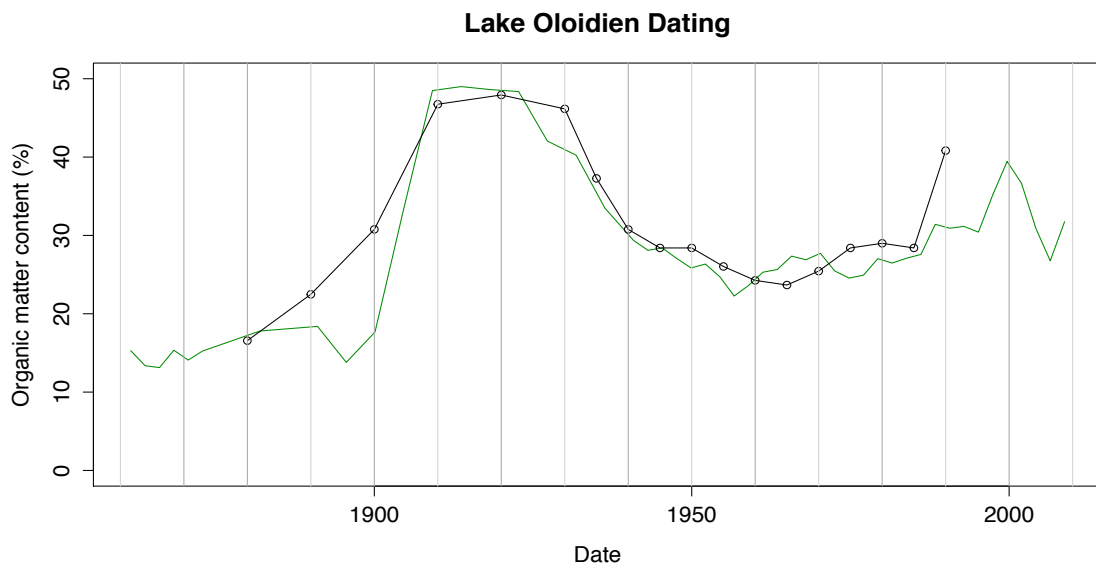


FIGURE 3.7: Lake Oloidien core G7 organic matter content (green) compared against organic matter content from Lake Oloidien (black) recorded by Verschuren et al. (1999).

3.2.3 Lake Elmentaita

The Lake Elmentaita core was not dated, and so other ways to compare the Lake Elmentaita core with the Lake Oloidien and Lake Bogoria cores had to be considered. These lakes experience different phytoplankton communities at different times due to their different bathymetry and salt concentrations. It is unlikely that organic matter content will be much use for a comparison. However, rainfall changes the same way across the region, and so the changes in elemental data are more likely to yield similarities since some elements tend to concentrate during lower lake water levels, whilst others increase

during higher rainfall as weathered rock is inwashed into the lake. The rate of weathering in the catchment should therefore be similar across all lakes in the region and so the Rb:Sr ratio can be compared. Since lake water depth changes occur across all lakes at the same time in response to rainfall changes (albeit at different rates), the Fe/Mn ratio was also be compared, but it should be noted that this ratio is less useful than the Rb:Sr ratio, since each lake has a different bathymetry and average depth.

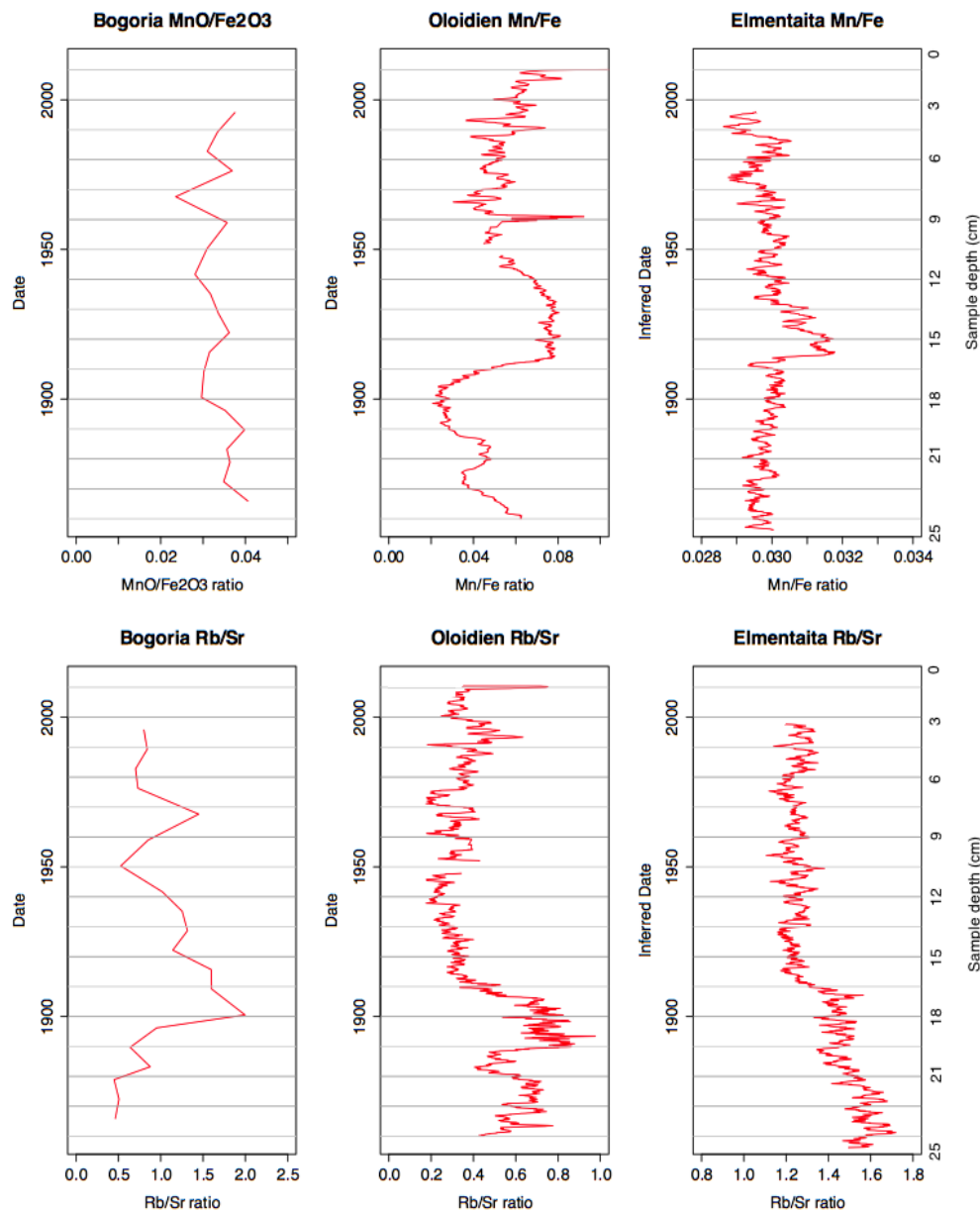


FIGURE 3.8: The Mn:Fe and Rb:Sr ratios for Lakes Bogoria, Oloidien and Elmentaita.

Figure 3.8 shows the Mn:Fe and Rb:Sr ratios for Lakes Bogoria, Oloidien and Elmentaita. It is not as easy to compare the bulk XRF data for Lake Bogoria with the ITRAX data for Lakes Oloidien and Elmentaita because the Lake Bogoria is very low resolution in

comparison. Also, the bulk XRF data does not have Mn and Fe data, so MnO/Fe_2O_3 was used. When compared to Lake Oloidien and Lake Elmentaita Mn:Fe ratios the MnO/Fe_2O_3 showed similar fluctuations (see Figure 3.8) and so was considered representative of the Mn:Fe ratio. This is based on the assumption that all of these lakes experienced similar changes in Mn:Fe ratio in response to changing environmental conditions, i.e. that lake water level reduces across all lakes at the same time (see Section 4.2.2), causing an increased oxygenation of the sediment.

The changes at the very top of the Elmentaita and Oloidien cores can be ignored. The Mn:Fe ratio changes for the Lake Oloidien and Elmentaita cores both had distinct changes that aligned for both ratios when if 25 cm at the Lake Elmentaita core was dated at 1856, including increased Mn:Fe ratios between 1915 and 1930, the increase in Rb:Sr ratio from 1906 to 1915 and low Rb:Sr ratios at 1990. The changes in ratios for lake Oloidien are more extreme, which may be a consequence of Lake Oloidien periodically joining and separating from fresher Lake Naivasha.

If this is correct, then the accumulation rate at Lake Elmentaita would be 0.264 cm yr^{-1} . The rest of the data following are presented with dates according to this estimate, but it must be emphasised that there has not been any follow up to confirm these dates.

These age models were applied to the cores and so all subsequent graphs of the Lakes Borgia, Oloidien and Elmentaita data show changes against time rather than depth.

3.3 LOI and TOC:TN

Loss on Ignition (LOI) is a well established method used for measuring the relative proportions of organic matter and carbonate contained in lake sediments (Dean, 1974). This is used as a proxy of overall lake productivity. The organic matter content is determined by weighing the samples before and after a 550°C ‘burn’. When the sediment is heated to 550°C , the organic material is oxidised to carbon dioxide and ash. In a second burn at 950°C , the carbonate in the sample is released as carbon dioxide, and the samples are then weighed again to determine the mass lost (Dean, 1974; Bengtsson & Enell, 1986).

The ratios of total organic carbon to nitrogen (TOC/N) in sediments can provide information about the origin of the organic matter it contains. The TOC/N ratios of terrestrial plants are ≥ 20 , and the TOC/N ratios of algae range between 4 and 10 (Meyers, 1994). Higher ratios TOC/N ratios in the lake sediments would therefore indicate that a higher proportion of the organic matter was washed in from littoral areas or rivers, and lower ratios would suggest that more of the organic matter was produced from within the lake. Burian (2010) measured TOC/N ratio of plankton at Lake Nakuru in April 2009 to be as low as 4.5-5.5; this measurement was made after 4 years of below

average rainfall when Lake Nakuru was unlikely to have received much organic carbon from the catchment in runoff or river inflow.

The total organic carbon and nitrogen can be measured using the ‘dry combustion’ or ‘suspension’ methods. Dry combustion is the established way to calculate TOC/N. However, the suspension method has also been developed and has been found to produce good results for homogenised material (Donald et al., 1973). The organic C/N ratio for the sediment samples was measured at the University of Southampton using the suspension method. This was achieved using freeze-dried samples that were finely ground ($<130\ \mu\text{m}$) and homogenised using a pestle and mortar. 30 mg of sample was then weighed into a vial and 30 ml of 0.22 M hydrochloric acid was added. The samples were run using an Analytik Jena 3100 Carbon Nitrogen Analyser, which purges the samples of inorganic material by adding an additional measure of 2 M hydrochloric acid before the analysis of the suspension using catalytic high temperature oxidation. Liquid blanks and standards were run to check the calibration.

The TOC/N ratio is used to identify the source of organic content of a the sediment, or the relative proportions of plant material from outside the lake to algal matter produced within it (Meyers & Ishiwatari, 1993). Low ratios are associated with productive, algae dominated lakes, and higher ratios are associated with a higher proportion of inwashed organic material since land plants contain more cellulose and thus higher carbon content and have TOC/N ratios of 20 and above.

All sample preparation and analysis for LOI and TOC/N for each core was undertaken by Sarah Ward, at the University of Southampton.

3.3.1 Lake Bogoria

Lake Bogoria is a very productive lake, usually containing high densities of *Arthrosphaera* as well as other cyanobacteria and green algae. There are no aquatic plants, and so most of the organic matter in Lake Bogoria sediments is from decomposing phytoplankton. The other major source of organic matter is from flamingo guano.

The organic matter profiles of the Lake Bogoria north basin core was generated using 81 samples from core G1, and 59 samples for south basin core SB1. The organic matter, carbonate content and TOC/N ratio for core G1 can be seen in Figure 3.9, and the organic matter content of the north and south basin cores can be seen in Figure 3.5, and the data can be seen in Tables 1 and 2 of the appendix. The north basin organic content fluctuates between 11% and 18% of the dry sample mass. The mean organic content of the samples is 14.37%. There is an increase in organic matter content between 1910 and 1925, and a relatively steady increase in organic content from 12% in 1840 to 17.5% in 2011.

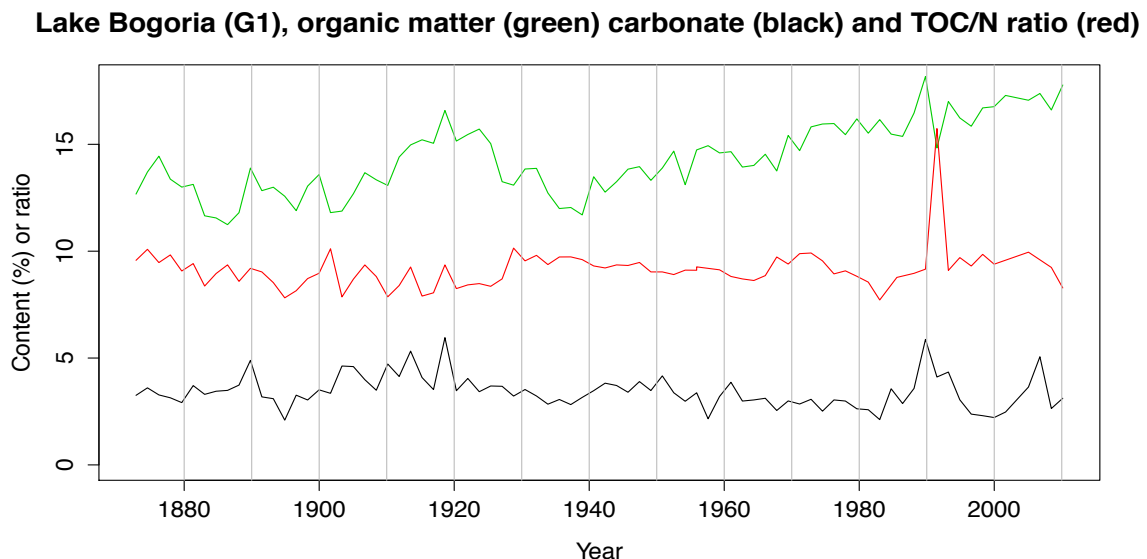


FIGURE 3.9: Lake Bogoria percent organic matter content (green), percent carbonate content (black), and TOC/N ratio (red) for core G1.

Carbonate content is fairly stable, with small deviations from an average of 3.5%. The most notable change is the increase to 5% between 1988 and 1992. The TOC/N ratio graph shows that the ratio for core G1 is predominantly low (8-10). There is a peak in 1991-1992, which corresponds with a drop in organic matter content. This occurred during a year of very low rainfall (see Figure 1.1) and suggests that Lake Bogoria contained a higher concentration of carbonates and low concentration of cyanobacteria, possibly a result of reduced lake water level.

3.3.2 Lake Olloidien

There are large fluctuations in the total organic matter content of the sediment at Lake Olloidien (see Figure 3.10, and the data in Table 10 of the appendix), the largest change is a dramatic increase in organic matter content reaching almost 50% between 1890 and 1900. This organic matter increase is attributed by Verschuren et al. (1999) to a decrease in the inwash of sediment from the catchment due to papyrus stands growing around the lake. The wet conditions allowed for this swamp to develop, causing sediment carried by runoff to deposit before reaching the lake, and so proportionally the amount of organic matter deposited increased during this time (graph *f* of Figure 3.6). Our own data shows the same organic matter profile (see the second graph of Figure 3.21), and also found an increase in organic carbon-nitrogen ratio during the peak in organic matter, suggesting that some organic matter was in-washed from the catchment due to high rainfall. Section *c* of Figure 3.6 shows the water depth in Lake Olloidien, and three occasions since 1980 where the water level has been high enough to overtop the sill separating Lake Olloidien from Lake Naivasha. The first was between 1880 and 1940, the

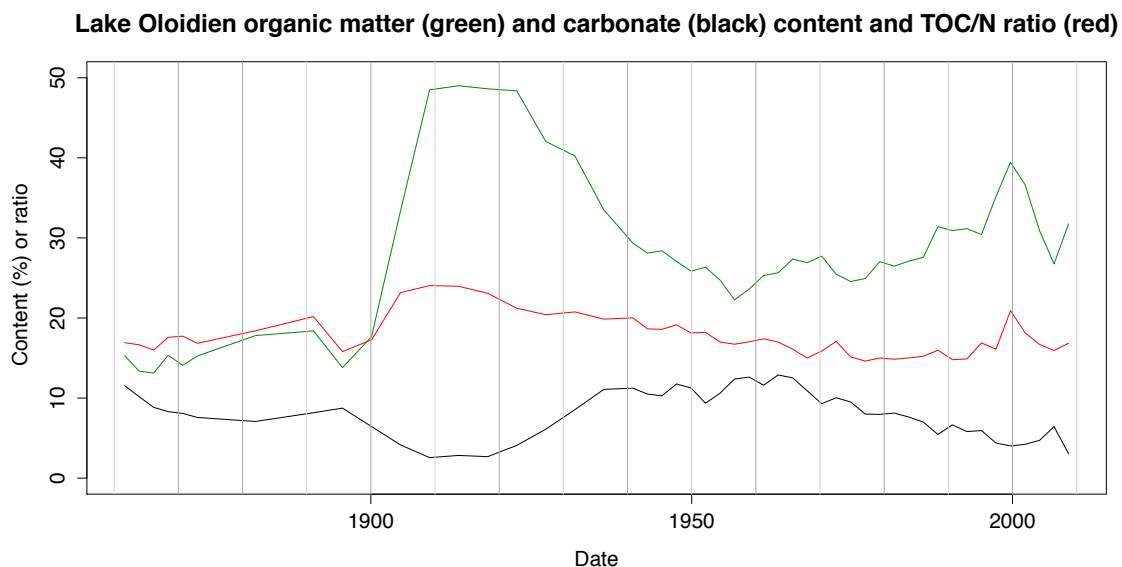


FIGURE 3.10: Lake Oloidien percent organic matter content (green), percent carbonate content (black), and TOC/N ratio (red).

second in the late 1960s, and the third around 1980 (Verschuren et al., 1999). During these events Lake Oloidien would have become much fresher. This is supported by an investigation into the diatom species composition by M. Leeson, a dissertation student at the University of Southampton who used core material from this project (unpublished, 2012). In Figure 3.11 the diatoms are grouped into fresh, fresh-saline and saline types. The diatom community during the organic matter peak (1880-1940) is dominated by *Aulacoseira ambigua*, a freshwater diatom, whereas before the 1880 peak from 40 to 45 cm (1865 to 1880) and in the samples that were studied above 25cm *Navicula elcab*, a saline diatom, were dominant. The oldest sediments below 45 cm (before 1865) contained more fresh-saline and fresh diatoms.

The lower carbonate levels suggest deeper lake water levels, which can be seen from the Verschuren data (Verschuren et al., 1999). Organic carbon-nitrogen ratio decreases as organic matter increases from 1935 towards the surface until 1990, which indicates that the increase in organic matter is due to increased productivity within the Lake Oloidien overall. There is another increase in organic matter content that coincides with an increase in organic carbon-nitrogen ratio at 1998 which is likely to be a smaller in-wash event.

3.3.3 Lake Elmentaita

The organic matter and TOC/N ratio can be seen in Figure 3.12, and the data can be seen in Table 15 of the appendix. The organic matter content varies between 7 and 15%, increasing from 7-8% between 1856 and 1910, to 9-10% from 1915 to 1965, and then

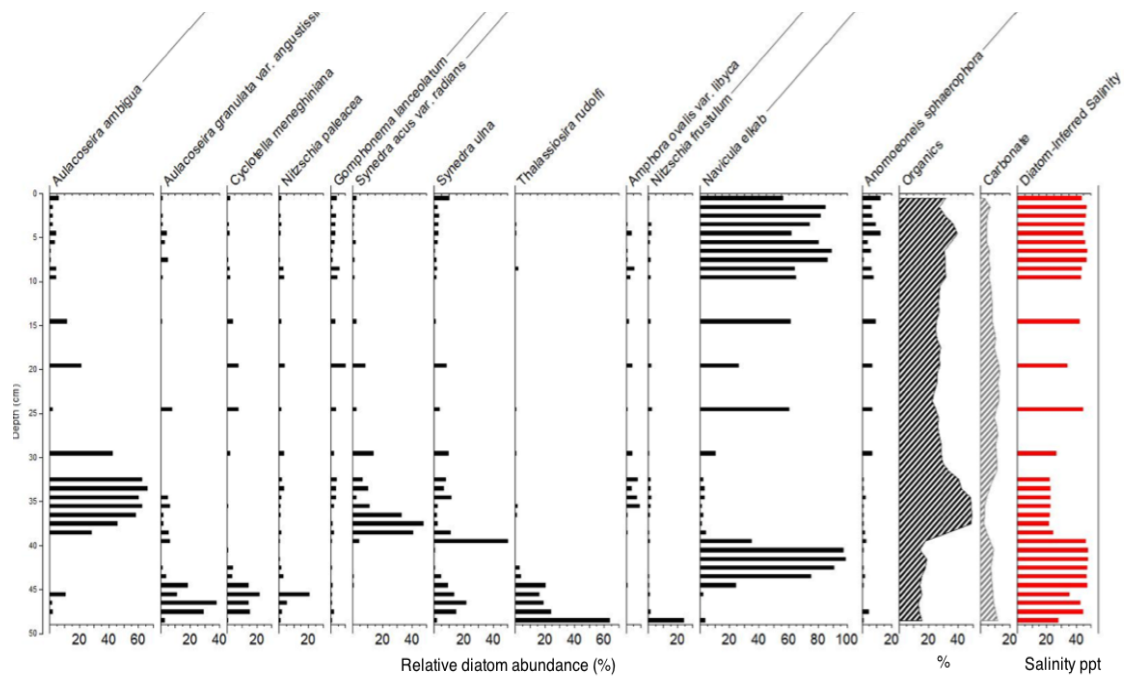


FIGURE 3.11: Lake Olloidien diatom analysis undertaken by M Leeson (unpublished, 2012) on the Lake Olloidien core. The y axis shows the core depth from 0 to 50 cm .

increases from 12% -15% from 1970 to 2011. The organic carbon-nitrogen ratio varies from 7-10 which is typical for algae dominated lakes.

The organic carbon-nitrogen ratio divides the core at 1940 between a state with higher TOC/N ratio to lower TOC/N ratio. This drop in TOC/N ratio as organic matter increases suggests that there has been an increase in lake productivity over time rather than the increase of inwashed material.

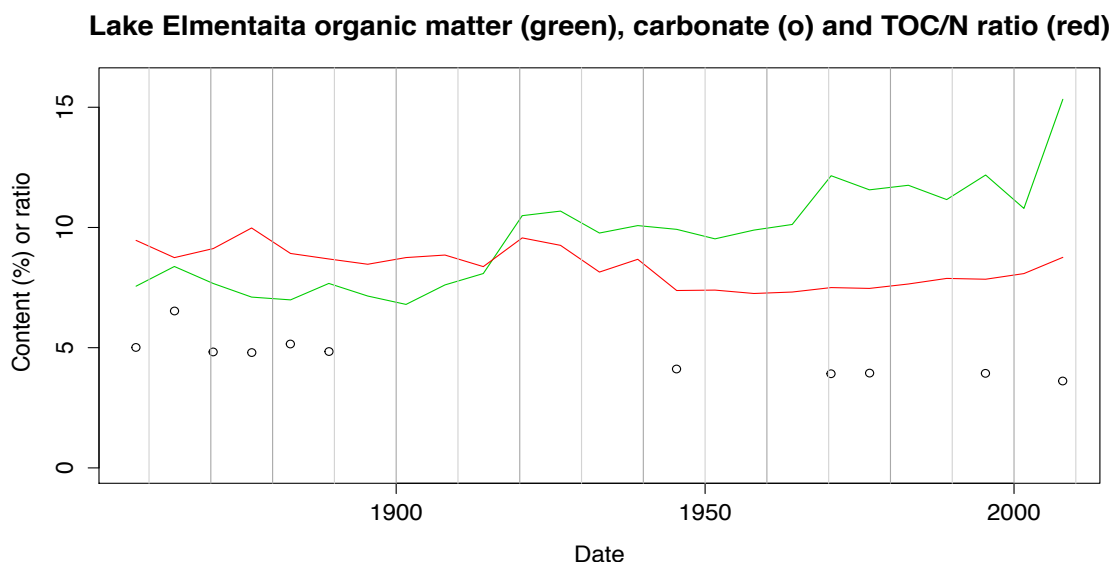


FIGURE 3.12: Lake Elmentaita percent organic matter content (green), percent carbonate content (black), and TOC/N ratio (red).

3.4 Pigments

Chlorophyll and carotenoid pigments found in lake sediments are the bio-chemical remains of plants and animals. Pigments are substances which selectively absorb and reflect light of particular wavelengths. Plants, for example, contain the pigment chlorophyll, and appear green because chlorophyll absorbs yellow and blue light, and reflects green light back to the observer. Carotenoids are another type of pigment also found in plants, and include lycopene, carotene, and lutein which reflect red, orange, or yellow light respectively.

When plant and animal remains are laid down in lake sediments, they often decay, leaving only bio-chemical fossils such as pigments and their derivatives (McGowan, 2007). These fossil pigments can be identified from lake sediments and used to estimate past lake productivity. They are associated with particular taxa, and can even be species specific; scytonemin for example, is a photo-protective pigment which is absorbs ultraviolet radiation that would otherwise damage cyanobacteria (Proteau et al., 1993). Taxon-specific fossil pigments can therefore be used to reconstruct past phytoplankton community structure as well as abundance (Zullig, 1981; Yacobi et al., 1990).

β -carotene (Leavitt et al., 1989, 1994), chlorophyll-a (Carpenter et al., 1986), and pheophytin-a pigments are relatively ubiquitous and are generally used as indicators of total lake productivity (Leavitt & Hodgson, 2001). Verschuren et al. (1999) used β -carotene to reconstruct total algal abundance for Lake Sonachi, a small soda lake in Kenya.

The taxon-specific pigments alloxanthin, diatoxanthin, myxoxanthophyll, lutein- zeaxanthin and chlorophyll-b are associated with cryptophytes, diatoms, filamentous cyanobacteria, green algae and cyanobacteria, and green algae respectively. Verschuren et al. (1999) identified the relative abundance of these taxon-specific pigments though the lake sediment record of Lake Sonachi, and used them to reconstruct the phytoplankton community structure. Hertzberg and Liaaen-Jensen (1966) found *Arthrosphaera* carotenes to be 46% myxoxanthophyll, 27% β -carotene, 15% zeaxanthin, and 3% echinenone. The myxoxanthophyll pigments are likely to be the best proxy for *Arthrosphaera*. Myxoxanthophyll was used as a proxy for 'filamentous cyanobacteria' by Verschuren et al. (1999).

Apart from being used to identify different taxa, the derivatives of chlorophyll and carotenoids can be used to investigate the characteristics of the lake sediments and water column through time. Grazing (Daley, 1973), oxygen availability, mixing regime, and light intensity all affect the way that pigments are transformed into their derivatives (Leavitt & Hodgson, 2001). Because of this, changes in the derivatives of these pigments throughout a sediment record can provide an indication of changes in physical lake conditions as well as the lake biota (Koopmans et al., 1996).

Liquid chromatography (HPLC) analysis is an established pigment analysis technique that has been used in the study of many lake ecosystems. It is one of the most rapid and accurate methods available for pigment analysis (McGowan, 2007). There are errors encountered using pigment analysis, as with other sediment proxies, where there is differential preservation of pigments (Leavitt & Hodgson, 2001). However, studies have found fossil pigments to be effective records of change in phytoplankton community structure (Vinebrooke et al., 1998).

Pigment analysis was used to gain more insight into what biota had produced the organic matter in the sediments, to find out what was growing in Lakes Bogoria, Oloidien and Elmentaita at the time each layer of sediment was deposited. The samples used for pigment analysis were freeze dried, ground and stored in a freezer to minimise pigment degradation. The pigment sample preparation and analysis was undertaken at the University of Nottingham by Sarah Ward under the instruction of Dr Suzanne McGowen, using High performance liquid chromatography (HPLC) using the Chen method (Chen et al., 2001). The pigments are first extracted from the samples using solvents, before being dried down and then mixed with a measured quantity of injection solvent which can then be run through the HPLC unit. The pigments are separated out by the HPLC unit which outputs a chromatogram report for each sample. The report contains data on peak retention times that are associated with different pigments and calibrated against a 'green standard'. The peak area is a measure of the amount of the pigment found in the sample. Each peak has an associated spectral signal which is used to identify specific pigments. Pigments that are degraded can appear less well defined

Pigment	Affinity (Leavitt & Hodgson, 2001)	Details
Chlorophyll-a	Plantae, Algae	Land and aquatic plants, Green algae i.e chlorophytes
Pheophytin-a	Chl-a derivative	
Chlorophyll-b	Plantae, Chlorophyta, Euglenophyta	Land and aquatic plants, Green algae, Unicellular green algae
Pheophytin-b	Chl-b derivative	
Alloxanthin	Cryptophyta	Cryptophytes -brown, red, or blue-green algae
Zeaxanthin	Cyanobacteria	
β -carotene	Plantae Algae	Land and aquatic plants, Green algae
Echinenone	Cyanobacteria	
Diatoxanthin	Bacillariophyta, Dinophyta, Crysophyta	Diatoms, Dinoflagellata -red-brown algae, golden-brown algae
Fucoxanthin	Dinophyta, Bacillariophyta, Crysophyta	Dinoflagellata -red-brown algae, Diatoms, Golden-brown algae
Canthaxanthin	Colonial cyanobacteria, Herbivore tissues	
Myxoxanthophyll	Colonial cyanobacteria	<i>Arthospira</i> (Hertzber and Liaaen-Jensen, 1966)
Oscillaxanthin	colonial cyanobacteria	Oscillatoriaceae
Aphanizophyll	N_2 -fixing cyanobacteria	Nostocales

TABLE 3.4: Pigments found in Lakes Bogoria, Olloidien and Elmentaita sediments.

or ‘fuzzy’, whilst some pigments break down into well known derivatives that can be easily identified (McGowen, pers. com.).

The pigments found in the soda lake sediments are summarised in Table 3.4.

3.4.1 Lake Bogoria

Pigment analysis of both the north (G1) and south (SB2) basin cores from Lake Bogoria was undertaken to explore the similarities and differences between these basins. The pigment data for the north basin can be seen in Figure 3.13, and in Tables 3, 4, 5 and 6 in the appendix. It is very likely that similar changes in lake water level occurred at Lake Bogoria and Lake Olloidien, although these changes are likely to be less extreme at Lake Bogoria because of its lower surface area to volume ratio. The leftmost graph in Figure 3.13 shows the depth at Lake Olloidien (Verschuren et al., 1999) for comparison with pigment changes. The most abundant pigment is aphanizophyll, a cyanobacteria pigment.

Aphanizophyll has a similar profile to zeaxanthin, myxoxanthophyll, echinenone and canthaxanthin which are also cyanobacteria pigments. Pheophytin-b is the second most abundant pigment, and has a similar profile to pheophytin-a, chlorophyll-a, chlorophyll-b, diatoxanthin and alloxanthin. Pheophytin-b is a breakdown product of chlorophyll-b, and so these pigments are both associated with plants and green algae. Diatoxanthin is associated with diatoms and is indicative of fresher conditions and a deeper lake water level in these hyper saline lakes. Alloxanthin is associated with cryptomonads (algae). Pheophytin-a is a breakdown product of chlorophyll-a, which is often a ubiquitous pigment, but is associated with other green algae pigments rather than the cyanobacteria pigments at Lake Bogoria. Therefore the pigments fall into two distinct groups, the cyanobacterial pigments, likely to indicate more saline conditions at Lake Bogoria, and the algae and diatom group, which indicate fresher water conditions.

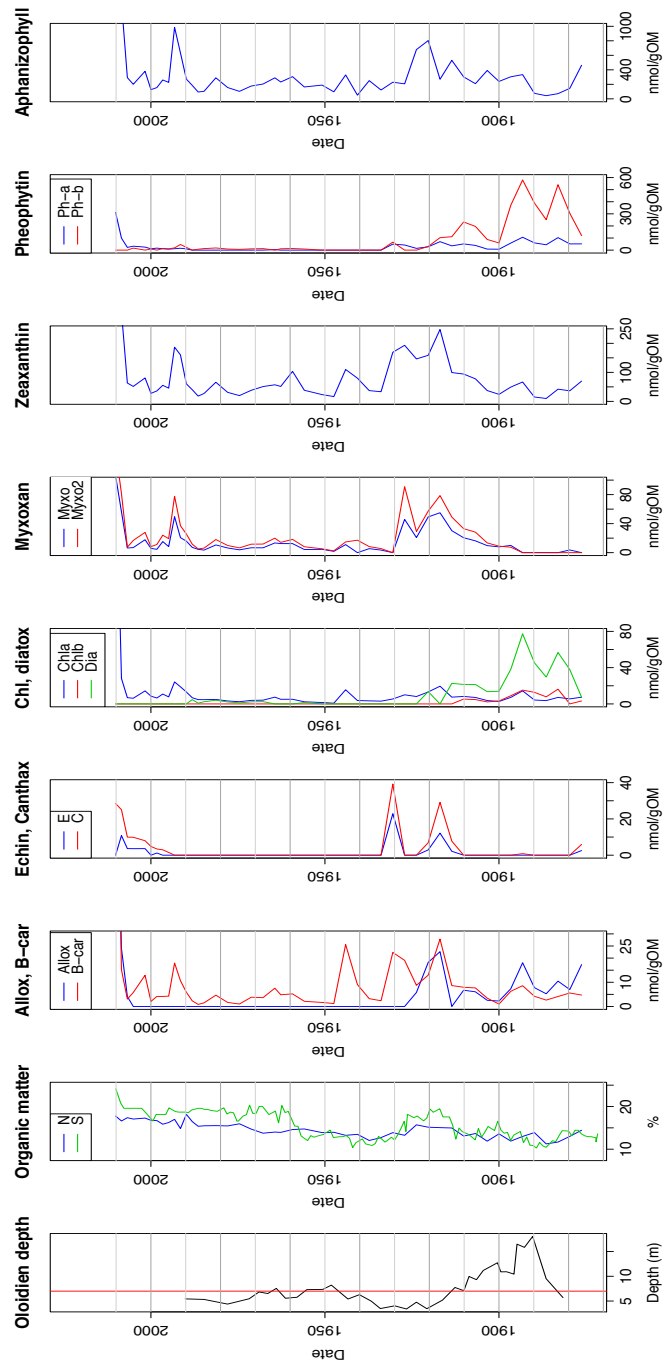


FIGURE 3.13: Lake Bogoria north basin (core G1) organic and pigment data. Pigment data are expressed in nanomoles per gram of organic matter ($\text{nmol g}^{-1}\text{OM}$). Oloidien lake depth (Verschuren et al., 1999) is for comparison.

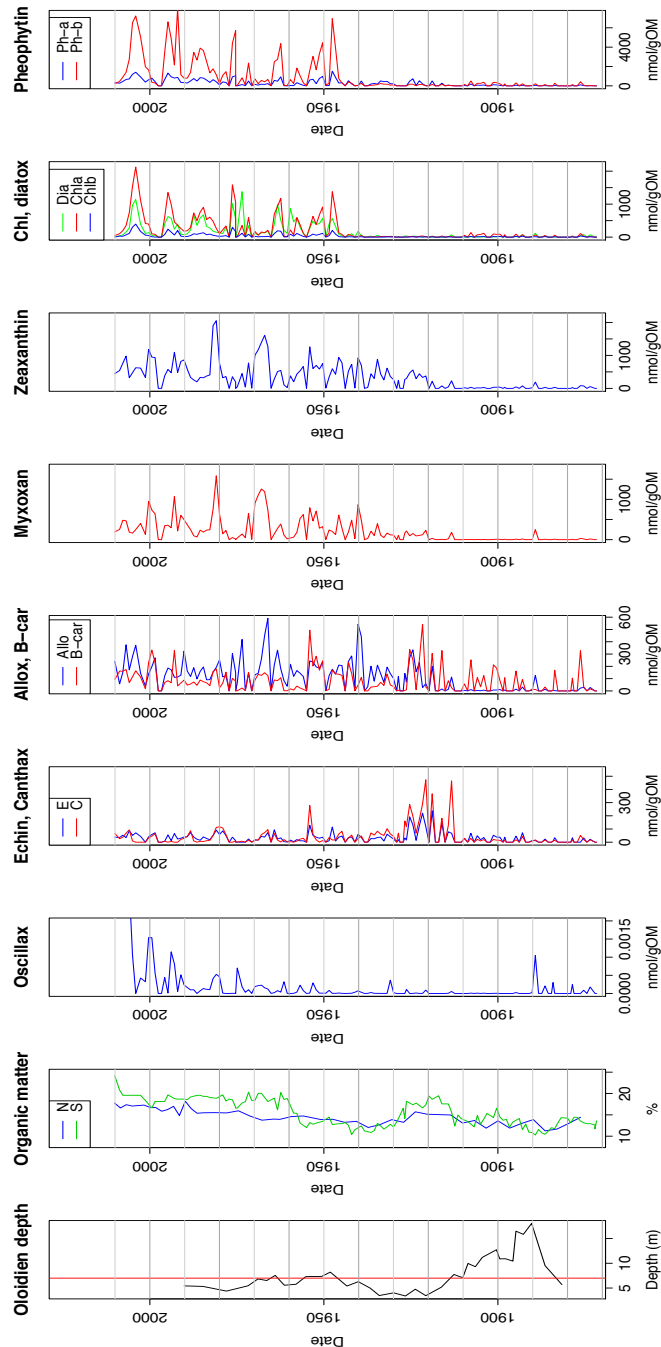


FIGURE 3.14: Dated Lake Bogoria south basin (core SB2) organic and pigment data. Pigment data are expressed in nanomoles per gram of organic matter ($\text{nmol g}^{-1} \text{OM}$). Oloidien lake depth (Verschuren et al., 1999) is for comparison.

The pigment data for the south basin can be seen in Figure 3.14. The south basin pigments also fall into two distinct groups which show similar profiles for the algal and diatom pigments, and the cyanobacteria pigments. There are many differences between the profiles for the north and south basin pigments, firstly the pigments in the south basin when they are preserved are approximately an order of magnitude greater in abundance. Aphanizophyll, the most abundant pigment in the north basin is not found in the south basin, whilst oscillaxanthin is found in the south basin in very low abundance but is not found in the north basin sediment. Most pigments in the south basin sediments older than 1910 either could not be found or were only present in very low abundances. Since chlorophyll-a and chlorophyll-b are relatively susceptible to degradation compared to other pigments (Leavitt & Hodgson, 2001) the reduced pigment concentration may be a result of degradation. Deeper lake water levels can also cause a reduction in pigment concentrations, which may contribute to the reduced pigment concentration in the south basin between 1890 and 1910. However, the chlorophyll pigments are in much lower abundances before 1940 in the south basin which also includes a period of low lake water level. This suggests that degradation is more likely to be the cause of the reduced pigment concentration in the south basin. The south basin is deeper than the north basin, which may explain why pigments in the north basin are preserved, whereas in the deeper south basin lake water levels have to reduce for at least a further 10 years before pigments begin to be preserved.

There are differences between the north and south basins that must account for the differences in pigment records. The north basin is sometimes fresher than the south basin because of the inflow of the Wasegus river, which brings in large amounts of silt during the wet season. The fresher conditions in the north basin may allow for different phytoplankton communities to grow in the north and south basins, and higher abundances of cyanobacteria are likely to occur in the south basin as a result. This is reflected in the higher organic matter content of the south basin sediment, which is 5% higher throughout much of the core, although the proportionally lower organic content of the north basin may also be due to the large amount of silt brought in by the Wasegus river into the north basin. The south basin is 5m deeper than the north basin at its deepest point, and conditions were found to be anoxic at the time of core collection rather than oxygenated as in the north basin. The south basin sediments had experienced no mixing since fine laminations could be seen which were not present in the north basin sediment. There is severe degradation of pigments in the south basin before 1910. Between 1895 and 1910 this degradation may be related to a deeper lake water level, since pigment degradation occurs in the water column as the organic material sinks to the lake bed. At low lake water levels resuspension of surface sediments may cause pigment degradation. However, this is not reflected in the north basin pigments which should be more exposed during the 1920-1930. Pigments degrade more quickly in oxygenated environments which is likely to explain the difference in abundance between the north and south basins. The lack of pigments in the south basin prior to 1910

cannot be attributed to reduced pigment production during the time because the organic matter profile shows the lake to be productive with between 10 and 16% organic matter content.

An ordination is undertaken to identify similarities and differences between samples. Detrended Correspondance Analysis (DCA) (Hill & Gauch, 1980), is typically used where environmental gradients vary significantly, in the case of these lakes there is significant variation in the concentration of salts from almost fresh to hypersaline. DCA is a well established technique (e.g. Khedr & El-Dermerdash, 1997; Ejrnaes, 2000; Wang et al., 2012) that uses an algorithm that involves the ‘reciprocal averaging’ (Hill, 1973) of sample values, to identify the largest correspondence between the rows and columns of the sample data. DCA is useful where there is no environmental data to compare these samples against, and allows the samples and pigments to be viewed together in the same plot so that the importance of pigments to each sample can be seen, as well as to identify which pigments vary together, and which occur more independently from each other. A DCA plot was made for the north basin pigments, and can be seen in Figure 3.15.

The pigments are grouped in the DCA plot (Figure 3.15) with the first group of pigments; chlorophyll-a, zeaxanthin, β -carotene and aphanizophyll grouped closely together with the majority of the sediment samples. The myxoxanthophyll pigments lie together within the same values on Axis 2 as the first group of pigments but lower values on Axis 2 which separates them out. A visual inspection of the pigment abundances in Figure 3.13 shows that these pigments vary together with sample depth. These pigments represent the cyanobacteria component of the phytoplankton community.

Canthaxanthin and echinenone have Axis 1 values that lie between the myxoxanthophyll pigments and the first group of pigments but has much higher Axis 2 values. The canthaxanthin and echinenone pigments appear at low levels in the same samples with the peak abundances of zeaxanthin, β -carotene and myxoxanthophyll between 1910 and 1935. Canthaxanthin is a very stable pigment that is associated with colonial cyanobacteria and herbivore tissues (Leavitt & Hodgson, 2001), which could indicate the presence of large flamingo populations.

Alloxanthin, chlorophyll-a2 (a chlorophyll degradation product) and pheophytin a have a similar Axis 1 value but are spread out along Axis 2. Alloxanthin is typically associated with a type of algae known as cryptomonads which have been found to be more dominant during crashes or smaller drops in the abundance of *Arthrosira* at lakes Nakuru and Bogoria (Kaggwa et al., 2012). When comparing the alloxanthin and myxoxanthophyll pigment profiles (Figure 3.13) it can be seen that there is a higher abundance of alloxanthin between 1975 to 1900 where there is coincidentally the least myxoxanthophyll in the core, when lake water levels are higher. There is also a peak in both pigments at 1917 which does not support the idea of an inverse relationship, although it is possible

that *Arthospira* was at high densities during this intermediate lake water level period and the extremely high rainfall in 1917 may have caused a freshening of the north basin at the mouth of the Wasegus river which allowed freshwater phytoplankton species to grow alongside *Arthospira*. This situation was observed in the July 2012 field trip after a period of very high rainfall (see Chapter 2).

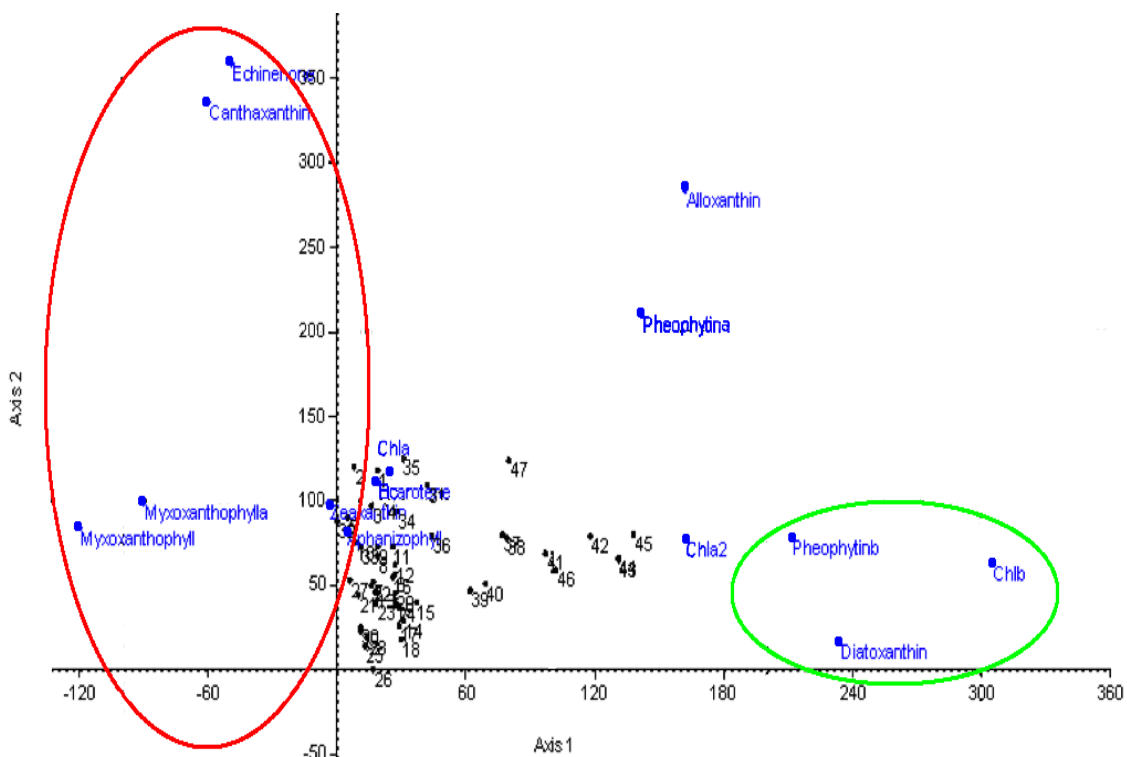


FIGURE 3.15: Lake Bogoria north basin DCA. The cyanobacteria pigments (echinenone, canthaxanthin, myxoxanthophyll) are highlighted in red, and the diatom and plant pigments are highlighted in green (pheophytin b, chlorophyll b and diatoxanthin). The other pigments are associated with green algae.

The variation in pigment composition has been reduced by the DCA to two variables and plotted against sample depth in Figure 3.16. The axes are most likely to represent green algae (Axis 1) and cyanobacteria (Axis 2). The Axis 1 profile has a striking similarity to the profile of Lake Oloidien water level between 1875 and 1920, with the higher Axis scores occurring when Lake Bogoria is fresher. Axis 2 (cyanobacteria) is generally dominant after 1910, when lake water levels are significantly lower. This supports the hypothesis that the ecosystems of the soda lakes can exist in different states during fresher and more saline periods which are more or less suited to flamingo populations. These results show that even Lake Bogoria, the most stable soda lake, has undergone fresher periods that allow increased competition between cyanobacteria and green algae, which may have reduced its reliability as a feeding lake for lesser flamingos.

To help understand the pigment data it is useful to compare the pigments found in lake Bogoria data with field observations made over long time periods. In the literature there are four studies that monitored the phytoplankton abundance over time. The

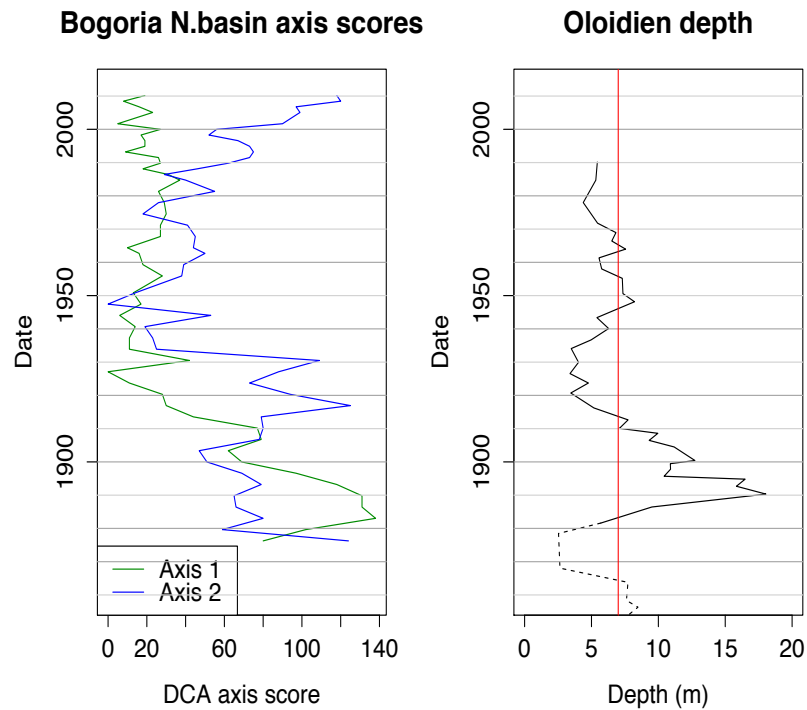


FIGURE 3.16: Lake Bogoria DCA Axis scores from the pigment data plotted against depth by Verschuren et al. (1999).

first was published by Ballot et al. (2004) (Figure 3.17), who studied the cyanobacteria community from June 2001 to September 2002. Measurements were made intermittently from monthly intervals to every few months. Schagerl and Oduor (2008) (Figure 3.18) sampled the phytoplankton community on a monthly to bi-monthly basis between November 2003 to February 2005. Krienitz and Kotut (2010) (Figure 3.19) monitored the phytoplankton community over the longest period of time from June 2001 to January 2010, sampling every 6 months to a year. The most recent study to date is by Kaggwa et al. (2012) (Figure 3.20) who sampled the lake weekly or bi-weekly from July 2008 to November 2009.

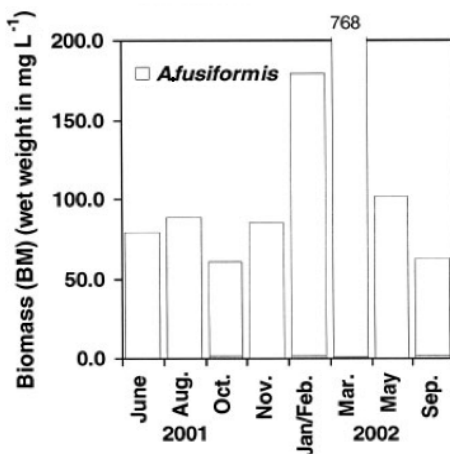


FIGURE 3.17: *Arthrosphaera* biomass 2001-2002, modified from Ballot et al. (2004).

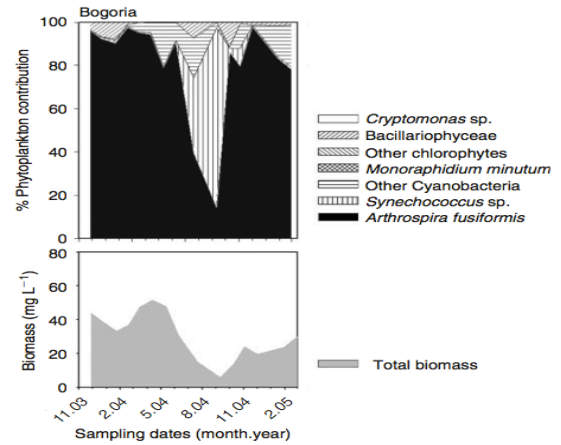


FIGURE 3.18: *Arthrosphaera* biomass 2003-2005, modified from Schagerl and Oduor (2008).

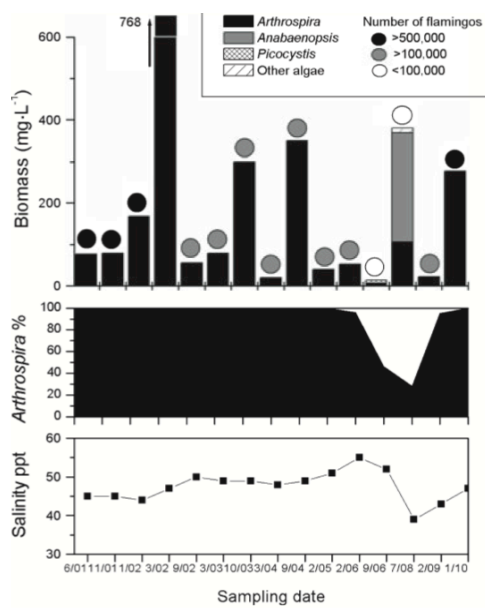


FIGURE 3.19: *Arthrosphaera* biomass 2001-2010, from Krienitz and Kotut (2010).

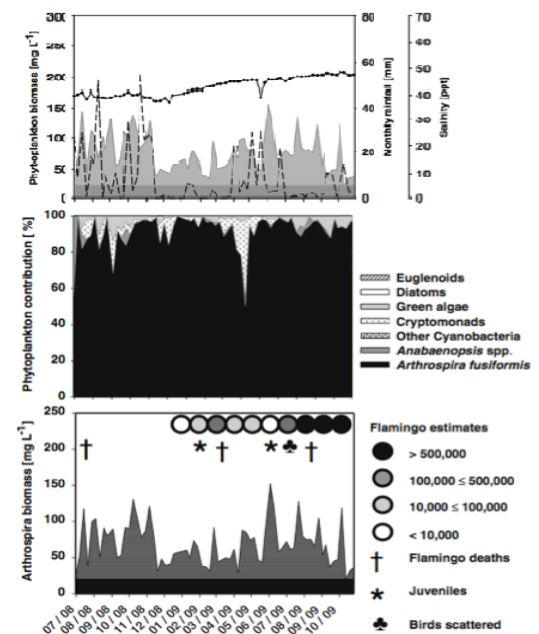


FIGURE 3.20: *Arthrosphaera* biomass 2008-2009, modified from Kaggwa et al. (2012).

The studies by Ballot et al. (2004) (Figure 3.17), Schagerl and Oduor (2008) (Figure 3.18) and Kaggwa et al. (2012) (Figure 3.20) are shorter, more detailed studies and lie within the study period of Krienitz and Kotut (2010) (Figure 3.19). These studies broadly agree with each other in terms of the *Arthrosphaera* biomass. However, there are differences which are likely to be a result of sampling at different times of day, on different days, or sampling from different basins. The *Arthrosphaera* abundance varies dramatically over short time periods as can be seen in Figure 3.20.

In the study by Krienitz and Kotut (2010) *Arthrosphaera* dominated the phytoplankton of Lake Bogoria throughout the majority of the study period, although its biomass fluctuated hugely from a minimum of 13 mg L^{-1} (Figure 3.19) in September 2006 to a maximum of 768 mg L^{-1} (Figures 3.17 and 3.19) in March 2002. The *Arthrosphaera* bloom in early 2002 does coincide with a peak in the cyanobacteria pigment abundances in the north and south basin pigment data (Figures 3.14 and 3.14), and there is a corresponding drop in in both the north and south basin cyanobacteria pigments in 2006. The most abundant cyanobacteria apart from *Arthrosphaera* were identified as *Anabaenopsis arnoldii*, *Arthrosphaera platensis* and *Synechococcus minutes*. The green algae included *Karatococcus* sp., *Picocystis salinarum* and *Monoraphidium minitum*, and cryptomonads were also present. Diatoms (*Nitzschia frustulum*) were found in the central basin by both Schagerl and Oduor (2008) and Kaggwa et al. (2012), although there were none found in the pigment analysis, which suggests that any diatoms that can grow in Lake Bogoria during more saline periods are subject to dissolution, and are not preserved in the sediment.

3.4.2 Lake Olidien

The pigment data for Lake Olidien are shown in Figure 3.21, and in the appendix, Tables 11 and 12. The myxoxanthophyll pigments were not always easy to identify from the spectra due to degradation of the pigments, and there is likely to be some missing data as a result. The same is true of diatoxanthin, since diatoms are known to be present throughout this particular core (Figure 3.11), yet the diatoxanthin pigment was not preserved between 1990 and 2011. (For a summary of the taxa indicated by different pigments see Table 3.4).

Aphanizophyll is the most abundant pigment in Lake Olidien, and is similar to the myxoxanthophyll profile. These cyanobacteria pigments are distinct from the other cyanobacteria pigments. The majority of the other pigments pheophytin a, pheophytin-b, chlorophyll-a, chlorophyll-a2, β -carotene, canthaxanthin, echinenone, zeaxanthin, diatoxanthin and alloxanthin are all similar. This suggests that at Lake Olidien there has often had a mixture of cyanobacteria and algae in the lake. Chlorophyll-b is only found in low abundance and does not appear to correlate with any other changes in Lake Olidien, although the presence of chlorophyll-b during high water levels in 1890-1891 may

be a result of expanding lake surface area causing vegetation around the lake edges to be submerged. Pheophytin-b is a degradation product of chlorophyll-b, and this peaks in 1905 and in the 1950s when Lake Olidien water levels were high enough to overtop the sill and join with Lake Naivasha. Diatoxanthin was not preserved at high lake water levels despite the presence of diatom frustules in the samples (see Figure 3.11), which suggests that when lake depth exceeds 7-8m, the pigments are degraded before they can be preserved in the sediment.

There is an increase in both algal and cyanobacterial pigments from 1990 to 2011 which is likely to be an indication of the improved preservation of the younger pigment material. This increase can also reflect an increase in overall lake productivity. Comparison with studies by Ballot et al. (2009), Figures 3.24, and Krienitz and Kotut (2010), Figure 3.25, show that there was a dramatic increase in *Arthospira* density from 2001 to 2010 that dominated primary production at Lake Olidien, which is reflected in the relatively large increase in zeaxanthin and aphanizophyll pigments during this period.

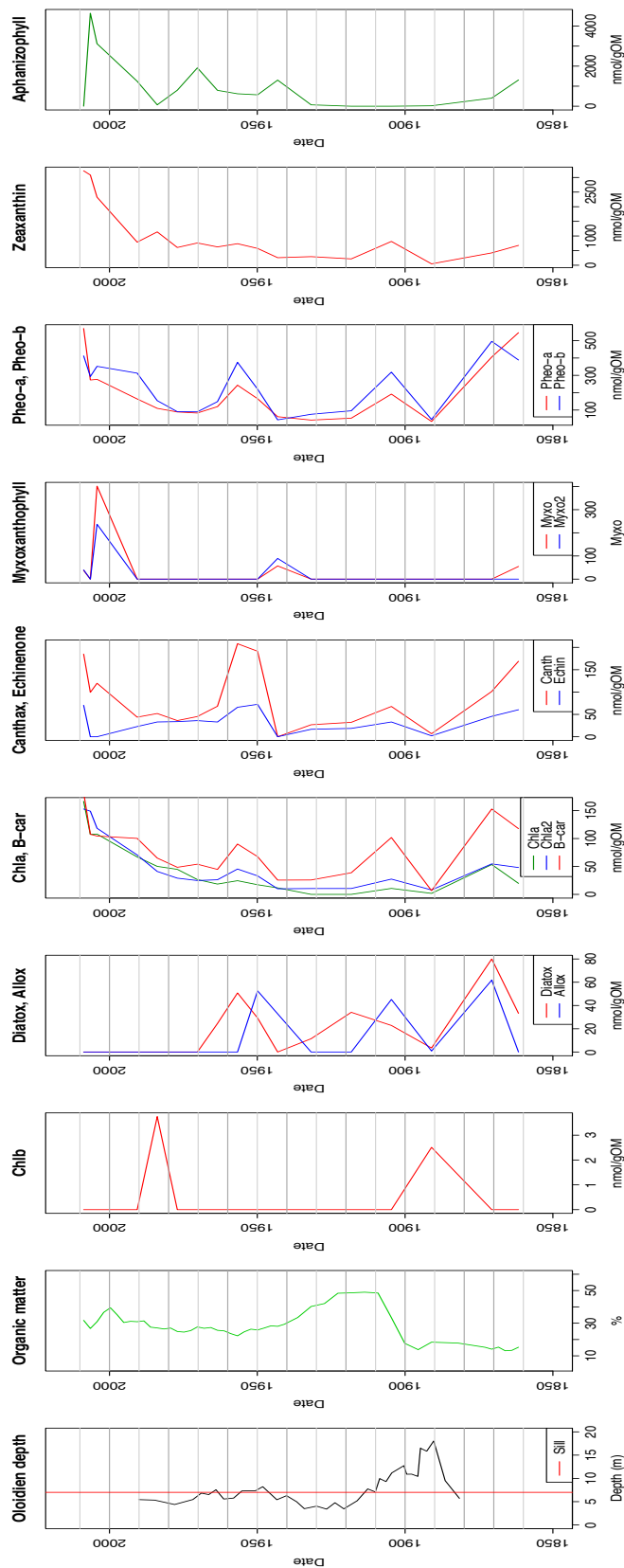
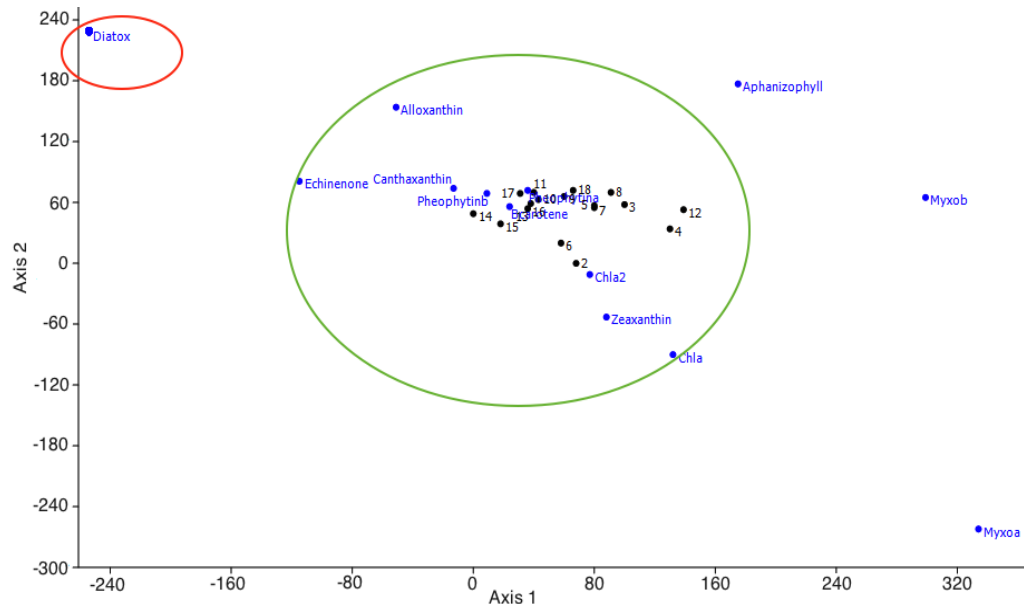


FIGURE 3.21: Pigment data for Lake Oloidien for pigments with complete profiles. Pigment abundance is expressed in nanomoles per gram of organic matter ($nmol\ g^{-1}OM$). Oloidien lake depth is from Verschuren et al. (1999).



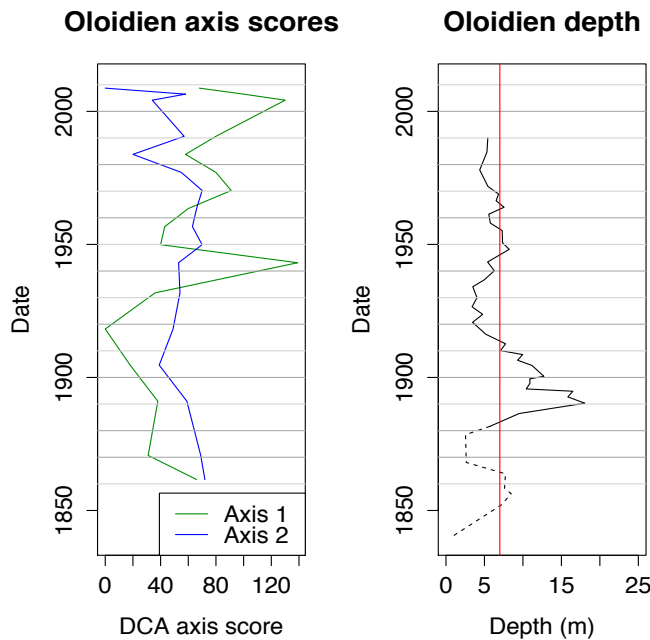


FIGURE 3.23: Lake Oloidien DCA Axis scores alongside Lake Oloidien depth (Verschuren et al., 1999).

community was sampled intermittently every few months from June 2001 to February 2005. This first study lies within the time frame of the longer term study by Krienitz and Kotut (2010) (Figure 3.25). Krienitz and Kotut (2010) monitored the phytoplankton community from June 2001 to January 2010, sampling every 6 months to a year during the interesting transition in phytoplankton community from years 2001 to 2010. The salinity increased from 1.5 to 5.5 ppt during this time, and two changes in phytoplankton community structure were observed. The first change was from coccoid green algae to coccoid cyanobacteria, with smaller populations of *Arthrosphaera* and *A. elenkinii* during 2001. The second change occurred in 2005-2006, when *Arthrosphaera* became the dominant species, and remained so for the duration of the study. After the sudden increase in *Arthrosphaera* in 2006 the lesser flamingo numbers increase from less than one thousand to more than twenty thousand.

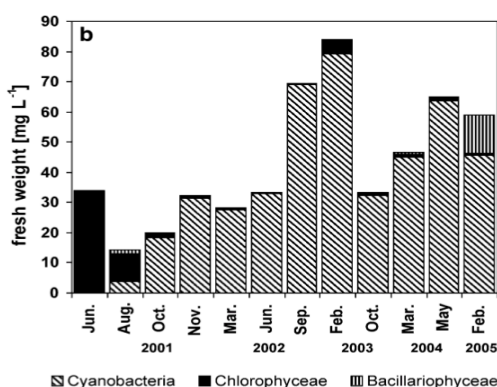


FIGURE 3.24: Lake Oloidien phytoplankton 2001-2005, from Ballot et al. (2009).

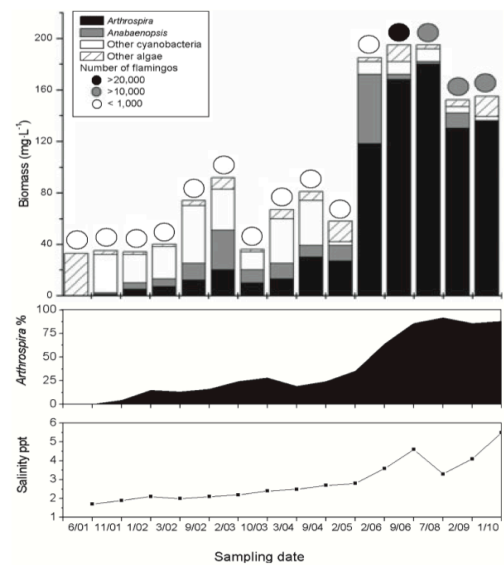


FIGURE 3.25: Lake Oloidien flamingo population, salinity, and algae composition and abundance 2001-2010, from Krienitz and Kotut (2010).

3.4.3 Lake Elmentaita

The pigment data for Lake Elmentaita can be seen in Tables 16 and 17 in the appendix. For a summary of the taxa indicated by different pigments see table 3.4. In Figure 3.26 it can be seen that Zeaxanthin is the most abundant pigment and has a similar profile to the organic matter abundance, suggesting that it represents overall lake productivity. The pigments generally increase in abundance towards the surface of the core. Fucoxanthin and diatoxanthin are both associated with diatoms. There is an increase in diatoxanthin and fucoxanthin in the 1920s. The increase in fucoxanthin may be more indicative of the rate of degradation of this pigment rather than simply representing diatom abundance (McGowan, pers. comm.), but it is more likely to be reduced as a result of high lake water levels between 1880s and 1910. The canthaxanthin abundance is similar to diatoxanthin abundance, which both peak during a period of low lake water level in the 1930s.

It was difficult to clearly identify echinenone and alloxanthin from the HPLC output. Alloxanthin was only identified in small amounts towards the top of the core with an abundance of $22 \text{ nmol g}^{-1} OM$ at the surface, suggesting that cryptomonads were present, but that there may be a high rate of degradation at Lake Elmentaita. No myxoxanthophyll was found in these samples, and although this could mean that *Arthrosphaera* may not historically be a significant component of the cyanobacteria community in this lake, the fuzzy signal profiles suggest that some pigments do not preserve well and it may not mean that they were not there. Since Lake Elmentaita is the most shallow lake of the three studied here, it is more prone to sediment resuspension and bioturbation

which increase exposure the light and oxygen. It has also been known to dry up in severe drought conditions which would expose the sediment and could cause damage to pigments as a result of higher temperatures, light and oxygen exposure. However, the presence of fucoxanthin suggests that preservation conditions are relatively good, and it may be that myxoxanthophyll is difficult to identify because it is only present in low abundances or is more susceptible to degradation in these conditions.

There is an increase in beta carotene, chlorophyll-a and zeaxanthin, which indicate an overall increase in phytoplankton productivity from this point onwards. Although there is little chlorophyll-b in the sediment, the peak between 1880 and 1930 and the increase in TOC/N ratio at this time suggest the inwash of plant material from outside of the lake. This would coincide with high lake water levels at the time if the inferred dates are correct.

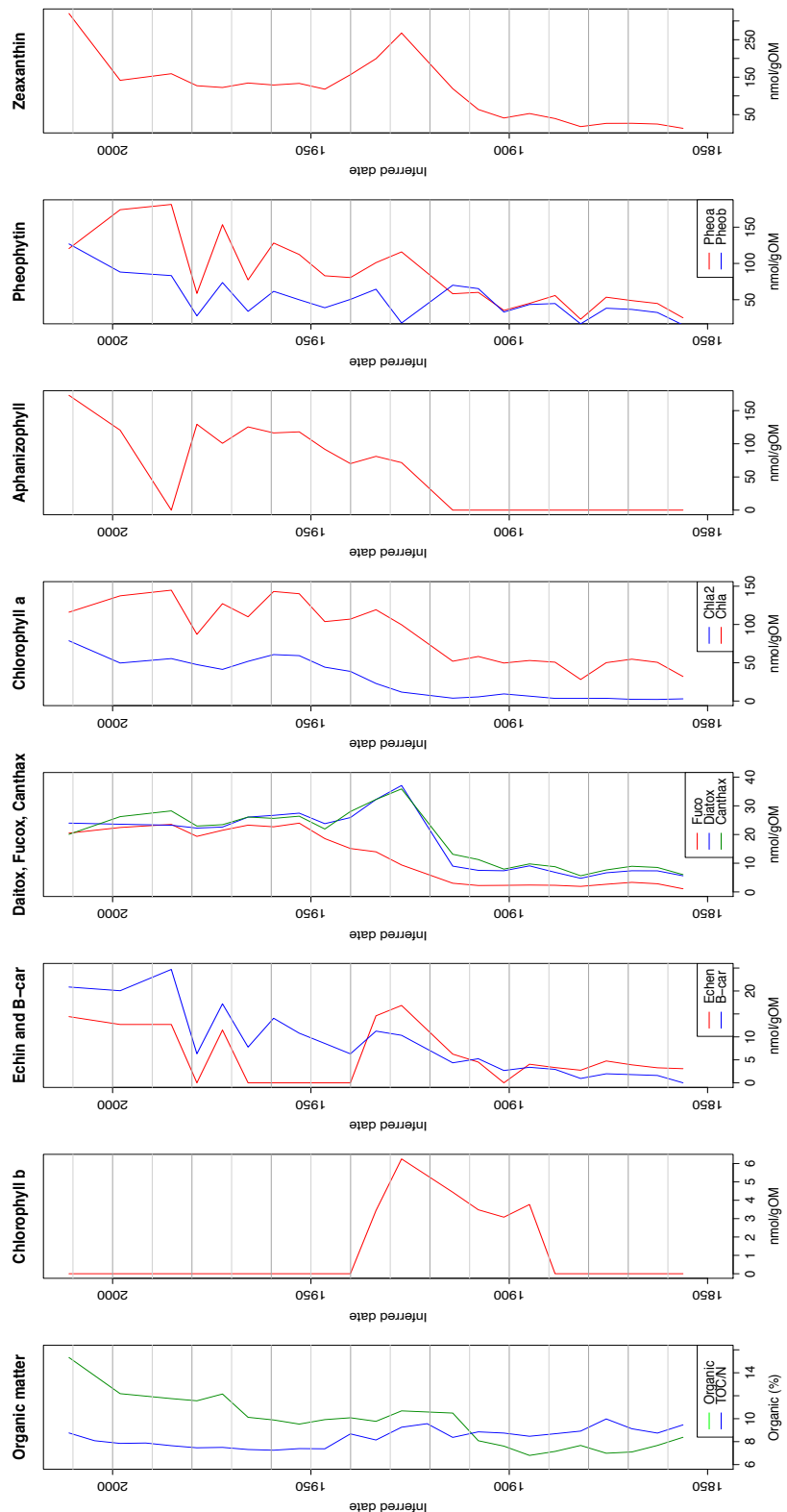


FIGURE 3.26: Lake Elementata pigment data expressed in nano moles per gram of organic matter ($nmol\ g^{-1}OM$).

The Detrended Correspondance Anaylsis (DCA) plots (see Figure 3.27) show the samples and pigments to be together in the same plot. The importance of pigments to each sample can be seen, and which pigments occur concurrently, and which occur independently from each other. Chlorophyll-b only appearing in a few samples and so was excluded the DCA.

The DCA plot shows the samples in two distinct groups. The pigments pheophytin-a and chlorophyll-a2 are both formed from the breakdown of chlorophyll-a, and are particularly important in the group of samples with the lower Axis 1 values. This group of samples (apart from sample 3) are all from the lower half of the core. These contain less of the cyanobacteria pigments and are strongly associated with the derivatives of chlorophyll-a pigments that suggest the lake was more algae or macrophyte dominated before 1925.

The second group of samples with the higher Axis 1 values are all from the more modern half of the core (1930 to 2011). These samples are grouped between the chlorophyll derivatives and cyanobacteria and the diatom pigments. This shows that these samples are likely to contain more cyanobacteria as well as diatoms and green algae, and suggests an overall increase in phytoplankton growth in Lake Elmentaita, which is more dominated by cyanobacteria growth.

The remaining pigments are pheophytin-b, a chlorophyll-b breakdown product, which lies on the opposite side of the plot to the aphanizophyll pigment. These pigments all lie around the edges of the DCA plot far from the sample dots and do not appear to account for a significant portion of the variation in the samples from the Lake Elmentaita core.

The DCA axes scores for Lake Elmentaita can be seen in Figure 3.28. Axis 1 appears to broadly represent a mixture of green algae, some cyanobacteria and diatoms. Axis 2 increases during lower lake water levels, and with increased echinenone abundance which would suggest it is representative of a cyanobacteria that appears in more saline conditions. Somewhat counterintuitively, chlorophyl-b and pheophytin-b are also present in higher abundances during lower lake water levels. By comparing these axes with the Lake Oloidien depth it can be seen that Axis 2 usually increases during drops in lake depth which would be expected since cyanobacteria usually dominates the soda lakes at higher salinities. It is difficult to know how meaningful these data are however when there is such severe pigment degradation without comparing these results with studies in the literature.

There are three studies of phytoplankton abundance at Lake Elmentaita in the literature. The first was a study of the cyanobacteria community by Melack (1988), who studied the phytoplankton community from February 1973 to March 1975. Ballot et al. (2004) (Figure 3.31) studied the cyanobacteria community intermittently every few months from June 2001 to September 2002. And thirdly, Schagerl and Oduor (2008) sampled

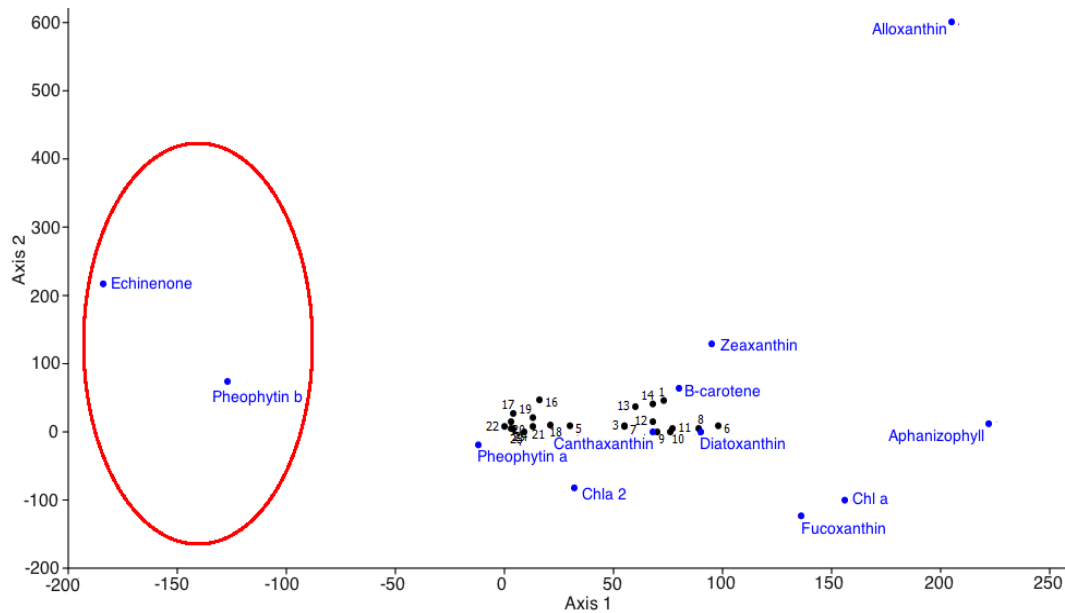


FIGURE 3.27: Lake Elmentaita DCA. The echinenone and pheophytin b pigments (highlighted in red) co-vary, the other cyanobacteria, diatom and green algae pigments all have similar profiles.

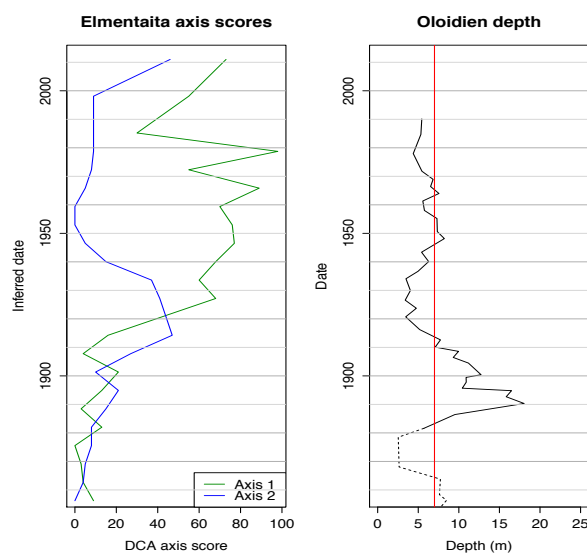


FIGURE 3.28: Lake Elmentaita DCA Axis scores plotted against depth.

the phytoplankton community on a monthly to bi-monthly basis between November 2003 to February 2005 (Figure 3.32). Melack (1988) found that the cyanobacteria *Spirulina platensis* (*A.fusiformis*) and *Spirulina laxissima* seen in Figure 3.29 both declined in 1973 as the salinity of the lake increased. *Anabaenopsis arnoldii* declined in a similar way to *Arthospira*, and the only copepod *Paradiaptomus africanus* disappeared by May 1973. The green algae *Selenastrum sp.* declined but then began to recover in 1974. Diatoms *Navicula elka* and *Navicula cryptocephala* increased in abundance during the study, as did *Nitzschia* sp. and *Anomoenis sphaerophora* (see Figure 3.30). *Nitzschia sigma* fluctuated around ca. 1×10^3 frustules/ml throughout the study. Lake water level declined from 1.1 to 0.65m during the study, and cyanobacteria declined dramatically after which benthic algae increased in abundance. Melack (1988) concluded that the loss of *P. africanus* and oxygenation of the sediments by the diatom community caused a reduction in the rate of nutrient recycling during this time. Unfortunately the pigment data is not of high enough resolution and the studies are too brief to be able to compare the changes directly with the pigment data. However, it can be concluded that there is a diverse phytoplankton community at Lake Elmentaita. These studies also show that total cyanobacteria biomass can change dramatically from month to month, as does the dominant cyanobacteria species. *Arthospira* often accounts for less than half of the total cyanobacteria biomass, with green algae and diatoms usually present in smaller abundances. The presence of a diverse phytoplankton community does agree with the DCA analysis of the pigment data for the core between 1915 and 2011 (see Figure 3.27).

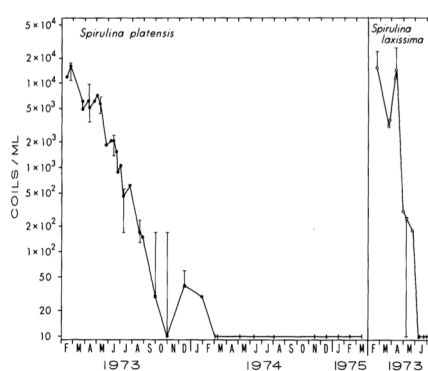


FIGURE 3.29: *Arthospira* abundance 1973-1975, (Melack, 1988).

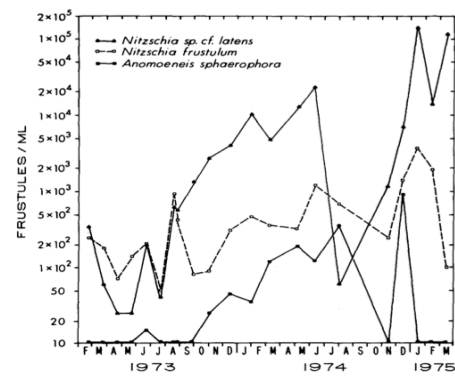


FIGURE 3.30: Diatom abundance 1973-1975, (Melack, 1988).

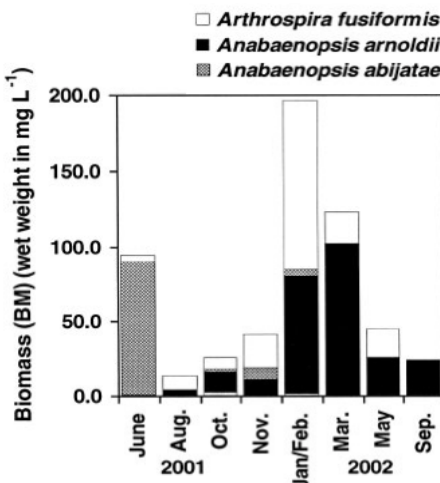


FIGURE 3.31: Cyanobacteria biomass 2001-2002, modified from Ballot et al. (2004).

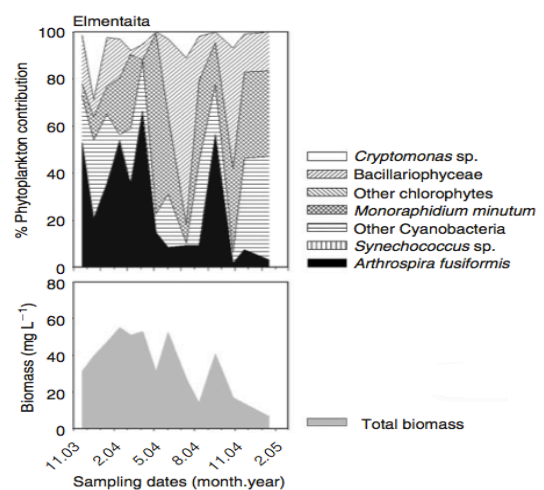


FIGURE 3.32: Phytoplankton composition 2003-2005, modified from Schagerl and Oduor (2008).

3.5 Nitrogen Isotopes

There are two stable nitrogen isotopes, ^{14}N and ^{15}N . Stable isotope analysis has been used to understand the movement of resources through an ecosystem (e.g. Burian et al., 2014), since the proportion of ^{15}N increases in each trophic level of a food chain (Boecklen et al., 2011). High flamingo populations should cause an enrichment in the ^{15}N isotope because of the relatively large amount of material that large flamingo populations would excrete into the lake, as well as the higher $\delta^{15}N$ value of feathers and dead flamingos that decompose in the lake and end up in the sediment. Larger flamingo populations should therefore increase $\delta^{15}N$ values in the sediments, and so ^{15}N may be a suitable flamingo proxy.

To explore the idea that N-isotopes could be used as a flamingo proxy 17 sub samples from the Bogoria North basin core (G1), and three flamingo dropping samples were sent to the British Geological Survey in Keyworth for analysis by Prof. Melanie Leng to explore the possibility that higher ^{15}N values in lake sediments could be linked to higher flamingo populations. The subsamples had been previously freeze dried and ground by Sarah Ward. Leng determined $^{15}N/^{14}N$ ratios on the N_2 gas produced by the combustion of the sediment samples in a Flash 1112 elemental analyser linked to a Delta+ mass spectrometer (ThermoFinnigan, Bremen). The $^{15}N/^{14}N$ ratios were calculated as $\delta^{15}N$ values versus atmospheric N_2 by comparison with calibrated USGS standards.

The nitrogen isotope data can be seen in the leftmost graph of Figure 3.33, and in Table 7 of the appendix. Lake sediment values were found to fluctuate between 7.0‰ and 9.2‰. *Arthrosphaera* does not fix nitrogen from the atmosphere (Vareschi, 1982; Zhang et al.,

2009), it has a lower $\delta^{15}N$ value of 4.1 (Burian et al., 2014). The higher $\delta^{15}N$ in the sediment is caused by an increase in material from consumers that cause fractionation of nitrogen isotopes. The flamingo guano samples had a $\delta^{15}N$ value of 5.1‰, which is higher than the *Arthrosphaera* value. Flamingo tissues are likely to be significantly higher than this, and may account for the higher sediment $\delta^{15}N$ values, which are likely to increase with high flamingo populations. Flamingos shed feathers into the lake, and also large numbers died at Lake Bogoria during the mortality events, particularly at the 1999-2000 event where 200,000 birds died, which is likely to have caused an increase in $\delta^{15}N$.

The flamingo census data is available for 1992 to 2010 for Lake Bogoria from annual counts undertaken by the Kenyan Wildlife Service, and personal observations from rangers that are used to counting flamingos from 2011 onwards. The flamingo population changes between only a few thousand and more than one million between 1991 and 2012, and these data were plotted alongside the $\delta^{15}N$ data for the same time period. The few $\delta^{15}N$ data points make it difficult to compare these data. But there are some clear changes in $\delta^{15}N$ sediment values suggests that it should be possible to identify the presence of large flamingo populations from higher resolution data.

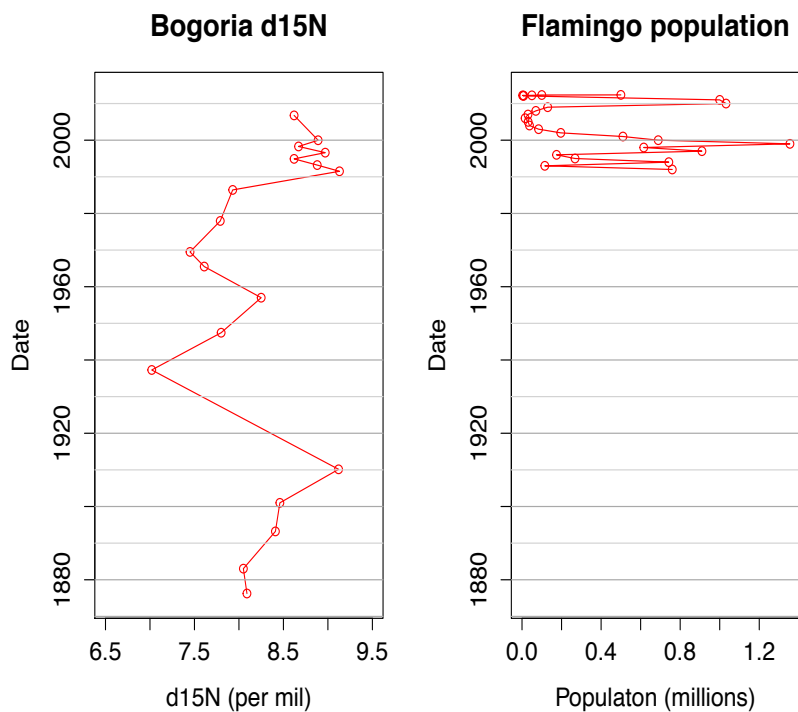


FIGURE 3.33: Lake Bogoria north basin $\delta^{15}N$ data and flamingo population data (Nature Kenya, NMK, KWS, Bogoria National Park rangers).

3.6 Geochemistry

The elemental composition and relative abundance of elements in a sediment sample reflect the changes in environmental and sedimentological conditions.

X-ray fluorescence (XRF) analysis is a non-destructive way to measure elemental profiles in lake sediment cores (Croudace et al., 2006). Either bulk analysis of samples can be used for extruded cores, or higher resolution ITRAX core scanning of cores that are split lengthways. An x-ray beam excites electrons in the sample, causing the atoms to become ionised by releasing electrons. To stabilise the atoms electrons from higher energy orbitals move to the holes in the lower energy orbitals of the atom, emitting a photon of a characteristic energy. The photons emitted from the surface of the sample are then detected and counted. Since the energies of these photons are associated with particular elements, the elemental composition of the sample can be found and the relative abundance of these different elements deduced from the counts of photons of different energies.

The ITRAX core scanners (Croudace et al., 2006) generate high-resolution elemental profiles, which can be interpreted to provide information about grain size and sediment inputs, as well as proxies for lake productivity and lake water level. Kylander et al. (2011) studied the associations between elements Ti, Rb, K, Zr, Si, Ca, Sr, Mn and Fe, and found that the strength of association varied with changes in lake state. Calcium abundance in lake sediments can be related to the precipitation of calcium carbonate (Cohen, 2003) and would indicate declining lake levels for the Kenyan soda lakes.

The advantages of the ITRAX method of elemental analysis is that it is fast, non-destructive and very high resolution. There are disadvantages of using this technique due to the difficulties of relating the semi-quantitative counts recorded by the ITRAX detector to actual elemental abundances (Croudace et al., 2006). The detector is also highly sensitive to undulations in the core surface, grain size, air pockets or water at the surface. These variations can cause the detector to move away from the surface of the sample, and this causes the overall counts to be reduced for these core sections. The ITRAX core scanner is not as sensitive to some elements as it is to others, and so counts can not always be relied upon to represent the true relative abundance of elements (Weltje & Tjallingii, 2008). The use of element ratios can help to reduce the noise in the data due to variation in the core. For example Ma/Ti has been used as an indicator of redox-related diagenesis and Ba/Ti has been used as an indicator of productivity (Croudace et al., 2006).

Weltje and Tjallingii (2008) proposed a log-ratio calibration model for converting these counts to a quantitative measurement of elemental composition. To apply this method to the soda lake cores grain size analysis and calibration is required.

Itrax core scanning was undertaken at the National Oceanography Centre at the University of Southampton. Preparation of the cores was undertaken by Sarah Ward, and runs on the Itrax core scanner were set up by Prof. Ian Croudace. The success of this approach to elemental analysis is highly dependent on whether the structural integrity of cores has remained intact. The cores from Lakes Elmentaita and Oloidien have a much lower water content than those at Lake Bogoria, but were still rather watery which made them difficult to split. However, the structural integrity of these cores had been preserved. The surface of the split cores was not smooth and flat as preferred but undulated and also contained air pockets, which makes interpretation of the data less straightforward.

The whole core brought back from Lake Bogoria was mixed through at least the first 50 cm, and so it was not possible to run it on the Itrax core scanner. Instead individual samples were used from a core that was extruded in the field and these were run as pellets on an XRF scanner. This method (Croudace & Gilligan, 1990; Jenkins, 1999; Croudace et al., 2006) is labour intensive and requires several grams of ground material which is pressed into pellets although these data are two orders of magnitude lower resolution than the ITRAX core scanner data, and due to the limited material remaining at this stage only 20 samples were run. The pellets were prepared by Sarah Ward, and run on the XRF scanner under the direction of Prof. Ian Croudace at the National Oceanography Centre, University of Southampton. The bulk XRF data for the south basin core (SB1) can be seen in Figures 3.34 and 3.35. The data can be seen in Tables 8 and 9 in the appendix. Rinsed sediment samples were used to remove the salts which were in such high concentrations in initial XRF runs that some elements were being obscured. As a result the soluble elements Na, K, Cl and S have been washed out and are not present in the data.

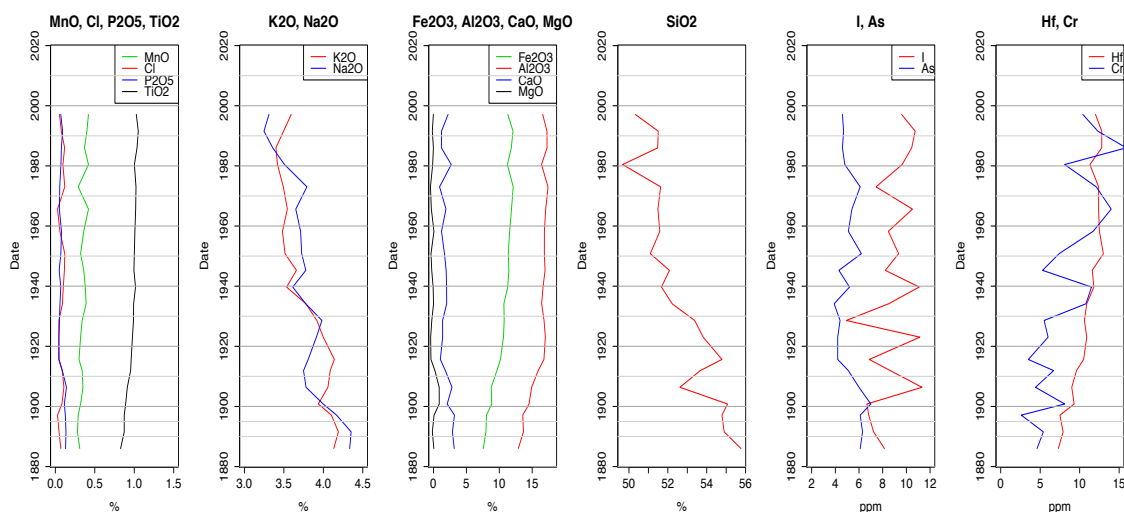


FIGURE 3.34: Lake Bogoria south basin XRF data (part 1).

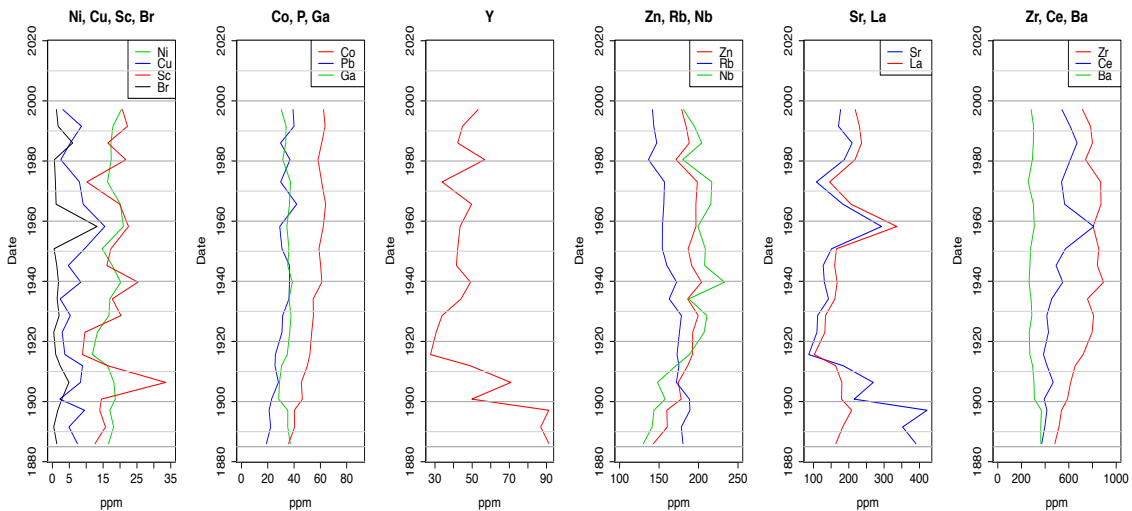


FIGURE 3.35: Lake Bogoria south basin XRF data (part 2).

The south basin sediment geochemistry reflects an origin from weathering of the distinctive alkali volcanic rocks, mainly trachyphonolite, basalts and phonolites (McCall, 1967) which contain high concentrations of Zr, Nb and Hf, and also high concentrations of rare earth elements like yttrium (Y), cerium (Ce) and lutetium (Lu). A Detrended Correspondance Analysis (DCA) was used to reduce the elemental data to two variables that could be plotted against sample depth. The DCA plot can be seen in Figure 3.36, and the sample depths and Axis scores can be seen in Table 3.5 and Figure 3.37.

The DCA plot shows that most variation occurs along Axis 1, which the samples are spread across relatively evenly, and that there is less variation in Axis 2. The samples are clustered into two main groups, with the deeper sediment samples highlighted in red (samples 19 to 23, which correspond to years 1906 to 1886) and the shallower samples are highlighted in green. To understand more about what gradients these axes represent the DCA Axis scores were plotted against Lake Oloidien depth and the Rb:Sr ratio in Figure 3.37.

It can be seen by comparing the Lake Oloidien depth and Axis 1 profile that Axis 1 appears to represent a Lake depth. Axis 1 was plotted against Lake Oloidien depth to give an R^2 value of 0.698, which suggests that Axis 1 is a good indication of lake depth. Rb:Sr ratio is used as a weathering proxy (Brass, 1975; Chen et al., 1999), and Axis 2 increases when there are higher Rb:Sr ratios. When Axis 2 is plotted against the Rb:Sr ratio the R^2 value is 0.708, which suggests that Axis 2 is a good indication of weathering rate.

The change in runoff and vegetation between wet and dry periods in the Lake Bogoria catchment is likely to be the cause of changes in the abundance of elements, either increasing them as weathered rock is inwashed into the lake or by leaching trace elements out of the soils. Strontium (Sr), Lanthanum (La) and Yttrium (Y) for example, increase

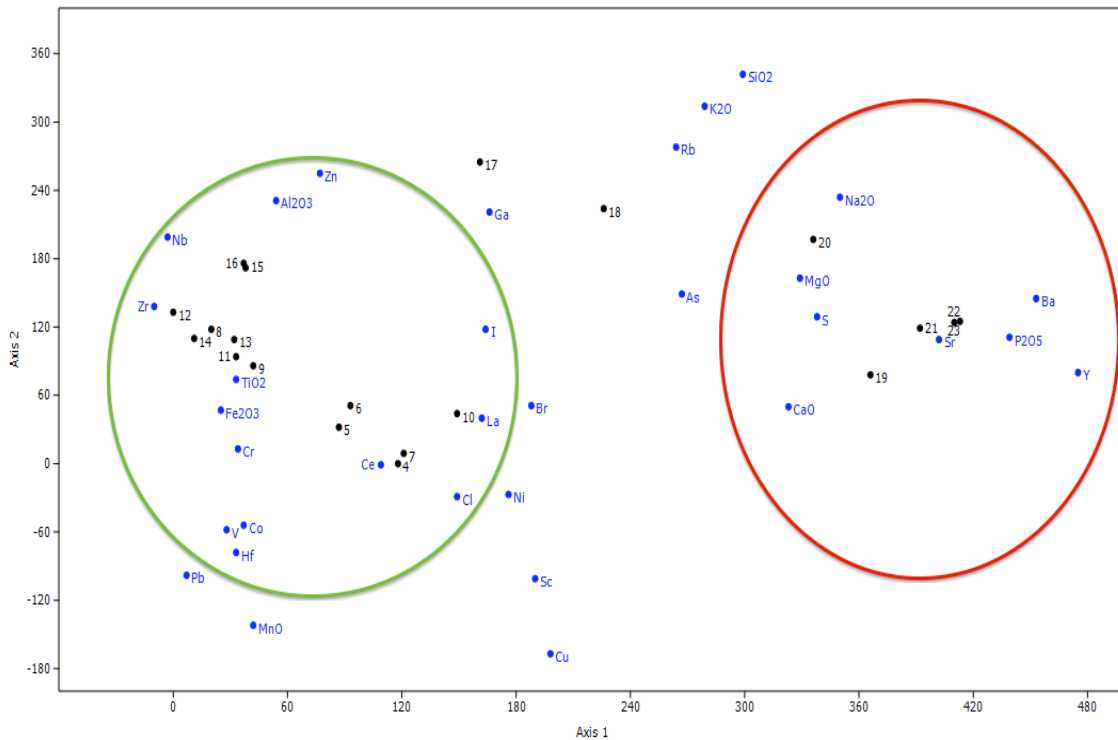


FIGURE 3.36: Lake Bogoria south basin XRF DCA. The older core samples are grouped together and are highlighted in red. The samples highlighted in green are younger sediments.

during wetter periods, suggesting that they are inwashed during periods of high rainfall (Figure 3.37). It may seem counterintuitive that weathering and lake water level are separate environmental gradients in the DCA, since high rainfall is often associated with increased weathering rates. However, the Eastern shore of Lake Bogoria meets the foot of a steep escarpment, and the increased rate of weathering during dry periods may be a result of reduced vegetation on this steep escarpment slope. During dry periods some material may be deposited by winds or as a result of landslides.

Date	Depth	Pellet number	Axis1	Axis2
1997.11	7.5	4	118	0
1991.56	10.5	5	87	32
1986.00	13.5	6	93	51
1980.44	16.5	7	121	9
1973.04	20.5	8	20	118
1965.63	24.5	9	42	86
1958.22	28.5	10	149	44
1950.81	32.5	11	33	94
1945.26	35.5	12	0	133
1939.70	38.5	13	32	109
1934.15	41.5	14	11	110
1928.59	44.5	15	38	172
1923.04	47.5	16	37	176
1915.63	51.5	17	161	265
1911.93	53.5	18	226	224
1906.37	56.5	19	366	78
1900.81	59.5	20	336	197
1897.11	61.5	21	392	119
1891.56	64.5	22	413	125
1886.00	67.5	23	410	124

TABLE 3.5: Lake Bogoria XRF DTC Axis scores.

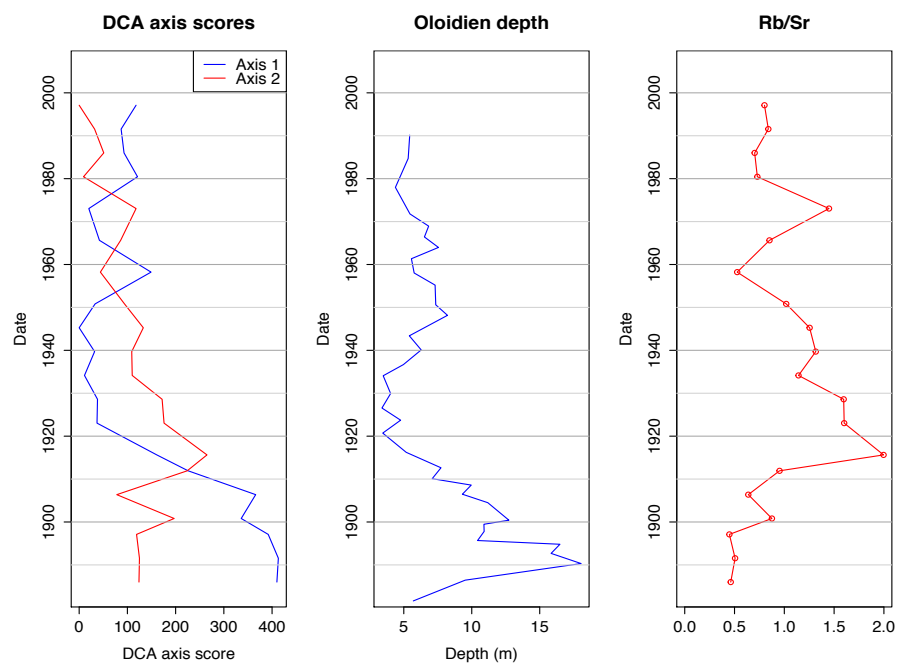


FIGURE 3.37: Lake Bogoria XRF Axis scores, Lake Oloidien depth, and Rb:Sr ratio.

3.6.1 Lake Oloidien

The ITRAX data can be seen in Figure 3.38, and is summarised in Tables 13 and 14 of the appendix. Since this core had a relatively high water content it did not split particularly well and so resulted a slightly uneven surface and there were a few air bubbles. Serious defects in the core surface meant that data recorded around 1950 had to be removed from the output. There is also an undulation at the very top of the core which can be seen as a spike in ‘peak area/kcps’ at 2011 in Figure 3.38. To even out the smaller changes in counts, the peak areas (the signal strength from each element) were divided by counts per second. The ITRAX data were smoothed using a 10 point average to reduce the amount of noise.

The geochemistry is reflective of the alkali volcanic rocks in the catchment, with a high abundance of Fe, Ca, K and Zn Figure (3.38). Iron is the most abundant element, and has a similar profile to Ca, Sr, Rb, K, Mn, Zr and Ti. These elements concentrate during lower lake water levels. Other elements including P, S, Cl and Cr increase when lake water levels are higher, suggesting that they are inwashed during heavy rainfall. There is a reduction in counts for several elements including zirconium (Zr) and calcium (Ca) between 1890 and 1920. During this period (Verschuren et al., 1999) suggests that there is a decrease in the inwash of sediment from the catchment due to papyrus stands growing around the lake, which is likely to be the cause of the low abundance of these elements during this period.

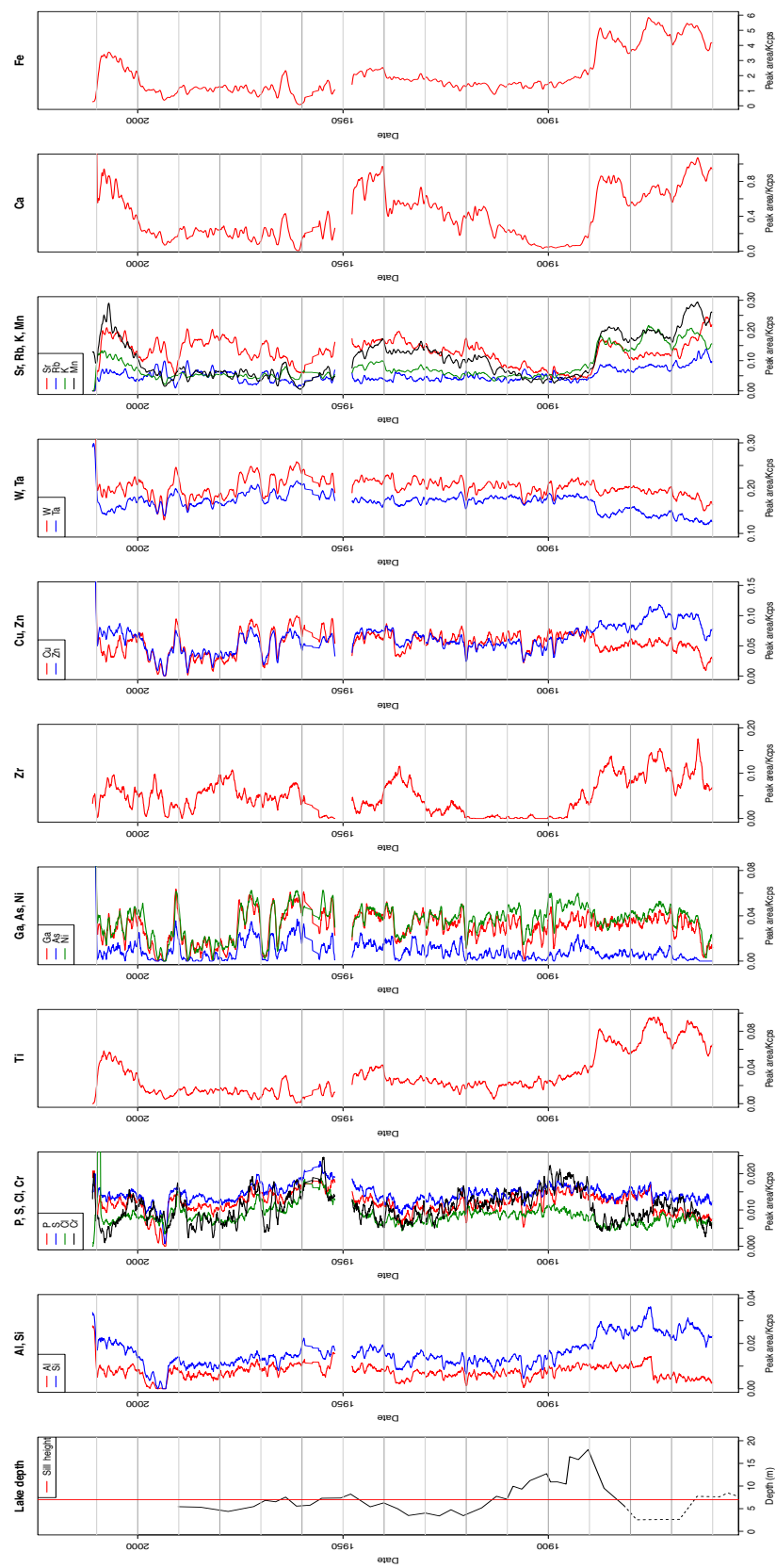


FIGURE 3.38: Lake Oloidien ITRAX elemental data. The x-axis is the signal strength from each element) divided by counts per second.

Detrended Correspondence Analysis (DCA) was used to reduce the elemental data to two variables that could be plotted against sample depth. The DCA plots can be seen in Figures 3.39 and 3.40, and the sample depths and Axis scores can be seen in Table 3.6 and Figure 3.41.

The DCA plot (Figure 3.39) shows that most variation occurs along Axis 1. The samples are clustered together in the plot, but on closer inspection (Figure 3.40), where samples 39-50 cm, which correspond to years 1862 to 1903, can be seen highlighted in red and are clustered together with the lowest Axis 1 values. Samples 34-39, which correspond to years 1906 to 1922, are highlighted in green and are clustered together with the lowest Axis 2 values.

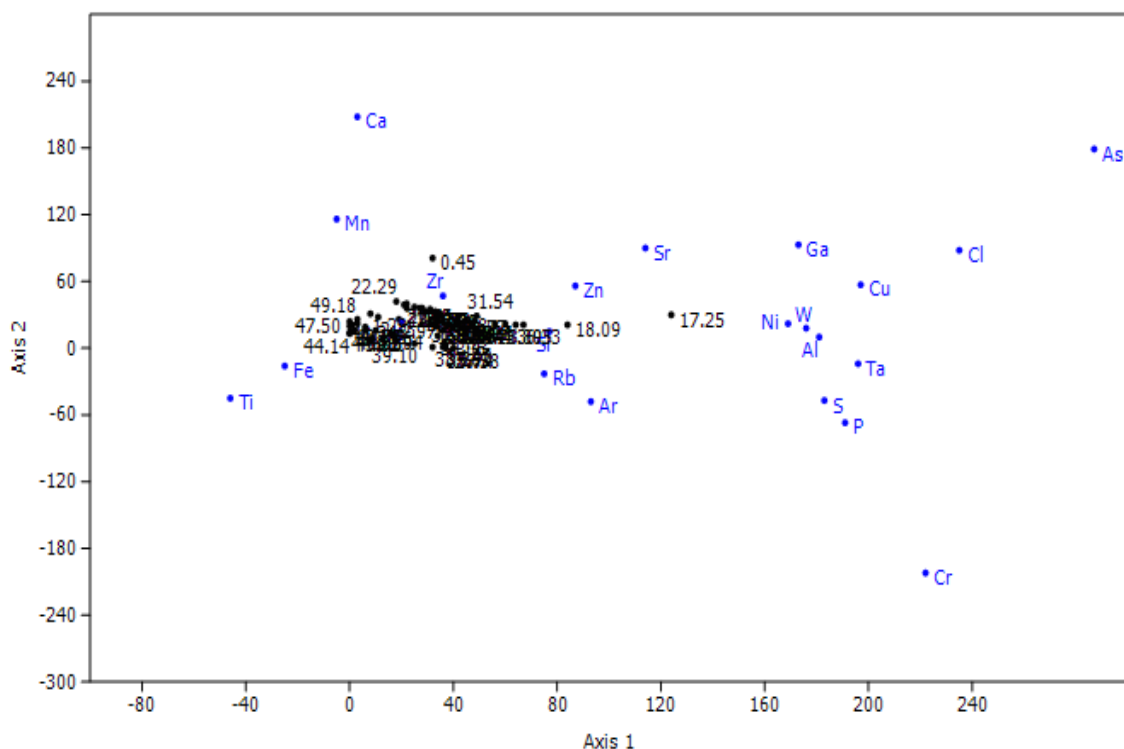


FIGURE 3.39: Lake Olloidien XRF DCA.

To understand more about what gradients these axes represent the DCA Axis scores were plotted against Lake Oloidien depth, Organic matter content, Rb:Sr ratio and Mn:Fe ratio in Figure 3.41. Unlike the Lake Bogoria geochemistry data there is not an obvious relationship between lake water level and either DCA axis. However, Axis 2 may be related to weathering by runoff, since it is lower during the period when papyrus reduced the sedimentation rate, and Axis 1 is potentially related to the deposition of eroded rock by wind because it increases during lower lake depths.

Ratios of different elements can be used to extract more information from elemental profiles. Rubidium to strontium ratio (Rb:Sr) is indicative of increased weathering and Mn:Fe ratios have been used as a proxy for anoxic conditions (e.g. Mackereth, 1966; Wersin et al., 1991), which would be expected to occur when the lake is deeper. The

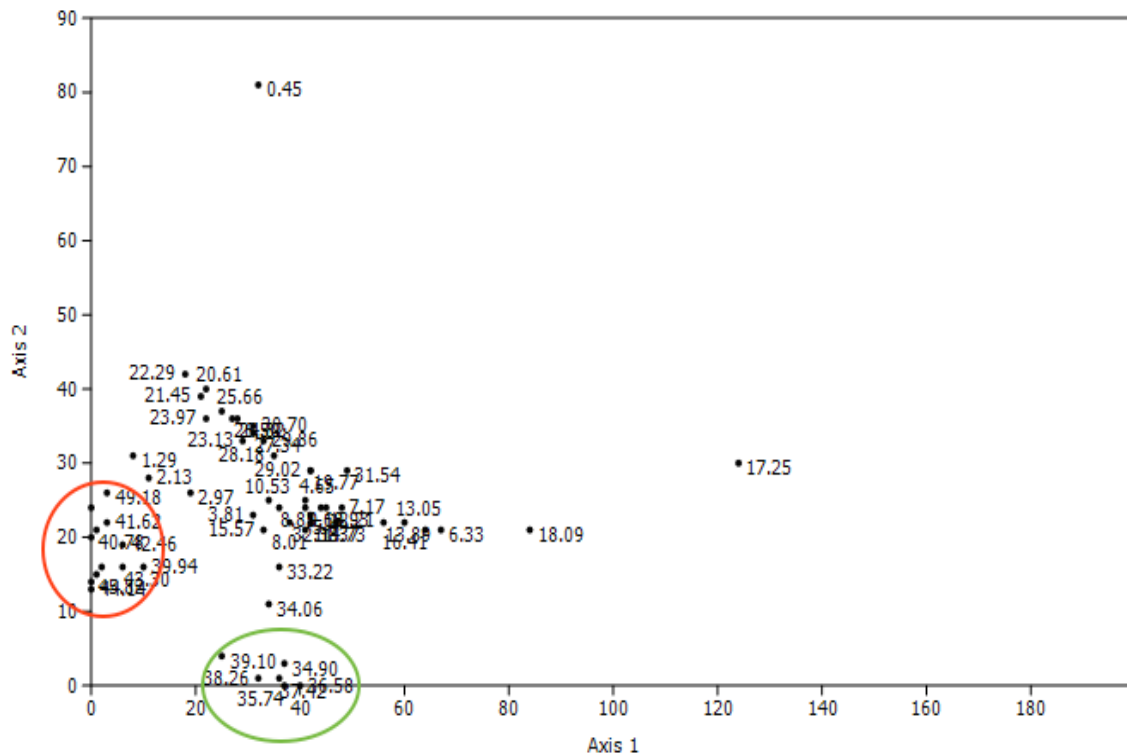


FIGURE 3.40: Lake Oloidien XRF DCA showing the sample depths only.

Mn:Fe and Rb:Sr ratios do not behave as would be expected since during periods of high lake water level Rb:Sr ratio would usually be expected to increase as weathering rates increase, whilst Mn:Fe ratio, as a proxy for anoxia, should be low during high lake water levels, although anoxic conditions can also be caused by eutrophication or reduced mixing of the water column as a result of lower wind speeds. The reduction in sediment inwashed as a result of papyrus stands resulted in a greater proportion of organic matter in the sediment (Verschuren et al., 1999). This is the reason that organic matter content is relatively high during this period at this time and coincides with low Axis 2 values the Mn:Fe ratio is low during this period would usually suggest anoxic conditions.

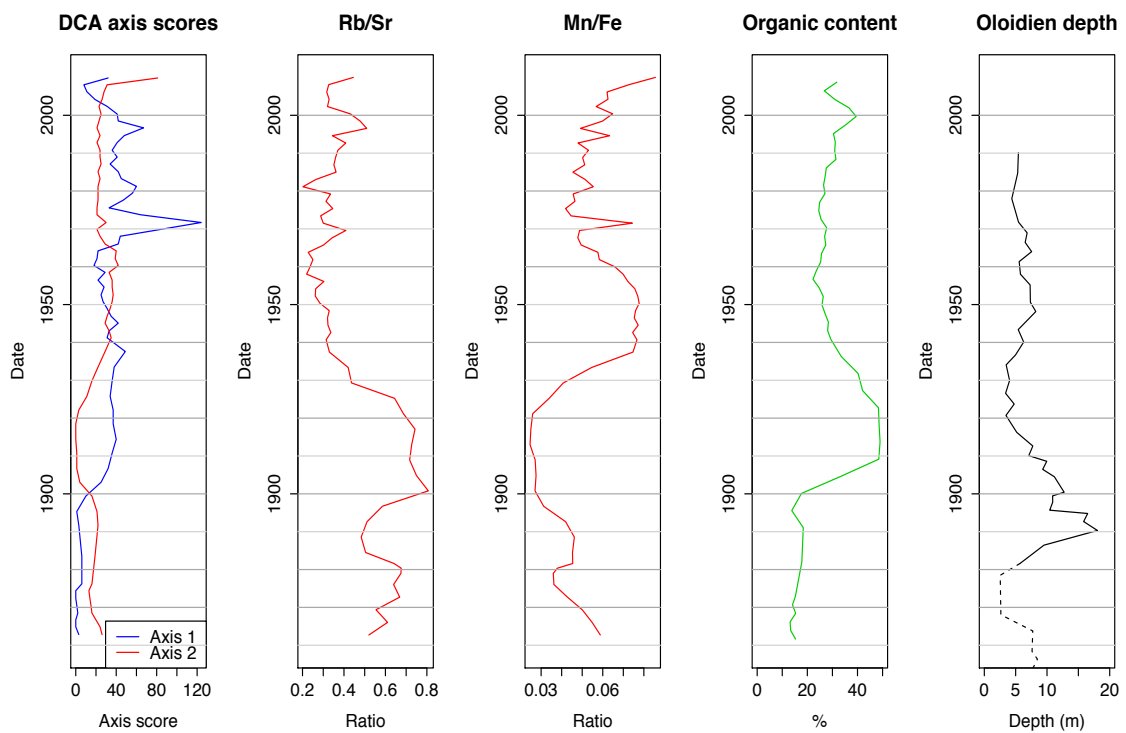


FIGURE 3.41: Lake Oloidien Itrax DCA Axis scores plotted alongside Rb:Sr ratio (a weathering proxy), Mn:Fe ratio (a proxy for sediment oxygen level), organic matter content, and Lake Oloidien depth from Verschuren et al. (1999).

Depth	Date	Axis 1	Axis 2	Depth	Date	Axis 1	Axis 2
0.45	2009.86	32	81	25.66	1952.59	25	37
1.29	2008.05	8	31	26.5	1950.77	27	36
2.13	2006.23	11	28	27.34	1948.95	31	34
2.97	2004.18	19	26	28.18	1946.91	35	31
3.81	2002.36	31	23	29.02	1945.09	42	29
4.65	2000.32	41	25	29.86	1943.05	33	33
5.49	1998.50	42	23	30.7	1941.23	31	35
6.33	1996.68	67	21	31.54	1937.59	49	29
7.17	1994.64	48	24	32.38	1933.50	38	22
8.01	1992.82	41	21	33.22	1929.86	36	16
8.85	1990.77	36	24	34.06	1925.77	34	11
9.69	1988.95	41	24	34.9	1922.14	37	3
10.53	1987.14	34	25	35.74	1918.50	37	0
11.37	1985.09	42	22	36.58	1914.41	40	0
12.21	1983.27	45	24	37.42	1910.77	36	1
13.05	1981.23	60	22	38.26	1906.68	32	1
13.89	1979.41	56	22	39.1	1903.05	25	4
14.73	1977.59	47	22	39.94	1899.41	10	16
15.57	1975.55	33	21	40.78	1895.32	1	21
16.41	1973.73	64	21	41.62	1891.68	3	22
17.25	1971.68	124	30	42.46	1883.50	6	19
18.09	1969.86	84	21	43.3	1876.23	6	16
18.93	1968.05	44	24	44.14	1874.41	0	13
19.77	1966.00	42	29	44.98	1872.36	0	14
20.61	1964.18	22	40	45.82	1870.55	1	15
21.45	1962.14	21	39	46.66	1868.50	2	16
22.29	1960.32	18	42	47.5	1866.68	0	20
23.13	1958.50	29	33	48.34	1864.86	0	24
23.97	1956.45	22	36	49.18	1862.82	3	26
24.82	1954.64	28	36				

TABLE 3.6: Lake Oloidien ITRAX DTC Axis scores.

3.6.2 Lake Elmentaita

The ITRAX data can be seen in Figure 3.42 and is summarised in Tables 18 and 19 in the appendix. The core from Lake Elmentaita had lower water content than the Lake Oloidien core which made it easier to split. There were small undulations in core surface and so peak areas (the signal strength from each element) was divided by counts per second. The ITRAX data were then smoothed using a 10 point average to reduce the amount of noise.

A visual inspection of Figure 3.42 shows the element abundances appear to be relatively stable, the main points to note are that calcium and silicon reduce from 25 to 17 *cm* before increasing again and remaining relatively constant throughout the rest of the core. The geochemistry is reflective of the alkali volcanic rocks in the catchment, with a high abundance of Fe, Ca and K. Iron (Fe) is the most abundant element, and has a similar profile to Ca, K, Mn, Si and Ti.

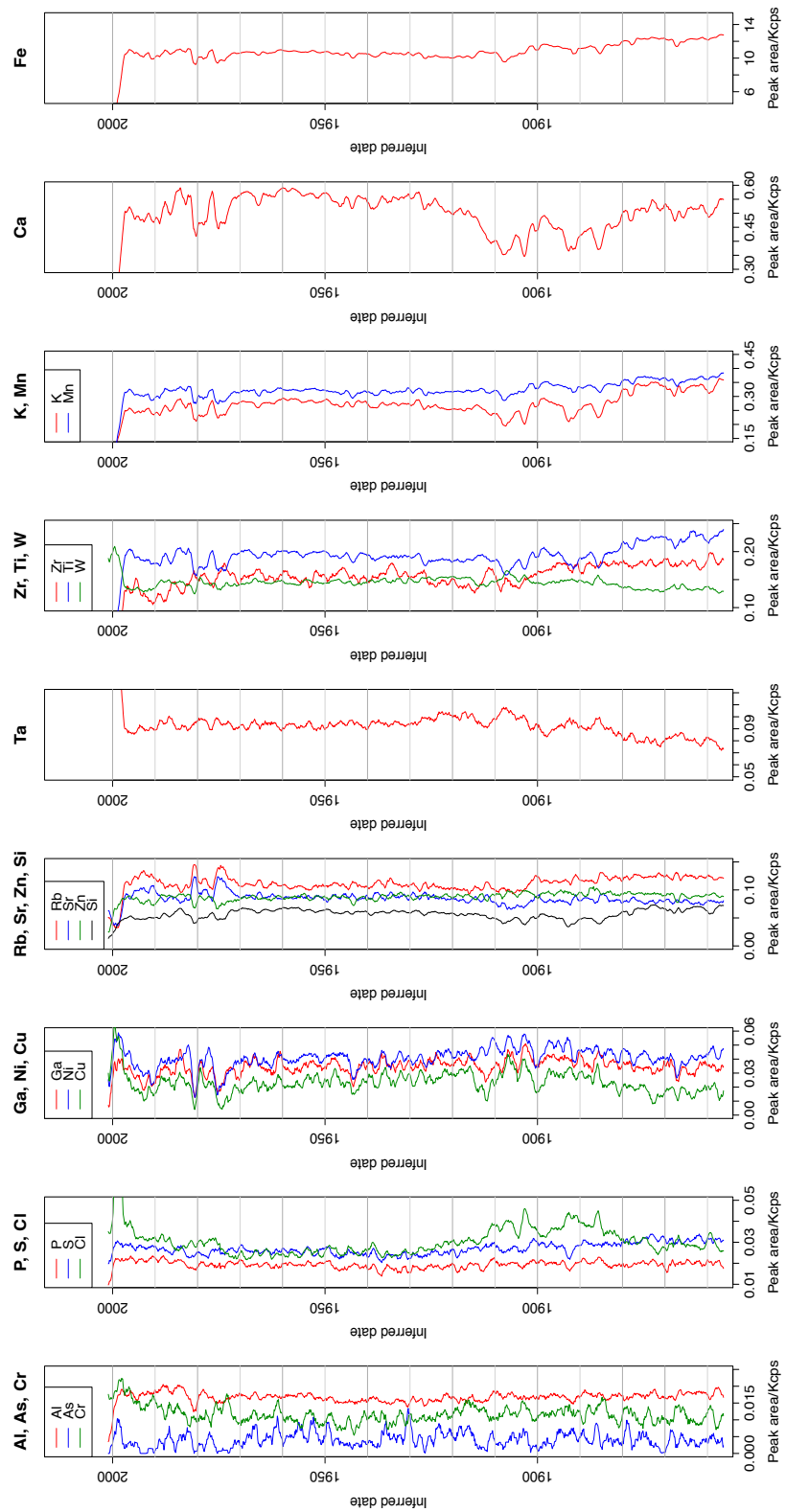


FIGURE 3.42: Lake Elmentaita ITRAX elemental data.

Detrended Correspondence Analysis (DCA) was used to reduce the elemental data to two variables that could be plotted against sample depth. The DCA plots can be seen in Figure 3.43, and the sample depths and Axis scores can be seen in Table 3.7 and Figure 3.44.

The DCA plot (Figure 3.43) shows that most variation occurs along Axis 1. Most of the samples have very little variation and have the same Axis 1 and Axis 2 values. The samples that are outside of this group are the youngest sediments, 2.05 to 4.94, which correspond to inferred dates of 1992 to 2003. When DCA was tried without the uppermost samples the DCA output was the same for the other samples, showing no variation in the older sediments.

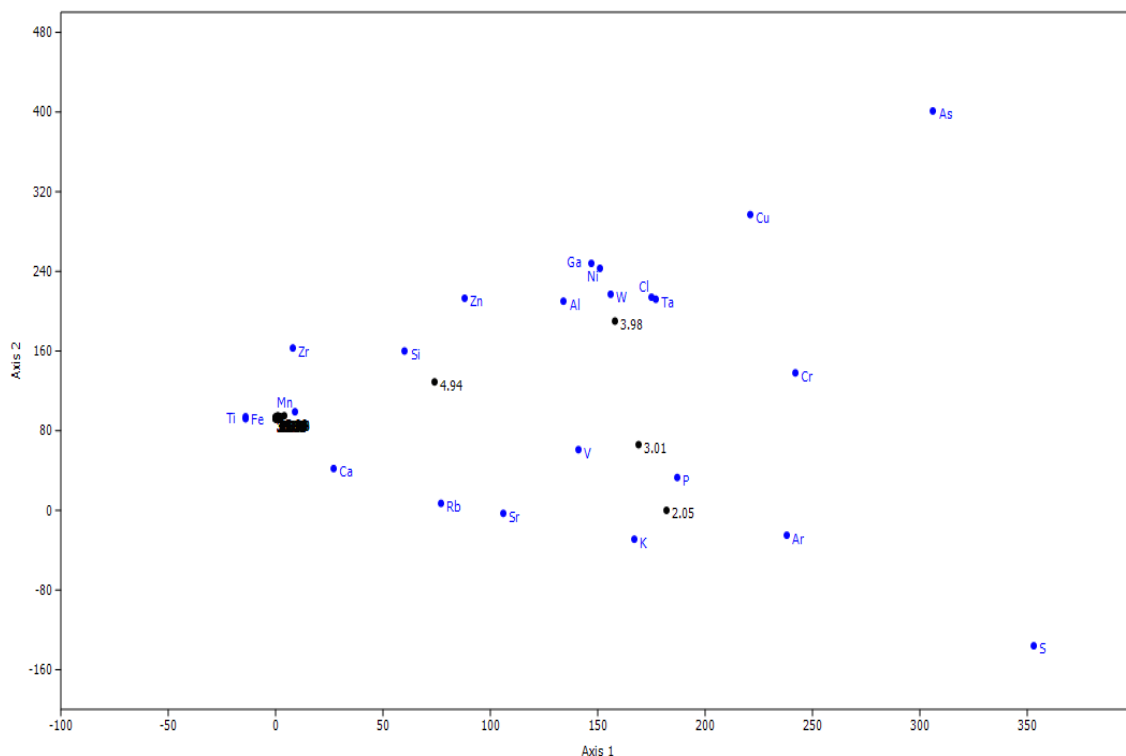


FIGURE 3.43: Lake Elmentaita XRF DCA, Axis 1 is the x-axis, and Axis 2 is on the y-axis.

The DCA Axis scores were plotted against Rb:Sr ratio, Mn:Fe ratio and Lake Oloidien depth, in Figure 3.44. The axes scores show no variation apart from at the surface. It is likely that mixing and bioturbation are the reason that there is such low variation in these data, since Lake Elmentaita is usually very shallow (<1 m deep).

Ratios of different elements can still be used to extract some useful information. Figure 3.44 shows the the Rb:Sr and Mn:Fe ratios, which have been used as proxies for weathering, and how oxygenated the sediment is respectively. Although at Lake Elmentaita Mn:Fe may relate to a different process, since Lake Elmentaita is very shallow. The periods with higher Mn:Fe ratios do appear to coincide with low lake water level on visual inspection, but changes in Mn:Fe may relate to different weathering processes during

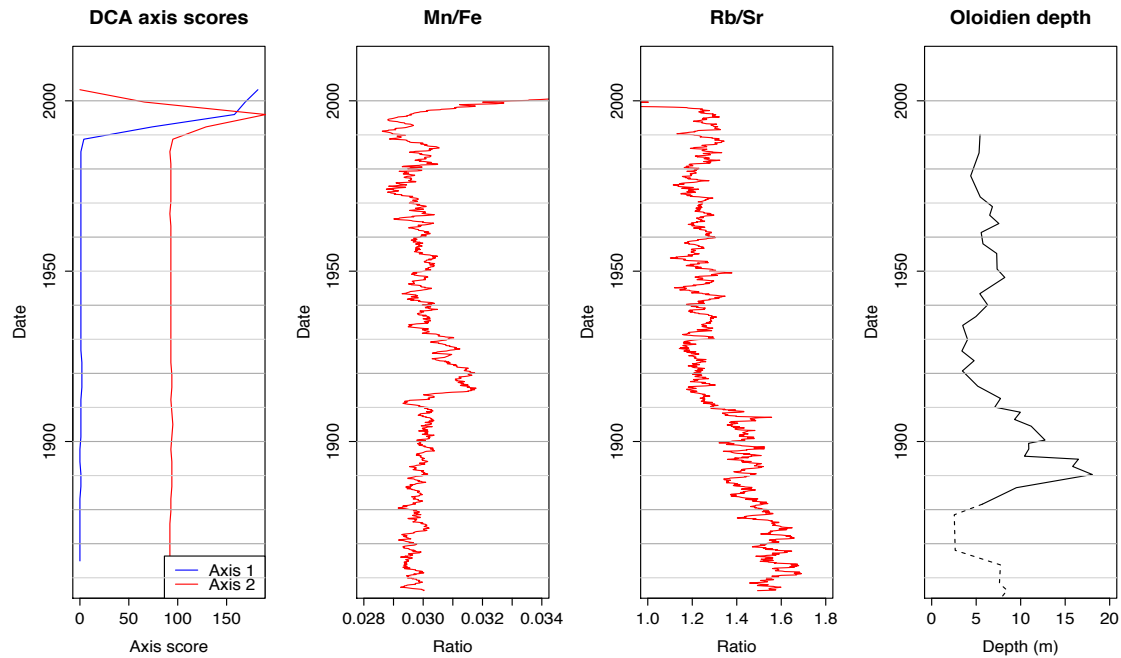


FIGURE 3.44: Lake Elmentaita ITRAX elemental data.

dry periods and the deposit of weathered rock by wind. It is likely that Lake Elmentaita dried up in the 1870s, so it is uncertain how meaningful this ratio is prior to 1880. It is possible that there was a break in the chronology during this time. Because of this, the ratios were plotted against lake water level for the sediments younger than 1880, and it was found that the Rb:Sr ratio correlated weakly with lake water level with an R^2 value of 0.415, whilst Mn:Fe ratio gave an R^2 value of only 0.258. This suggests that weathering has increased when lake water levels are higher at Lake Elmentaita. This is in contrast to Lake Bogoria, which sits at the bottom of a steep escarpment slope, where weathering increased during dry periods. Lake Elmentaita is situated in much flatter terrain away from the rift escarpments, and so the dominant weathering mechanism is more likely to be a result of rainfall.

Date	Depth	Axis 1	Axis 2	Date	Depth	Axis 1	Axis 2
2003.26	2.05	182	0	1930.48	21.33	1	93
1999.64	3.01	169	66	1926.82	22.3	1	93
1995.97	3.98	158	190	1923.19	23.26	2	93
1992.35	4.94	74	129	1919.53	24.23	2	94
1988.73	5.9	4	95	1915.91	25.19	2	94
1985.06	6.87	1	92	1912.28	26.15	1	93
1981.44	7.83	1	93	1908.62	27.12	1	94
1977.78	8.8	1	93	1905.00	28.08	1	95
1974.16	9.76	1	93	1901.34	29.05	1	94
1970.49	10.73	1	93	1897.71	30.01	0	93
1966.87	11.69	1	92	1894.05	30.98	0	94
1963.25	12.65	1	93	1890.43	31.94	1	94
1959.58	13.62	1	93	1886.80	32.9	1	94
1955.96	14.58	1	93	1883.14	33.87	0	93
1952.30	15.55	1	93	1879.52	34.83	0	93
1948.67	16.51	1	93	1875.85	35.8	0	92
1945.01	17.48	1	93	1872.23	36.76	0	92
1941.39	18.44	1	93	1868.61	37.72	0	92
1937.76	19.4	1	93	1864.94	38.69	0	92
1934.10	20.37	1	93				

TABLE 3.7: Lake Elmentaita ITRAX DTC Axis scores.

3.7 Discussion

The reason for using a palaeolimnological approach was to understand how phytoplankton and potentially flamingo populations have changed at these lakes over the last 100+ years. To do this organic matter abundance, pigment, and elemental data were obtained for analysis.

3.7.1 Lake Bogoria

A south basin core was successfully dated using a gamma ray spectrometer, where a distinct ^{210}Pb decay curve was identified. The range in the accumulation rate errors for ^{210}Pb is 0.47 cm yr^{-1} to 0.56 cm yr^{-1} . A clear ^{137}Ce peak was also identified, and the accumulation rate estimated from the spread of the ^{137}Ce signal to be 0.51 to 0.61 cm yr^{-1} . The average accumulation rate for the south basin of Lake Bogoria was estimated from these data to be 0.54 cm yr^{-1} . The north basin accumulation rate was estimated by comparing the correlation between the organic matter contents of the north and south basin and was found to be slightly higher at 0.59 cm yr^{-1} . The age model was applied to the other Lake Bogoria palaeodata, a summary of which can be seen in Figure 3.46.

Although there were similar trends in organic matter content, the south basin contained a slightly higher proportion of organic matter than the north basin. This is likely to be

a result of changes in rainfall being exacerbated due to the Wasegus river inflow into the north basin. The Wasegus river freshens the north basin during wet periods relative to the south basin, and can carry high amounts of eroded material from the catchment, which is also likely to account for the higher accumulation rate in the north basin. The difference in organic matter content between the north and south basin is more pronounced after 1960, which suggests an increase in erosion in the Bogoria catchment. Kenya has experienced rapid population growth from approximately 8 million in 1960 to 46 million in 2014. The increasing pressure on resources has increased deforestation and overgrazing problems, and since the 1960s intensive agricultural farming methods have become widely implemented in Kenya. These activities all accelerate erosion.

The largest differences between organic matter abundance in the north and south basins occur between 1915 and 1930, and between 1960 and 1980, which correspond with peaks in the Rb:Sr ratio which is used as a weathering proxy. Lake Bogoria depth changes are expected to occur at the same time as those at Lake Oloidien because of the regional rainfall signal (see Figure 4.7), although changes at Lake Bogoria are expected to be less extreme due to the much lower surface area:volume ratio compared with Lake Oloidien. The geochemistry DCA Axis 1 values co-varied with change in lake water level, giving an R^2 value between lake water level and Axis 1 of 0.698 this suggests that during wet periods, weathering is primarily caused by runoff. Rb:Sr ratio was found to have an inverse relationship with lake water level, and t co-vary with the geochemistry DCA Axis 2 values, with an R^2 value between Axis 2 and Rb:Sr ratio of 0.708. The Rb:Sr ratio and lake water level do not co-vary as might be expected, since weathering is usually assumed to be predominantly caused by the in wash of weathered material by runoff. However, the impact of vegetation growth during wetter periods at Lake Bogoria is unknown. It is possible that in dry periods weathering by wind erosion and landslides becomes more important as a the cause of weathering, since the Eastern shore of Lake Bogoria meets the foot of a steep escarpment where landslides and erosion by wind may increase if vegetation cover is reduced.

The north and south basins showed significant differences in the pigment data, with a more continuous record of the fossil pigments in the north basin, although the abundance of these pigments is very low for most pigments in the south basin between 1870 and 1910. Since the phytoplankton communities in the Lake Bogoria are expected to be similar in the north and south basins these differences are likely to be primarily caused by different rates of degradation. The highest pigment abundances occur in the south basin during periods of low lake water level, which suggests that during high lake water levels pigment degradation increases in the south basin. Pigments preserve best in cold, dark, anoxic environments (Leavitt et al., 1994), and so in very shallow basins degradation will be increased due to exposure to light, oxygen, higher temperatures and bioturbation. In deeper basins, although conditions may be dark and anoxic which is ideal for pigment preservation, pigments can spend longer in the water column before reaching the lake

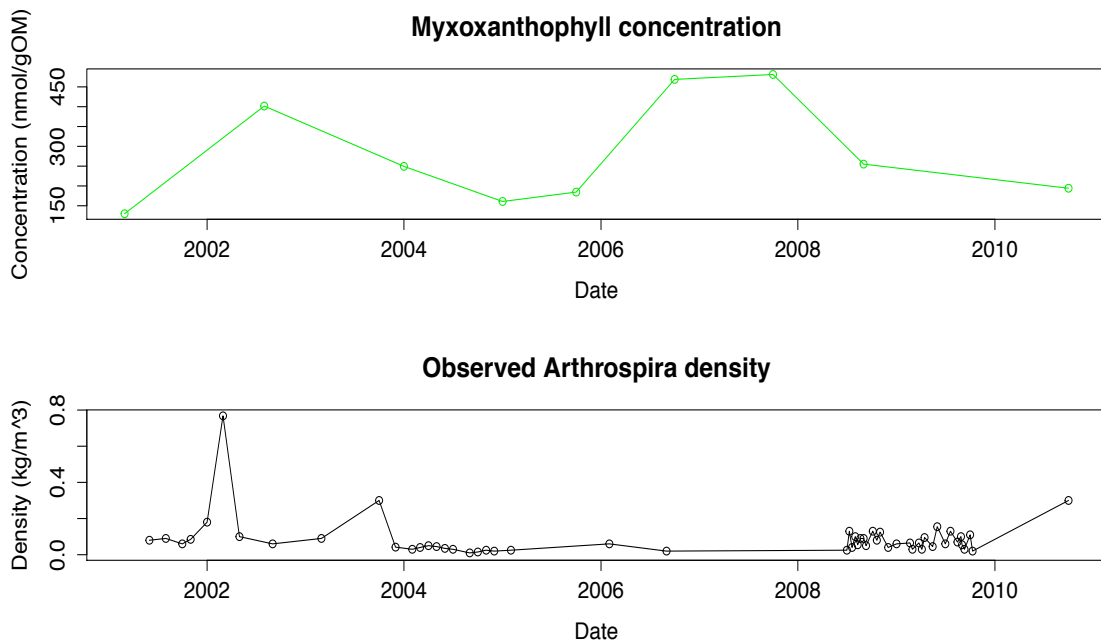


FIGURE 3.45: The myroxanthophyll pigment concentration from the south basin of Lake Bogoria and the observed *Arthrosphaera* density at Lake Bogoria from (Ballot et al., 2004; Schagerl & Oduor, 2008; Krienitz & Kotut, 2010; Kaggwa et al., 2012).

can be degraded before they reach the sediment water interface (McGowen, pers. com.). The north basin is 6m shallower than the south basin, and is also close to the mouth of the Waseges river which brings in silt-laden water from the catchment. This is likely to account for the low abundance of pigments in the south basin before 1910-1940. For example, zeaxanthin (a ubiquitous pigment) is found in very low abundance in the south basin before 1910, diatoxanthin, the chlorophyll pigments and their derivatives are all in very low abundance before 1940 (Figure 3.14). These pigments are associated with land and aquatic plants, algae, diatoms and cyanobacteria, and since there is still a high proportion of organic matter in the sediments during this time, these low pigment abundance's cannot be attributed to low lake productivity.

Crashes in *Arthrosphaera* were observed in 1978, 2001 and 2004 at Lake Bogoria. The pigment data shows a reduction in the cyanobacteria pigments in 2000-2001 which may be related to the 2001 crash. The organic matter profile does not reflect this crash in *Arthrosphaera*, probably because of the large amount of organic matter that would sink to the lake bed during a crash masks the period of lower lake productivity during the recovery, although the south basin shows a small reduction in productivity.

The south basin is periodically or permanently anoxic, and the sediments are undisturbed by resuspension, whereas the north basin may be susceptible to some disturbance since laminations were not seen in the north basin cores. This may be the reason why the pigments that are preserved in the south basin are approximately ten times more abundant than those found in the north basin.

The pigment DCA Axis 2 values correspond to the cyanobacteria pigments, which suggests that Lake Bogoria is most productive at lower lake water levels, where there is an increase in organic matter content in the sediments and cyanobacteria pigments usually dominate the phytoplankton community. There are fluctuations between algae and cyanobacteria in Lake Bogoria, although *Arthrosphaera* is usually dominant. There is a description of a change in phytoplankton occurring at Lake Bogoria by Krienitz and Kotut (2010), who observed a change in cyanobacteria community structure in 2006 where green picoplankton *P. salinarum* was dominant in the lake. *Arthrosphaera* had recovered to make up one third of the cyanobacteria population by 2008, and the remaining cyanobacteria consisted of lumps of *Anabaenopsis* sp., which disappeared by 2009, allowing *Arthrosphaera* to dominate once more (Krienitz & Kotut, 2010). This change can be seen in the pigment data for Lake Bogoria from the south basin. The pigment data from the south basin (Figure 3.14) shows nine peaks in green algae pigments that often occur during lower abundance of cyanobacteria pigments between 1940 and 2011. These peaks occur over time periods from one year to five years, and suggests that Lake Bogoria is likely to have experienced this shift in phytoplankton community more frequently than expected.

Myxoxanthophyll pigment concentration for the south basin of Lake Bogoria was plotted against the observed data in Figure 3.45. The observed data is not continuous, and most are single data points which may belie the overall trend in *Arthrosphaera* density, which makes it difficult to compare to average densities output by the pigment data. On visual inspection there appears to be some similarity in the profiles of the observed data and myxoxanthophyll concentrations before 2006, but it is difficult to draw a meaningful comparison.

The potential for nitrogen isotopes to be used as a flamingo proxy was investigated. *Arthrosphaera* has a lower $\delta^{15}N$ value of 4.1 (Burian et al., 2014) compared with the sediment which fluctuated between 7.0 and 9.2. Flamingos shed feathers into the lake, and also large numbers died at Lake Bogoria during the mortality events, particularly at the 1999-2000 event where 200,000 birds died, which corresponds to an increase in $\delta^{15}N$. Canthaxanthin is associated with colonial cyanobacteria and herbivore tissues (Leavitt & Hodgson, 2001). There are peaks in canthaxanthin between 1910 and 1930 that occur during low lake water levels in the north and south basins of Lake Bogoria, and corresponds with a high $\delta^{15}N$ value, which could lend support to the hypothesis flamingos can increase $\delta^{15}N$ values. The nitrogen isotope data $\delta^{15}N$ data appears on visual inspection, similar $\delta^{15}N$ changes to pigment DCA Axis 2 values which describes cyanobacteria abundance. Flamingos are likely to be at Lake Bogoria in large populations during these periods. However, when these data are plotted against each other the R^2 value is only 0.271. Higher resolution $\delta^{15}N$ will be needed, as well as other proxies for flamingo abundance such as the use of remote sensing to identify congregations (discussed in Section 3.8.2), before any conclusion can be drawn about how useful $\delta^{15}N$

might be as a proxy for flamingo populations. Since flamingos at Lake Bogoria tend to congregate in the central basin near the hot springs on the western shoreline, it would be useful to undertake nitrogen isotope analysis on a core from the central basin.

During 2012 Lake Bogoria water levels were increasing and there were high numbers of flamingos feeding on *Arthrosphaera* in the central and southern basins. However, the north basin was freshened by the high inflow from the Wasegus river. This caused the establishment of swamp around the north basin and the sudden increase in freshwater species normally found at the freshwater Lake Baringo to the north (pers. obs., 2012). The flamingo population was still significantly greater than the numbers of other bird species, and it is likely that flamingos have still been able to feed on *Arthrosphaera* at Lake Bogoria during higher lake water levels in the past which may account for the relatively consistent $\delta^{15}N$ levels before 1910. During this time Lakes Nakuru, Elmentaita and Oloidien were probably too fresh for *Arthrosphaera* to grow (as was the case in 2012). As a result flamingos may have congregated at Lake Bogoria and other more hyper saline lakes such as Lake Logipi during high lake water levels.

The palaeodata from the Lake Bogoria cores shows that Lake Bogoria experienced much fresher conditions between 1870 and 1810, which allowed for fresher water phytoplankton to compete with cyanobacteria. Overall productivity is lower during wetter periods, and the phytoplankton community is more diverse. In drier periods cyanobacteria dominates the phytoplankton community and overall productivity is higher. Lake Bogoria is likely to be stronghold for flamingo populations even during higher lake water levels, although the myxoxanthophyll pigment profiles show that large fluctuations in *Arthrosphaera* abundance was likely. In order for large flamingo populations to survive, other lakes must also be able to support high densities of *Arthrosphaera*.

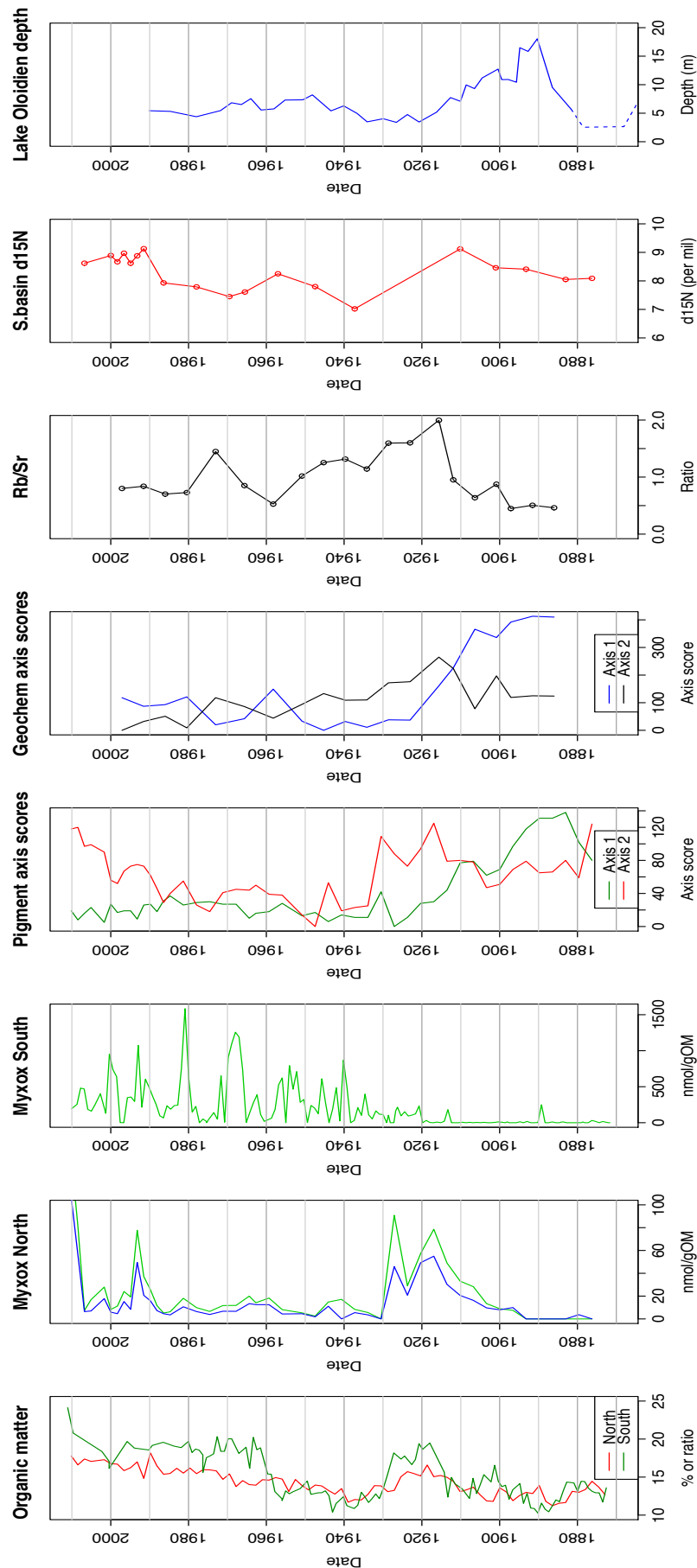


FIGURE 3.46: A summary of the Lake Bogoria data, including the organic matter content (lake productivity), myxoxanthophyll pigment concentration (a proxy for *Arthrosira* abundance) in the north and south basins, pigment DCA Axis 1 (green algae and diatoms) and Axis 2 scores (cyanobacteria), geochemistry DCA Axis 1 (weathering by runoff or lake depth) and Axis 2 scores (weathering during dry periods by wind and landslides), Rb:Sr ratio (weathering), $\delta^{15}\text{N}$ data (flamingo populations), and Lake Oloidien depth data (Verschuren et al., 1999).

3.7.2 Lake Oloidien

The Lake Oloidien core was dated by comparing the organic matter profile to the Verschuren et al. (1999) data. The accumulation rate was lower than the accumulation rate at Lake Bogoria averaging 0.44 cm yr^{-1} , apart from between the years 1900 and 1940, where accumulation is reduced to 0.22 cm yr^{-1} by swamp and papyrus stands that cause the weathered rock carried by runoff to precipitate before it reaches the lake (Verschuren et al., 1999). This reduction in weathered rock causes a relative increase in the proportion of organic matter during this period, which can be seen in the summary of the Lake Oloidien palaeodata in Figure 3.47.

The pigment data contained high concentrations of cyanobacteria pigments aphanizophyll and zeaxanthin. As for Lake Bogoria, the interpretation of the data is not straight forward since the pigment data do not directly represent the abundance of different flora. This is because of differential preservation. It is likely that there are much higher abundances of cyanobacteria pigments than pigments associated with green algae or diatoms at Lake Oloidien because during fresher water periods the lake productivity is likely to reduce, and degradation of pigments occurs during high lake water levels as they sink towards the lake bed. During lake water levels below 7m preservation rate increases, as does lake productivity at lower water levels. Axis 1 of the pigment DCA was representative of cyanobacteria pigments, and Axis 2 a mixture of green algae and cyanobacteria. Higher resolution data would be useful to improve the interpretation of the Lake Oloidien results.

The elemental data suggest that there was increased weathering in the catchment before 1925. The organic material in the lake at this time appeared to be dominated by a diverse phytoplankton community (Axis 2 of the DCA axis score), with cyanobacteria pigments (Axis 1) dominating the phytoplankton community from the 1995-2011. It is likely that *Arthospira* dominated the phytoplankton community during this period because the myxoxanthophyll pigment (associated with *Arthospira*) is present. It was found that there is a more diverse phytoplankton community at Lake Oloidien, although cyanobacteria could dominate during low lake water levels, which suggests that Lake Oloidien has been able to support some of the lesser flamingo population during low lake water levels.

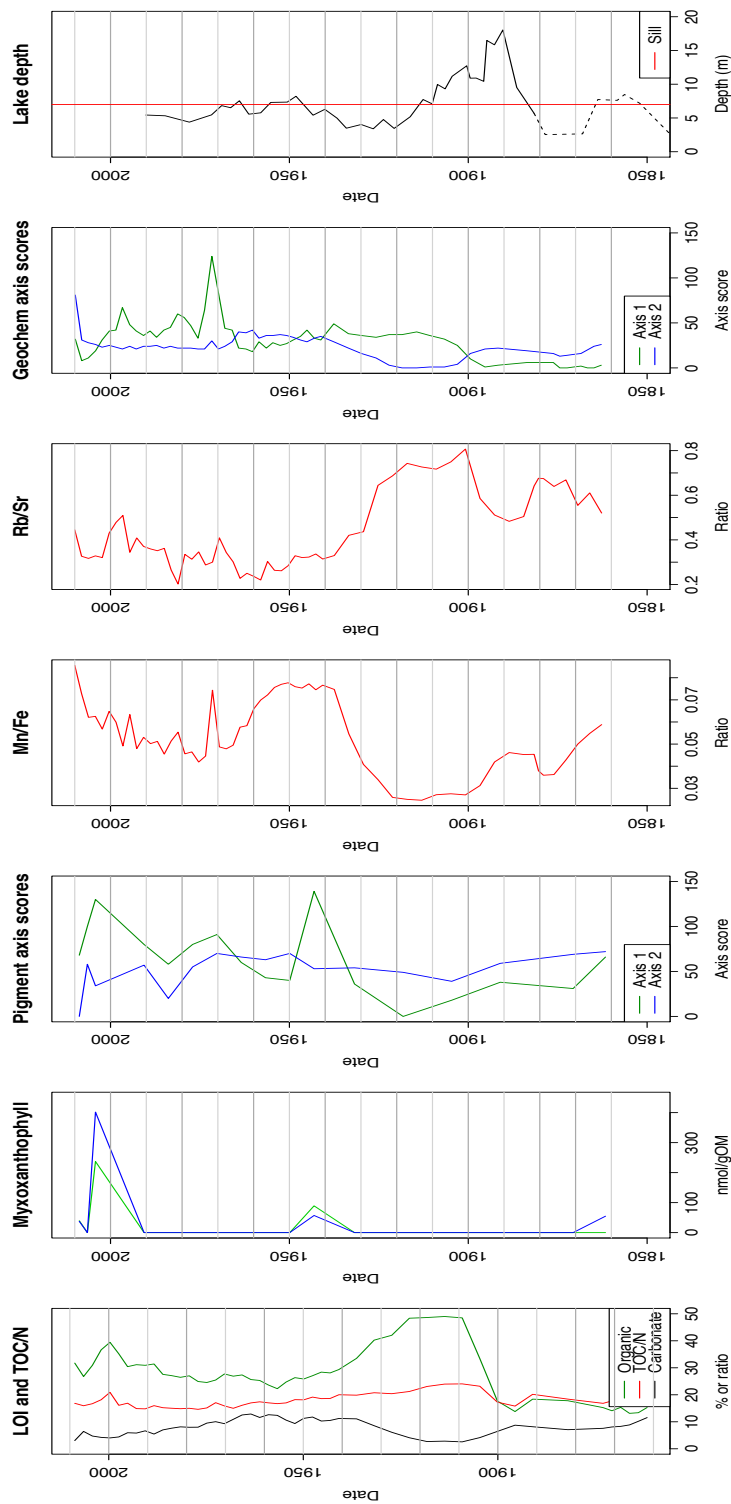


FIGURE 3.47: A summary of the Lake Oloidien data, organic matter content (productivity), and reduced sedimentation between 1900 and 1940, mycoxanthophyll (*Arthrospira*), pigment DCA Axis 1 (green algae, diatoms and cyanobacteria) and Axis 2 (green algae, diatoms and cyanobacteria) scores, Mn:Fe ratio (sediment oxygen level) the Rb:Sr ratio (weathering by wind), Axis 1 (weathering by wind), Axis 2 scores (weathering by runoff), and Lake Oloidien depth data by Verschuren et al. (1999).

3.7.3 Lake Elmentaita

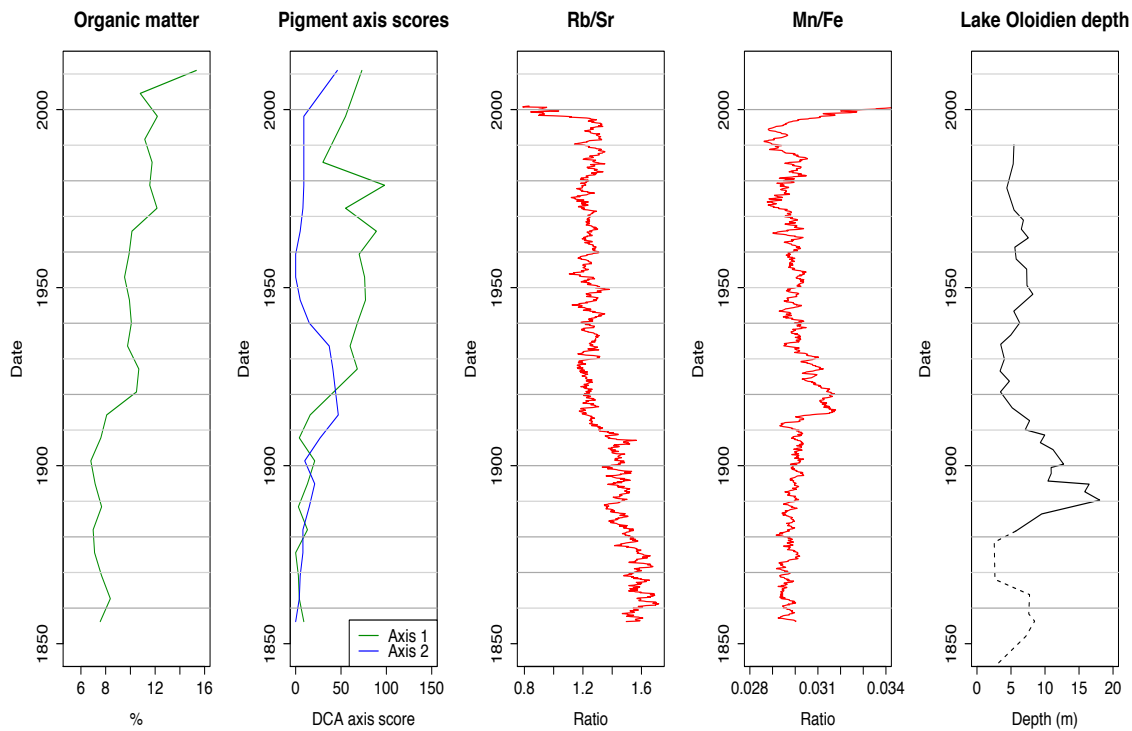


FIGURE 3.48: A summary of the Lake Elmentaita data, including the organic matter content, pigment DCA Axis scores, Rb:Sr and Mn:Fe ratios, alongside Lake Olloidien depth data by Verschuren et al. (1999).

A summary of the Lake Elmentaita palaeolimnological data can be seen in Figure 3.48. Lake Elmentaita dates were estimated by comparing the Mn:Fe and Rb:Sr elemental ratios with those of Lakes Bogoria and Olloidien. The Mn:Fe ratio changes for the Lake Olloidien and Elmentaita cores both had distinct changes that aligned for both ratios when a 25 cm of the Lake Elmentaita core was dated at 1856. If this is correct, then the accumulation rate at Lake Elmentaita would be 0.264 cm yr^{-1} , which is the lowest accumulation rate of the three lakes in this study.

It is logical that Lake Elmentaita would have a lower accumulation rate due to the nature of the sediment collected from each lake; the Lake Elmentaita core was much denser and it was more difficult for the gravity corer to penetrate the lake bed. Lake Olloidien was more watery and contained more organic material but could still be transported whole without mixing the sediment. By contrast at Lake Bogoria the high water content of the sediment meant that the core tube only felt resistance at around 80 cm depth and it was impossible to transport without mixing the material. This was due to the very high productivity in Lake Bogoria and the corresponding high sedimentation rate. Lake Olloidien was less productive, and Lake Elmentaita the least productive lake with the lowest sedimentation rate. The accumulation rate estimate is supported by the increase in Mn:Fe ratio at low lake water levels in the 1920s and 1930s, which suggests

an increase in oxygenation of the sediments, and by the low pigment concentrations found before 1900 in the Lake Elmentaita sediments, which may reflect a reduction in lake productivity during higher lake water levels in fresher conditions.

The organic matter content increased throughout the Elmentaita core, and may be related to increased nutrient concentrations, and general lower lake water levels after 1910 causing an increase in lake productivity.

The pigment data showed that most pigments co-varied together (DCA Axis 1), suggesting a diverse phytoplankton community, apart from one cyanobacteria pigment (DCA Axis 2) that increased when Axis 1 values were low. This suggests that cyanobacteria can dominate the Lake Elmentaita phytoplankton community, during lower lake water levels. Myxoxanthophyll was not identified in the sediments, despite observations by Melack (1988), who found *Arthrosphaera* growing in Lake Elmentaita throughout 1973 when lake water levels were low. It was also growing in Lake Elmentaita in 2007 (Adeka et al., 2008). It is likely that myxoxanthophyll has been present in Lake Elmentaita during low water levels, but has degraded in the sediments or is in such low abundance that it is difficult to detect. During this time benthic diatoms may also have increased in abundance, since diatoxanthin was found to peak in the 1930s, and benthic diatoms can grow on the lake bed where flamingos have been seen to feed during periods of low food abundance. Canthaxanthin is associated with cyanobacteria and herbivore tissues, and although the peak in diatoxanthin and canthaxanthin could be caused by improved preservation of pigments it may also be caused by an increase in benthic diatom abundance. This seems counterintuitive since the salinity of Lake Elmentaita would increase during low lake water levels. However, Lake Elmentaita is less saline than Lake Bogoria, and the data suggests that there is usually a diverse phytoplankton community usually exists at Lake Elmentaita, which becomes more suitable for benthic diatom growth as lake water levels reduce (as more light reaches the lake bed), and at very low lake water levels *Arthrosphaera* is likely to begin to dominate the phytoplankton community. An increase in benthic diatom abundance or *Arthrosphaera* would make Lake Elmentaita a more suitable feeding site for lesser flamingos, which could be the cause of the increased canthaxanthin abundance.

The dates could be confirmed using ^{210}Pb dating as was used successfully for the Lake Bogoria core. However, the sediment is likely to be more disturbed at Lake Elmentaita because of the low lake water levels (usually less than 1m) and may not produce a clear decay curve. Future work to support the dating model for these cores could include pollen 3.8.1.

The palaeolimnological data is useful for identifying changes in lake phytoplankton. The pigment and organic matter data has identified fluctuations between algae and cyanobacteria at hypersaline Lake Bogoria, and a more diverse phytoplankton community and probably macrophytes at Lakes Oloidien and Elmentaita which have fresher conditions.

The geochemistry data has been useful in comparing regional changes, the Rb:Sr ratio was used as an indication of the amount of weathering in a catchment, and showed similar fluctuations between lakes that allowed for Lake Elmentaita dates to be inferred. These data show how variable phytoplankton has been at Lakes Bogoria, Elmentaita and Oloidien have been during the past 100-150 years, and are useful for comparing with the model outputs to help understand if the model is behaving correctly. These palaeolimnological data show that changes at these soda lakes can be rapid and of high magnitude.

3.8 Future work

3.8.1 Pollen

If pollen from plant species that have been introduced into the region can be identified in the core, then it is possible to estimate the date of the samples where these species appear in the sediment record. Many exotic species have been introduced into Kenya from the 1800s onwards to provide fast growing building materials, fuel or food. Pollen from some of these species are likely to be present in the sediments of Lakes Bogoria, Elmentaia and Oloidien. Some examples include maize, *zea mays*, which first appears in Lake Boringo sediments at ca. 1800, pine, *Pinus patula*, and white cedar, *cupressus lusitanica*, which were introduced by europeans in 1910 (Kiage & Liu, 2006). In the 1960s intensive agriculture became established as pastoralists began intensively growing crops such as maize. Prosopis, *Prosopis juliflora*, is an invasive species that was initially introduced in the Boringo district in 1983 as part of a government initiative to provide a fast growing tree that could be used for fuel, but has since spread widely in the Marigat region and is now invading the Lake Bogoria National Reserve (pers. obs.).

3.8.2 Remote sensing

To reach remote and challenging locations can be prohibitively expensive. A remote sensing approach is often used for remote locations since it is much more economical with respect to time and the cost of reaching the same locations to make direct observations. There are errors associated with these methods, particularly when struggling with the limitations of low resolution images.

Barber-Meyer et al. (2007) used satellite imagery to estimate the size of emperor penguin colonies in the Antarctic. A supervised classification of the Quickbird satellite images was achieved using aerial photographs of the accessible penguin colonies, and this classification algorithm was then applied to the satellite images of the inaccessible colonies. Supervised classification involves the manual selection of land cover training sets from an image. A land cover classification algorithm can use these training sets to identify

which spectral signatures are associated with each land cover class. It can then evaluate every pixel in the image and assign it to one of the land cover classes. This method enabled relative penguin abundances to be estimated to the nearest few thousand, which is sensitive enough to identify catastrophic changes in penguin population (Barber-Meyer et al., 2007). This approach could be used to identify flamingo populations. Quickbird, launched in 2001, and has a spatial resolution of 65 cm , which means that each pixel in the satellite image corresponds to 65 cm on the ground surface. Since the study by Barber-Meyer et al. (2007), WorldView-1 and WorldView-2, have been launched, both have a resolution of 50 cm . GeoEye-1, launched in 2008, collects the highest resolution commercially available images, with a resolution of 41 cm in panchromatic mode. It is possible to buy some of this high resolution data, although it may be limiting for small projects. The cheapest Geo-eye product costs US\$11.50 per square km , which to cover the area of Lake Bogoria once would cost approximately US\$550. Quickbird images would cost US\$18 per square km .

The Landsat satellite series have collected images at a resolution of 30 m since the launch of Landsat-1 in 1972. These images are now free, and are the longest time series of images available. Given the lack of sensitivity to changes in penguin population using Quickbird images of 0.65m resolution (Barber-Meyer et al., 2007), it would seem unlikely that flamingo populations could be estimated using images of 30 m resolution. However, it may be possible to measure the ‘pinkness’ of pixels to try and identify the presence of flamingos, and when the lesser flamingos are grouped together around the lake shore they should be identifiable using landsat images. If this was a viable method it could at least be used to identify periods when a large proportion of the total flamingo population was in one location.

Landsat images have been used to measure changes in lake surface areas (Tebbs, 2013), which could be used alongside other water level proxies. Tebbs et al. (2013a) also used remote sensing to identify the surface areas between which breeding islands are available at Lake Natron. The cyanobacteria abundance for the time periods where breeding islands are available at Lake Natron could also be explored using Landsat images (Tebbs et al., 2013b).

Satellite imagery may be useful for identifying flamingo populations. Landsat images were selected and a location where most flamingos tend to congregate (pers. obs.) was located in two images and compared with the help of Robin Wilson at the University of Southampton. The flamingos can be clearly identified in the red pixels in Figure 3.49, and are absent or in low numbers in Figure 3.50. The flamingos are at a high density in Figure 3.49 and identifying smaller groups would be increasingly difficult. However, using landsat images can definitely be used to identify large congregations of flamingos. It may be possible to identify breeding populations at Lake Natron using these images. However, it would be a significant amount of work to create an algorithm to identify populations automatically, and beyond the scope of this project.

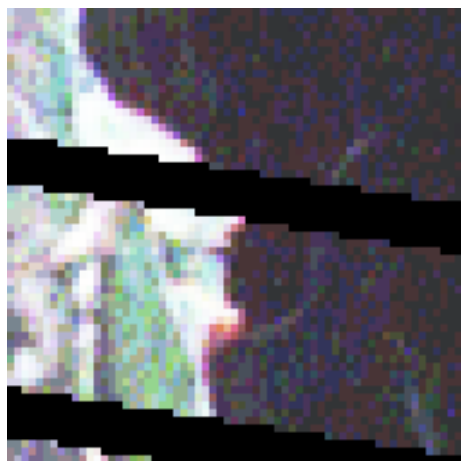


FIGURE 3.49: Loburu hot springs with flamingos



FIGURE 3.50: Loburu hot springs without flamingos

Chapter 4

Hydrological model

This chapter describes the hydrological model. The literature review (Section 4.1) relates the model to previous work, and then in Section 4.2, the final model is described and the model output can be seen in Section 4.3. The outputs from the hydrological model are then used as inputs to the *Arthrosipa* and flamingo models, which are described in Chapters 5 and 6 respectively. The model was written in java in a text editor called Sublime Text, and version control was managed using GitHub.

4.1 Literature review

There are many physical parameters that could be considered for a hydrological model. The change in lake water level for any lake depends on the water balance. Broadly, this is the balance between the amount of water entering the lake catchment by precipitation, and the water leaving the catchment by evaporation and out-flowing rivers.

$$\Delta V = P + R + Gi - E - Go \quad (4.1)$$

Where ΔV is the change in volume, P is precipitation, R is run-off, Gi is groundwater input, E is evaporation, and Go is groundwater output. There is no surface outflow term for endorheic lakes.

Precipitation in the catchment finds its way into the lakes in different ways. This includes direct precipitation, runoff, and groundwater sources like the hot springs. Water leaves the lake by evaporation or by seeping through the lake basin into the bedrock. In the case of a closed soda lake such as those considered here, evaporation and groundwater flow are the only outlets. The precipitation that enters the lake directly depends on the surface area of the lake, and the amount of run-off depends upon the catchment size, as well as the amount of water diverted from rivers upstream for domestic use or crop irrigation. The volume of lake water lost by evaporation depends upon the surface

area of the lake and the ratio of volume to surface area, determined largely by the lake bathymetry.

Three hydrological models are described below. They differ in complexity, and could be applied to the soda lakes to explore past changes.

A hydrological model of Lake St. Lucia, a shallow estuarine lake in Southern Africa, was developed by Hutchinson and Midgely (1978). They used coupled mathematical models to model the runoff from the catchment into the lake, as well as the flow through the lake towards the sea. The catchment model was calibrated using rainfall data, and limited river gauge and evaporation records. The lake was represented by a series of storage cells. The affect of lake bathymetry on the lake surface area was simplified by using a depth vs area curve for each cell. For each monthly iteration the change in water stored in each cell was calculated from the inflow to the lake cell minus the volume of water evaporated from the lake surface. Salt concentration change was calculated using dispersion and advection equations. Advection, the mass transport of salts by water moving from one cell to another, was calculated in the model using the rate of flow between the cells. Dispersion was calculated by considering the cross sectional area between adjoining cells and the salinity gradient across the join. The model was found to reproduce lake water levels and salt concentrations reasonably well, but there were difficulties when considering the estuary part of the lake which connected it with the sea due to variations in the size of the estuary mouth (Hutchinson & Midgely, 1978). This complication would not affect a model of the soda lake basins.

Bergner et al. (2003) modelled the water balance for Lake Naivasha. This model calculates the lake level of Lake Naivasha using an energy budget algorithm. This approach allows the rate of evaporation to be modelled by considering incoming and outgoing radiation at the earth-air and water-air interface. Other parameters used in the model were calculated by averaging weather station data across the lake catchment. The model parameters were thoroughly tested using modern climate parameters and was then applied to palaeoclimate conditions. The modelled palaeolake levels agreed well with evidence of past lake levels observed during field visits. The total uncertainty was calculated by comparing rainfall amounts predicted using the modern lake water balance model with the basin averaged rainfall recorded from weather stations. The error was calculated to be less than 15% (Bergner et al., 2003).

Becht et al. (2006) modelled the water balance of lakes Naivasha, Elmentaita and Nakuru using a simple hydrological model. The model includes inflows from rivers and rain that falls directly onto the lake surface, outflows of evaporation, and a groundwater flow component. The model calculates the change in lake volume every month in m^3 using a water level:lake surface area:lake volume relationship for each lake generated using lake bathymetry maps.

$$\delta V = R + (P - E)SA + G + Aq \quad (4.2)$$

Where V , P and E are as above for equation 4.1, runoff, R is more specifically defined as the river inflow to the lake, G is regional groundwater flow, and SA is the lake surface area. Aq is the aquifer flow between the lake and a hypothetical dynamic groundwater aquifer. The functionality of the model is described in more detail in Becht and Harper (2002), where the model was originally constructed for Lake Naivasha. The inputs to the model were based on real data from the catchment of each lake, including average rainfall and river flow records. Groundwater flow data was based on the analysis of the O-18 and H-2 stable isotopes naturally found in lake water and the optimization of groundwater flow parameters in the groundwater flow model (Becht et al., 2006).

The model reproduced observed lake water levels well for each lake with an error of less than 2m. The groundwater flow was calibrated so that lake water level levels were reproduced as accurately as possible. However, the ‘groundwater flow’ actually absorbs the errors from missing data and aspects of the hydrological cycle not included in the model. These results are encouraging because the simplicity of the model and the small number of input parameters required to reproduce lake water level mean that it is much more easily applied to other lakes, and indeed the model was applied successfully to lakes in Ethiopia (Ayenew & Becht, 2008).

The hydrological model by Becht and Harper (2002) is the simplest model and has been successfully applied to different lakes in the Rift Valley, including lakes Elementaita and Nakuru. It would be sensible to use this model as a starting point for the flamingo soda lakes in this study. It is likely that other soda lakes such as Bogoria and Natron have not been included by Becht et al. (2006) because there are insufficient river inflow data for Bogoria, and hardly any data at all available for Lake Natron. Lake Natron also has a more complex aspect to evaporation from the lake surface because of the high salt concentration. To apply this model to other lakes, the parameters would have to be estimated and the output compared with remotely sensed lake surface area and rainfall data.

4.2 Overview

A simple hydrological model was written in java to calculate the change in lake depth, surface area, volume and salinity in response to rainfall over a series of monthly time-steps. The way that a lake responds to rainfall depends upon its catchment area, runoff and bathymetry. Bathymetry was described using a simple depth:surface area curve,

with volume estimated from the surface area, depth, and by approximating the shape of the lake basin using simple geometric shapes (described later in section 4.2.1).

The hydrological model for these lakes is relatively simple because there is no outlet apart from evaporation for the soda lakes (Figure 4.1). The only lakes with outflows in the region are the fresher lakes Baringo and Naivasha. The outflow for these two lakes occur underground as water seeps through the lake sediment and through the faults, preventing the build up of salts seen in other lakes.

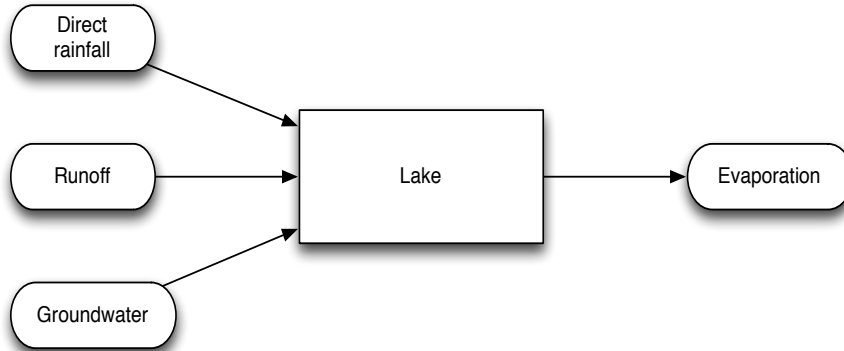


FIGURE 4.1: Hydrological model flow chart

There is uncertainty regarding the large groundwater component to the inflow for each lake, and the surface runoff inflows which are approximated from rainfall due to a lack of data available for river discharge in the catchments of these lakes.

The volumes of water to be added by direct rainfall, groundwater inflow, and runoff, and the volume to be subtracted due to evaporation for each month are calculated separately according to Equation 4.2.

$$V_t = V_{t-1} - EA_t + DR_t A_t + RO_t^x + GW_t^y \quad (4.3)$$

Where V_t is the lake volume at time t , V_{t-1} is the lake volume in the previous time step, E is the evaporation rate, A is the lake surface area, DR is direct rainfall, RO is the volume of runoff entering the lake from the catchment, x is a factor used to amplify runoff during periods of higher rainfall, GW is the volume of water inflowing as groundwater, amplified by y . The lake volume is updated daily.

The lake water volume is then updated by these values and the depth and surface area of each lake are updated. The model then outputs the hydrological parameters for each lake including monthly water level and surface area at each iteration.

4.2.1 Bathymetry

There are low resolution bathymetry maps available in the literature for Lakes Bogoria, Elmentaita, Nakuru, and Oloidien, and Logipi. The bathymetry of Lake Magadi was estimated using google Earth images because it is a more complex shape and could not be approximated as a circular basin. There was no data for Lake Natron, apart from its estimated depth and diameter, and so Lake Natron bathymetry was estimated assuming the basin is a very shallow circular pan. The concentration of salts in the lake at each volume was calculated from the data in tables based on the lake volume, by assuming the lake held a fixed mass of salts that changed in concentration as lake volume change occurred according to Tables 4.1 to 4.6. When the lake depth ($depth_{new}$) was between two depths in the bathymetry data ($depth_1 < depth_{new} < depth_2$) the new salinity ($salinity_{new}$) was estimated using a linear equation:

$$gradient = \frac{salinity_2 - salinity_1}{depth_2 - depth_1} \quad (4.4)$$

$$constant = salinity_1 - gradient * depth_1 \quad (4.5)$$

$$salinity_{new} = gradient * depth_{new} + constant \quad (4.6)$$

Where $salinity_1$ is the salinity at $depth_1$, and $salinity_2$ is the salinity at $depth_2$.

These salinities are theoretical and are the result of the depth:area curve used, and the assumption that salts will be evenly distributed throughout the lake irrespective of lake depth, mixing or salinity. In reality when lake water level reduces and salinity increases dramatically salt precipitates out of the water column. However, the salinity above which *Arthrosphaera* can grow (in the *Arthrosphaera* model this is estimated to be in the region of 100 ppt) is unimportant to the model because *Arthrosphaera* will not be present, and so modelling the precipitation of salts was not considered. The data used in the model can be seen in Tables 4.1, 4.2, 4.3, 4.4, 4.5 and 4.6.

Max depth	Surface area (km^2)	Volume (km^3)	Salinity (ppt)
0	0	0	200
1	28	0.009	151
2	75	0.034	41
3	150	0.084	17
4	169	0.147	10
4.5	189	0.172	8
5	250	0.214	6.7
5.25	300	0.229	5.9

TABLE 4.1: Lake Logipi bathymetry and salinity estimated using data from Castanier et al. (1993).

Max depth	Surface area (km^2)	Volume (km^3)	Salinity (ppt)
0	0	0	1000
2.5	5.8	0.048	800
3.5	10.4	0.12	496
4.5	14.5	0.22	277
5.5	19.1	0.35	172
6.5	22.6	0.49	123
7.5	24.3	0.61	99
8.5	25.5	0.72	83
9.5	27.2	0.86	70
10.3	34.0	1.17	52
12	40	1.6	37
15	65	3.2	18
18	100	4.0	15

TABLE 4.2: Lake Bogoria bathymetry and salinity estimated using data from Hikley et al. (2003) and Ballot et al. (2004).

Max depth	Surface area (km^2)	Volume (km^3)	Salinity (ppt)
0	0	0	1000
0.1	5	0.0002	500
0.5	12	0.0017	272
1.4	28	0.01	47
2.7	32	0.024	20
3.4	38.2	0.03	14.6
4.4	47.5	0.048	9.8
6	60	0.08	6

TABLE 4.3: Lake Nakuru bathymetry and salinity estimated using Vareschi (1982).

Max depth	Surface area (km^2)	Volume (km^3)	Salinity (ppt)
0	0	0	100
0.1	4	0.007	60
0.3	10	0.014	30
0.4	10.5	0.021	20
2.5	20	0.034	12
4	40	0.05	8.5

TABLE 4.4: Lake Elmentaita bathymetry and salinity estimated using data from Melack (1988).

Max depth	Surface area (km^2)	Volume (km^3)	Lagoon salinity (ppt)
0	0	0	1000
1	30	0.01	563
2	39	0.023	244
3	100	0.056	100
5	143	0.15	37
5.2	180	0.16	34
5.4	200	0.177	31
5.5	220	0.184	30

TABLE 4.5: Lake Magadi bathymetry and salinity. Bathymetry and salinity was estimated using google earth and data from Becht et al. (2006).

Max depth	Surface area (km^2)	Volume (km^3)	Lagoon salinity (ppt)
0	0	0	1000
0.5	81	0.013	415
1.0	400	0.08	70
1.5	600	0.18	31
1.8	804	0.26	18
2.1	900	0.33	12
2.4	1000	0.5	8

TABLE 4.6: Lake Natron bathymetry and salinity. Bathymetry and salinity estimated using data from Tebbs et al. (2013a).

4.2.2 Rainfall

The rainfall data used in the model has been compiled from different sources (Figure 4.2). Rainfall data has been provided by the Kenyan Meteorological Office (KMO) for Lakes Nakuru (1970 to 2011), Bogoria (1977 to 2003) and Oloidien (1970 to 2009). Annual Lake Nakuru rainfall data (1904 to 1973) recorded by the Kenyan Meteorological Office has been found in the literature (Masaya, 1975). The monthly data was approximated from the annual rainfall by multiplying the annual rainfall by the average proportion of annual rainfall that falls in each month. Lake Elmentaita is 20 km from Nakuru and so the rainfall data was applied to Lake Elmentaita in the absence of rainfall gauge data. The Tropical Rainfall Measuring Mission (TRMM) is a nasa satellite used to gather tropical rainfall data. TRMM aims to improve our knowledge about land-air-sea interactions in the tropics, which should improve the global circulation models used to explore climate change (NASA, 2014). Rainfall data was estimated for all lakes from the Lake Nakuru data from 1904 to 1970 by using the deviation from average annual rainfall and applying this deviation to average annual rainfall calculated from the TRMM or KMO data available, and from 1970 to 1998 where there is missing data Narok annual rainfall data was used for Lakes Logipi, Bogoria and Magadi in the same way to estimate missing monthly data.

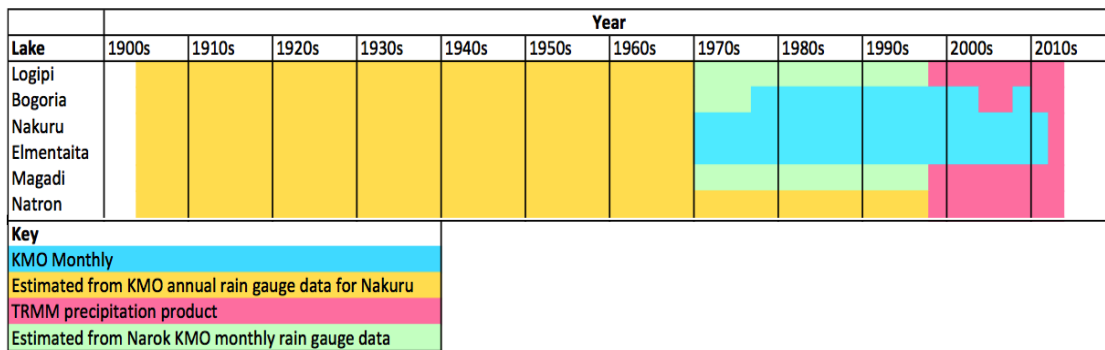


FIGURE 4.2: Rainfall data sources.

Google Earth Engine is a new platform providing access to a catalogue of remote sensing images and the tools for researchers to gather data from thousands of these images in a short space of time using cloud computing. It is currently still in development, but research carried out using Google Earth Engine has already been published in major journals (e.g. Hansen et al., 2013).

TRMM data has been extracted for each lake using Google Earth Engine to provide rainfall data for each lake from 1998 to 2013. The pixels in TRMM images are 25 km resolution. To get the rainfall at each lake the lake boundaries were digitised in Google Earth and were then imported into Google Earth Engine. The 25 km TRMM pixels overlaying the lakes were then divided into 5 km pixels, so that the proportion of each

pixel covering a particular lake could be taken into account. The temporal resolution of TRMM data is three hours. The 3-hourly data was summed over every month for each sub-pixel, and then the monthly rainfall was calculated by averaging over the number of pixels in or crossing the lake boundary. To compare the results of the remotely sensed rainfall data with the rainfall station data the data was plotted for visual inspection for the lakes with overlapping data (see Figures 4.3, 4.4 and 4.5) and the root-mean-square error (RMSE) was calculated for each lake. The rainfall data from Tebbs (Tebbs et al., 2013a; Tebbs, 2013) using TRMM data was also compared with our TRMM data (Figure 4.6) to compare the results.

To see how the rainfall at each lake fluctuates across the region, the deviations from the average rainfall at each lake were plotted for 1998 to 2012 (see Figure 4.7) the trends for each lake are similar, which suggests that the annual lake Nakuru data could be used in conjunction with the average monthly rainfall proportion calculated from the TRMM data to generate a relatively realistic rainfall dataset going back to 1904. There is one significant deviation from the overall trend which is for Lake Bogoria in 2002. This would not be the case if the TRMM data was used rather than the rain gauge data which is much higher in 2002, suggesting that the rain gauge reading may not always be reliable (see Figure 4.3). Possible causes of differences between the rainfall gauge data and TRMM data is that rainfall gauges are point sources rather than representative of the region. The lakes can generate their own weather and if the gauge is not very close to the lake then it is likely that the rainfall gauge will record lower rainfall values than occurs at the lake. Lower readings can also be a result of water beading on the walls of the gauge cylinder, and there is also the potential for human error unless data collection is automated.

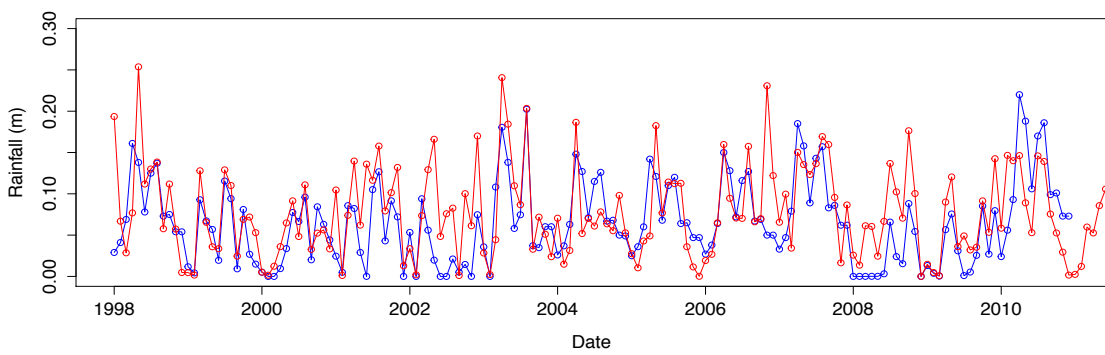


FIGURE 4.3: Lake Bogoria meteorological data (blue) were compared with TRMM data (red). The Root Mean Squared Error (RMSE) is 0.048.

Currently the only rainfall data for Lakes Logipi, Magadi and Natron are the TRMM data. The remaining rainfall data for these lakes was estimated from longer term rainfall datasets. There is monthly rainfall data for Narok for the period 1970 to 1998. Narok

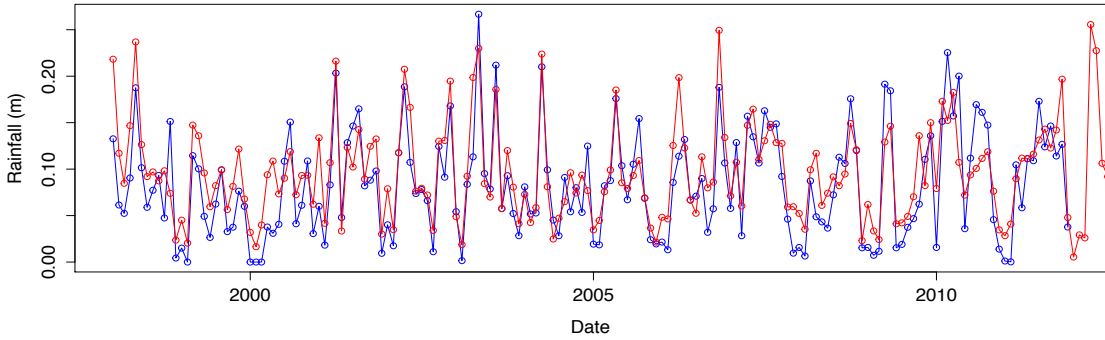


FIGURE 4.4: Lake Nakuru meteorological data (blue) were compared with and TRMM data (red) and gave an RMSE of 0.035.

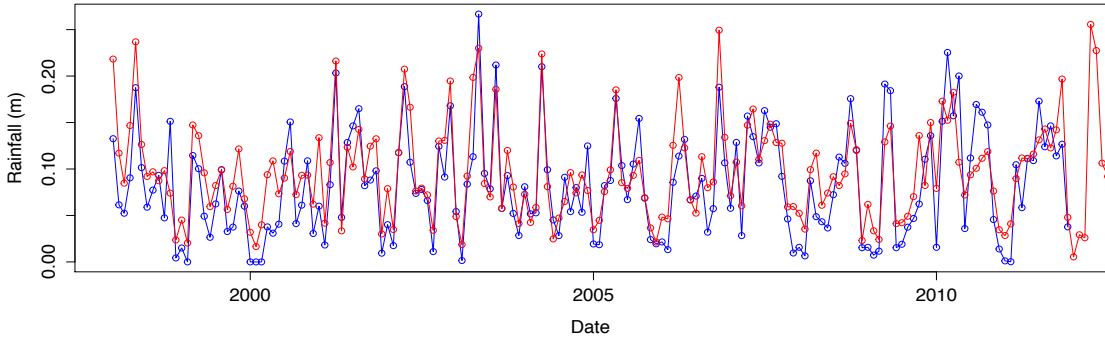


FIGURE 4.5: Lake Elmentaita meteorological data (blue) were compared with TRMM data (red) and gave an RMSE of 0.035.

is 100 km to the North of lake Magadi, and as can be seen from Figure 4.7, the Narok deviations are very similar to those for Lake Magadi.

Since the rainfall data fluctuates in a similar way across the region, it was decided that the deviation from the average rainfall for one lake could be used to estimate the rainfall at another where there is missing data.

The average monthly rainfall was estimated for Lakes Logipi, Natron and Magadi using the TRMM rainfall data and comparing with the average monthly rainfall for Narok from 1970 to 1998. There are some missing rainfall data and for these months the hydrological model will use average monthly rainfall values to calculate lake water level. For 1904 to 1970 annual Lake Nakuru data was used to estimate monthly rainfall at all lakes.

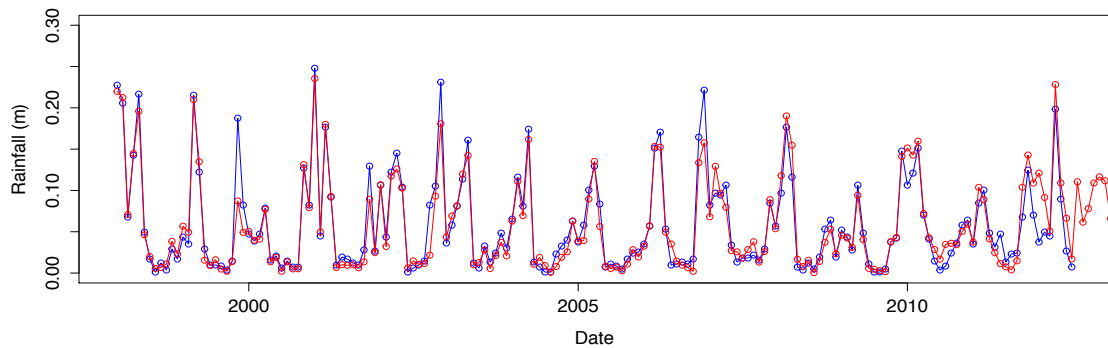


FIGURE 4.6: Lake Natron data from Tebbs et al. (2013a) and Tebbs (2013) (blue) were compared with TRMM data (red) and gave an RMSE of 0.018

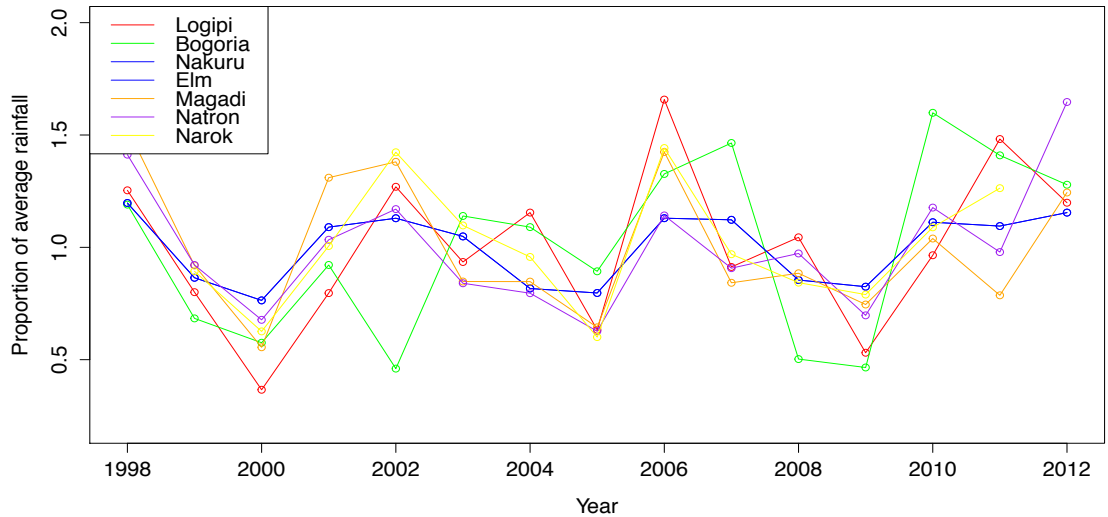


FIGURE 4.7: The proportional deviation from the average annual rainfall (1.0), from 1998 to 2012 using TRMM data where there is no rainfall gauge data for each lake.

4.2.3 Evaporation

Since the lake network transects the equator, changes in insolation and temperature over time were ignored, and evaporation rate was made constant at each lake. The evaporation rate at each lake can be seen in Table 4.7.

4.2.4 Runoff

The runoff term accounts for river inflow to the lakes and was estimated in the absence of river inflow data. The percentage of the catchment rainfall to reach the lake can be roughly estimated using a simplified hydrological spreadsheet model (Table 4.7). The deficit between evaporation and direct rainfall must be made up by inflow to maintain

lake water levels. It can be seen in Table 4.7 that very little of the rainfall falling in the Bogoria, Nakuru and Elmentaita catchments reaches these lakes. Much of the rainfall in tropical climates is quickly evaporated, or will be taken up by plants depending on the amount of vegetation, and some will infiltrate the soil and rock and become groundwater. The amount of runoff depends on many different factors including soil type, vegetation cover and abstraction by humans. The average runoff for Lake Nakuru was calculated using average rainfall and groundwater inflow data to produce a very low value of only 1.11% of Lake Nakuru's total inflow, only 0.34% of the total rainfall falling in the catchment. Raini (2006) suggested that 3.2% of the potential catchment runoff reaches Lake Nakuru. However, this volume would exceed the deficit caused by evaporation, and even if groundwater was not an inflow to Lake Nakuru, only a maximum of 1.5% of the catchment runoff would need to reach the lake to maintain the water level, and therefore 0.34% is a reasonable estimate. It is possible that the groundwater inflow estimated by Becht and Harper (2002) use different rainfall and evaporation values than are found in Table 4.7 since they are not specified in the paper. A cutoff parameter was used to prevent runoff reaching some lakes during periods when rainfall was reduced below a certain proportion of the average monthly rainfall expected.

There is no groundwater or runoff data available for Lakes Natron, Magadi and Logipi. In order to maintain lake water levels the deficit remaining once direct rainfall is subtracted from evaporation must be the sum of runoff and groundwater inflow. It was found that the proportion of groundwater inflow must be relatively low in order for the lakes to be able to fluctuate between the same limits as the observational data, particularly for Lake Logipi, which was forced to high average lake depths unless groundwater inflow was reduced to very low levels (Table 4.7). As a result of these low groundwater inflows, runoff in these catchments is much higher than expected compared with the Lake Elmentaita catchment runoff of 2.01%. Some of this difference may be a consequence of the more arid environments in which lakes Logipi, Magadi and Natron are situated, but is likely to also absorb other fluctuations in groundwater inflow change that have not been accounted for in the model.

Since there was no continuous data available for river inflow, modelled runoff was set as a rain dependent parameter that is equal to a proportion of the rainfall landing in three 'zones' around a lake (Figure 4.8). Studies of some soda lakes in the Kenyan Rift Valley suggest a three month lag time in lake water level response to rainfall (Vareschi, 1982). To emulate this the lake catchment is divided into three equal zones that store rainfall. At the beginning of each month rainfall falls and is stored in each zone. Then rainfall stored in zone one (closest to the lake) moves into the lake in the same month, and water is transferred from zone two to zone one, and from zone three to zone two, with zone three store then becoming zero until the next month's rainfall. This allows for a lag time of three month's for the rainfall landing in the outer zone of the lake catchment to reach the lake.

	Logipi	Bogoria	Nakuru	Elmentaita	Magadi	Natron
Evaporation ($m\ yr^{-1}$)	2.3 ₁₅	2.6 ₂	1.8 ₃	1.8 ₃	2.43 ₁	2.43 ₁
Direct rainfall ₄ ($m\ yr^{-1}$)	0.389	0.845	0.923	0.923	0.657	0.705
Groundwater inflow ($m\ yr^{-1}$)	0.06 ₁₀	1.200 ₁₀	0.857 ₇	0.400 ₁₀	0.71 ₈	0.6 ₁₀
Runoff ($m\ yr^{-1}$)	1.851 ₁₀	0.555 ₁₀	0.02 ₉	0.477 ₁₀	1.063 ₉	1.125 ₁₀
Direct rainfall (% of total inflow)	16.9	32.5	51.3	51.3	27.0	29.0
Groundwater (% of total inflow)	2.6	46.15	47.6	22.2	29.2	24.7
Runoff (% of total inflow)	80.5	21.34	1.11	26.5	43.7	46.3
Catchment size (km^2)	720 ₁₁	1500 ₁₂	1800 ₁₂	500 ₁₂	1000 ₅	1000 ₅
Lake area (km^2)	5-200 ₁₁	34 ₁₂	28 ₁₂	20 ₁₂	100 ₁₃	81-804 ₁₄
Lake area (% catchment)	13.9	2.27	1.56	4.0	10.0	40.0
Runoff (% of catchment)	66.1	1.49	0.34	2.01	16.2	63.8

TABLE 4.7: Inflows and outflows calculated or estimated for each lake. 1. Evaporation for Lake Magadi (Becht et al., 2006) was also used for Lake Natron as these lakes experience similar environmental conditions. 2. Renaut and Tiercelin (1993). 3. Nakuru evaporation was estimated from the other hydrological data as it was not specified in the Becht and Harper (2002) or Becht et al. (2006) hydrological models. Since Lakes Nakuru and Elmentaita are only 20 km apart, and no evaporation value was found for Lake Elmentaita, the same value was used for both lakes. 4. Calculated as the average of the available annual rainfall data for each lake as seen in section 4.2.2). 5. Speculative starting point for the model parameterisation in the absence of measured parameters. 7. Becht and Harper (2002). 8. Becht et al. (2006). 9. Calculated from the other hydrological data, the runoff value makes the total inflows equal to the rate evaporation. 10. Estimated based on surface area data using the hydrological model. 11. Junginger (2011). 12. Oduor and Schagerl (2007b). 13. Matagi (2004). 14. Tebbs et al. (2013a), Tebbs (2013). 15. Nyenzi et al. (1981).

The total potential runoff was determined by the volume of runoff in zone 1, which is the runoff that will enter the lake this month, and the deviation of this month's rainfall from average annual rainfall (calculated from the whole rainfall dataset). It has been found for the Lake Nakuru drainage basin that proportionally less runoff reached the lake during drier periods (Murimi & Prasad, 2005), and so the runoff was made proportional to the amount of monthly rainfall. The runoff is therefore reduced during drier than average months and increased during wetter than average months. This response is amplified by a parameter called 'runoff power'. The proportion of runoff that enters a lake is determined in the model by the total potential runoff raised to a runoff-power. This runoff-power is different at each lake to allow for differences in catchment, lake size, and absorb variations in soil properties, abstraction, evaporation, transpiration and land use.

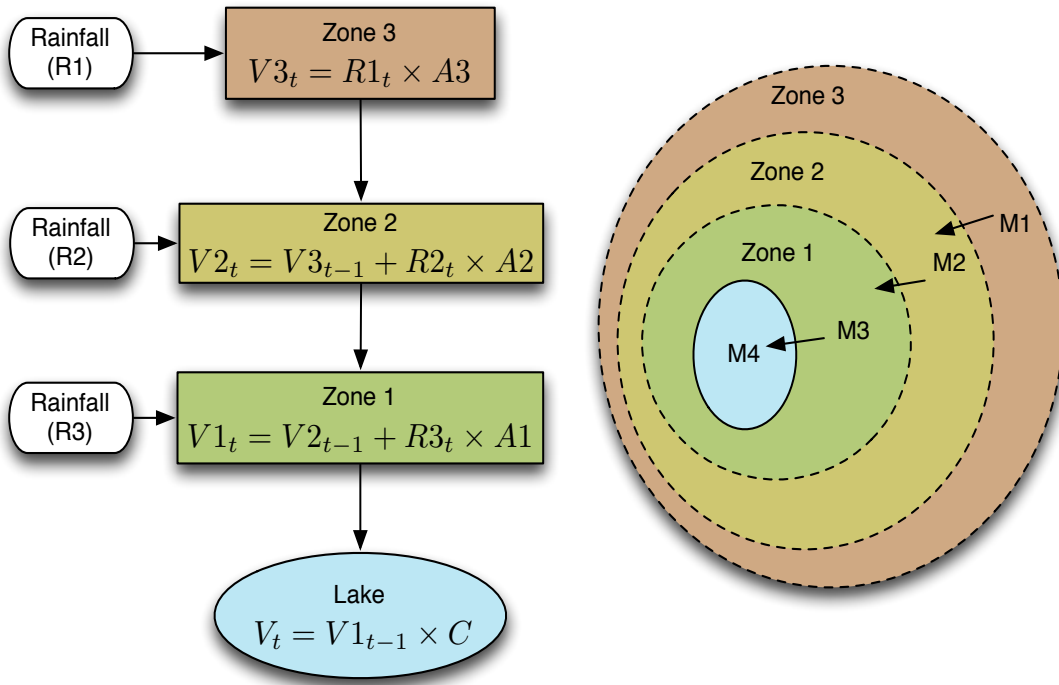


FIGURE 4.8: When rainfall occurs in the lake catchment, it moves through runoff ‘zones’ towards the lake at a rate of one zone per month. V_{nt} is the volume of water in zone n at time t , R_{nt} is the volume of rainfall landing in the zone n at time t . A_n is the area of the zone n , which is one third of the total catchment area in size.

4.2.5 Groundwater flow

Annual groundwater flow estimates were taken from the literature or were parameterised by running the hydrological model with different values until average lake water levels were within the limits of observed lake water levels (Table 4.7).

The total potential groundwater flow into the lake is determined by a deviation from the average groundwater flow identified in the literature by some proportion. This proportion is found by dividing the average monthly rainfall over n months by the average annual rainfall (of the whole rainfall dataset). The average groundwater potential is therefore higher during wetter phases and lower in drier phases. The sensitivity of groundwater inflow to rainfall also increases as the time lag is reduced. The groundwater lag and the number of months over which groundwater inflow was averaged therefore both reduce the sensitivity of the lake in response to rainfall changes as they are increased. A cutoff parameter was used to allow for a disconnection between the groundwater aquifer and the lake during periods when rainfall was reduced below a certain proportion of the average monthly rainfall expected.

4.2.6 Fitting groundwater and runoff parameters

A hill climber algorithm was used to perturb the number of months that groundwater was averaged over, and the groundwater lag in months, as well as the runoff and groundwater powers. The hill climber algorithm ran for 1000 iterations, picking values for each parameter randomly within the range allowed. The model was then run using these perturbed parameters. The root mean squared error (RMSE) between surface area output by the model, and observed surface areas was then calculated from Landsat satellite images by Tebbs et al. (2013a) and Tebbs (2013). If the new RMSE error was smaller, the inputs that produced the smaller RMSE result were recorded. There was no surface area data available for Lake Magadi.

The hill climber algorithm identified parameters that produced similar surface area output data for most lakes. However, Lakes Logipi and Magadi were prone to very high lake water levels that exceeded the limits of the bathymetry data. The cutoff parameter was then explored. It was found that the cutoff parameter did not improve RMSEs for three lakes, but for Lake Logipi it caused surface areas to behave more like observed surface areas, and improved Lake Elmentaita and Lake Magadi surface areas by moderating dramatic increases in surface area that cause surface areas to increase beyond the bounds of lake bathymetry data. The final values can be seen in Table 4.8. The sensitivity analysis can be seen later in Table 4.9.

Lake	Lag (months)	GW average (months)	Runoff power	GW power	Cutoff proportion	RMSE (km^2)	RMSE % lake SA
Logipi	3	1	0.175	1.46	0.05	45.858	22.929
Bogoria	9	31	-0.017	0.49	0	1.411	4.151
Nakuru	2	37	0.039	0.694	0	3.943	8.301
Elmentaita	3	3	1.96	-0.353	0.1	3.943	19.716
Magadi	9	28	-0.21	1.1	0.1	*	*
Natron	9	28	-0.21	1.1	0	234.369	29.150

TABLE 4.8: The initial groundwater lag, number of months groundwater inflow is averaged over, and the associated root mean squared error (RMSE) between the model and observed lake surface areas. *There is no observational data to compare with Lake Magadi surface areas, so parameters from Lake Natron were used because it is the closest Lake to Lake Magadi, with similar rainfall and the same catchment size used for the purpose of this model.

4.2.7 Time step

The hydrological model resolution is limited by the monthly rainfall data. However, a monthly time step causes dramatic changes in lake water level at the start of each month and unrealistic perturbations to the NPZ model. The hydrological model was

given a daily time step by simply dividing monthly rainfall by the number of days so that changes in lake water level occurred more gradually.

4.2.8 Data for validation

Water level data is published in the literature for Lakes Nakuru and Elmentaita which was digitised for comparison with the model output (Ayenew & Becht, 2008). Some of the significant changes in lake water level have been noted in the literature and agree with the lake water level data such as the falling lake water levels in 1973 and 1974 which coincided with a decrease in flamingo population at Lake Nakuru (Milbrink, 1977); the drought of 1993 to mid-1997 was recorded to result in a falling lake water level (Odada et al. unpublished); Lake Nakuru was seen to dry up during 1944-1946 and July 1961 (Vareschi, 1982), and from 1979 to 1982, Lake Nakuru water level was above 4m (Vareschi, 1982). Heavy rains in 1954 and 1956 coincided with a significant lake water level rise and a dramatic decline in flamingo population at Lake Nakuru (Brown, 1973).

The lake surface area data for years 1999 to 2012 were estimated from Landsat images by Tebbs, 2012 (unpublished). These were compared with surface areas output by the model. River gauge data does exist for some rivers that flow into Lakes Nakuru and Elmentaita. However, attempts to gain permission to access this data were unsuccessful.

Other observations include the heavy rains in the Kenyan Rift Valley in 1937 and 1961, which coincided with an increase in the flamingo population in western Uganda (Din & Eltringham, 1976) suggesting that the East African population can migrate to other regions during conditions that cause low food abundance in their usual feeding lakes.

4.2.9 Initial conditions

The average depth for each lake found in the literature was used as the starting depth. Volume of runoff stored in each catchment zone initially set to zero. The groundwater inflow was initially set as the average monthly groundwater inflow found in the literature for each lake. Because it is not possible to know the precise conditions in 1904 when the model is started the first year outputs reflect the model settling down as the water balance finds equilibrium.

4.2.10 Parameterisation

The hydrological model was run using the data from Table 4.7 and average annual monthly rainfall to make sure that the average water level was maintained for each lake.

The other groundwater and runoff parameters used in the hydrological model can be seen in Table 4.8. If this set of parameters is realistic then this difference could be attributed to differences in local geology. However, the average runoff used in the model for Lake Bogoria is higher than expected for a lake with such a large catchment, and this is the reason why Lake Bogoria is less stable than expected. Because of this it is more likely that these are not optimal parameters. It may be that since there is less variation in Lake Bogoria surface area and depth in response to changes in rainfall compared with the other lakes, there will be more combinations of parameter values that will produce similar outputs, and so identifying the most realistic combination of parameters using a hill climber algorithm is more difficult. It should also be remembered that groundwater and runoff parameters absorb changes in all the other variables that have not been accounted for specifically, such soil type and vegetation cover.

The RMSE for lakes Logipi and Natron are much higher than the RMSE for Lakes Bogoria, Nakuru and Elmentaita. This is likely to be because the least bathymetry data was available for Lakes Logipi and Natron.

The cutoff proportion was included for lakes Logipi, Elmentaita and Magadi to reduce the inflows to these lakes during months of low rainfall. Where the deviation in the monthly rainfall from the average monthly rainfall is below this cutoff value, then there is a disconnect between the groundwater aquifer so that no groundwater flows into the lake. There is also no additional rainfall stored as runoff in the catchment and runoff inflow is also zero for that month. This only occurs when rainfall is one twentieth of the average monthly rainfall for Lake Logipi, and when rainfall is one tenth of average monthly rainfall for Lakes Elmentaita and Magadi. The other lakes produced less accurate surface areas when cutoffs were considered (Table 4.8).

4.3 Results

Lake surface areas compared relatively well with the observational data (see Figures 4.9 and 4.10). Lake Elmentaita also had a large RMSE of 19.7% of its lake surface area (Table 4.8), despite RMSE values that were similar to Lake Nakuru (only 3.943 km^2) because of its relatively small lake surface area. Despite the variation in the availability of observed data for different lakes, and the estimation of several hydrological parameters, the model represents the changes in surface area well for Lakes Bogoria and Nakuru with RMSE values between 4% and 8.3% for the lake surface areas, and 19% for Lake

Elmentaita. These errors are comparable with the (Bergner et al., 2003) error of $<15\%$. Lakes Logipi and Natron had much higher RMSEs, possibly because the bathymetry data for Lakes Logipi and Natron was much sparser than for the other lakes. Although the error for Lakes Logipi, Elmentaita and Natron are large, a visual inspection of the outputs shows that they surface area output by the model is still similar to observed lake surface areas.

Lake Logipi and Natron model surface areas still agree well with the observational data, especially considering that lake surface area is very sensitive to changes in such shallow lakes, which means that the estimated bathymetry and hydrological parameters must be reasonable for the time period where surface area data is available. The output for Lake Elmentaita surface area is very similar to observational data but the observational data shows that the model does not capture the sudden drops in lake surface area that are caused by lower than average rainfall. This may be an issue relating to changes in the inflows that is not considered in the model. The affect of a disconnection from the groundwater aquifer and runoff during drought periods was explored for Lake Elmentaita, but this did not improve lake surface areas or capture the sudden drops in surface area during low rainfall periods. It is possible that the runoff and groundwater parameters would need to vary to capture these fluctuations, either during wet and dry periods, or to reflect other changes in the catchment which are not accounted for in this model. There is no surface area data available to compare with the lake Magadi surface areas, and so similar parameters were used to those for Lake Natron.

Lake depth data was only available for Lakes Nakuru and Elmentaita. The outputs and observational data can be compared in Figure 4.11. The lake depths fluctuate between the upper and lower limits of the observed depth data for these two lakes, although there are some significant differences between the observed and modelled outputs. The RMSE for Lakes Nakuru and Elmentaita depths is 1.22 m, and is 0.88 m respectively. This is a large error for such shallow lakes where the average depth is between 1 m and 2 m. However, this is comparable to the error in the Becht et al. (2006) model ($<2\text{m}$) which output lake depths for Lakes for Naivasha, Nakuru and Elmentaita. The Lake Nakuru depth output shows similar relative changes, with increases and decreases in depth usually occurring at the same time in both datasets. There are large differences in the average depths for some time periods, particularly prior to 1965, and in the late 1970s where the model output depth of Lake Nakuru is approximately 2 m higher than the observed data. The Lake Elmentaita depth output has similar problems, and is more stable than the observed data which does not allow for the lake to dry up during drought periods.

The model parametrisation was made using the observational surface area data because this is available for five of the six lakes, whereas depth data is only available for two. The surface area observational data is only available from the 1990s onwards, and so the hydrological model is likely to work well for the modern catchments but does not account

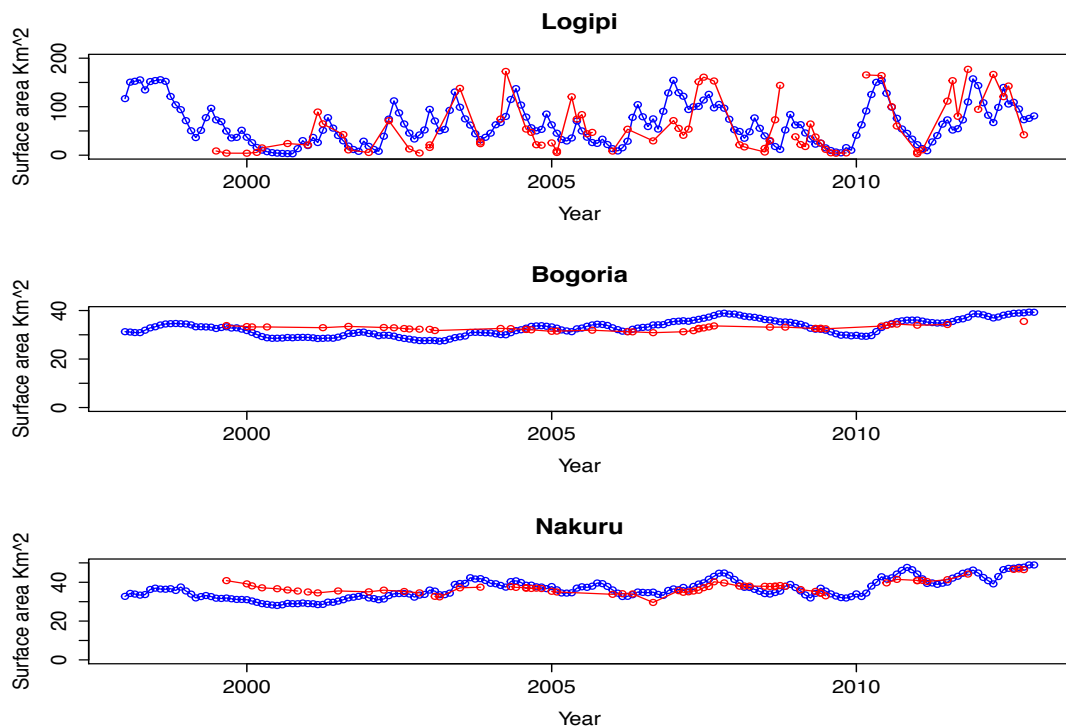


FIGURE 4.9: Lakes Logipi, Bogoria and Nakuru surface area output by the hydrological model (blue) show a good comparison with the surface area data (red) from Tebbs et al. (2013a), Tebbs (2013).

for the changes in the catchments that have occurred between 1904 and the 1990s, such as deforestation, increased use of intensive farming methods and water abstraction due to larger human populations.

Since most of these lakes receive a large proportion of inflow from groundwater, the discrepancies may be due to the way in which groundwater changes are implemented in the model.

Groundwater lag times varied between 3 and 9 months, with the sensitivity of the groundwater aquifer to changes in rainfall (average groundwater) varying between 1 and 37 months. The runoff and groundwater powers differ for each lake to amplify or dampen the response to changes in rainfall in order to produce surface areas that are more similar to observed surface area data. The parameters used in the hydrological model for runoff and groundwater inflow are optimised for the highly simplified version of these processes used in the model and do not necessarily represent real numbers that can be measured in the field. The purpose of the hydrological model is to produce similar behaviour to that seen in the observational data, such as increased sensitivity to rainfall for shallower lakes, which is observed in the Lake Logipi, Magadi and Natron surface area outputs. Another important characteristic is the relative stability of deeper lakes, especially Lake Bogoria, which is captured well by the hydrological model.

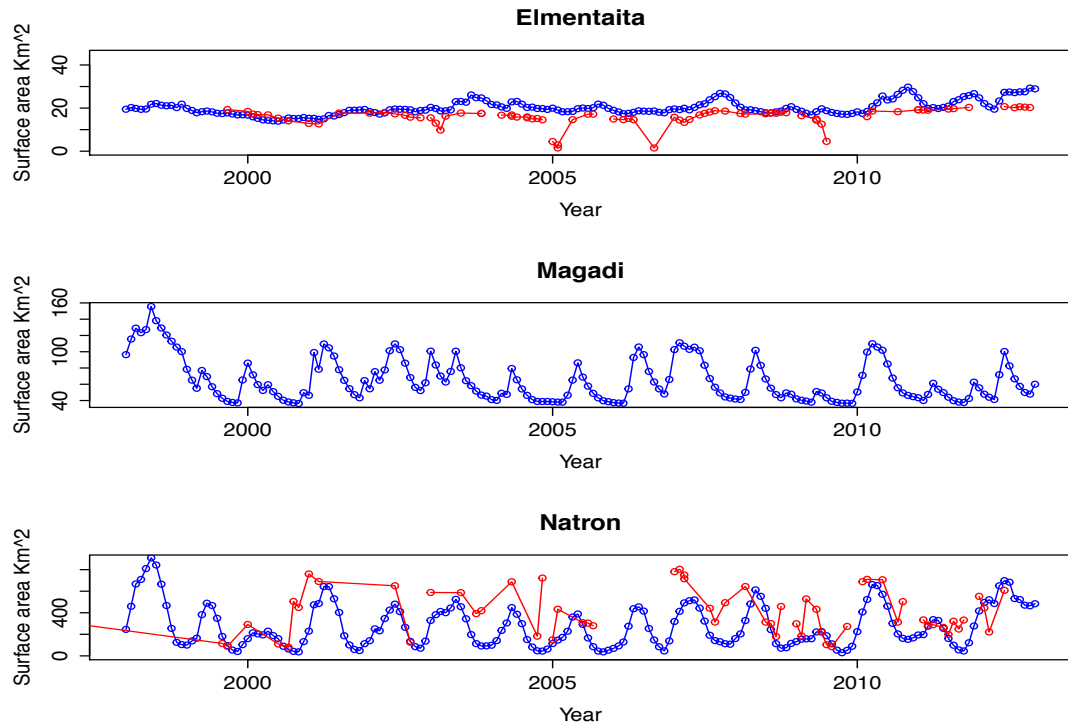


FIGURE 4.10: Lakes Elmentaita, Magadi and Natron surface area output by the hydrological model (blue) show a good comparison with the surface area data (red) from Tebbs et al. (2013a), Tebbs (2013), but there was no surface area data available for Lake Magadi.

The hydrological model outputs data with a similar range to observational depth and surface area data, and produces lake surface areas that are similar to observed lake surface areas. The differences between lake depth data and the earliest surface area data are likely to be due to changes in runoff or groundwater flow parameters over time, which is not accounted for in this model. Despite this the model can be considered to broadly represent these flamingo lakes, and is an adequate platform from which to model *Arthrosphaera* abundance and explore flamingo population changes.

4.3.1 Sensitivity Analysis

To explore the sensitivity of the hydrological model the groundwater and runoff parameters were varied one at a time for each lake. The runoff and groundwater powers were varied by 10%, and average months groundwater and lag were varied by ± 1 month, since they have a monthly resolution (Table 4.9). The RMSE is shown in terms of percent lake surface area. It can be seen that for all apart from Lake Elmentaita, the lake surface area varies by less than 1% in response to the changes in runoff and groundwater parameters. Lake Elmentaita is much more sensitive to changes in average groundwater and runoff powers causing large increases in error. This is partly because Lake Elmentaita has the smallest lake surface area, which makes it more sensitive than large lakes

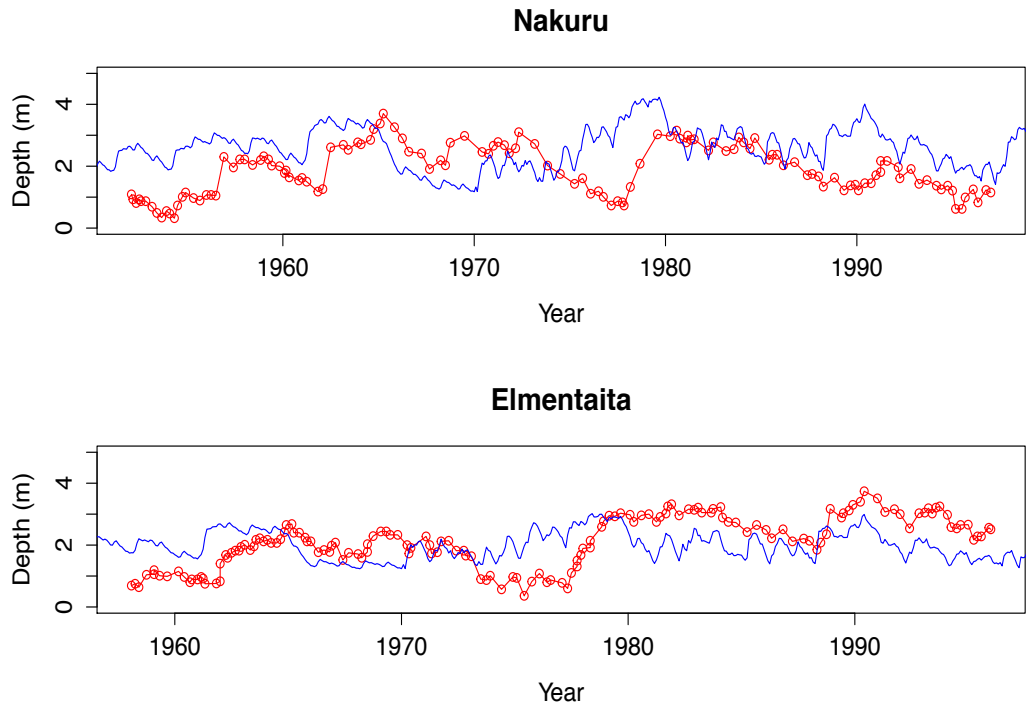


FIGURE 4.11: Lake Nakuru and Elmentaita depth output by the hydrological model (blue) compared with Ayenew and Becht (2008) depth data (red). The RMSE for Lake Elmentaita is 0.88 m, and for Lake Nakuru is 1.22 m.

Lake	Best error (% surface area)	Lag ± 1 (% surface area)	GW average ± 1 (% surface area)	Runoff power $\pm 10\%$ (% surface area)	GW power $\pm 10\%$ (% surface area)
Logipi	22.929	23.188	22.939	23.171	22.980
Bogoria	4.151	4.153	4.328	4.578	4.428
Nakuru	8.301	8.933	8.987	8.957	9.108
Elmentaita	19.716	19.785	31.298	38.752	19.834
Natron	29.150	29.173	29.163	29.811	29.151

TABLE 4.9: The RMSE in terms of percent lake surface area when each parameter was varied individually (where the RMSE is the average RMSE as a result of perturbing the parameter in both directions e.g. by Lag ± 1).

to what appear initially to be small RMSE values. Runoff power is the most sensitive parameter for most lakes. The error increases for lakes that are larger as a proportion of their catchment area (Table 4.7) and are more sensitive to changes in runoff.

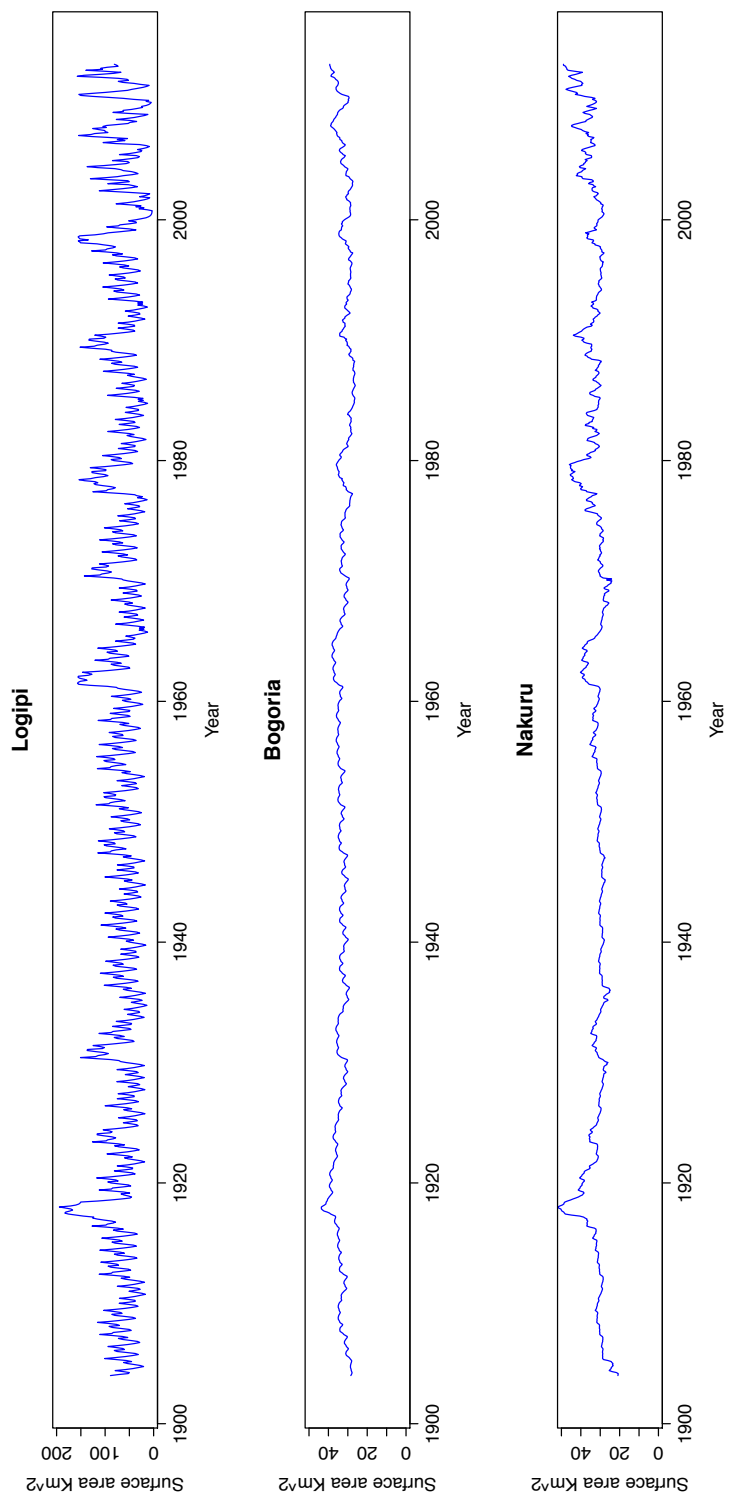


FIGURE 4.12: Lake surface area (km^2) output by the hydrological model for lakes Logipi, Bogoria and Nakuru.

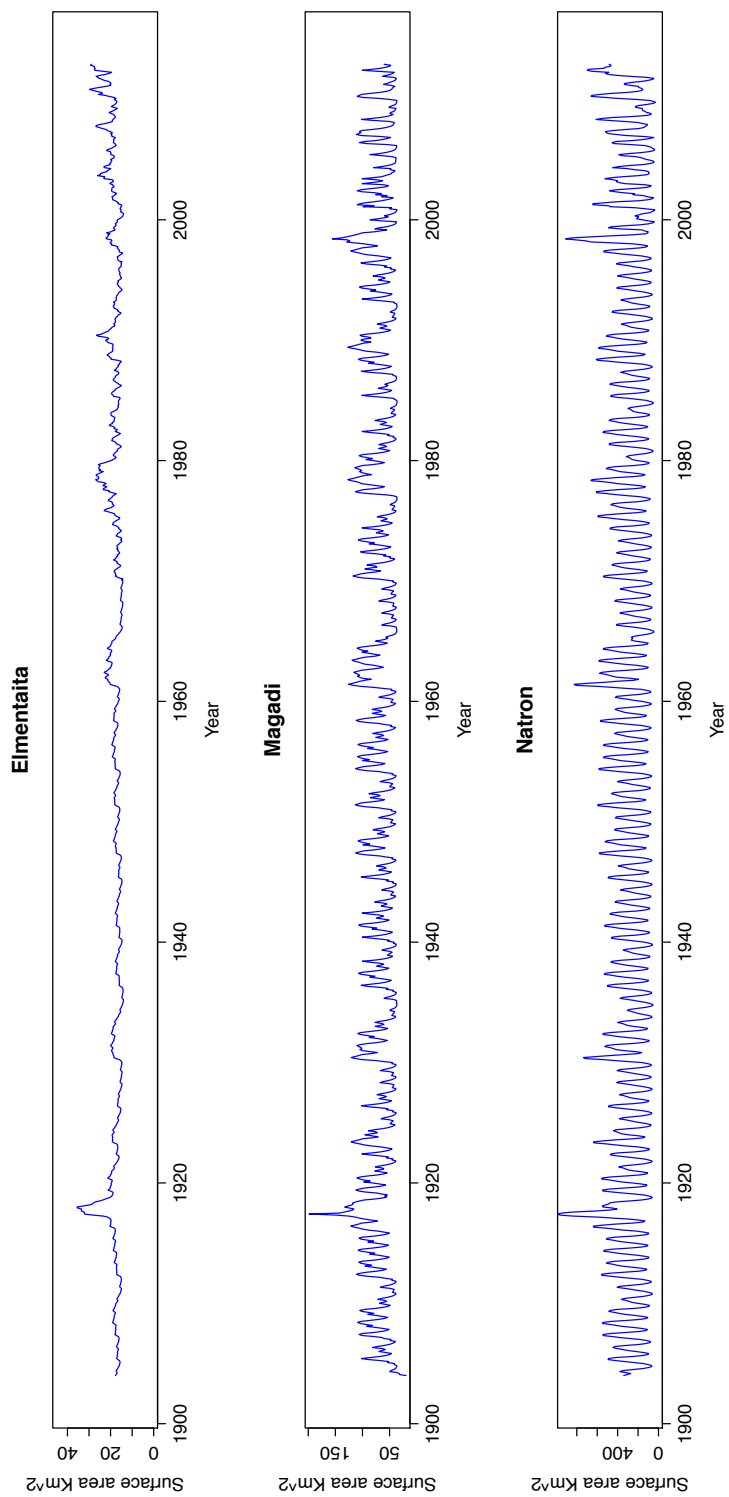


FIGURE 4.13: Lake surface area (km^2) output by the hydrological model for lakes Elmentaita, Magadi and Natron.

Chapter 5

Arthrosphaera abundance model

This chapter describes the *Arthrosphaera* model. The literature review (Section 5.1) relates the model to previous work, and then in Section 5.2, the final model is described and the model output can be seen in Section 5.3. The outputs from the hydrological model are then used as inputs to the flamingo model 6. The model was written in java in a text editor called Sublime Text, and version control was managed using GitHub.

5.1 Literature review

5.1.1 *Arthrosphaera*

Cyanobacteria dominate many eutrophic Rift Valley lake flora, including that of Lakes Bogoria, Nakuru and more recently at Lake Olidien, and has periodically dominated the phytoplankton community in Lake Elmentaita. At Lake Bogoria the species of cyanobacteria present were identified by Schagerl and Oduor (2008) as *Arthrosphaera fusiformis*, *Arthrosphaera platensis*, *Synechocystis minutus*, *Synechocystis* sp., *Anabaenopsis arnoldii* and *Anabaena* sp. There were also species of chlorophyceae (green algae) present; *Mororaphidium minutum* and *Keratococcus* sp. were sporadically observed. Bacillariophyceae (diatom) species *Nitzschia frustulum*, *Navicula elka* and *Navicula halophila* have also been identified although their presence is rare or sporadic (Schagerl & Oduor, 2008). *Arthrosphaera* usually dominates at Lake Bogoria, with a biomass accounting for over 80% (Schagerl & Oduor, 2008) of the total phytoplankton community, and has been measured at up to 97% of the phytoplankton biomass (Ballot et al., 2004).

Some fluctuations have been sudden, with dramatic changes in phytoplankton abundance and species composition. At Lake Bogoria there have been collapses in *Arthrosphaera* abundance which have an associated temporary increase in phytoplankton diversity until the recovery of *Arthrosphaera* (Melack, 1976). The earliest known decline in biomass occurring in 1978 (Vareschi, 1987). Other declines in *Arthrosphaera* have been recorded

more recently, in October 2001 (Harper et al., 2003) and from July to September 2004 (Schagerl & Oduor, 2008). *Arthrosphaera* biomass fluctuates more frequently in the other shallower lakes.

There is limited data recording *Arthrosphaera* abundance for any of the soda lakes and hence a limited understanding of exactly how cyanobacteria species respond to changing conditions. Melack (1988) studied lake Elmentaita from February 1973 to August 1974, during which time the lake water level was decreasing, causing an increase in conductivity from 19.1 to 27 mmhos cm^{-1} . *Arthrosphaera* declined in abundance, causing an increase water transparency and benthic algae primary productivity. *Paradiaptomus africanus* was the only copepod (small crustacean) identified in Lake Elmentaita at this time, and was present in high abundances in February and March 1974, but had disappeared from the lake by May. A sudden increase in benthic diatom abundance was noted in August 1973. Flamingos initially left the lake as the phytoplankton declined in abundance, but began to return as the abundance of benthic diatoms increased. There was an increase in the abundance of nanoplankton, which are not a viable food source as they are too small to be filtered by lesser flamingos, since flamingos can only filter particles between $800 \mu\text{m}$ and $50 \mu\text{m}$ in size. The same process occurred in Lake Nakuru, starting in January 1974, with similar changes in lake biota (Vareschi, 1982). Melack (1988) proposes a theory for the changes in the lake during declining water levels, suggesting that salinity changes by $>5 \text{ mmhos cm}^{-1}$ per month, and is $>25 \text{ mmhos cm}^{-1}$, the nitrogen fixing copepod *P. africanus* can no longer tolerate the lake water. Without *P. africanus*, there is a reduction in nutrient recycling. The combination of a lower nitrogen availability and an increase in salinity allows nanoplankton to outcompete *Arthrosphaera* (Melack, 1988).

Schagerl and Oduor (2008) measured environmental variables and phytoplankton abundance monthly from November 2003 and February 2005 at lakes Bogoria, Nakuru and Elmentaita. They used redundancy analysis to investigate the significance of conductivity, temperature, light attenuation, nitrate ammonium, total phosphorus and silica to phytoplankton growth. They found that generally species diversity decreased with increased water temperature and conductivity. More specifically *Arthrosphaera* sp. was associated with light attenuation and nitrate concentration, although these two environmental variables only accounted for 36% of the variation. *Arthrosphaera* has been shown to tolerate the wide fluctuations in conductivity at the soda lakes (Vareschi, 1982), and *Arthrosphaera* abundance was not been directly attributed to salinity changes in the study by Schagerl and Oduor (2008). However, Schagerl and Oduor (2008) and Kaggwa et al. (2012) both plot graphs of phytoplankton abundance and rainfall against time, and months with high rainfall often coincide with a reduction in phytoplankton abundance. Since rainfall at these lakes during the rainy season is often concentrated into a short intense downpour in the afternoons, these rainfall events will have an impact on the surface temperature and salinity in the epilimnion, reducing salinity and temperature

for a short period at the surface. Heavy rainfall will also cause the in-wash of suspended solids that will reduce the transparency of the water, and bring a pulse of nutrients from the catchment into the lake. Either one or a combination of these factors is likely to cause the reduction in cyanobacteria abundance.

Kebede and Ahlgren (1996) isolated *Arthrosphaera* from soda Lake Chitu in Ethiopia and studied its growth under different light intensities. They found a maximum specific growth rate of 1.78/day and optimum light for growth of 332 micromol *photons/m²/s* in their culture medium (Kebede & Ahlgren, 1996). Kebede (1997) then tested the response of the *Arthrosphaera* to changing salinities (see Figure 5.1).

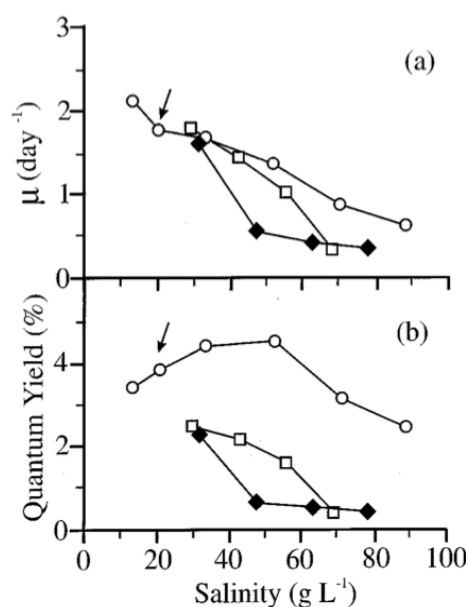


FIGURE 5.1: Specific growth rate (a) and quantum yield (b) in response to different salinities resulting from different salts $NaHCO_3$ (circles), $NaCl$ (squares), and Na_2SO_4 (diamonds). The control is marked by the arrow (Kebede, 1997).

Kebede then varied the concentrations of salts in different cultures and ran growth experiments under the optimum irradiance of 332 micromol *photons/m²/s* at 30C (Kebede, 1997). For each salinity the ions were the same as their original medium concentrations and then variations were made to some anions.

The results (Figure 5.1) show the growth of *Arthrosphaera* once a steady state was achieved in each solution. It was suggested that *Arthrosphaera* can adapt to stresses in alkaline solutions better than in more saline SO_4^{2-} dominated solutions, and that if a lake were to become more saline than alkaline due to environmental changes that *Arthrosphaera* would begin to lose its competitive advantage allowing for other salt tolerant species to grow.

Jimenez et al. (2003) studied the conditions for growth of *Arthrosphaera* in a mediterranean climate, and created a mathematical model for the prediction of yield for *Arthrosphaera* cultivated in ponds in Southern Spain. They studied the physiochemical and biological

variables: pH, dissolved oxygen concentration, temperature, conductivity and irradiance, biomass concentration and yield. The study of the significance of these variables was restricted by the upper and lower limits that these variables naturally achieved in these ponds in the mediterranean climate. The temperature, for example, did not exceed 28°C, whereas the maximum growth occurs at 35°C (Richmond, 1986), also conductivity of the ponds did not vary significantly (22 to 28 $mS\ cm^{-1}$), and so no conclusions could be drawn about the sensitivity of *Arthrosphaera* to changes in conductivity.

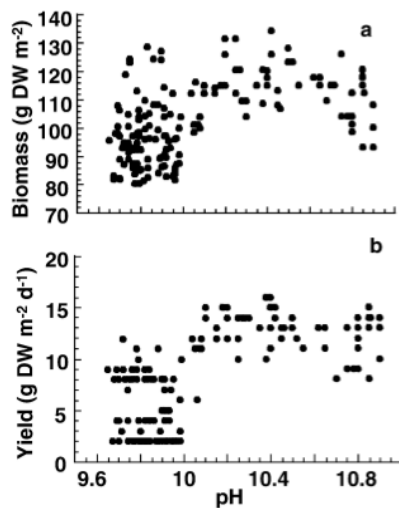


FIGURE 5.2: *Arthrosphaera* biomass and yield (Jimenez et al., 2003).

During the study it was found that *Arthrosphaera* biomass increased linearly between 10 and 25mg/L of dissolved oxygen, but decreased when dissolved oxygen increased beyond 25mg/L. Yield also increased linearly with the culture temperature between 10°C and 28°C, and with irradiance which was limited in the study to $2.1 \times 10^4\ kJ/m^2$, and biomass was unable to reach carrying capacity in this range. pH was found to control maximum density and productivity of *Arthrosphaera*, which were both optimal between pH 9.5 to 10.5, but did not grow well below pH 8, and below a pH of 9.5 other microalgae could grow and compete with *Arthrosphaera* (see Figure 5.2).

Oduor and Schagerl (2007a) investigated phytoplankton biomass in response to ion content, and nutrients and conductivity in Lakes Bogoria, Elmentaita and Nakuru. It was found that nitrate-N, conductivity, phosphorus and light availability were the most important variables to phytoplankton biomass. Nutrients were not found to be limiting phytoplankton growth at Lakes Bogoria and Nakuru but there was some phosphorus deficiency found at Lake Elmentaita.

Krienitz et al. (2013) monitored the change in the Lake Olloidien basin of Lake Naivasha as it became increasingly saline and the yield of *Arthrosphaera* increased to dominate primary production. Between 2001 to 2005 salinity was at 2 ppt, and the phytoplankton was dominated by coccoid green algae and coccoid and colonial cyanobacteria. In 2006 salinity reached 3 ppt, where there was massive growth in *Arthrosphaera*. Heavy rain

then caused an increase in lake water levels causing salinity to reduce to 2.2 ppt in January 2013, but *Arthrospira* still remained at 100%. Experiments with this strain of *Arthrospira* found the yield to be highest at 8.5 ppt salinity (see Figure 5.3). Vonshak (1997) found that *Arthrospira* doubled in a time period of between 11 and 20 hours.

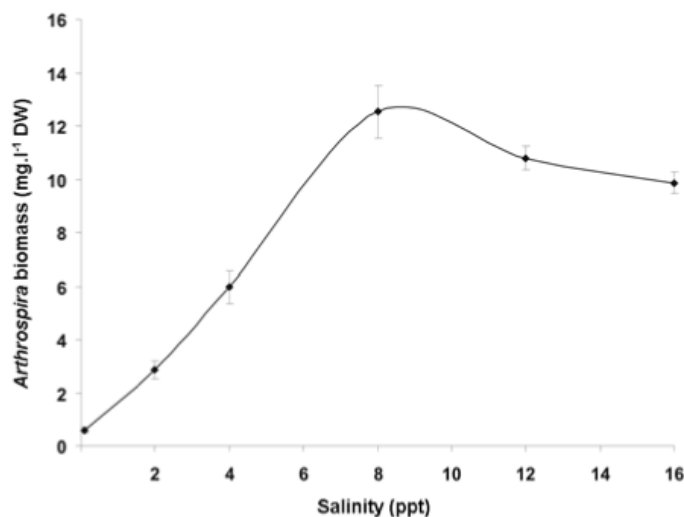


FIGURE 5.3: *Arthrospira* yield (Krienitz et al., 2013)

It would seem logical that *Arthrospira* decline occurs across all soda lakes in the Rift Valley in response to the same rainfall or drought event. Whether this actually happens is unknown, since the records of phytoplankton abundance by Krienitz and Kotut (2010) are not made over a long enough time period to allow much comparison. Changes are likely to be affected by local climate variation and will certainly be affected by the topography of the lake bed. There is variation in the amount of rainfall across the Rift Valley with elevation. However, it is unlikely that some lakes would receive rainfall when others do not during the same rainy season. It could be expected that changes will occur in response to the same flood or drought event across all lakes. However, changes in lake phytoplankton are likely to be observed earlier and more frequently in shallower lakes. The analysis of cores from Lakes Bogoria, Nakuru and Elmentaita might make this clearer, since observational records of past fluctuations are sporadic, and there are conflicting reports of phytoplankton abundance in the literature. Another consideration is that the water balance of many soda lakes is being negatively impacted by human activity, particularly as a result of river water being diverted for irrigation of crops. This problem is an ever more pressing one as an increasing human population puts huge pressure on finite natural resources. Currently the impact of human activity upon lesser flamingo populations is unknown.

5.1.2 Modelling

Ecologists are interested in environmental problems such as declining populations, the increase in numbers of an invasive species and the impact of human activity in ecosystem dynamics. To improve our understanding about how ecosystems function and to investigate changes in these systems modelling has become a well established approach (e.g. An, 2012; Bodin & Saura, 2010; Nezen & Arujo, 2011; Gentleman, 2002). A conceptual model of the system can be used to identify the important state variables and processes. In the case of an ecosystem where there are many different interacting components, the most common conceptual model is a flow diagram containing the ‘state variables’, or organisms in the ecosystem. The flow of energy or interactions between these organisms is indicated using arrows (e.g. Figure 5.4). To move onto a simple computer model the interactions shown on this diagram need to be made into operations that can be followed in an algorithm, and can be expressed either mathematically or using a rule based model or a combination of both.

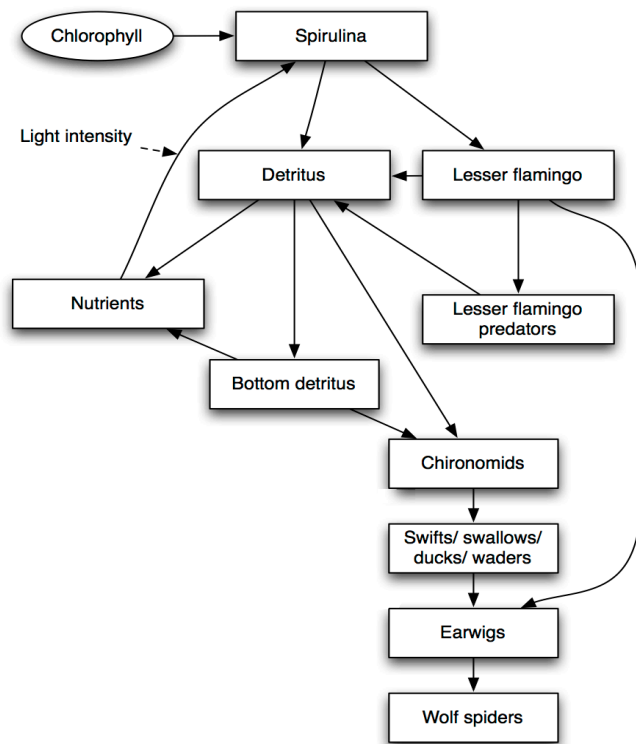


FIGURE 5.4: A conceptual model of some interactions in the Lake Bogoria ecosystem. Spirulina is the common name for *Arthrospira fusiformis*, the cyanobacteria consumed by flamingos (source: pers. obs. and Harper, pers. com.)

To model the rates of change in ecosystem state variables requires the quantitative formalisation of the interactions between. If enough is known about these interactions then the differential equations governing the interactions in the model will represent the behaviour in the real ecosystem well enough for useful insights and conclusions to be drawn from the model. One of the earliest population models developed is the Lotka-Volterra model. The Lotka-Volterra model was developed in the 1920s to describe interactions between two fish species (Lotka, 1925). It consists of a pair of interdependent differential equations describing the growth of a predator and prey population (see equations 5.1 and 5.2).

$$\frac{dx}{dt} = \alpha x - \beta xy \quad (5.1)$$

$$\frac{dy}{dt} = \delta xy - \gamma y \quad (5.2)$$

The prey equation (equation 5.1) shows that the change in number of prey (x) with respect to time is equal to the growth (αx) minus the rate of predation (βxy), where y is the number of predators. Similarly the rate of change in predator numbers (equation 5.2) is dependent upon the growth rate (δxy), and death rate (γy) of the predators. This model only considers the number of predators and prey, and is based upon many assumptions about the environment such as an unlimited supply of food for prey. Despite their simplicity the Lotka-Volterra equations have been widely used and developed to describe other interactions such as parasite-host (e.g. Nowak & May, 1994), competition (e.g. Neuhauser & Pacala, 1999), and coevolution (e.g. Saloniemi, 1993).

Early models of marine ecosystems considered the interaction of nutrients (N), phytoplankton (P), zooplankton (Z) and sometimes included detritus (D) (e.g. Steele, 1974; Wroblewski, 1989). A conceptual NPZ model can be seen in Figure 5.5, where the boxes contain the state variables, these state variables are usually represented in terms of concentration of a limiting nutrient. The interactions are shown by the arrows between the state variables. An NPZ model describes these interactions by using a series of differential equations.

NPZ models have since been widely used in marine ecological models (Gentleman, 2002). They have been developed to include multiple planktonic functional types (e.g. Totterdel, 1993), and more recently have also been used as the basis for general circulation models (e.g. Moore et al., 2002). Phytoplankton and zooplankton have also been split into different planktonic functional groups (Steele & Mullin, 1977). Fasham et al. (1990) modelled nutrient and plankton dynamics in the oceanic mixed layer using a detailed NPZDB model, where B is bacteria, and nutrients (N) are separated into three different types of dissolved nitrogen. This model produced net primary production cycles of phytoplankton and was used in a North Atlantic Ocean general circulation model.

The increasing complexity of NPZ models does not always lead to an improvement in their accuracy, and can even reduce it (Hastie & Tibshirani, 2009). Turner et al. (2014)

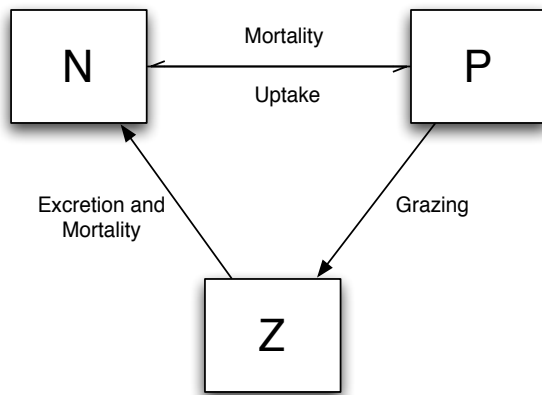


FIGURE 5.5: A conceptual NPZ model.

applied four different NPZ models that are widely used and heavily cited in the literature to an estuarine environment and compared their behaviours alongside a model written specifically for their chosen location. These models (Fasham et al. (1990), Steele and Henderson (1992), Franks (2002), Arismendez et al. (2014)) varied in number of state variables, number of interactions and mathematical formulation. Turner et al. (2014) found that the model written purposely for the study site did produce more accurate primary productivity results, but overall there was very little difference between the outputs given by different models. This suggests that unless it is directly relevant to the research question, adding extra complexity to NPZ models is unnecessary.

Starfield et al. (1989) explored a low resolution rule based model to simulate the changes in biota in lake cells in response to physical changes in Lake St. Lucia, an estuarine lake in South Africa. To do this the range of physical and ecological states of the lake were discretised. The physical parameters considered were salinity, lake water level and season. Salinity was attributed six possible states, state 1 was freshwater, with a salinity range (0-4 ppt). Higher salinity state had a larger range than the last and was adjusted to the tolerance ranges for key organisms. The abundance of 13 plant and animal species was represented by five states that increased on an exponential scale. Rules were used to determine the reaction of plants and animals to the physical conditions of the lake. The model was used as an exploratory tool rather than used to make real predictions. It was incomplete and no sensitivity analysis or validation was conducted. However, the idea of using a series of states based on the tolerance range of different organisms may be useful for a model of the soda lakes where salinity and lake water level are crucial to the functioning of the ecosystem (Starfield et al., 1989).

Arthospira fusiformis is the name of the cyanobacteria that lesser flamingos consume in East Africa. It is found in high abundances in hyper-saline-alkaline lakes, where it tends to dominate the phytoplankton community. *Arthospira* grows in highest abundance at high salinities when lake conditions have been relatively stable. In lakes like

Lake Bogoria, growth is possibly light limited because there is a high concentrations of nutrients in Lake Bogoria which allows *Arthrosphaera* to reach very high densities. In this situation the light available for photosynthesis becomes limited due to self-shading. In relatively fresher water *Arthrosphaera* must compete with a much more diverse phytoplankton community and may also be consumed by zooplankton and fish (Section 5.1.1).

In saline environments cells can be stressed by the effect of salts on osmosis across cell membranes. Salt stress can affect photosynthesis and increase respiration because it takes more energy to maintain a cell where the gradients across cell membranes are high (Sudhir & Murthey, 2004). Vonshak et al. (1988) found that *Arthrosphaera* responded to increased salt concentrations by increasing respiration rates.

Most NPZ models do not consider variable salinities like those seen in the soda lakes. Griffin et al. (2001) modelled phytoplankton densities in an NPZ model for variable salinities, where the respiration rate of phytoplankton was dependant upon salinity. Dube et al. (2012) applied Griffin's parabolic functions to mortality rather than respiration rate, in an NPZD model of an estuarine environment with a strong salinity gradient.

5.2 Overview

An NPZF model was used, where P and Z are restricted to single classes of *Arthrosphaera* and zooplankton respectively, and F is lesser flamingos. Flamingo energy budget and behaviour are modelled separately (Chapter 6). However, it is important to acknowledge the impact of flamingos on both the nutrient cycle and phytoplankton abundance in the NPZ model, since flamingos can congregate in very large numbers in the soda lakes, and are the primary phytoplankton consumers during higher salinities where zooplankton are not present.

The assumptions in the *Arthrosphaera* model are:

1. *Arthrosphaera* growth is a function of light intensity and nutrient availability.
2. *Arthrosphaera* mortality rate is a function of salinity.
3. Lesser flamingos are the primary consumers of *Arthrosphaera* during higher lake salinities, and zooplankton are the primary consumers at low salinities.
4. *Arthrosphaera* growth and mortality occurs in the same way at each lake.

The NPZF model is described below. The equations for this model were taken from Fasham et al. (1990), and adapted to exclude bacteria, detritus or multiple size classes of phytoplankton and zooplankton. The simplification of the Fasham model was desirable

because the aim of this model is to produce similar behaviours to those observed in the soda lakes (the dramatic fluctuations in phytoplankton abundance) without increasing the complexity any further than is necessary, particularly since relatively little is known about the interactions within these lakes.

$$P = P_{t-1} + P_g - P_r - P_{cZ} - P_{cF} - P_m - H_{vg} \quad (5.3)$$

$$N = N_{t-1} - P_g + P_r + P_m + Z_r + Z_m + P_{cF} - H_{mld} \quad (5.4)$$

$$Z = Z_{t-1} + P_{cZ} - Z_r - Z_m - H_{vg} \quad (5.5)$$

Where P and Z are in terms of the amount of nutrient (nitrite) stored in phytoplankton and zooplankton biomass respectively, and N is the free dissolved nutrient available in the lake for P to consume.

Equation 5.3 describes the change in phytoplankton (*Arthrosipa*) concentration, where P_{t-1} is the concentration of phytoplankton in the previous time step, P_g is the nitrogen newly stored as phytoplankton due to growth, P_r is the nitrogen lost by phytoplankton as a result of metabolic activity, P_{cZ} and P_{cF} is the phytoplankton consumed by zooplankton and flamingos respectively, P_m is the phytoplankton mortality term, and H_{mld} is a dilution term which traditionally decreases the the concentration of phytoplankton or nitrate if the mixed layer depth increases. However, in the soda lakes *Arthrosipa* tends to be concentrated in the top 5 cm of the water column (Harper, pers. com.). Since *Arthrosipa* can control its buoyancy using vacuoles (Choong-Jae et al., 2007) and zooplankton are motile creatures that are assumed to be able to overcome mixing of the water column, rather than using H_{mld} the change in volume for growth (H_{vg}) of phytoplankton and zooplankton in the soda lakes was assumed to occur as a result of change in the lake surface area rather than changes in mixed layer depth. The nutrient concentration is still affected by changes in mixed layer depth (Equation 5.4).

The P_{cF} term in Equations 5.3 and 5.4 describes the instantaneous conversion of nutrients from P to N by flamingos via their metabolism, and makes the simplification that flamingos do not store N in their bodies. This simplification was made to reduce the model complexity since it removed the requirement for the transfer of N between different lakes by flamingos to be modelled.

Equation 5.4 describes the change in nutrient concentration, where N_{t-1} is the concentration of nitrogen in the form of nitrate in the previous time step, P_g is the nitrate removed by the growth of phytoplankton, P_r and Z_r is the nitrate added by phytoplankton and zooplankton as a result of metabolic activity (respiration), and P_m and Z_m is

the nitrate added by phytoplankton and zooplankton mortality. Equation 5.5 describes the change in zooplankton concentration where Z_{t-1} the concentration of zooplankton in the previous time step. Concentrations of nitrate contained in P and N are measured in moles per cubic meter ($mol\ m^{-3}$), and are assumed to be homogeneous within the mixed layer depth of the lake.

Each term in Equations 5.4, 5.3 and 5.5 are described by Equations 5.6 to 5.16.

5.2.1 Phytoplankton

Phytoplankton growth (P_g) occurs when light energy is converted into chemical energy via the per capita growth rate (P_{ss}):

$$P_g = P_{ss} P_{t-1} T \quad (5.6)$$

The phytoplankton per capita growth rate (P_{ss}) is limited by light availability and nitrate concentration independently:

$$P_{ss} = \frac{V_p \alpha I_z}{\sqrt{V_p^2 + \alpha^2 I_z^2}} \times \frac{N_{t-1}}{k_N + N_{t-1}} \quad (5.7)$$

Where V_p is the maximum growth rate in moles per day, I_z is the irradiance at depth z , N_{t-1} is the nutrient concentration in the last time step and k_N is the half saturation constant for nutrient uptake. The photosynthesis-irradiance or PI curve has a linear initial slope (α) where the rate of photosynthesis increases proportionally with irradiance. The average irradiance was used for the 12 daylight hours, and during the night growth equals zero.

Irradiance at the average *Arthospira* depth (I_z) is dependent on the light attenuation coefficient K , and D , the depth of the phytoplankton.

$$I_z = I \times 10^{-KD} \quad (5.8)$$

Where I is irradiance at the surface in Wm^{-2} .

Light attenuation is calculated by:

$$K = k_w + k_p \frac{P_{t-1}}{D} \quad (5.9)$$

Where k_w is the light attenuation due to water, and k_p is the light attenuate due to the phytoplankton in the water.

Respiration and non-grazing mortality are both loss terms that are traditionally described in terms of a linear and non-linear function respectively. If salinity is optimal then this would still be the case. However, if the affect of variable salinity is taken into account and Griffin's parabolic functions are used to modify respiration rate when salinity increases beyond the optimal salinity, the respiration equation also becomes non-linear (Griffin et al., 2001):

$$P_r = \begin{cases} p_r P_{t-1} T, & \text{if } S \leq S_{optP} \\ p_r P_{t-1} T \left((\beta_p - 1.0) \left(\frac{S}{S_{optP}} \right)^2 - (2(\beta_p - 1.0)) \left(\frac{S}{S_{optP}} \right) + \beta_p \right), & \text{if } S > S_{optP} \end{cases} \quad (5.10)$$

Where β_p is the value of P_r when $S = 2 \times S_{optP}$, T is the time step as a proportion of one day (e.g. if the time step is one hour, the proportion = 1/24), and p_r is the respiration constant in moles of nitrate per day.

The phytoplankton consumed by zooplankton P_{cZ} is synonymous with zooplankton growth:

$$P_{cZ} = \frac{g Z_{t-1} P_{t-1} T}{k_g + P} \quad (5.11)$$

Where g is the maximum grazing rate (or zooplankton growth rate) and k_g is the half saturation constant for grazing.

The non-grazing phytoplankton mortality equation was modified (see Equation 5.12) to allow for increased mortality during high rainfall events, and is applied when monthly rainfall R_m is greater than R_{opt} , which is the 'optimal monthly rainfall' or the rainfall above which *Arthospira* mortality begins to increase as a result of high rainfall events.

The non-grazing mortality of phytoplankton, P_m :

$$P_m = \begin{cases} p_m P_{t-1}^2 T, & \text{if } R_m \leq R_{opt} \\ p_m P_{t-1}^2 \left(\frac{R_m}{R_{opt}} \right)^2 T, & \text{if } R_m > R_{opt} \end{cases} \quad (5.12)$$

Where p_m is the non-grazing mortality rate.

The volume where phytoplankton can grow, H_{vg} , changes as a result of lake surface area changes, causing the dilution or concentrate of the phytoplankton. The lake surface area change is an output of the hydrological model, and the volume for phytoplankton growth is:

$$H_{vg}(t) = \begin{cases} V_d - V_{d-0.05}, & \text{if } d \geq 0.05m \\ V_d, & \text{if } d < 0.05m \end{cases} \quad (5.13)$$

Where V_d is the volume of the lake at its current maximum depth d , and $V_{d-0.05m}$ is the volume of the lake at depth - 0.05m, the depth in the water column where *Arthrosphaera* is found (Harper, pers. com.).

5.2.2 Zooplankton

Growth of zooplankton occurs as a result of the grazing of phytoplankton P_{cZ} (Equation 5.11). It is assumed that the nitrate removed from phytoplankton by zooplankton is all converted into zooplankton. Zooplankton is not found in hyper saline conditions, but becomes important at lower salinities.

In the same way that phytoplankton respiration is affected by increased salinity S , zooplankton respiration Z_r is assumed to be a linear function until the optimal salinity S_{optZ} is reached, beyond which respiration begins to increase:

Zooplankton respiration Z_r is:

$$Z_r = \begin{cases} z_r Z_{t-1} T, & \text{if } S \leq S_{optZ} \\ z_r Z_{t-1} \left((\beta_z - 1.0) \left(\frac{S}{S_{optZ}} \right)^2 - (2(\beta_z - 1.0)) \left(\frac{S}{S_{optZ}} \right) + \beta_z \right), & \text{if } S > S_{optZ} \end{cases} \quad (5.14)$$

Where T is the time step as a proportion of one day and z_r is the respiration constant.

Where β_z is the value of Z_r if $S > S_{optZ}$.

Mortality of zooplankton, Z_m is:

$$Z_m = z_m Z_{t-1}^2 T \quad (5.15)$$

Where z_m is the mortality rate of zooplankton.

5.2.3 Nutrients

Nitrate is distributed throughout the mixed layer, which is estimated to be 2.5m from Harper et al. (2003). Traditionally the dilution term is not concerned with changes in basin depth, but changes in mixed layer depth as a result of changing wind speed. Because there is no wind speed data available the mixed layer depth is assumed to be

constant, and the volume of the mixed layer changes as a result of changing lake surface area and depth, which is often less than 2.5m in these soda lakes:

$$H_{mld}(t) = V_d - V_{d-x} \quad (5.16)$$

Where V_d is the volume of the lake at its current maximum depth (d), and V_{d-x} is the volume of the lake that is below the mixed layer depth. $x = 2.5m$ if depth is greater than the mixed layer depth, and $x = 0m$ if depth is shallower than the mixed layer depth.

5.2.4 Flamingos

The flamingo model is explained in full in Chapter 6, but it is necessary to mention them here as part of the NPZF model.

The phytoplankton consumed by flamingos P_{cF} is calculated differently because flamingos move from one lake to another, and each individual requires different amounts of phytoplankton depending upon its total mass and the mass of its fat reserves (see Chapter 6.2). The P required by a flamingo is calculated (in kg per day) in the flamingo energy budget model (see Section 6.2.2). The concentration of nitrate contained in phytoplankton in the lake must therefore be converted to a density of *Arthospira* in kg per cubic m.

For each time step the flamingos remove a proportion of phytoplankton from the lake, and the new density and nitrate concentration is calculated. Flamingos will continue to feed during each time step until they have met their individual requirements for the day, or until the density of phytoplankton reduces below a minimum threshold. This incremental approach prevents large populations of flamingos removing all of the phytoplankton from a lake, and allows the phytoplankton density to gradually reduce until it is too low for flamingos to gain more energy than it costs to feed on low densities of phytoplankton.

The excretion of nutrients back into the lake by flamingos is assumed to be equivalent to the nitrate removed by flamingos each day (Equation 5.17). The impact of flamingos on the soda lakes in this model is therefore to increase the rate of nutrient cycling.

$$P_{cF} = \sum_{n=1}^N cPkg_n T \quad (5.17)$$

Where P_{cF} is the sum of the P removed by a population of N flamingos. Pkg is the P consumed by flamingo n in kg in time step T , and is an output of the flamingo model. Constant c is used to convert P from kg to moles of nitrate. The value for c was

estimated using the following logic: *Arthrosphaera* is 70% protein (Cohen, 1997). Proteins are made of amino acids which are estimated to constitute of 25% nitrogen (14/55, where 14 is the molecular weight of nitrogen and 55 is the total molecular weight of an average amino acid), if 25% of the protein contained in *Arthrosphaera* is nitrogen, then 17.5% of *Arthrosphaera* by mass is nitrogen. There are 0.041kg of nitrogen in 1mol, which is 71.43mol/kg of Nitrogen. The moles of nitrogen in one kg of *Arthrosphaera* is therefore $71.43 \times 0.175 = 12.5\text{mol kg}^{-1}$.

5.2.5 Parameters

	Symbol	Value	Units	Reference
<i>Environmental parameters</i>				
Irradiance	I	200	$W\text{ m}^{-2}$	Ashfaque (2000)
Light attenuation by water	k_w	0.04	m^{-1}	Fasham et al. (1990)
Mixed layer depth	x	2.5	m	
<i>Phytoplankton parameters</i>				
Light attenuation by phytoplankton	k_p	0.03	m^{-1}	Fasham et al. (1990)
Photosynthesis-Irradiance curve initial gradient	α	1.1	$(W\text{ m}^{-2})^{-1}\text{d}^{-1}$	Zengling and Kunshan (2009)
Maximum growth rate	V_p	2.136	d^{-1}	Kebede (1997)
Respiration rate	p_r	0.05	d^{-1}	Fasham et al. (1990)
Non-grazing mortality	p_m	0.09	d^{-1}	Fasham et al. (1990)
Half-sat. for nutrient uptake	k_N	0.5	$mol\text{ m}^{-3}$	Free parameter
Optimal salinity	S_{optP}	10	ppt	Kebede (1997)
Optimal rainfall	R_{opt}	0.09	$m\text{ month}^{-1}$	Free parameter
Maximum salinity	S_{maxP}	100	ppt	Free parameter
Phyt. lost by respiration when salinity = $2 \times S_{optP}$	β_p	1.2	d^{-1}	Free parameter
Depth of <i>Arthrosphaera</i> kg to moles constant	D	0.05	m	Harper, pers. com.
	c	12.5	$mol\text{ kg}^{-1}$	
<i>Zooplankton parameters</i>				
Maximum grazing rate	g	1.0	d^{-1}	Fasham et al. (1990)
Half-sat. for ingestion	k_g	1.0	d^{-1}	Fasham et al. (1990)
Optimal salinity	S_{optZ}	10	ppt	Ooyo-Okoth et al. (2011)
Maximum salinity	S_{maxZ}	40	ppt	Free parameter
Zoopl. lost by respiration when salinity = $2 \times S_{optZ}$	β_z	2.0	d^{-1}	Free parameter
Respiration rate	z_r	0.1	d^{-1}	Fasham et al. (1990)
Mortality rate	z_m	0.05	d^{-1}	Fasham et al. (1990)

TABLE 5.1: Parameters used in the NPZF model.

5.2.6 Time step

The NPZ model is updated on an hourly time step. This is small enough to prevent the NPZ model from crashing in response to large changes, but large enough to prevent the overall model runtime from becoming excessive.

5.2.7 Initial conditions and input data

The model was written in Java using the parameters in Table 5.1. The initial hydrological parameters are set by the hydrological model outputs, which also determine the salinity at each lake.

The rainfall data is described in section 4.2.2.

The observed total nitrogen has been measured at Lakes Nakuru and Bogoria ranges between 0.008 and 0.8 $mol\ m^{-3}$ (Krienitz & Kotut, 2010). Even if all of this was in the form of nitrate, it would only be enough to produce a maximum of 0.064 $kg\ m^{-3}$ of *Arthrosipa*. To produce the minimum density for flamingos to survive on *Arthrosipa*, the concentration of nitrate would have to be 1.25 $mol\ m^{-3}$, and to reach the maximum observed density at Lake Bogoria of 0.768 $kg\ m^{-3}$ much higher concentrations of up to 9.6 $mol\ m^{-3}$ would be needed. The total nitrate available in each lake was varied manually between 1.25 and 9.6 $mol\ m^{-3}$, and the most sensible outputs in terms of *Arthrosipa* density range chosen.

The initial values are shown in Table 5.2.

Lake	Total nitrate ($mol\ m^{-3}$)
Logipi	3.5
Bogoria	9.6
Nakuru	5.5
Elmentaita	3.5
Magadi	2.5
Natron	3.5

TABLE 5.2: The total nitrate available in each lake.

5.2.8 Data for validation

There are some data for *Arthrosipa* abundance at lakes Bogoria, Elmentaita and Nakuru from Ballot et al. (2004), Schagerl and Oduor (2008), Krienitz and Kotut (2010) and Kaggwa et al. (2012). Most of these data are measured on a monthly basis, although Kaggwa et al. (2012) was more detailed. These results can be compared with the model output to see if there is any similarity. However, even some of the overlapping observed

data do not agree (Schagerl & Oduor, 2008; Krienitz & Kotut, 2010), perhaps because of density changes throughout the course of each day in response to insolation, and there is spatial variation in density across each lake.

Ooyo-Okoth et al. (2011) found that when salinity increased beyond 17 *ppt* at Lake Nakuru, the zooplankton community reduced. *Arthrosphaera* was found by Kebede (1997) to grow best at low salinities of 10 *ppt* in laboratory conditions. However, densities of *Arthrosphaera* have been found to be highest in Lake Nakuru at salinities of 51 *ppt* in 2005 (Ooyo-Okoth et al., 2011), and at 45 *ppt* at Lake Bogoria in 2002 (Krienitz & Kotut, 2010). The high density of *Arthrosphaera* at these higher salinities may reflect a lack of competition or grazing by zooplankton which inhibits the density of *Arthrosphaera* at lower salinities.

Key features that it is hoped that the model will output:

1. Behaviour of the NPZ model varies for each lake.
2. Rapid fluctuations in the NPZ output in response to changing lake water levels.
3. *Arthrosphaera* growth will only occur in lakes with very high average salinities (>100 *ppt*) during flood periods, there will be a high dissolved nitrate concentration and growth will be limited by salinity.
4. In lakes with medium to high salinities (40 to 100 *ppt*) *Arthrosphaera* will usually dominate and growth will usually be limited by nutrient availability. There may be periods of higher salinity where growth becomes salinity limited, or periods of lower salinity where growth becomes limited by zooplankton.
5. In lakes with low salinity (<40 *ppt*), *Arthrosphaera* growth is usually limited by zooplankton.
6. Lake Bogoria, being the deepest lake, has the most consistently high *Arthrosphaera* density, although there is still significant variation in density and occasional ‘crashes’ in *Arthrosphaera* density.

5.3 Results

The *Arthrosphaera* density and nitrate concentrations output by the initial NPZ model without flamingo grazing can be seen in Figures 5.6 to 5.10. Note that the outputs can have different scales on the y-axis to allow for clearer presentation of the data.

It is encouraging to see that the same model outputs significantly different behaviour for each lake. Some lakes exhibit rapid cycling of the NPZ model in response to changing lake water levels, and for lakes with higher salinities these periods become less frequent and are interspersed with longer periods of nitrate limited *Arthrosphaera* growth and low

zooplankton concentrations. Lake Magadi is too saline to allow P or Z growth apart from during very high water levels.

Lake Logipi (Figure 5.6) *Arthospira* density fluctuates significantly in response to changing salinity. Zooplankton concentrations are able to increase during very high lake water levels (e.g. in 1917, the late 1970s and 1997) causing *Arthospira* densities to be suppressed slightly, but zooplankton is not usually present at Lake Logipi. Flamingos have been observed in large numbers at Logipi during periods of low food abundance at Lakes Nakuru and Bogoira, suggesting that there may be an increase in *Arthospira* at Lake Logipi during higher regional water levels (BBC Earth and W. Kimosop pers. com., and Tebbs (2013)).

Lake Nakuru (Figure 5.7) exhibits periods of stable high *Arthospira* density at low to intermediate water levels when salinity is between 40 and 60 ppt zooplankton cannot grow. At higher salinities *Arthospira* begins to reduce as growth is inhibited by salinity. At lower lake water levels when salinity is <40 ppt, zooplankton cause the moderation of *Arthospira*. This output is similar to Kaggwa et al. (2012) observational data, where *Arthospira* density ranges from 0 - 0.25 kg m^{-3} .

Arthospira density oscillates at Lake Elmentaita in response to changes in zooplankton concentration. Unlike the other lakes zooplankton is always present in Lake Elmentaita due to its lower salinity, and since lake volume changes significantly at this shallow lake in response to rainfall the concentrations of N , P and Z are also changing rapidly as they are diluted and concentrated by the lake, but also because the system does not get a chance to reach equilibrium since N , P and Z are continually adjusting to changing conditions. Densities range between 0 and 0.2 kg m^{-3} , which is similar to Ballot et al. (2004) observational data where *Arthospira* ranges from 0 to 0.11 kg m^{-3} . This means that although *Arthospira* density can be high enough for flamingos to graze at Lake Elmentaita, it is only available for brief periods in low concentrations that are unlikely to support large numbers of flamingos. The pigment data for Lake Elmentaita (Figures 3.26 and 3.28) suggests that there is a diverse phytoplankton community at Lake Elmentaita, including some cyanobacteria. Lesser flamingos have been found feeding at Lake Elmentaita, although normally on diatoms at times of low *Arthospira* abundance at other lakes. It is likely that the *Arthospira* is outcompeted in Lake Elmentaita by other phytoplankton, and is also grazed upon by fish which have been introduced to the lake during fresher water periods.

Lake Magadi (Figure 5.9) is extremely saline, apart from at high water levels when salinities reduce enough for *Arthospira* to begin to grow. During wetter periods when the other soda lakes have become too fresh for *Arthospira* to grow in high densities, Lake Magadi may have been suitable for *Arthospira* growth and been a refuge for flamingos. There are few observations of Lake Magadi but flamingos have been seen feeding on diatoms in low numbers (Harper, pers. com.).

Arthrosphaera density at Lake Natron (Figure 5.10) is particularly important, since it must produce enough *Arthrosphaera* to allow flamingos to breed at the lake when islands are available. Lake Natron salinity fluctuates dramatically causing periods of low lake water level where *Arthrosphaera* cannot grow, and then as lake depth increases the salinity drops to tolerable levels where *Arthrosphaera* can grow at densities approaching 0.3 kg m^{-3} . This is a response to the rapidly changing lake surface areas of these very shallow hypersaline lakes, where small rainfall events can cause relatively large changes in lake surface area and salinity. For lesser flamingos to breed successfully at Lake Natron *Arthrosphaera* must reach densities of 0.25 to allow parent flamingos with less time to feed the ability to maintain their fat reserves (Pennycuick & Bartholomew, 1973), and breeding islands must also be available.

The NPZ model outputs are characteristic of each lake, and similar to the kinds of behaviour expected as a result of their salinity and bathymetry. Rather than expecting to output changes that are identical to the few studies that have documented *Arthrosphaera* densities, the aim of this model is to capture the characteristic behaviour of each lake in response to rainfall changes.

The impact of including a mortality term related to the freshwater input due to high rainfall (Equation 5.12) is illustrated by Figures 5.11 and 5.12. Lake Bogoria is the most stable lake, with relatively low fluctuations in salinity in a smaller range of 40 to 80 *ppt*. Figure 5.11 shows the output for the unmodified mortality equation, where *Arthrosphaera* density only fluctuates between 0.3 and 0.5 $kg\ m^{-3}$. Although this agrees with observations that Lake Bogoria is a stronghold for lesser flamingos due to frequent high concentrations of *Arthrosphaera*, it does not exhibit the more dramatic fluctuation's in *Arthrosphaera*, or the large range in densities that has been observed (0.1 to 0.768 $kg\ m^{-3}$) (Krienitz & Kotut, 2010). On reviewing the literature the most dramatic *Arthrosphaera* density changes occurred at Lake Bogoria when lake water volume changed significantly and also after a sudden large rainfall event, where an influx of fresh water fell onto the lake surface (Schagerl & Oduor, 2008; Kaggwa et al., 2012). This freshening of the surface water where *Arthrosphaera* grows can change salinity too quickly for *Arthrosphaera* to adapt or can change the conditions beyond the tolerance of *Arthrosphaera*. During months of higher rainfall the temperature of water at the lake surface will drop, the radiation incident on the waters surface will reduce and there will be a freshening of the surface waters where *Arthrosphaera* grows. This relatively sudden change in conditions is the likely cause of sudden reductions on *Arthrosphaera* biomass shown in wetter months. To include this in the NPZ model the mortality term for P was modified so that when Lake Bogoria received high rainfall, mortality of P was reduced according to equation 5.12 which can be seen in Figure 5.12. The output for *Arthrosphaera* density fluctuates between 0.08 and 0.4 $kg\ m^{-3}$, more widely than for Figure 5.11, with sudden drops in *Arthrosphaera* density which will cause flamingos to search elsewhere for food.

The when flamingo grazing is included in the NPZ model, the flamingos can have an impact on the abundance of *Arthrosphaera* by consuming a significant proportion of the total daily growth. Figures 5.13 to 5.18 show the affect of flamingos on *Arthrosphaera* at each lake by the resident flamingos for one run of the model with a start population of one million flamingos. To make the output easier to read, a subset of the data is shown for the period 1920 to 1950.

Lake Logipi (Figure 5.13) is not frequently occupied by flamingos because the *Arthrosphaera* abundance is not usually stable for long periods. When flamingos are present at Logipi the populations consumed up to 50% of the daily *Arthrosphaera* growth.

Lake Bogoria (Figure 5.14) is continually occupied by flamingos in high numbers, because *Arthrosphaera* density is early always above the minimum threshold for flamingos to feed effectively. The flamingos consume up to 30% of the daily growth of *Arthrosphaera* during periods of higher density, but when the density drops to below 0.2 kg m^{-3} , the flamingos can consume as much as 60% of the daily growth.

Lake Nakuru (Figure 5.15) is usually occupied by flamingos in low numbers, because although *Arthrosphaera* is often available, it is not as reliable a food source as Lake Bogoria. At Lake Nakuru flamingos have a larger impact on *Arthrosphaera*, consuming up to 80% of daily growth.

Lake Elmentaita (Figure 5.16) is usually occupied by flamingos in low numbers. At Lake Elmentaita, on the occasions when flamingos can feed on *Arthrosphaera*, they have a large impact, consuming up to 80% of daily growth.

At Lake Magadi (Figure 5.17), there are only a few occasions when *Arthrosphaera* is available during periods of high water level. Because *Arthrosphaera* only grows at low densities the flamingo population can have a large impact on daily growth of *Arthrosphaera* despite the large size of Lake Magadi (approximately 100 km^2), consuming up to 40% of the daily growth.

Lake Natron (Figure 5.18) is usually occupied by flamingos because they attempt to breed during periods when islands are available. Lake Natron is the largest lake (up to approximately 800 km^2), and so flamingos do not usually have much impact on daily *Arthrosphaera* growth, consuming up to 20% when the largest population of more than 600,000 flamingos is at Lake Natron. The output for Lake Natron is characteristic of this lake since *Arthrosphaera* must be abundant when breeding islands are available (see Figure 5.19), to allow the flamingos to breed successfully.

Breeding events at Lake Natron can be seen in Figure 5.19. These events can only occur during the right conditions, when islands are available to nest on, and *Arthrosphaera* is available. The top graph in Figure 5.19 shows the *Arthrosphaera* density at Lake Natron, with the threshold above which flamingos can feed (0.1 kg m^{-3}) marked by a horizontal line. The middle graph shows the depth of Lake Natron, and when the depth is between

the two horizontal lines islands are available at Lake Natron. The bottom graph shows the percentage of the flamingo population sitting on eggs (in black), and the number of fledgelings produced (in red) as a percentage of the total flamingo population. The green line shows periods when both islands and food are available at Lake Natron.

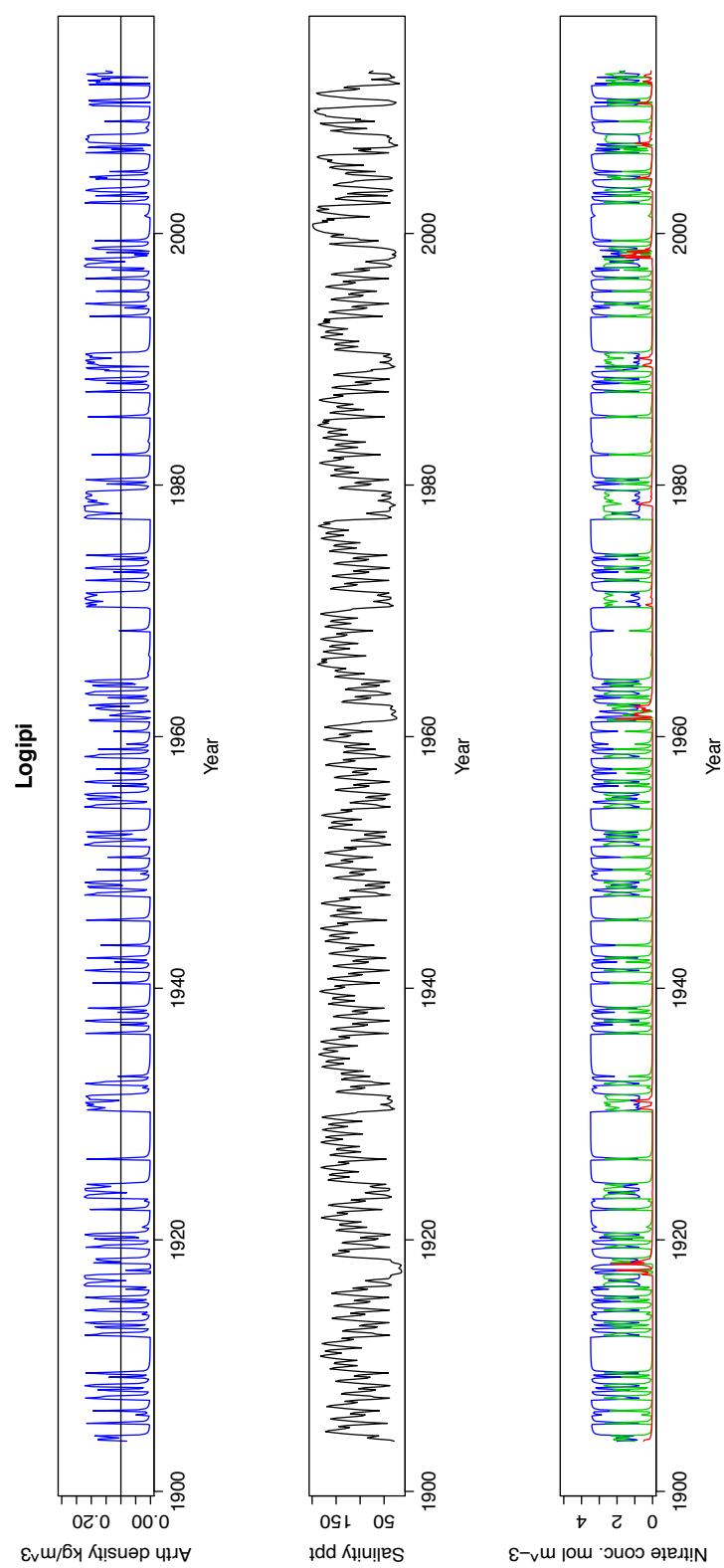


FIGURE 5.6: Lake Logipi *Arthrosphaera* density (top) output by the NPZ model, salinity output by the hydrological model (middle), and the concentration of dissolved nitrate (in blue), *Arthrosphaera* (P) nitrate concentration (in green), and zooplankton (Z) concentration (in red) (bottom). The *Arthrosphaera* density threshold above which flamingos can feed is marked at 0.1 kg m^{-3} .

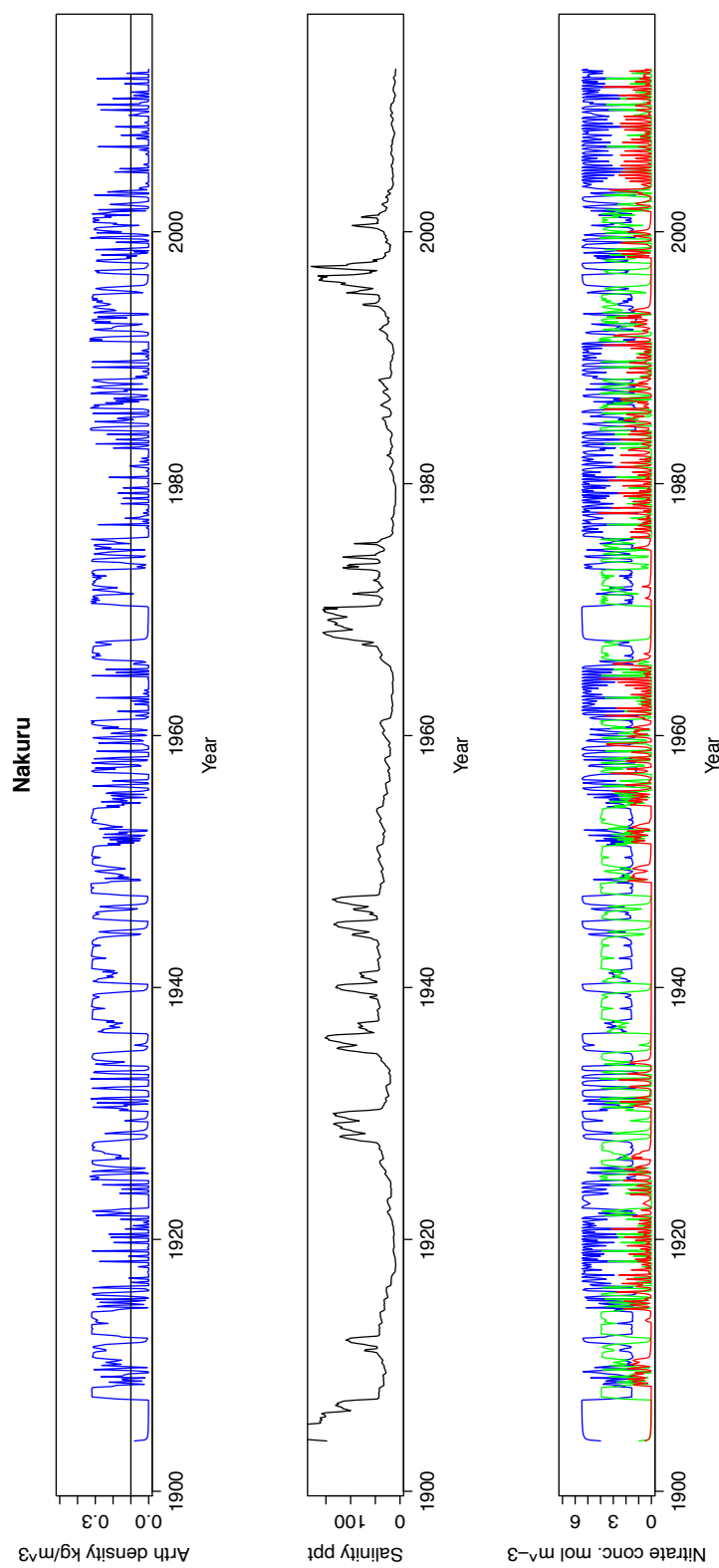


FIGURE 5.7: Lake Nakuru *Arthrospira* density in kg m^{-3} (top) output by the NPZ model, salinity output by the hydrological model (middle), and the concentration of dissolved nitrate (in blue), *Arthrospira* (P) nitrate concentration (in green), and zooplankton (Z) concentration (in red) (bottom). The *Arthrospira* density threshold above which flamingos can feed is marked at 0.1 kg m^{-3} .

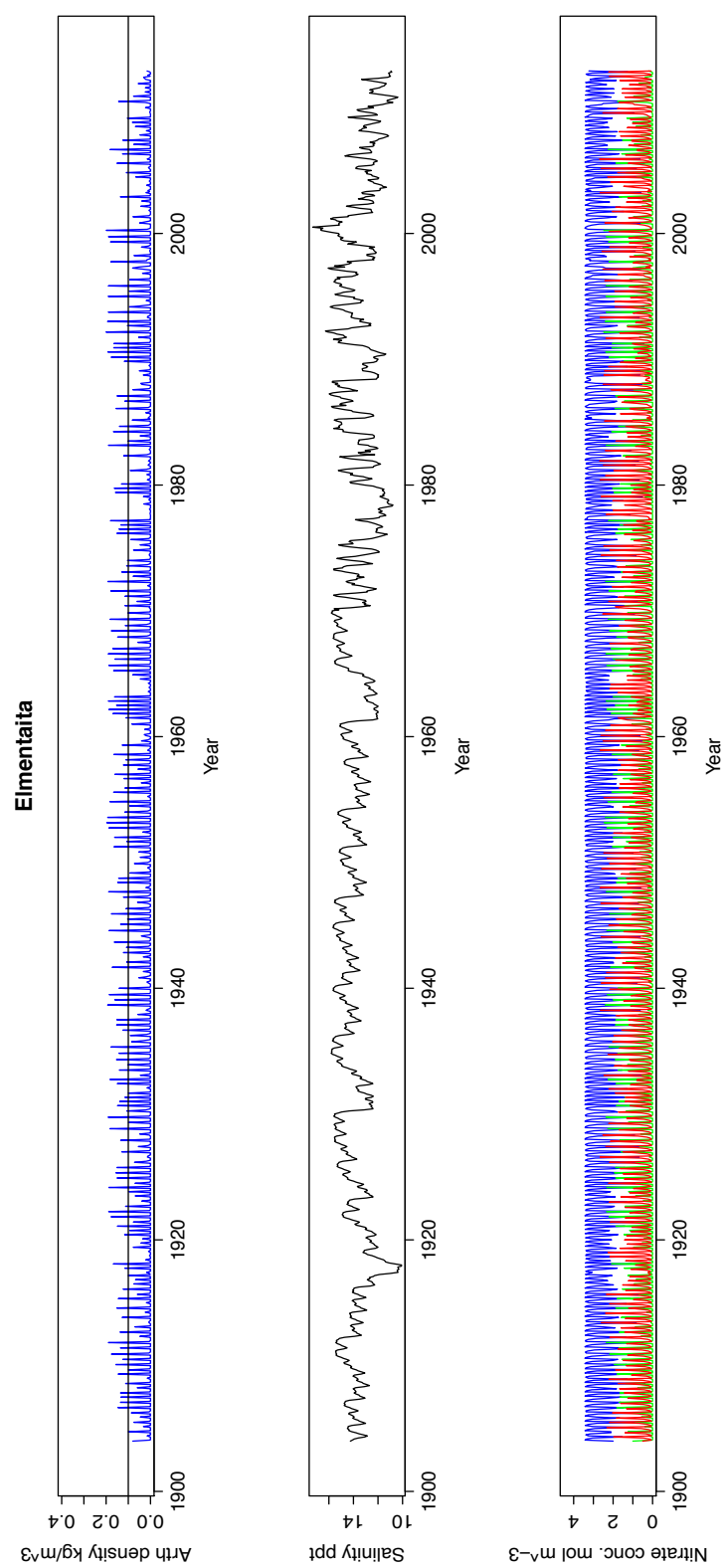


FIGURE 5.8: Lake Elementaita *Arthrosphaera* density (top) output by the NPZ model, salinity output by the hydrological model (middle), and the concentration of dissolved nitrate (in blue), *Arthrosphaera* (P) nitrate concentration (in green), and zooplankton (Z) concentration (in red) (bottom). The *Arthrosphaera* density threshold above which flamingos can feed is marked at 0.1 kg m^{-3} .

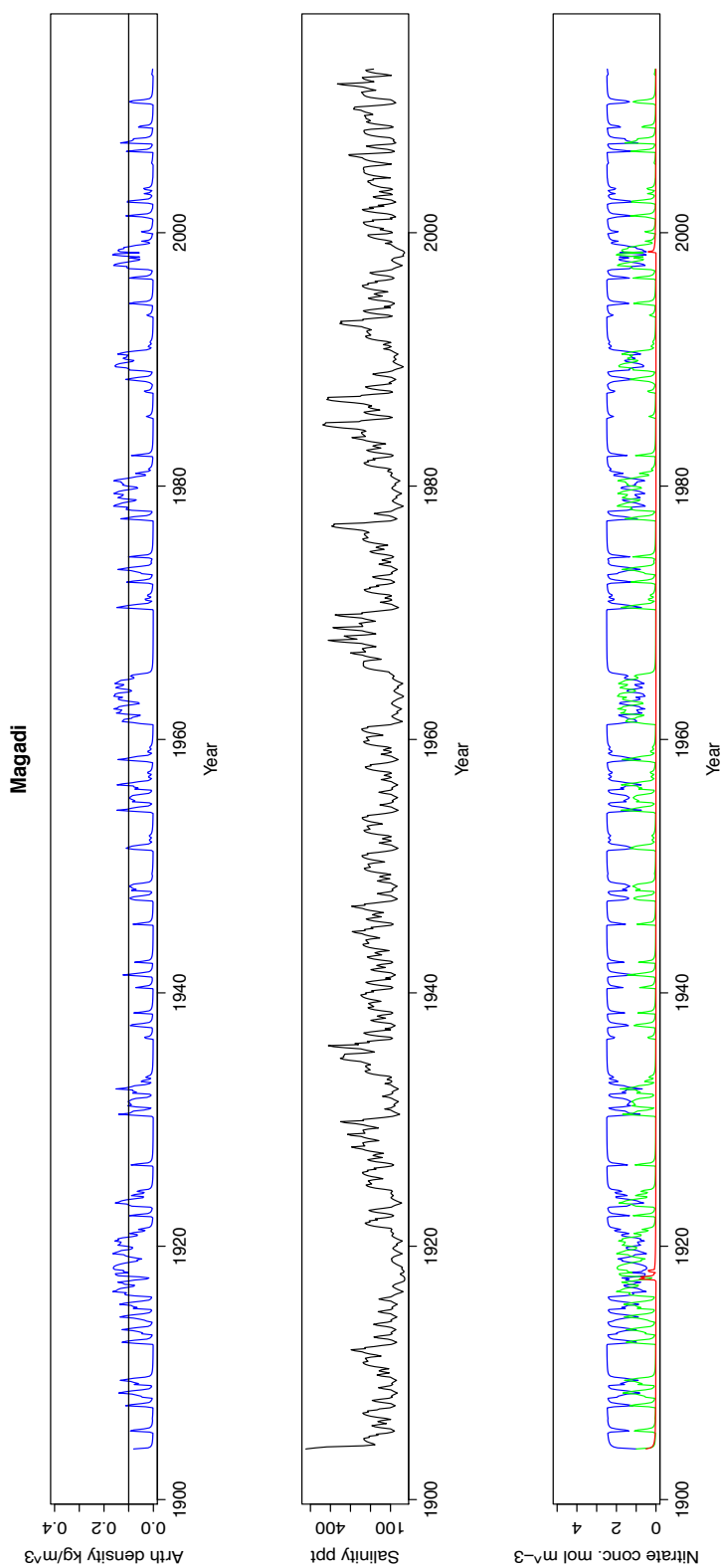


FIGURE 5.9: Lake Magadi *Arthrospira* density (top) output by the NPZ model, salinity output by the hydrological model (middle), and the concentration of dissolved nitrate (in blue), *Arthrospira* (P) nitrate concentration (in green), and zooplankton (Z) concentration (in red) (bottom). The *Arthrospira* density threshold above which flamingos can feed is marked at 0.1 kg m^{-3} .

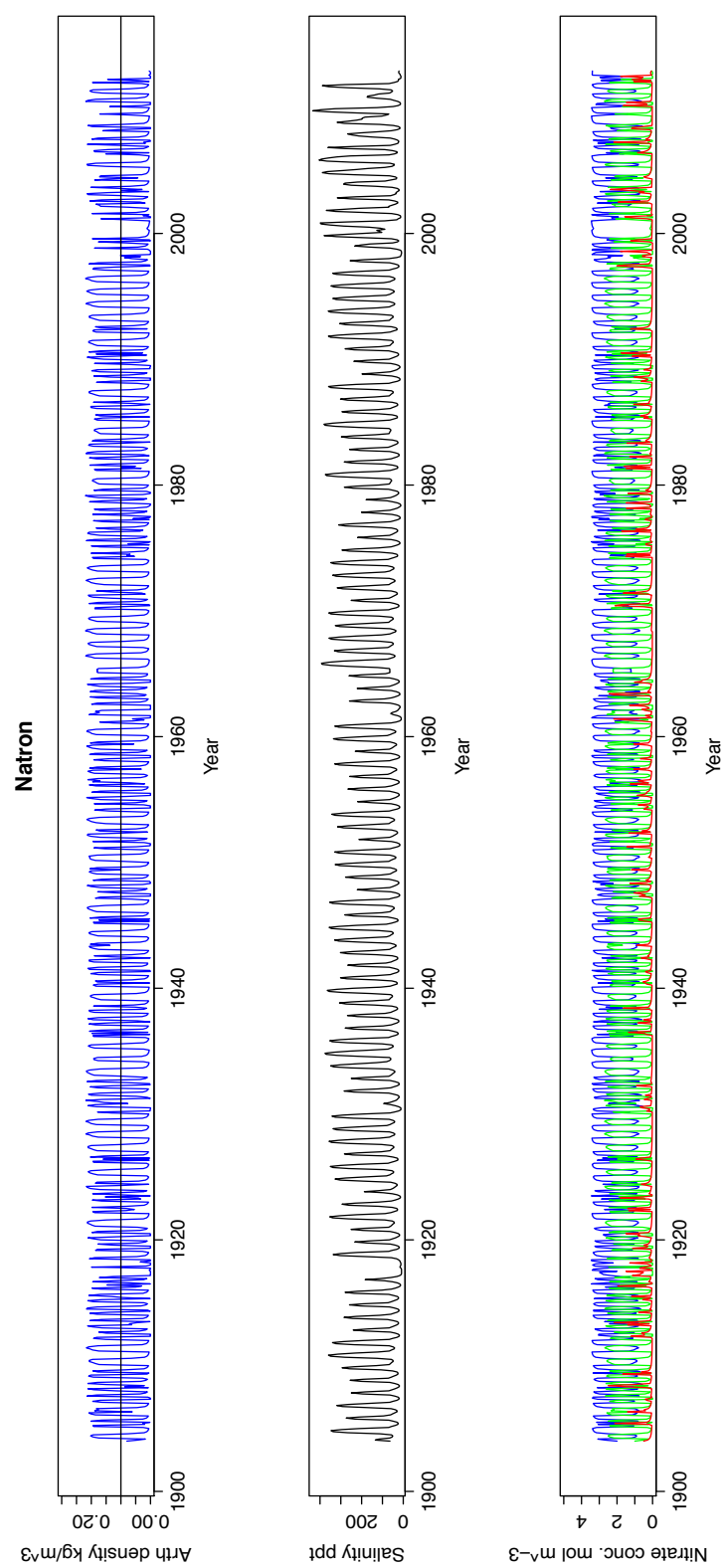


FIGURE 5.10: Lake Natron *Arthrosphaera* density (top) output by the NPZ model, salinity output by the hydrological model (middle), and the concentration of dissolved nitrate (in blue), *Arthrosphaera* (P) nitrate concentration (in green), and zooplankton (Z) concentration (in red) (bottom). The *Arthrosphaera* density threshold above which flamingos can feed is marked at 0.1 kg m^{-3} .

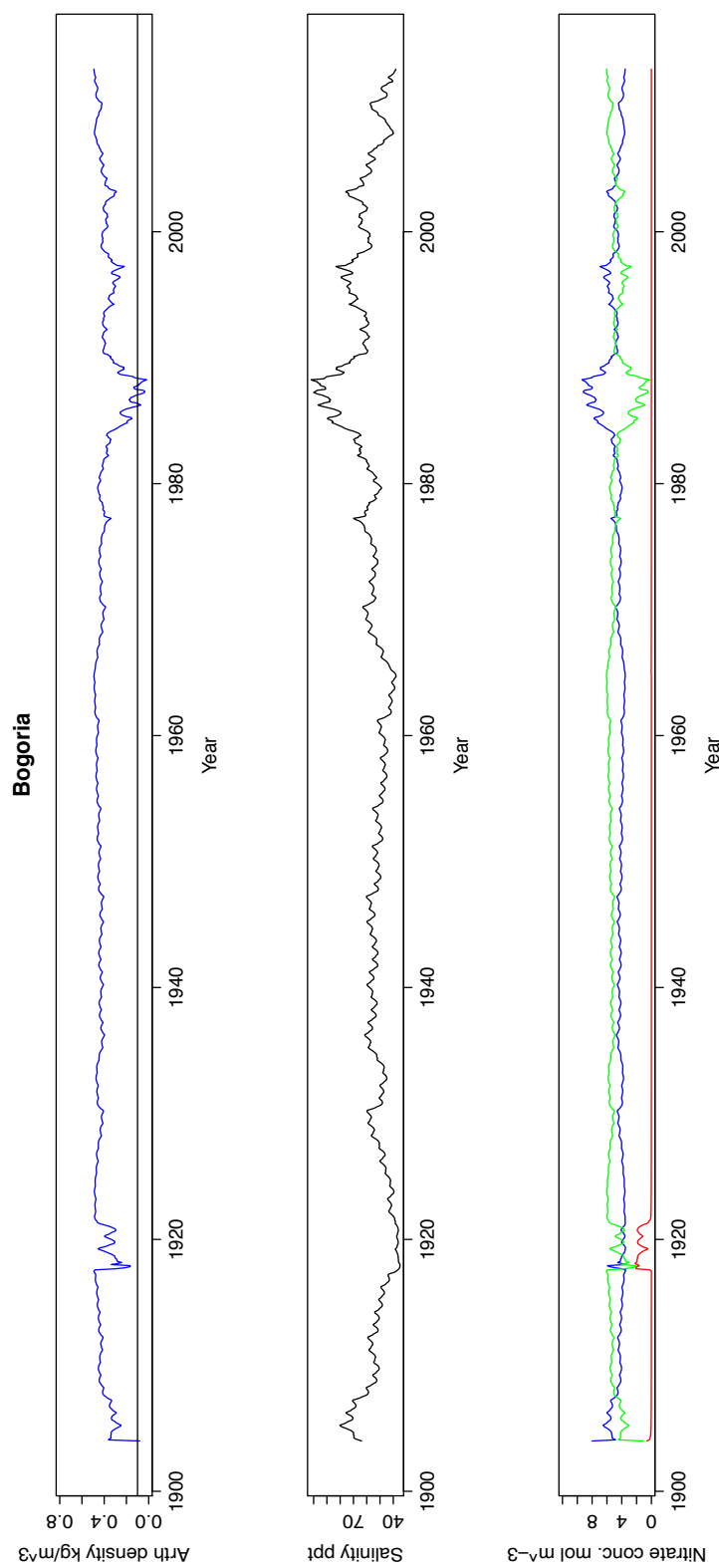


FIGURE 5.11: Lake Bogoria outputs by the NPZ model with an unmodified mortality term. *Arthrospira* density (top), salinity output by the hydrological model (middle), and the concentration of dissolved nitrate (in blue), *Arthrospira* (P) nitrate concentration (in green), and zooplankton (Z) concentration (in red) (bottom). The *Arthrospira* density threshold above which flamingos can feed is marked at 0.1 kg m^{-3} .

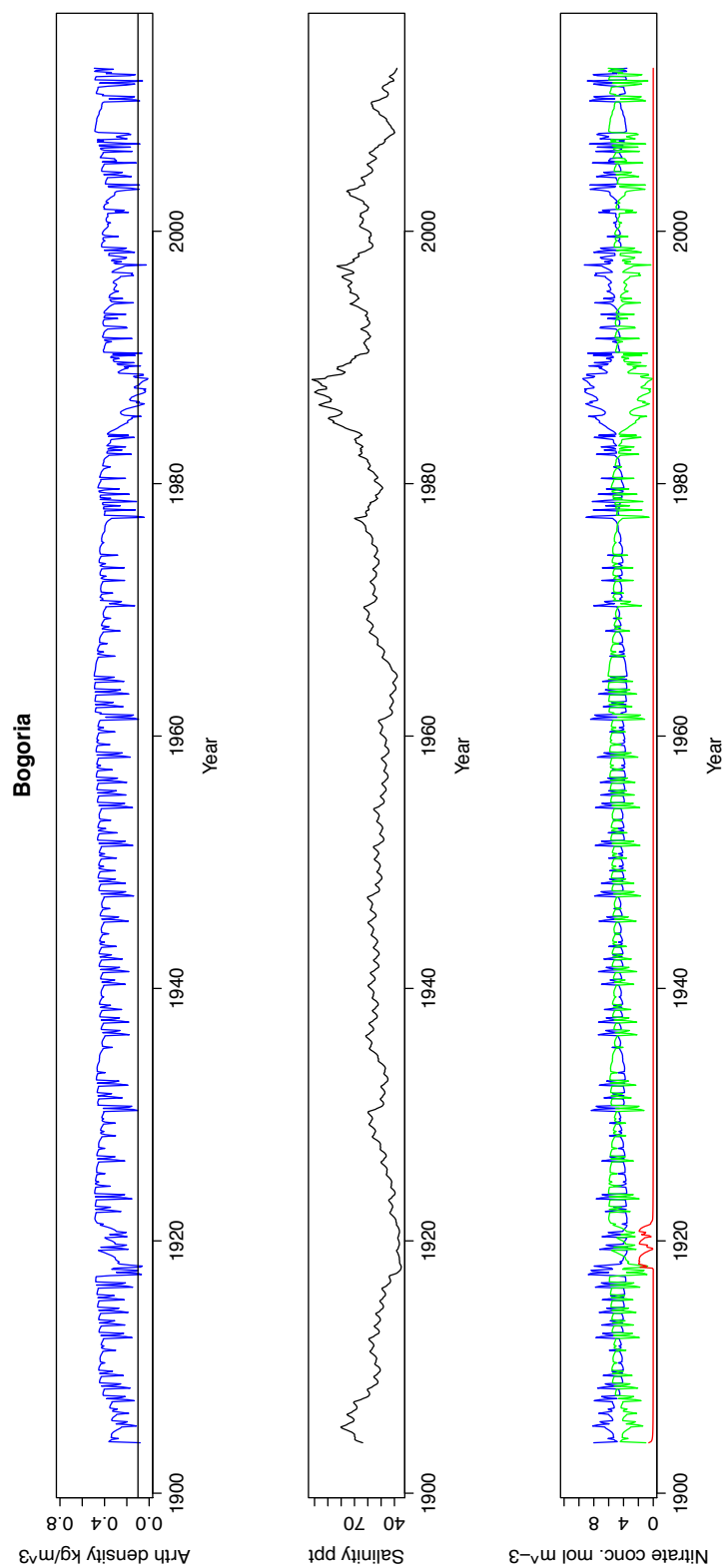


FIGURE 5.12: Lake Bogoria outputs by the NPZ model with a modified mortality term. *Arthrosphaera* density (top) output by the NPZ model, salinity output by the hydrological model (middle), and the concentration of dissolved nitrate (in blue), *Arthrosphaera* (P) nitrate concentration (in green), and zooplankton (Z) concentration (in red) (bottom). Mortality of P increases during high rainfall events. The *Arthrosphaera* density threshold above which flamingos can feed is marked at 0.1 kg m^{-3} .

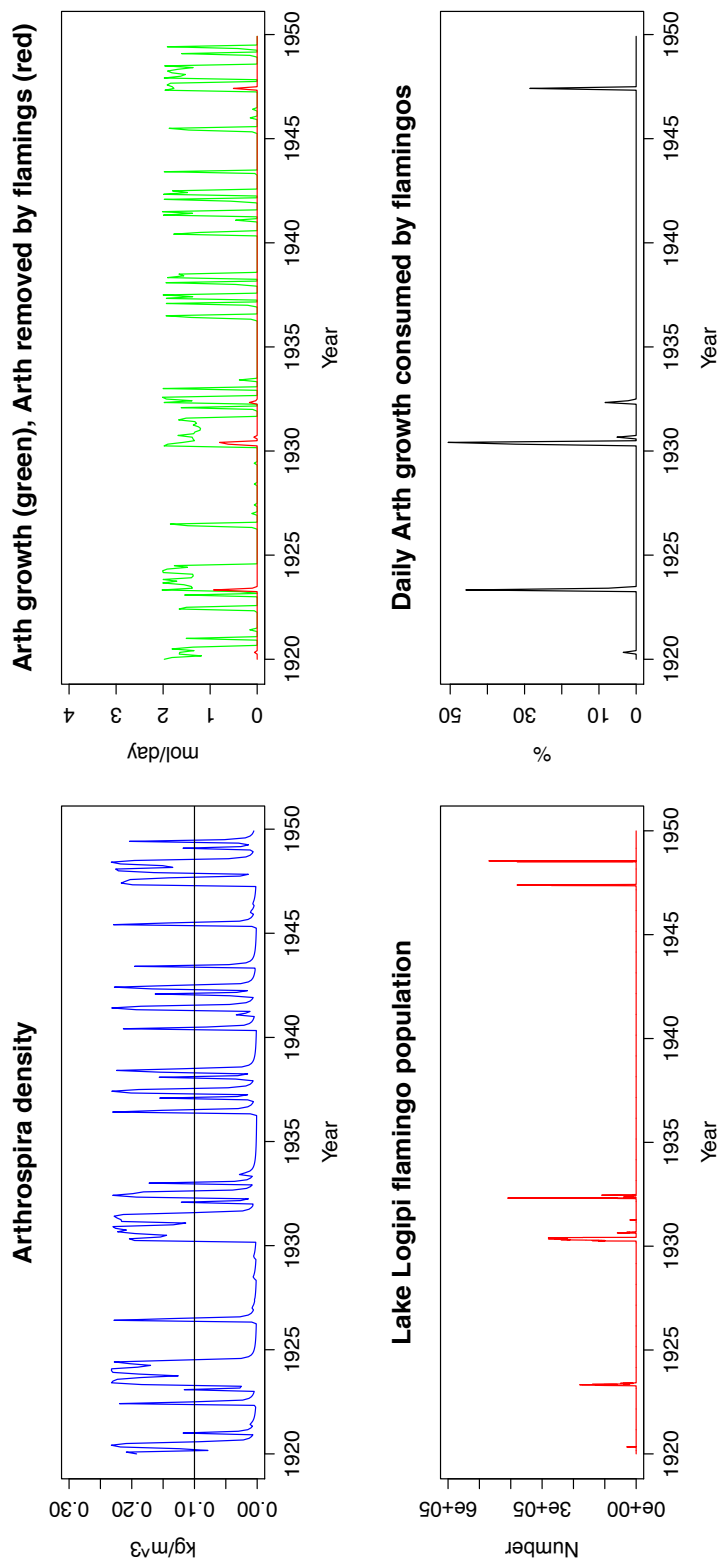


FIGURE 5.13: Lake Logipi NPZF model output. The *Arthrospira* density threshold above which flamingos can feed is marked at 0.1 kg m^{-3} .

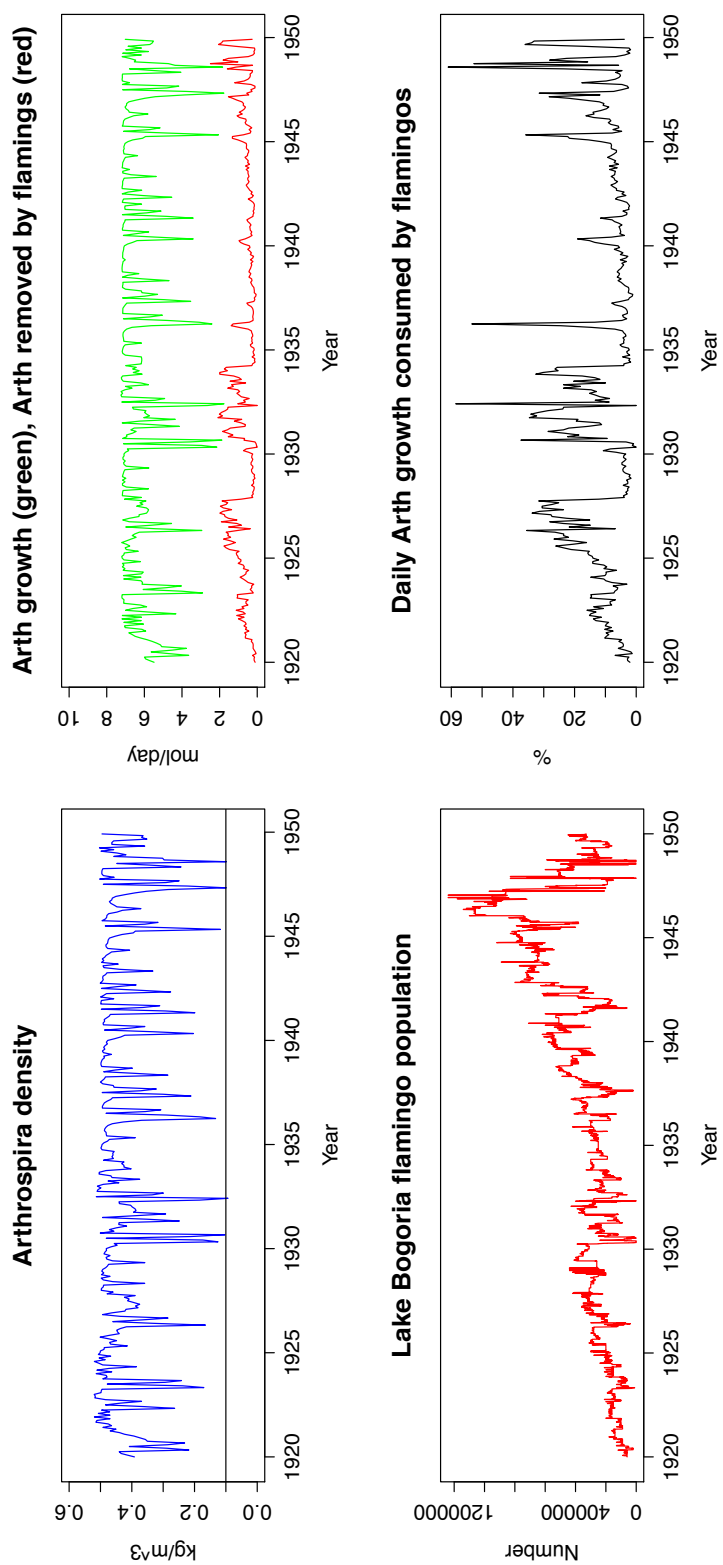


FIGURE 5.14: Lake Bogoria NPZF model output. The *Arthrospira* density threshold above which flamingos can feed is marked at 0.1 kg m^{-3} .

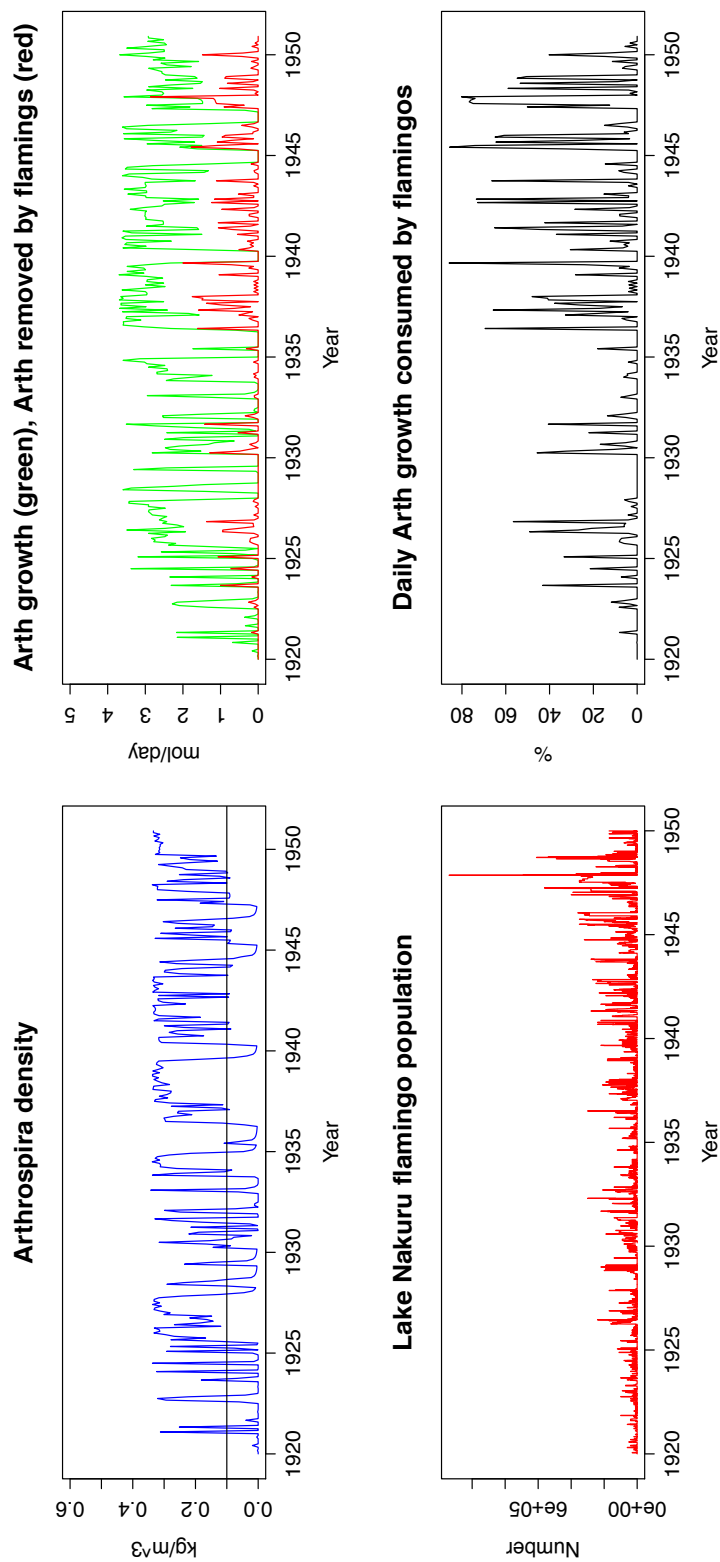


FIGURE 5.15: Lake Nakuru NPZF model output. The *Arthrospira* density threshold above which flamingos can feed is marked at 0.1 kg m^{-3} .

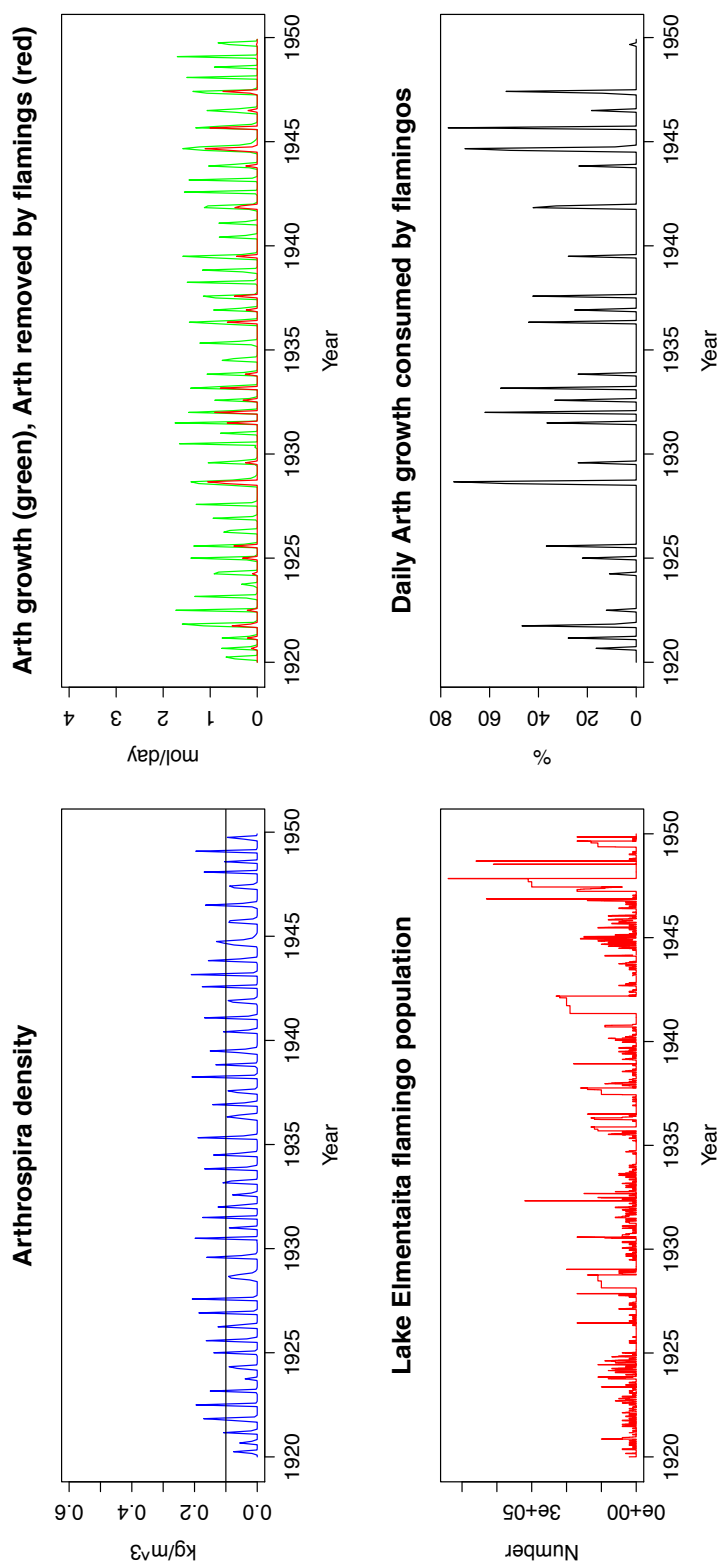


FIGURE 5.16: Lake Elmentaita NPZF model output. The *Arthrospira* density threshold above which flamingos can feed is marked at 0.1 kg m^{-3} .

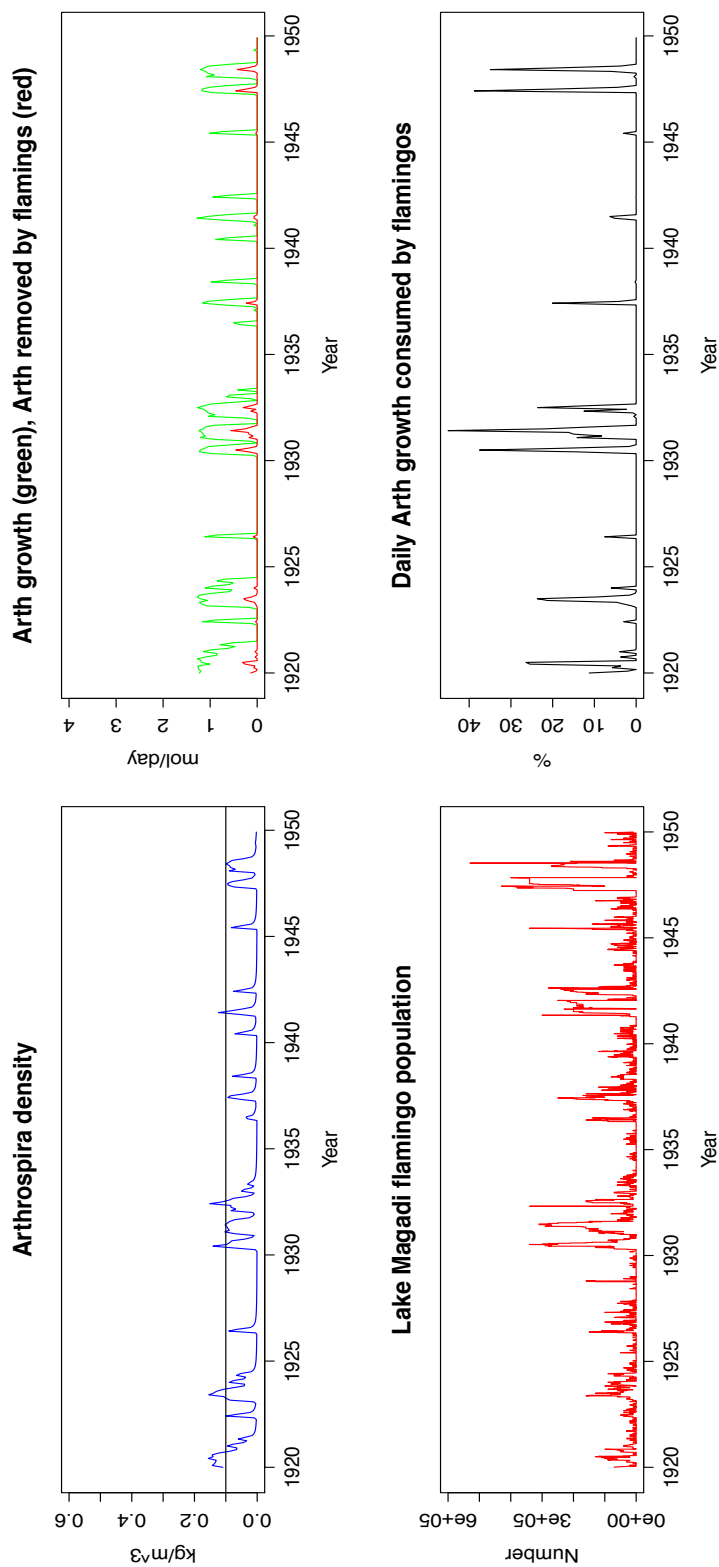


FIGURE 5.17: Lake Magadi NPZF model output. The *Arthrospira* density threshold above which flamingos can feed is marked at 0.1 kg m^{-3} .

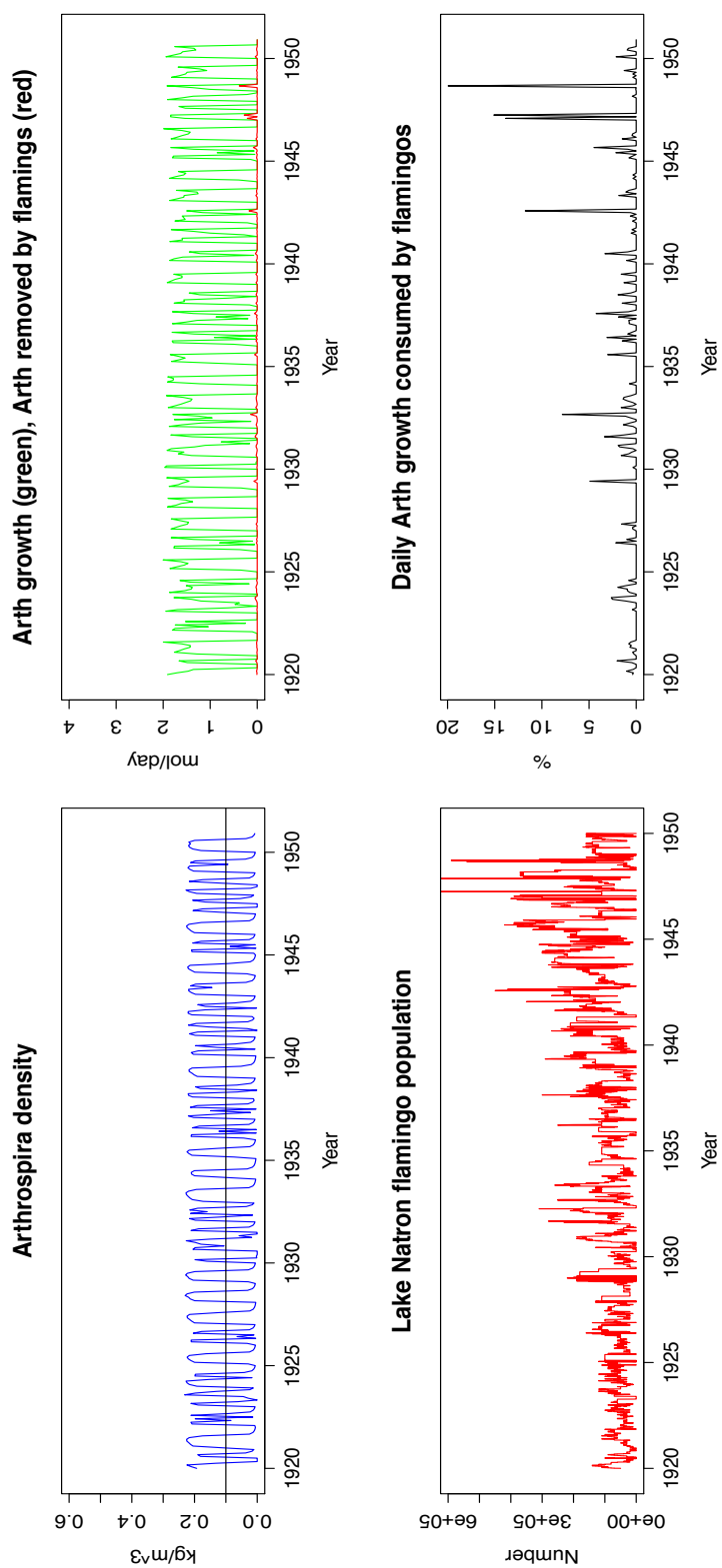


FIGURE 5.18: Lake Natron NPZF model output. The *Arthrospira* density threshold above which flamingos can feed is marked at 0.1 kg m^{-3} .

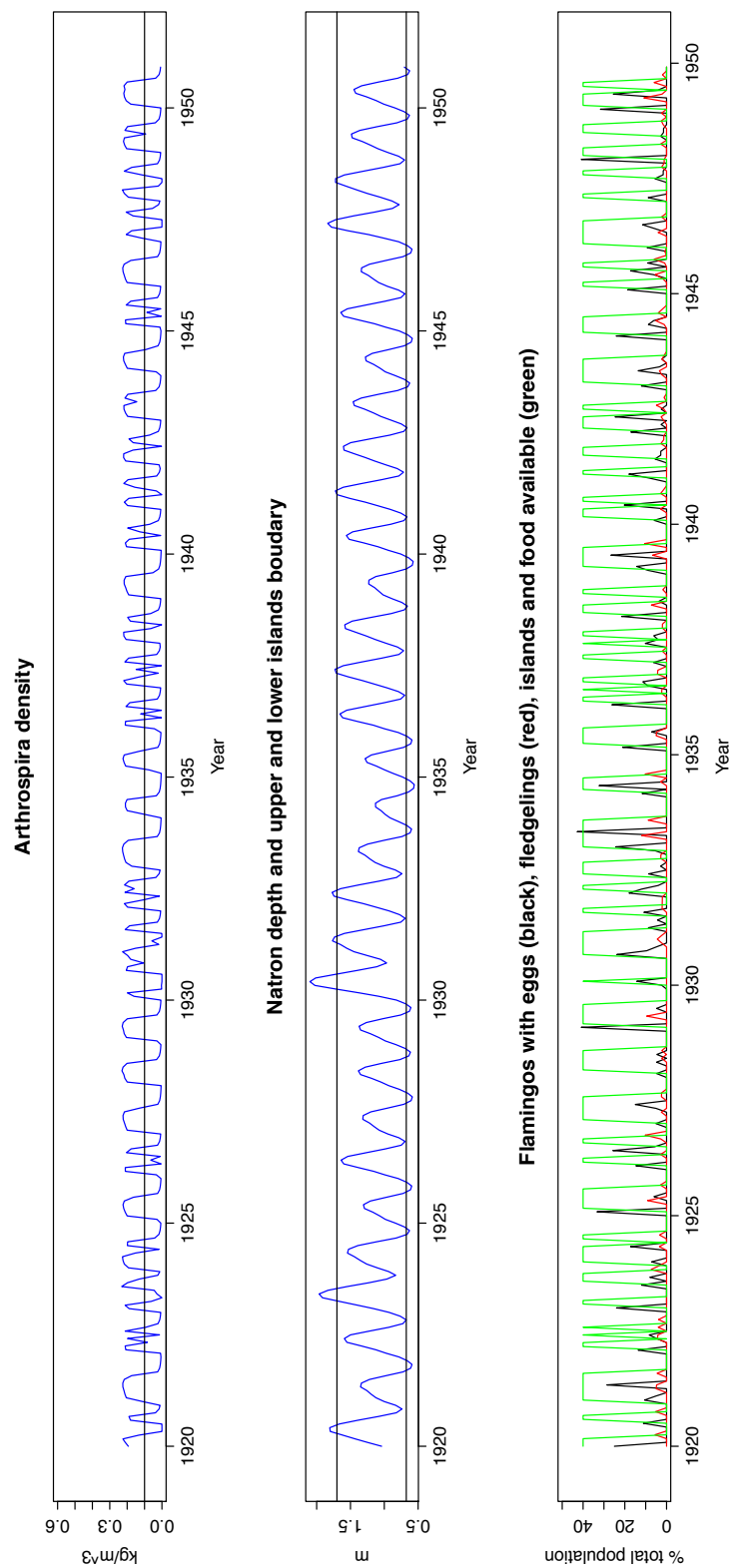


FIGURE 5.19: Flamingos can only breed at Lake Natron if both islands and food are available. This is achieved by the model, which outputs many successful breeding attempts. The *Arthrospira* density threshold above which flamingos can feed is marked at 0.1 kg m^{-3} (leftmost graph), and the depths between which breeding islands are available are highlighted (middle graph).

Overall the NPZ model outputs the key behaviours that are observed in the Kenyan soda lakes. There are rapid fluctuations in response to changing lake water levels, and different behaviour output by the NPZ model at each lake. There are have been three observed crashes in *Arthrosphaera* abundance at Lake Bogoria, in 1978, 2001 and 2004. The NPZ model output *Arthrosphaera* crashes in the late 1970s, and around 2004 at low lake water levels, after high rainfall but not in 2001. This suggests that the 2001 crash may have been caused by factors not considered by the model or perhaps that Lake Bogoria is more sensitive to changes than the *Arthrosphaera* parameters currently allow.

Because of its very high average salinity ($>100\text{ ppt}$) *Arthrosphaera* growth only occurs at Lake Magadi during flood periods. In Lake Bogoria *Arthrosphaera* will usually dominates and growth is usually limited by nutrient availability, apart from during periods of higher salinity where growth becomes salinity limited, or the flood period in 1917 where growth becomes limited by zooplankton because of the lower salinity. The outputs for Lakes Logipi, Nakuru, Elmentaita, Magadi and Natron exhibit rapid changes, but the deeper lakes output longer periods of stability in terms of *Arthrosphaera* abundance, than the shallower lakes.

Crashes in *Arthrosphaera* density are caused in most lakes when the thresholds for *Arthrosphaera* growth have been exceeded. However, at Lake Bogoria crashes in *Arthrosphaera* are more often the result of large rainfall events that shock *Arthrosphaera* growing at the surface of the lake, because it is very stable compared with the other lakes.

Flamingos can abstract a large proportion of daily *Arthrosphaera* growth when there are low densities of *Arthrosphaera* or large numbers of flamingos at one lake. It is possible that a large number of flamingos will limit the *Arthrosphaera* density at these lakes.

5.3.1 Sensitivity Analysis

Since there is little data with which to compare the NPZ model output, and the aim of the model is to capture the characteristic changes at each lake, it is challenging to measure the accuracy of the outputs of the NPZ model quantitatively. Instead the sensitivity of the NPZ model was explored by varying the free parameters one at a time for each lake, and the change in the outputs were compared by visual inspection. The free parameters (see Table 5.1) are the half saturation coefficient for the uptake of N by P (k_N), the loss of P and Z by respiration when salinity is twice the optimal salinity (β_P and β_Z respectively), the optimal rainfall (R_{opt}), and the maximum salinities for P and Z (S_{maxP} and S_{maxZ}).

Tables 5.3 and 5.4 show the characteristics of each lake and the changes that occur when each parameter is varied by $\pm 10\%$.

The lower the half saturation constant (k_N), the more quickly P can grow for the same N concentration. This is because P becomes more efficient at consuming N . The P

concentration output by the model is not very sensitive to increase in N half saturation constant.

The P respiration parameter (β_P) increases the rate of P respiration at higher salinities, which is why P is reduced when β_P increased at higher salinities, and therefore lakes with higher average salinity are more sensitive to β_P . At lower salinities β_P does not affect P output. The lake most affected by changes in β_P is Lake Magadi because of its very high salinity. Although little is known about P growth at Lake Magadi, it is likely that P is absent or very low in abundance during wet phases.

The Z respiration parameter (β_Z) increases the rate of Z respiration at higher salinities, which will cause it to predate more on P . The only real difference for increase in Z is to increase magnitude of nutrient cycling at low salinities <25 ppt, as Z becomes more sensitive to changes in salinity, and reduce the rate of nutrient cycling at salinities 25-40 ppt, where respiration rates are higher causing lower Z concentrations.

Bogoria is the only lake that shows any sensitivity to change in rainfall by 10%. This is because Lake Bogoria is hyper-saline, and the freshening of the surface by rainfall has a larger affect on the phytoplankton community compared with the fresher lakes. At Lake Bogoria *Arthrosira* density is generally very high, but crashes in *Arthrosira* are known to occur, and there is still a high variation in density in observed data (see Figure 3.20). The impact of rainfall at Lake Bogoria on *Arthrosira* density can be seen in Section 5.3.

The output is not very sensitive to a 10% change in P and Z maximum salinity. The most notable difference being that the time period where Z can grow at high average salinity lakes during flood periods (e.g at Lake Magadi from 1910 to the early 1920s, Figure 5.9) is extended by a few months by an increase in Z maximum salinity, and vice versa for a lower S_{maxZ} , but this does not change the character of these lakes.

In summary, the changes in the free parameters explored here do not change the character of Lakes Logipi, Nakuru, Elmentaita or Natron, and only cause very small changes to the N P and Z outputs. The only notable changes occurred for Lakes Bogoria and Magadi. The characteristic Lake Bogoria output was changed by an increase in optimal rainfall, which prevented crashes in *Arthrosira* density from occurring. Lake Magadi was sensitive to changes in β_P which prevented the growth of P at Lake Magadi during flood events. It is unknown whether P has grown in Lake Magadi during these periods.

This chapter described the NPZF model used to output *Arthrosira* densities at six soda lakes between 1904 and 2012. The lesser flamingos move between these lakes in search of the *Arthrosira* (P) output by the NPZF model and nesting opportunities. The next chapter gives an overview of flamingo behaviour and describes the model used to simulate flamingo population change and distribution. The flamingo model feeds back

flamingo population distribution data to the NPZF model to allow for the abstraction by flamingos at each lake.

Characteristics	Logipi	Bogoria	Nakuru	Elmentaita	Magadi	Natron
NPZ cycling: rate	Low	Low	High at high LWL, low at low LWL	High	V.low	Low
P	V.low, but high for short periods	High with crashes	High P phases, unstable P phases	Low, unstable	Low at high LWL	High at mid LWL
Z	Only present at high LWL	Only present at v.high LWL	Present at mid-high LWL	Ubiquitous, unstable	None or low at v.high LWL	None or low at v.high LWL
Parameter						
$k_N + 10\%$	-	-	-	-	-	-
$k_N - 10\%$	-	-	-	-	-	-
$\beta_P + 10\%$	Reduced frequency of P peaks	-	-	-	No P growth	-
$\beta_P - 10\%$	Increased frequency of P peaks	-	-	-	Increased frequency of P peaks	-
$\beta_Z + 10\%$	-	Increase in NPZ cycling magnitude	Reduced cycling rate and magnitude	-	-	-
$\beta_Z - 10\%$	-	Decrease in NPZ cycling magnitude	Increased NPZ cycling rate and magnitude	-	-	-

TABLE 5.3: The change in NPZ characteristics for each lake when free parameters in the NPZ model are varied by $\pm 10\%$. The NPZ cycling, P and Z rows describe the main characteristics of each lake when the final parameter values are used. The parameters are then varied and any change in characteristics (made by visual inspection) is noted. LWL is short-hand for lake water level, and “-” is used where there is no qualitative change in the NPZ output. This means that any change in N, P and Z is very small e.g. change in P density of $< 0.01 \text{kgm}^{-3}$, which is negligible compared with the threshold above which flamingos can feed at 0.1kgm^{-3} , and also that any small change in N, P and Z is as expected according to the parameter that is being varied.

Characteristics	Logipi	Bogoria	Nakuru	Elmentaita	Magadi	Natron
NPZ cycling: rate	Low	Low	High at high LWL, low at low LWL	High	V.low	Low
P	V.low, but high for short periods	High with crashes	High P phases, unstable P phases	Low, unstable	Low at high LWL	High at mid LWL
Z	Only present at high LWL	Only present at v.high LWL	Present at mid-high LWL	Ubiquitous, unstable	Low at v.high LWL	Low at v.high LWL
Parameter						
$R_{opt} + 10\%$	-	No P crashes	-	-	-	-
$R_{opt} - 10\%$	-	-	-	-	-	No P peak in 1917
$S_{maxP} + 10\%$	-	-	-	-	-	-
$S_{maxP} - 10\%$	-	Reduced P in late 1980s at high salinity	-	-	-	-
$S_{maxZ} + 10\%$	-	-	-	-	-	-
$S_{maxZ} - 10\%$	-	-	-	-	-	-

TABLE 5.4: The change in NPZ characteristics for each lake when free parameters in the NPZ model are varied by $\pm 10\%$. The NPZ cycling, P and Z rows describe the main characteristics of each lake when the final parameter values are used. The parameters are then varied and any change in characteristics (made by visual inspection) is noted. LWL is short-hand for lake water level, and “-” is used where there is no qualitative change in the NPZ output. This means that any change in N, P and Z is very small e.g. change in P density of $< 0.01 \text{kgm}^{-3}$, which is negligible compared with the threshold above which flamingos can feed at 0.1kgm^{-3} , and also that any small change in N, P and Z is as expected according to the parameter that is being varied.

Chapter 6

The lesser flamingo model

This chapter describes the flamingo model. The literature review (Section 6.1) relates the model to previous work, and then in Section 6.2, the final model is described and the model output can be seen in Section 6.2.8. The hydrological, *Arthospira* and flamingo models are then used to test hypotheses about changes in the flamingo population in Chapter 7. The model was written in java in a text editor called Sublime Text, and version control was managed using GitHub.

6.1 Literature review

6.1.1 Flamingo distribution and abundance

Flamingos move between different soda lakes in what can appear to be an unpredictable fashion. Until recently the East African flamingo population was assumed to be genetically isolated from the population in southern Africa. This was based on the assumption that flamingos would not be capable of flying the 2,200 *km* distance between southern and East African lakes non-stop, and given that there have been no observations of flamingos resting at lakes en route. There has been evidence however of interchange between these two regions. Breeding colonies in southern Africa have been observed in numbers which far exceed the resident southern African flamingo population (Simmons, 2000). These observations have been found to coincide with lower than expected numbers in East Africa. Lesser flamingos have also been found to store fat like other migratory birds which would theoretically allow them to make the journey non-stop between regions (Simmons, 2000).

It has been difficult to count the total population of lesser flamingos in East Africa. Flamingo numbers have been recorded in the literature by different scientists (e.g., Brown & Root, 1971; Vareschi, 1987; Tuite, 1979; Childress et al., 2007) using differing methods. Visual estimates are likely to have a high margin of error associated

with them, particularly when made from the ground rather than from the air. It is also difficult to estimate total population since the population may be spread across many different lakes, and can move frequently between different lakes, so a census must be undertaken across as many lakes in the East African Rift Valley as possible.

Tuite (1979) showed that aerial photography can be used to make far more reliable estimates of flamingo populations. However, this method of counting flamingos is still rarely used. It is perhaps no surprise that counts using different methods by Vareschi (1987) and Tuite (1979) in August and September 1974 gave very different results. It is probably unwise to take records of flamingo abundance in the literature as anything more than a rough guide to the abundance of lesser flamingos, unless they have been made using a more reliable method such as aerial photography.

Early estimates of total population in East Africa vary between one and five million (Brown, 1973; Khal, 1975), which makes it difficult to know the true extent of population decline. Bartholomew and Pennycuick (1973) used aerial photographs across 24 lakes in Kenya and Northern Tanzania on 28-30th March 1969. They counted the total population at that time as 1,043,816 birds. This method is much more reliable, but has not been used in many population censuses.

The lesser flamingo population is considered a “near-threatened” species (IUCN, 2006) after the East African population was widely regarded to have halved from two million in the 1950’s (Brown, 1973) to 1.2 million in 2010 (Nature Kenya, NMK, KWS). To estimate the decline in flamingo populations given that they may move between East and southern Africa, it is more useful to take the populations in both regions into account. A recent estimate by Simmons (2000) estimates the decline in flamingo population using a revised estimate of total flamingo populations in southern and East Africa initially made by Kahl (1975), and compares this with numbers counted by the African Waterfowl Census by Wetlands International. The most comprehensive census was made in 1994 during which most of the East African population was counted. Simmons found that the lesser flamingo population in southern Africa has declined from 55,000 in 1975 to 40,000 in 1994-7, a decline of 27%. The total population of southern and Eastern Africa was estimated to have declined by 21%, from 5,057,000 to 4,000,000 birds. This estimate is far more optimistic than previous estimates, and was made using more reliable data. The conservation status of lesser flamingos has not changed in response to this estimate, and the actual trend in lesser flamingo population is still debatable. The long term trend in lesser flamingo population is still uncertain since this change in population occurs over 20 years, which is only about half the estimated life span of a lesser flamingo. This trend could be the result of unfavourable breeding conditions over the past twenty years, and may be related to the pressure that humans put on natural resources. Whether this trend is short-lived or not, any potential recovery in lesser flamingo population is likely to be hindered by the exploitation of natural resources by humans. Currently there are proposals to dam the Ewaso Ng’iro, a major inflow to Lake Natron, which could

have catastrophic affects on the breeding success of lesser flamingos in East Africa if it was allowed to go ahead. If the lake water level is stabilised at a level that prevents flamingos from breeding, their only major breeding site would be unsuitable (BirdLife International, 2000).

There are no records of flamingo movements in response to food abundance before 1972. However, in 1937, 1954, 1956 and 1961 heavy rains in the Eastern Rift Valley were associated with large fluctuations in flamingo numbers. In 1954 and 1956 most of the flamingos at Lake Nakuru left the lake (Brown, 1973, 1971a), and in 1937 and 1961 there was an increase in lesser flamingo population at lakes in Western Uganda (Din & Eltringham, 1976).

Movements of lesser flamingos after periods of drought or heavy rain are most likely to be associated with a reduction in food availability. On these occasions either the sudden dilatation in salt concentration at the lake surface by a large rainfall event, or the overall salinity change within the lake moving beyond the tolerance of the phytoplankton dominating the lake flora at that time cause a change in the availability of *Arthrosphaera*. The sudden reduction in salinity in soda lakes recorded by Leslie Brown between 1954 and 1956 coincided with changes in the phytoplankton abundance and community structure. At other times when lake level has declined, the salinity can increase beyond the tolerance of *Arthrosphaera*. An example of this was seen by Vareschi (1987), when studying the flamingo population at Lake Nakuru from 1972 to December 1974. In May 1972 Vareschi found *Arthrosphaera* abundance to be >150 mg DW per litre of lake water. Around this time there were an estimated 1.5 million flamingos on the lake. *Arthrosphaera* abundance began to slowly reduce before declining suddenly in February 1974 to 80 mg DW per litre. This occurred during a time where lake level was reducing and conductivity was increasing. A decrease in flamingo population at Lake Nakuru was observed during this time. The remaining flamingos had to change their grazing habits in order to make the most of the low food abundance by spending up to 80% of their time feeding, either from patches of denser algae or by grazing on diatoms found on the mudflats.

The distribution and density of lesser flamingos in response to changes in phytoplankton abundance was studied by Tuite (2000) between 1962 and 1976. Tuite found that lesser flamingos were concentrated at lakes Bogoria and Nakuru when blooms of *Arthrosphaera* dominated the lake phytoplankton. In March 1969 more than 600,000 were at Lake Bogoria, and about 300,000 were at Lake Nakuru. In 1973 there were approximately 100,000 and 800,000 at lakes Bogoria and Nakuru respectively. On both these occasions nearly the entire East African lesser flamingo population was thought to be concentrated on these two lakes. The observations over the following three years showed a reduction in the total number of flamingos across all lakes in East Africa to between 380,880 in February 1975, and 540,724 in January 1976. The abundance of *Arthrosphaera* was low during this time, and flamingos fed instead upon benthic diatoms, their secondary food source, and were dispersed across many lakes. This dispersion is necessary because the

overall biomass of benthic diatoms is low compared with blooms of *Arthrospira*, and they also grow much more slowly (Tuite, 2000).

Lakes Bogoria and Nakuru are particularly important feeding grounds when there are blooms in *Arthrospira*, with Lake Bogoria being capable of supporting several million lesser flamingos during these events (Pennycuick & Bartholomew, 1973). If flamingo population abundance could be reconstructed for Lake Bogoria using lake sediments, it may be possible to estimate the total East African lesser flamingo populations in the past c.a 150 years and give a better indication of whether flamingo population decline is a recent phenomenon or if it is part of a longer-term trend.

6.1.2 Breeding of lesser flamingos

Brown (1955) discovered the breeding colonies of the lesser flamingos at Lake Natron, and gave the first detailed information about flamingo breeding behaviour. There have been reports of flamingo nests found at other lakes, including Lake Nakuru (Someren, 1922; Mackworth-Praed & Grant, 1952; Meinertzhagen, 1958), Lake Bogoria (Akeley, 1912) and Lake Rudolf in 1957. These reports are vague, with no mentions of chicks hatched on these nests. It is likely that these were practice nests, since no fledglings were observed, and lesser flamingos have built practice nests at Lake Bogoria in recent years. The only well documented case of lesser flamingos successfully breeding outside of Lake Natron in East Africa was during 1962, after unprecedented rainfall in 1961 diluted the caustic waters of Lake Magadi (Brown & Root, 1971). This was an unusually large nesting colony, but this breeding attempt would have been nearly a complete failure without human intervention. The flamingos were not isolated from the shore and so predators like hyenas could reach the nests, and the soda lake water, even diluted by the rains, caused the death of large numbers of chicks as the salts built up into large clumps on their legs. A rescue effort freed 27,000 of these chicks, and many more were saved by pumping fresh water into the areas where the birds were congregating (Brown & Root, 1971). Lake Magadi is also a less suitable location for nesting because there is not enough food available for the flamingos, which flew to Lake Natron to feed.

Lake Natron is the only regular breeding site for lesser flamingos in East Africa. At this lake lesser flamingos build nests on isolated mudflats far from the shore. There are two main breeding sites; the Gelai mudflat site is located close to the lagoon in the southern part of the lake, and the other is the Shombole site; an expanse of trona that has cracked into polygonal plates, located eleven or twelve kilometers south of the Shombole mountain at the Northern end of the lake. This site is further from freshwater and slightly less favoured compared to the Gelai site (Brown & Root, 1971).

When flamingos breed they first build nests out of the mud and trona, scooping it with their bills into a mound several inches above the ground, a process that may take up to six weeks (Brown, 1971b). A depression is made in the top where the egg is laid.

Year	Location	Months	Eggs laid	Young hatched	Success (%)
1953	None				
1954	Natron	June-Aug	150,000	60,000	40
1955	None				
1956	Natron	Mar	35,000	900	3
1957	Natron	Oct-Dec	770,000	400,000	70
1957	Rudolph	June	30,000		
1958	Natron	Oct-Dec	560,000	400,000	71
1959	Natron	Feb	3000		
1959	Natron	Nov-Dec	215,000	0	0
1960/1	Natron	Nov-Jan	300,000	80-100,000	27-33
1961	None				
1962	Magadi	Jul-Sept	1,100,000	350-400,000	32-36
1963	Magadi	Aug-Sept	0		
1964				<10,000	
1965	Natron	Oct-Nov		<100,000	
1966	Natron	Oct-Nov		<100,000	
1967	Natron	Oct-Nov		<100,000	
1968	None				
2002/3	Natron	Oct-Jan	high numbers		
2003/4	Natron	Oct-Jan	high numbers		
2012	Natron	Nov-Jan	175,000	120,000	

TABLE 6.1: Lesser flamingo breeding events, the data between 1953 and 1968 are summerised by (Brown & Root, 1971). The 2002-4 data are from Childress et al. (2007). The numbers for the 2012 event were from (Birdlife International, 2012).

An egg is incubated for 28 days before it hatches, and it usually takes 70-75 days for a flamingo chick to develop and become fully fledged. The success rate of nesting attempts by flamingo colonies can vary hugely from 0-75%. Despite the isolation from predators afforded by breeding sites at Lake Natron, the average success rate is still only about 42%. Success is dependent on climate conditions and the size of the colony, with larger colonies being more successful under the same conditions. Observations of flamingos at Magadi suggest that smaller colonies of flamingos are more likely to desert their nests and young (Brown & Root, 1971).

Breeding events have been recorded sporadically in the literature, with the most detailed work on flamingo breeding habits undertaken by (Brown, 1973). The information on breeding events found in the literature is summarised in Table 6.1.

Although lesser flamingos breed at various times throughout the year, the breeding season is generally between October and December. Large nuptial displays are often seen when very large numbers of flamingos congregate. These nuptial displays have often been seen at Lake Nakuru in the weeks or months preceding breeding events (Brown, 1955).

Breeding at Lake Natron was prevented or limited by high water levels during 1961 to

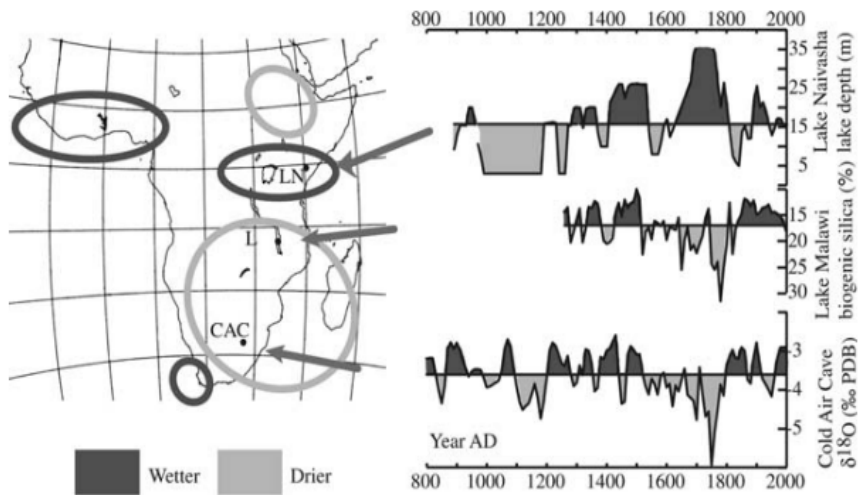


FIGURE 6.1: The amount of rainfall varies differently in East and southern Africa in response to El Niño and La Niña oscillations (Holmgren & Oberg, 2006). During the La Niña phase, East Africa receives higher than average rainfall, while in southern Africa there is below average rainfall, and the opposite occurs during the La Niña phase.

1965, but lesser flamingos still attempted to breed in other locations. In 1955 intense nuptial displays were seen at Lake Nakuru, coinciding with the right water depth at Lake Natron. Despite this activity no breeding was found to occur during that year. The reason for this is unknown, although it is speculated that food abundance may have been low at this time which may have reduced the likelihood of breeding. It has been suggested more recently that lesser flamingos from East Africa may fly to southern Africa to breed at the Sua Pan. The Sua Pan in Botswana is one of the sites where lesser flamingos have been sighted in large numbers (Borello et al., 1998), and is considered an important breeding site for lesser flamingos. Breeding was seen at Sua Pan in 1996, 1997, and 1998, with up to 110,000 adult birds present in 1997 (McCulloch & Borello, 2000). Sua pan is only suitable after the rains fill the salt pan with water and it becomes a saline lake. How it is that flamingos would know when to move between the East and southern regions is a mystery. It is a huge distance to travel in the hope that conditions would be suitable, but despite the questions surrounding this behaviour, there are some interesting conditions that make it a viable strategy. Palaeoclimate reconstructions of rainfall in East and southern Africa (see Figure 6.1) show that it is often, but not always the case, that droughts in East Africa correlate with higher than average rainfall in southern Africa in response to the La Niña events. This would mean that when *Arthrosphaera* abundance in East Africa reduces as lake water levels decline, flamingos are likely to find food and suitable breeding grounds in southern Africa. The breeding seen at Sua Pan in 1996-8 coincided with lower than average water levels, and low numbers of flamingos in East Africa (Nasirwa, 2000).

6.1.3 Modelling

6.1.3.1 Time-energy budget models

Time-energy budget models are constructed by monitoring the amount of time spent by an organism undertaking different activities, such as feeding and resting, and calculating the energy expended by multiplying the metabolic cost of each activity by the time taken to complete it. This requires knowledge of the daily activity, mass, and metabolic rates of the organism. The metabolic rates can be measured by measuring the oxygen consumption of an organism undertaking particular activities in a laboratory. In the field doubly labeled water (DLW) can be used which involves injecting an animal with water containing known isotope ratios, and recapturing the same organism after a period of activity and measuring the change in isotope ratios in the blood. Biotelemetry can be used to monitor heart rate of animals in the field, which is then used to estimate metabolic cost for different activities. Biotelemetry involves capturing the animal and fitting sensors to it, releasing it back into the environment and then monitoring its activity remotely. This is not suitable for small animals since the weight of the sensors will begin to affect the animal behaviour. Another way to estimate metabolic cost of activities is to capture animals before and after an activity and weigh them to calculate fat loss (Goldstein, 1988).

Fort et al. (2011) compared different methods of modelling sea bird energetics, specifically for the great cormorant *Phalacrocorax carbo* with a ‘direct’ measurement of DLW, which can be used to estimate mean energy expenditure. They compared allometric equations, time-energy budget models, and thermodynamics models and found that the results of the time-energy budget model were closest to the doubly labeled water (DLW) result with only a 5.3% over-estimation for energy expenditure compared with a 9.9% overestimation for the thermodynamic model, and an overestimation of 16.6% by the allometric equations (Fort et al., 2011). These results showed that the time-energy budget model approach predicted the energy budget for the great cormorant (*Phalacrocorax carbo*) most accurately. This may be surprising since the thermodynamic model considers a much wider array of variables than the time-energy budget model. As well as mass, metabolism and behavioural parameters the thermodynamic model requires many more morphological and physiological parameters as well as climate data to run (Fort et al., 2011). It may be that the large number of variables accumulated a large error in the thermodynamics model in this case, which is where simpler models are beneficial.

6.1.3.2 Dynamic energy budget models

One way to model complex systems is to use systems dynamics models. System dynamics models were founded by Forrester in the 1950’s, as a way to capture the emergent behaviour of complex interactions by modelling complex systems as a set of stocks and

flows, considering feedbacks and time lags. In many complex systems the cause of a problem may be indirect and may have been caused some time before any change is observed in the system (Scholl, 2001). System dynamics models are therefore more likely to identify the true cause of a problem, and allow the investigation of what changes must be made to improve the system. System dynamics has been applied predominantly in the fields of business management, economic systems and urban dynamics (e.g., Forrester, 1971). A similar approach has been developed in biological systems that tends to deal with individuals rather than aggregated populations, and is known as dynamic energy budget (DEB) modelling.

Dynamic energy budget (DEB) models are used to describe the energy flow through organisms at an individual based level. The general DEB model has been constructed on the principal that mass and energy are conserved, and that most organisms function using the same metabolic processes (Kooijman, 2001). The model considers stocks and flows of energy, where energy is extracted by an organism from the environment and stored in reserves (stocks) before being mobilised and allocated to maintenance, growth, maturity or reproduction. The state of the organism and the availability of food affect the rates at which energy flows through the organism, is allocated to different processes or stored. The reserves of energy allow organisms to survive in a fluctuating environment, and is key to a DEB model.

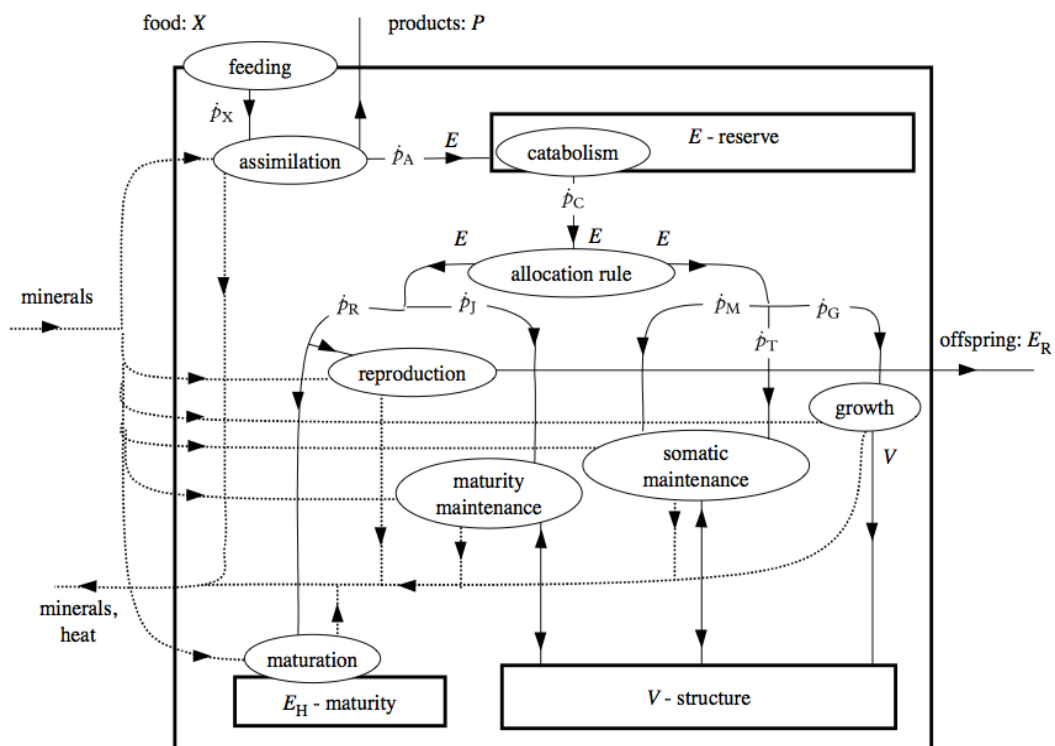


FIGURE 6.2: The standard DEB model. The square represents the organism, the ovals are processes, and rectangles are state variables. The arrows show the flow of energy in the form of reserves (E), structure (V), minerals, food (X), products (P) or reproduction (E_R) Figure taken from (Sousa et al., 2008).

Figure 6.2 shows the standard DEB model which is applicable to most heterotrophic unicellular organisms and animals (Sousa et al., 2008). The general organism in this model consume one energy source, and consists of one reserve, one structure, and metabolic processes (Nisbet et al., 2000). The flow of energy between the state variables is determined by a set of differential equations which are based on empirical observations of organisms and assumptions based on the laws of physics. The general model can usually be made species specific by changing the model parameter values, which include the surface area and length of the organism, and the size of the energy reserve, and the cumulative energy investment required to reach different levels of maturity. Maturity is important in DEB models because it allows the organism to behave differently at different stages in its life, embryos do not feed or reproduce for example, but when they are mature enough to be born feeding begins, and then later on when puberty is reached energy can be invested into reproduction.

Much of the energy is used by an organism to maintain its complexity, which is consistent with the laws of thermodynamics. The second law states that entropy can only increase, which means that the energy or order in any system or object flows from high to low to become more disorganised, with a lower potential energy, until it reaches a zero entropy state where the system or object has no potential energy remaining. It has been found that living organisms do not violate the second law because they maintain a low entropy state by consuming low entropy (food) and excreting high entropy (waste), acting as a kind of heat pump that extracts work from low entropy to maintain its low entropy state (Schneider, 1994).

To construct a ‘standard’ species specific DEB model in accordance with (Sousa et al., 2008) twelve parameters need to be measured or estimated. Some parameters are easier to measure than others; body mass and length of an organism can be measured in a non-destructive way and are relatively straight forward, but the reserve and structure are more difficult, and have to be related to a variable that can be measured directly. The metabolic processes are also difficult to study because they are interdependent (Kooijman et al., 2008). Kooijman et al. (2008) states that all the parameters required for a DEB model can be derived from the organism maximum length and observations of growth and reproduction at different constant food densities. It may be possible to estimate these parameters for one species from a reference species using scaling relationships, with the reference ideally within the same taxa and as similar to the species of interest as possible. Estimating these parameters is challenging because for many species it is not possible to monitor the energetics in the field, particularly for a constant food abundance. It is likely that the life span of the organism is much greater than the timespan of the project, and so it is not possible to follow the same individual. Many also move over great distances.

Nisbet et al. (2010) investigated the usefulness of DEB models by modelling the zooplankton *Daphnia*. They used information about growth and reproduction of the species

from the literature to obtain a subset of the parameters for a standard DEB model. The simplified DEB model only considered size of the zooplankter, and the distinction between juvenile and adult life stages. The simple DEB model was able to predict growth and reproduction of individuals in response to food abundance, and so the conclusion drawn in this paper was that a simplified version of the standard DEB model is still a viable approach to modelling the growth and reproduction of organisms, and has the advantage of reducing the number of parameters needed, particularly those which are very difficult to measure. The cost is that the reserve component is ignored which is a key part of the DEM model and necessary where there are fluctuations in food availability (Nisbet et al., 2010). The difficulty of constructing even simple DEB models is the lack of data available for the parameterisation for many species, and the large error that would accumulate from estimates of several of these parameters may prevent a realistic model of a particular species being constructed.

The large fluctuations in food density in the rift valley soda lakes make the concept of reserves important to any model of lesser flamingos. If the concept of a reserve can be incorporated into a model of the lesser flamingos it is much more likely to show realistic behaviour. The large number of parameters required for a DEB model of lesser flamingos is likely to cause problems. However, it may be possible to use a simplified version and estimate certain parameters from reference species.

6.1.3.3 Cellular Automata

The lake ecosystems in East Africa are relatively simple due to the extreme conditions. However, so little data is available about the important interactions within these lakes that it is not possible to use differential equations to describe them. When there is limited data available, rule-based models have often been used to model complex systems.

Behaviour that cannot be predicted by studying the component parts of a system is called emergent behaviour. It is often the emergent behaviour that we are interested in when studying an ecosystem, and because ecosystems are complex systems we cannot always model this behaviour by using a set of deterministic mathematical equations alone.

Rule based models can be used to explore complex phenomena without the input of any physical, chemical or biological information about the organisms, but may be constructed by simply using observations of the emergent behaviour of the organisms. These cellular automata and agent based models models use simple rules to govern the interactions, and have been used to model populations of organisms such as ant colonies and flocking birds (e.g., Bajec et al., 2007).

A cellular automaton (CA) model consists of a grid of cells, where each cell can occupy a different state. Simple rules can be used to mimic the complex interactions and processes that occur in a real system. The different parameters of the system can then be explored without the need for huge memory requirements and will also minimise processing time. These advantages make cellular automata a good way to model biological systems. A disadvantage of this approach is the lack of precision. However, it is still possible to achieve insights into real phenomena, obtain information that can guide experimentation, or identify which processes are unimportant or unlikely to cause certain behaviour (Ermentrout & Edelstein-Keshet, 1993). This section focuses on deterministic CA models, where the domain is a fixed lattice, and each cell has an associated state that is determined at each time step by the states of the neighbouring cells.

A well known example of a deterministic CA is the ‘game of life’, which was devised by Conway in 1970 (Gardner, 1970). In this model the state of an individual cell is determined by the states of the neighbouring eight cells. Each cell can be in one of two states: either ‘alive’ or ‘dead’. Once an initial configuration of cells in a grid are elected to be on, the following rules are applied to each cell for a number of iterations:

- ‘Reproduction’: any dead cell with three live neighbours becomes a live cell.
- ‘Under-population’: any live cell with less than two live neighbours dies.
- ‘Overcrowding’: Any live cell with more than 3 live neighbours dies.
- Any live cell with two or three neighbours lives.

The game of life model produces interesting behaviour for particular combinations of initial ‘live’ cells which illustrates the concept that complexity can emerge from a set of simple rules. Figure 6.3 shows how one configuration of live cells changes over time in a simple CA model. There are many different configurations that produce interesting patterns.

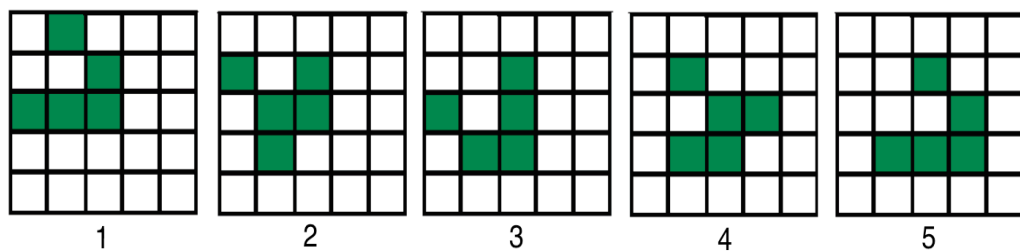


FIGURE 6.3: The numbered grids show how the configuration of live cells (highlighted in green) in grid 1 changes with each time step in accordance to the game of life rules. This configuration produces a repeating pattern that moves across the grid, and is known as a ‘glider’ because of the way it moves.

Cellular automata are not confined to single species models, but have also been used to model multiple species, evolution, and extinction events (e.g., Solé & Manrubia, 1996; Amaral & Meyer, 1999).

A simple cellular automata model was used by Bahr and Bekoff (1999) to model the vigilance of birds grazing in a flock. They did this by filling a grid of cells with birds, represented either as '1' for a scanning bird, or '0' for a feeding bird. At each time step, scanning birds or birds that have looked up from feeding assess their eight neighbouring cells and decide to scan or feed depending upon the proportion of neighbours that are scanning or feeding. If more birds are scanning the bird is more likely to feed, if more are feeding then the bird is more likely to scan. If there are equal numbers scanning and feeding then the bird is equally likely to do either in the next time step. This simple model reproduced behaviour observed in real flocks, such as the observation of increased vigilance around the edges of a flock and increased vigilance in flocks with a larger perimeter to size ratio (Bahr & Bekoff, 1999).

6.1.3.4 Agent based models

The second type of CA model consists of a discrete spatial grid on which agents move and interact using rules. These are called 'agent based' models. When modelling the behaviour of individuals in a population agent based models can be used. 'Agents' refers to the individuals in these models. In an agent based model a set of simple rules is created which governs the way that agents move and interact with each other, and are usually driven by random events. The probabilistic nature of agent based models means that different outcomes are possible for the same initial configuration. When the model is run the emergent behaviour of the agents can then be observed and compared with observations of the behaviour in the real environment.

The complex patterns seen in flocks of birds, swarms of bees, schools of fish and the organisation of ant colonies are some of natures most fascinating spectacles. It had been thought that the complex patterns observed in nature cannot emerge in the absence of a leader, and in the case of flocking birds it was postulated that a leader must be transmitting signals throughout the flock telepathically or using electromagnetic fields (Selous, 1931). Models of flocking behaviour have shown that a leader is not necessary for these patterns to emerge, but they may instead be produced as a result of the decisions made independently by each individual (e.g. Reynolds, 1987).

In an agent based model an agent typically moves across a grid of cells (the environment), or a network. This grid may hold information in each cell about the environment at that particular location, such as food abundance, which may affect the behaviour of an agent looking for food. Or the environment can simply be an empty space in which individuals interact, such as in the case of one of the earliest agent based models called "Boids". Boids was developed by Craig Reynolds in 1986 to simulate the flocking behaviour of birds (Reynolds, 1987). In this model each bird is an agent which navigates a two dimensional grid (representing the sky) using three simple rules:

1. Avoid collisions with neighbouring boids.

2. Attempt to travel at the same speed as neighbouring boids.
3. Attempt to stay near neighbouring boids.

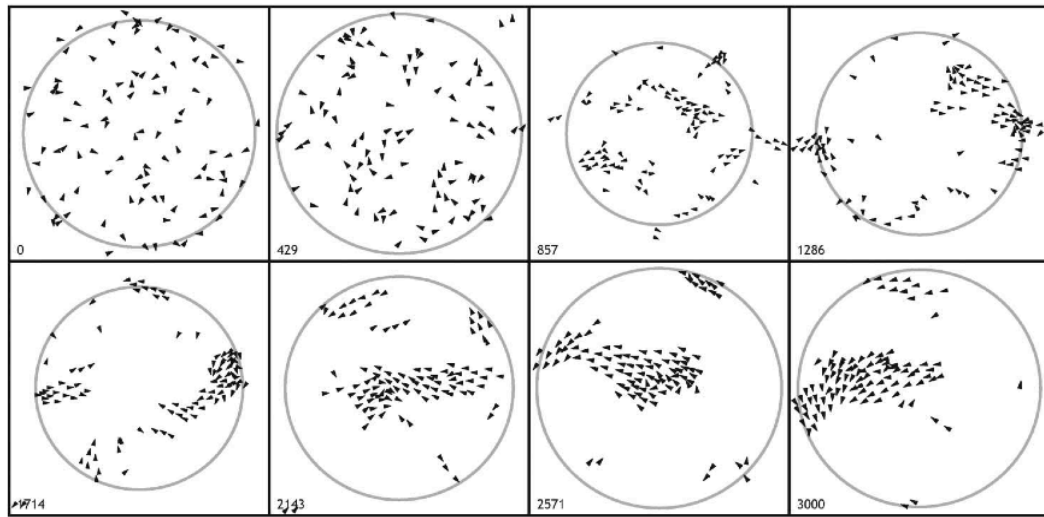


FIGURE 6.4: Snapshots of a simulated flock during one run. Each triangle is a boid with direction indicated by the apex of the triangle. The circle is the environment within which the flock tries to confine itself (Bajec et al., 2007).

Each boid has a velocity which consists of a speed and a direction of travel. The velocity is modified for each boid after each time-step in the model depending upon the location of neighbouring boids. The behaviour of a flock of boids in the simulations appears to the observer to be similar to real flocking behaviour in nature (see Figure 6.4). The success of simulations like this has often been subjectively judged by observers. A quantitative validation of the accurate these simulations has only been developed more recently for flocking behaviour. The idea being that a flock is a set of boids that influence each other whether directly due to close proximity, or indirectly by being part of the same flock (Bajec et al., 2007).

Roberts (1997) describes the relationship between flock size and the number of birds that need to depart from a group in response to a decision or disturbance before the whole flock takes flight. This may need to be considered when modelling flamingo movements between lakes, and could easily be incorporated into an agent based model.

Rule based models have been applied to explore many different types of animal behaviour and organisation. They are particularly useful where complex interactions occur that would be difficult to model using a series of deterministic equations. In the context of flamingo modelling, they would be most useful in terms of determining changes in flamingo behaviour such as when a flamingo decides to leave a lake, which lake the flamingo moves to next, and when they decide to breed. The cellular automata aspect is useful since each lake can be treated as a cell which flamingos can inhabit, and becomes more or less attractive to flamingos depending on food availability and the inclination of flamingos to breed. The flamingos would act as agents, moving between the lakes.

The agent based approach could also be used to investigate the transmission of disease through a population of flamingos under different conditions. The random event element that is used in agent based modelling would be used in terms of flamingo decision making, for example, when fat reserve is reducing, lesser flamingos would be increasingly likely to search elsewhere for food, rather than being triggered by the food density passing a threshold.

6.2 Overview

The aim of the flamingo model is to investigate the 27% decline in population identified by Simmons (2000). To investigate the change in flamingo population and population distribution it was necessary to construct three models drawing on a combination of systems dynamics, mathematical and agent based modelling techniques. The first model simulated lake water level change, the second, *Arthrosphaera* growth, and the third, flamingo population dynamics (Table 6.2). Each model is interlinked; the outputs from the hydrological model feed into the *Arthrosphaera* model, *Arthrosphaera* growth outputs and lake water level are inputs to the flamingo model, and flamingo population abundance and distribution feed back into the *Arthrosphaera* model (see Figure 6.5).

Model	Driving parameters	Outputs
Hydrological	Rainfall	Lake water level, Salinity
Arthrosphaera	Rainfall, lake water level, flamingo population	<i>Arthrosphaera</i> density
Flamingo	<i>Arthrosphaera</i> density	Flamingo population abundance and distribution

TABLE 6.2: Model overview.

The driver for these models is rainfall. The flamingo population is highly itinerant, and to model this behaviour an individual agent based approach was considered to be most suitable. The flamingo energetics are modelled to allow for the condition of the flamingos to be taken into account, since a flamingo is unlikely to breed if it does not have the energy reserves needed to raise a chick in the extreme conditions at Lake Natron, and flamingos must also be able to survive periods of low food abundance. Flamingo behaviour was based on observations of flamingos in the field by researchers such as Brown (1973), and was implemented using a rule based model.

The estimations and simplifications required to produce this model mean that it cannot be expected to reproduce the exact changes that happen over time, or be used as a predictive model. Instead the model is best thought of as a tool used to explore the internal consistency of theories regarding the soda lake ecosystems and flamingo behaviour. The capacity of the model to be predictive is limited since it has been constructed to function

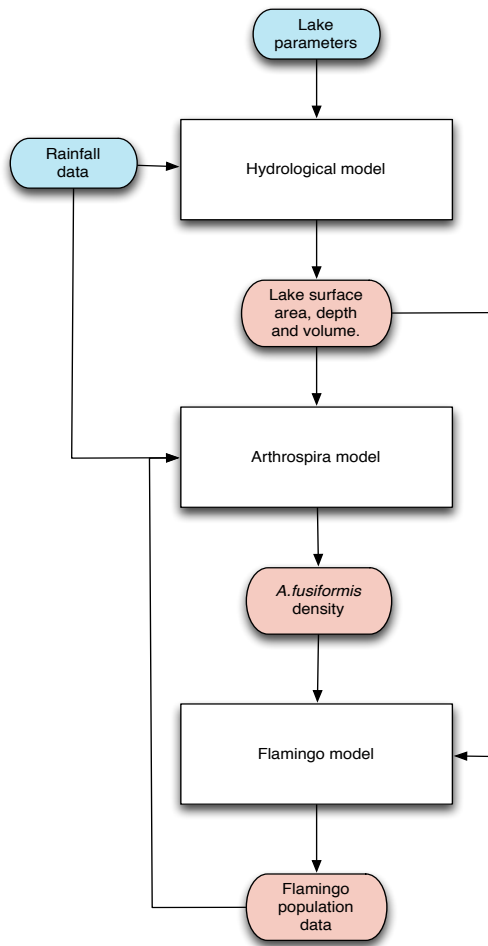


FIGURE 6.5: The model structure.

within the range of lake water level change that has been observed in the literature (e.g. Harper et al., 2003; Melack, 1988; Castanier et al., 1993). However, there is potential to improve the model to cope with more dramatic changes, such as the very dry period in the 1870's, and the very high lake water levels between 1880 and 1910. This would also allow for experimenting with rainfall data generated to simulate variations on future climate change scenarios which forecasts a wetter environment for East Africa. The model currently produces similar behaviours to those seen in the lake network, and exploration of the model behaviour has allowed insights into the emergent behaviour of flamingo populations and raised new questions that will help to direct further experiments and development of the hypotheses.

The flamingo model has two aspects to it; firstly the flamingo energy budget, which calculates the energy flow through individual flamingos or groups of flamingos and the size of their energy reserve, and secondly the rule based flamingo behaviour aspect, which models decisions such as whether to gather in large groups, breed, or move to a different lake. The basic flamingo model limits causes of death to old age and starvation, but death

by disease and toxicosis are also considered in Chapter 7, where different hypotheses for the reduction in flamingo numbers is explored.

6.2.1 Flamingo behaviour

Flamingos respond to many stimuli such as changes in food availability, the sudden availability of a breeding site, rough or smooth lake water, water depth, the rockiness of the shore beneath their feet, the availability of drinking water, the abundance of predators or disturbance by tourists. There are many different aspects of flamingo behaviour that impact the overall population abundance and distribution. Flamingo feeding behaviours were observed by Robinson in 2008 (Robinson, 2008). Four different feeding behaviours were observed at Lake Bogoria, including stand and swim filter feeding, wet mud feeding and deep water feeding. These different feeding behaviours occurred in different places in the lake, and it was suggested that feeding behaviour depends on the presence of predators and the topography of the lake bed as well as food abundance and distribution (Robinson, 2008). Population scale behaviours include movement from one lake to another, flocking behaviour, en-masse courtship dancing, moulting and breeding events. The important aspects of flamingo behaviour to this model are population changes in terms of distribution, overall population size, and breeding events. The conditions that cause them to change their behaviour are primarily changing food availability and the inclination to breed. Other behaviours have been ignored or categorised to simplify the model. It is unlikely that differentiating between different feeding behaviours, for example, is required considering the broader aims of this model.

Flamingos make decisions about when to exhibit different behaviours depending upon their individual condition and the state of their surroundings. These decisions include when to move from one lake to another, what direction to fly in order to move to a new lake, and when to engage in courtship behaviour and fly to the breeding lake to make a breeding attempt. The decisions represented in the model depend on *Arthrospira* density (e.g. Vareschi, 1987; Tuite, 2000), flamingo population distribution (e.g. Brown, 1955), fat reserve of the individual flamingo (Simmons, 2000), inclination to breed (Brown, 1955, 1973) and the availability of breeding sites (e.g. Brown, 1973; Tebbs et al., 2013a). These were chosen as the most likely flamingo-specific parameters to affect overall population change and distribution. Other factors such as predation at non-breeding lakes were not taken into account because most predation occurs by scavengers that take advantage of flamingos that are already injured or weak (Brown & Root, 1971). These decisions include an element of chance, for example a flamingo is *more likely to*, but not guaranteed to move from one lake to another under particular conditions. This part of the model is non-deterministic and can produce different outcomes with each run of the model for the same initial conditions. An overview of the thresholds for flamingo behaviour is outlined in Table 6.3.

A flow diagram showing the decisions undertaken by a flamingo can be seen in Figure 6.6. The main behaviours are also described below in Sections 6.2.1.1 to 6.2.1.5:

6.2.1.1 Feeding

Feeding behaviour is highlighted in orange in the flamingo behaviour flow chart (Figure 6.6). Flamingos feed on *Arthrospira* when it is in densities above the minimum threshold. If no *Arthrospira* is available they feed on diatoms, which are assumed to always be available but can be overgrazed where a large proportion of the total flamingo population are feeding on diatoms at the same lake. Feeding behaviour is explained in more detail in the energy budget description, Section 6.2.2.

6.2.1.2 Courtship

Courting occurs when a flamingo is in a flock of flamingos with a high average fat reserve ($>90\%$), has a high fat reserve itself ($>90\%$), is of breeding age (>6 years), is in a flock that is greater than the minimum size for a breeding colony ($>10,000$ individuals), is not already nesting or raising a chick, and has not already nested in the last 12 months.

6.2.1.3 Breeding

Flamingos begin a breeding attempt when the number of flamingos that have engaged in courtship is greater than the minimum size for a breeding colony. If the flamingos are not already at the breeding lake, Lake Natron, then they will fly to Lake Natron. If Lake Natron is suitable for breeding, with islands available, and *Arthrospira* above the minimum threshold, then they begin nesting. This causes the number of hours that each flamingo is able to feed each day to reduce to 12 hours because of the time required to care for the eggs or chicks. If conditions at Lake Natron remain good for breeding, a flamingo will nest for 40 days (this allows for building the nest and incubation), after which the chick hatches, and then requires another 60 days care before it can survive without its parents. When a fledgeling is old enough to survive alone, the parent flamingos finish breeding and a new flamingo object is created at Lake Natron.

Flamingos will desert nests if the breeding islands become unavailable, or food abundance reduces below a level where parent flamingos are able to maintain their fat reserves at above 30%. If the latter happens, parent flamingos are forced to abandon their nests and search for food, ending the breeding attempt. Breeding behaviour is highlighted in green in the flamingo behaviour flow chart (Figure 6.6).

6.2.1.4 Flight

The direction in which a flamingo will fly is determined by the lake that it previously arrived from, and whether it is in the northernmost or southernmost lake. When a new flamingo is initialised or a flamingo does not remember a previous location, and has a 50:50 chance of flying north or south if not at the northernmost or southernmost lake. A flamingo remembers its previous location for a ten days, and any flight will occur in a direction away from the previous lake if this is the case. If a flamingo is in the northernmost lake, it will always fly south, and if in the southernmost lake it will always fly north.

There are four reasons that a flamingo will fly from one lake to another:

1. No food: If the energy balance of a flamingo is negative (see Section 6.2.2), the flamingo is not nesting or raising a chick, and its energy reserve is greater than the minimum required for flight, it will search the next three lakes north or south along the Rift Valley (the lakes lie in a north-south direction, in order: Logipi, Bogoria, Nakuru, Elmentaita, Magadi, Natron from north to south), stopping at the first with enough *Arthrospira* to feed. If no *Arthrospira* is available the flamingo must eat diatoms, and will instead fly to the lake with the lowest flamingo population, where there will be less competition for diatoms. A flamingo with a very low energy reserve (< 10%) cannot search elsewhere for food, but is left behind by the rest of the flock where it dies of starvation or recovers if food availability increases.
2. Not enough flamingos: If a flamingo has a high reserve mass (> 90%) and is not nesting or raising a chick it will search the next three lakes along the Rift Valley and move to the lake with most flamingos in order to engage in courtship (see Section 6.2.1.2) .
3. Exploration: If a flamingo has a high fat reserve (> 75%), it is not nesting and food is available at its current location, a flamingo may explore other lakes to make sure it is in the best feeding location, which will allow the flamingo to spend less time feeding and more time engaging in other activities like preening and resting. The chance that a flamingo will search for a higher density food source is described by Equation 6.1:

$$F_{explore} = 1 - (D_{lake}/D_{max}) \quad (6.1)$$

Where $F_{explore}$ is the chance that a flamingo will explore other lakes to find the best food source, D_{lake} is the density of *Arthrospira* at the current location of the flamingo, and D_{max} is the maximum density that has been observed in the soda lakes. The lower the density at the flamingo's current location, the more likely it

it to search for higher food densities elsewhere. If a flamingo does explore other lakes, it will search three lakes and move to the lake with the highest food density.

This occurs only when the fat reserve of an individual flamingo is above a minimum threshold. The threshold of $> 75\%$ was chosen, since it is likely that a flamingo will search for the best food source in order to be in good condition for breeding before searching for flamingos to engage in courtship with. However, it is unlikely that a flamingo would waste energy searching for alternative food sources if fat reserves were low and could be replenished at its current lake.

4. Not at breeding lake: If a flamingo has engaged in courtship and is ready to breed but is not at Lake Natron, it will fly directly to Lake Natron.

The flight behaviour is highlighted in blue in the flamingo behaviour flow chart (Figure 6.6). It is within the ‘Am I ready to breed?’ box in Figure 6.6 where flamingos may decide to search for flamingos which to engage in courtship with according to reason 2 in the above list.

6.2.1.5 Death

A flamingo can die in the model from old age or starvation. A flamingo that reaches ‘old age’ (40 years) has a 1/100 chance of death every month until it reaches the age of 50 years, when it will be removed from the model.

A flamingo dies of starvation when its fat reserve runs out. This will happen when flamingos are feeding on diatoms during periods of low *Arthrosphaera* abundance if the population is greater than the carrying capacity at a particular lake.

6.2.1.6 Changing behavioural state

Flamingos occupy three different behavioural states in the model; resting, feeding and flying. The way that flamingos change from one state to another is shown in Figure 6.7 and is explained below.

1. Flamingos change from resting to feeding behaviour at the beginning of each day if they have not flown overnight (which happens at the start of each daily time step), once the daily energy requirement for that flamingo has been calculated.
2. Flamingos do not usually change from feeding to flying directly, since they usually consume enough food earlier in the day, allowing them to rest before flying overnight to a different location.
3. A flamingo does not change from a flying state to resting.

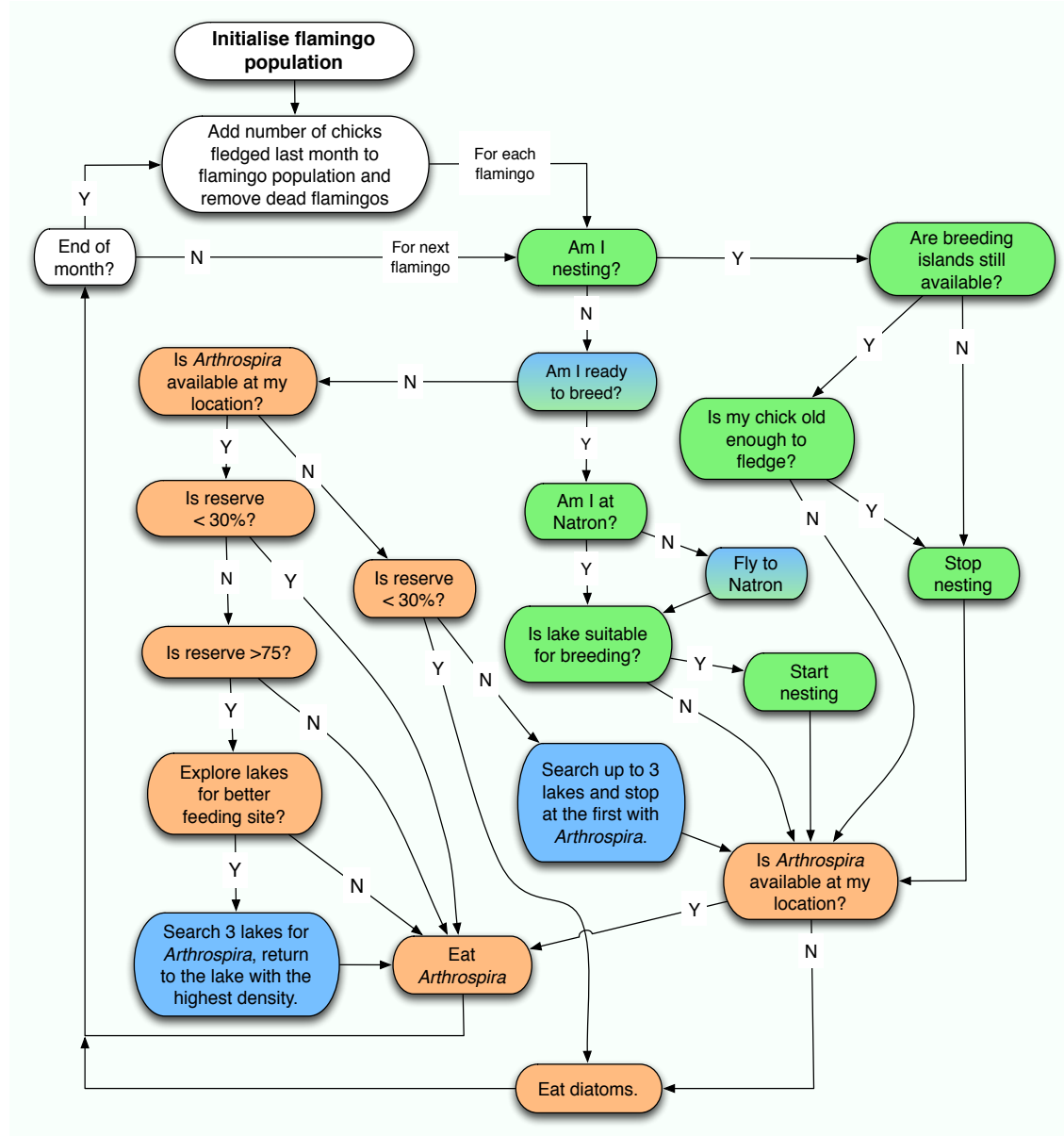


FIGURE 6.6: The flamingo behaviour model. The green boxes relate to breeding behaviour, the blue to flight from one lake to another, and the orange boxes to feeding behaviour.

4. A flamingo will change from a resting to flying state if it had already consumed enough food earlier in the day which allowed time to rest before flying to another lake, or if the food density is too low to feed, causing the flamingo to wait in a resting state until it could fly overnight (at the start of the next daily time step) to another lake.
5. A flamingo will change from flying to feeding behaviour if it has flown overnight and finds a lake with a food supply.
6. A flamingo changes from feeding to resting when it has consumed enough food to meet its energy requirements during the day.

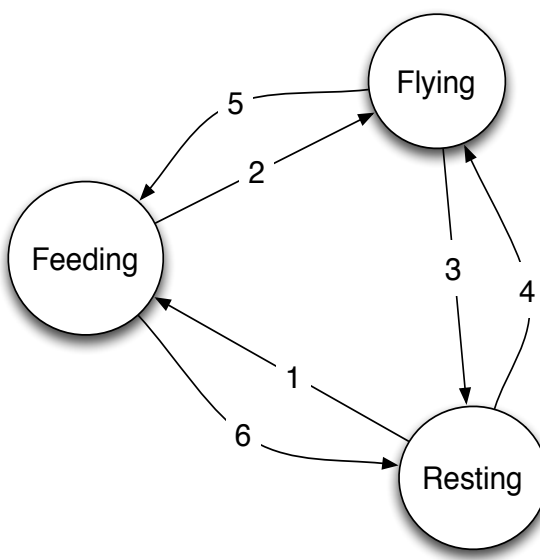


FIGURE 6.7: Flamingos occupy either a resting, feeding or flying behavioural state. The numbered arrows show the interaction between these states and are explained below.

6.2.1.7 Parameters

Each behaviour that a flamingo undertakes only occurs under particular conditions. The conditions are summarised in Table 6.3. The values used for these parameters can be seen in Table 6.4.

The minimum population for courtship and breeding to occur was 10,000 individuals. This number was chosen since the smallest recorded breeding event by Brown & Root (1971) was only of 3000 eggs, which means that at least 6000 flamingos would be breeding in this event, and the numbers were rounded up to 10,000 since there were likely to be more than 6,000 flamingos present.

Behaviour	Conditions
Eating <i>Arthrospira</i>	<i>Arthrospira</i> at current location exceeds minimum threshold.
Leaving a lake in search of food	<i>Arthrospira</i> is below the minimum threshold. A flamingo is increasingly likely to search elsewhere if <i>Arthrospira</i> density is low. Energy reserves are above the minimum for flight.
Leaving a lake in search of flamingos	A flamingo will search elsewhere for flamingos if the current flock is lower than the number needed to stimulate courtship.
Inclination to breed	If a flamingo is sexually mature, has a large energy store, and has not reared young in the last 12 months, its status is designated as 'in breeding condition'.
Courtship	The flamingo is in 'breeding condition', the flamingo is in a large flock, a large proportion of the flock are sexually mature and are also in breeding condition.
Nesting	The flamingo is in breeding condition, has engaged in courtship, is located at Lake Natron, a nesting site is available, and food can be found nearby.
Raising young	The flamingo has been nesting for over one month. The nesting site is still available.
Deserting nests	A flamingo is increasingly likely to desert a nest if fat reserve reduces below the threshold below which a flamingo must urgently search for food, or if nests become flooded or stranded.
Death	Flamingo reaches old age, or starves to death due to low food availability.

TABLE 6.3: Lesser flamingo behaviour and the conditions under which this behaviour occurs in the flamingo model. The values used to implement these conditions can be seen in Table 6.4.

Parameter	Value	Units	Reference
Minimum <i>Arthrospira</i> density for feeding	0.1	$kg\ m^{-3}$	Pennycuick and Bartholomew (1973)
Minimum time between breeding events	12	months	Free parameter
Minimum reserve for food exploration	75	%	Free parameter
Urgent food hunt reserve level	<30	%	Free parameter
Minimum reserve for breeding	90	%	Free parameter
Minimum reserve for flight	10	%	Free parameter
Time before flamingo forgets previous lake	10	days	Free parameter
Time before a chick can fledge	70	days	Brown (1973)
Breeding age	72	months	V. Robinson (2013), pers. com.
Time to build a nest	40	days	Brown (1973)
Average breeding success	42	%	Brown (1973)
Old age	40	years	Free parameter
Maximum age	50	years	*
Minimum size of breeding colony	10,000	flamingos	**
Maximum number of lakes searched per flight	3	lakes	Free parameter
Maximum observed <i>Arthrospira</i> density	0.7	$kg\ m^{-3}$	Krienitz and Kotut (2010)

TABLE 6.4: The values of the parameters and thresholds which determine flamingo behaviour. *Based on the recent recovery of a ring from a dead wild flamingo found at Lake Bogoria in February 2013 which puts the age of that particular flamingo at 51 years. **Based on observations of breeding colony size by Brown & Root (1971).

6.2.2 Flamingo energy budget

The mathematical energy budget model uses time energy budget modelling and includes the energy reserve concept from dynamic energy budget modelling (described in Section 6.1.3). The energy budget model calculates the change in the energy-reserve-mass of a flamingo using basic physics principles such as energy conservation and calculates the energy cost of flight as flamingos move from one lake to another. There are no data available on the metabolic cost of different activities for the lesser flamingo, and so apart from comparing the metabolic cost of activities for flamingos to that of other birds such as geese, the cost of different activities have to be estimated from first principles and using the basic characteristics of lesser flamingos such as the average height, mass, and bill size. The flamingo energy budget model is outlined in Figure 6.8.

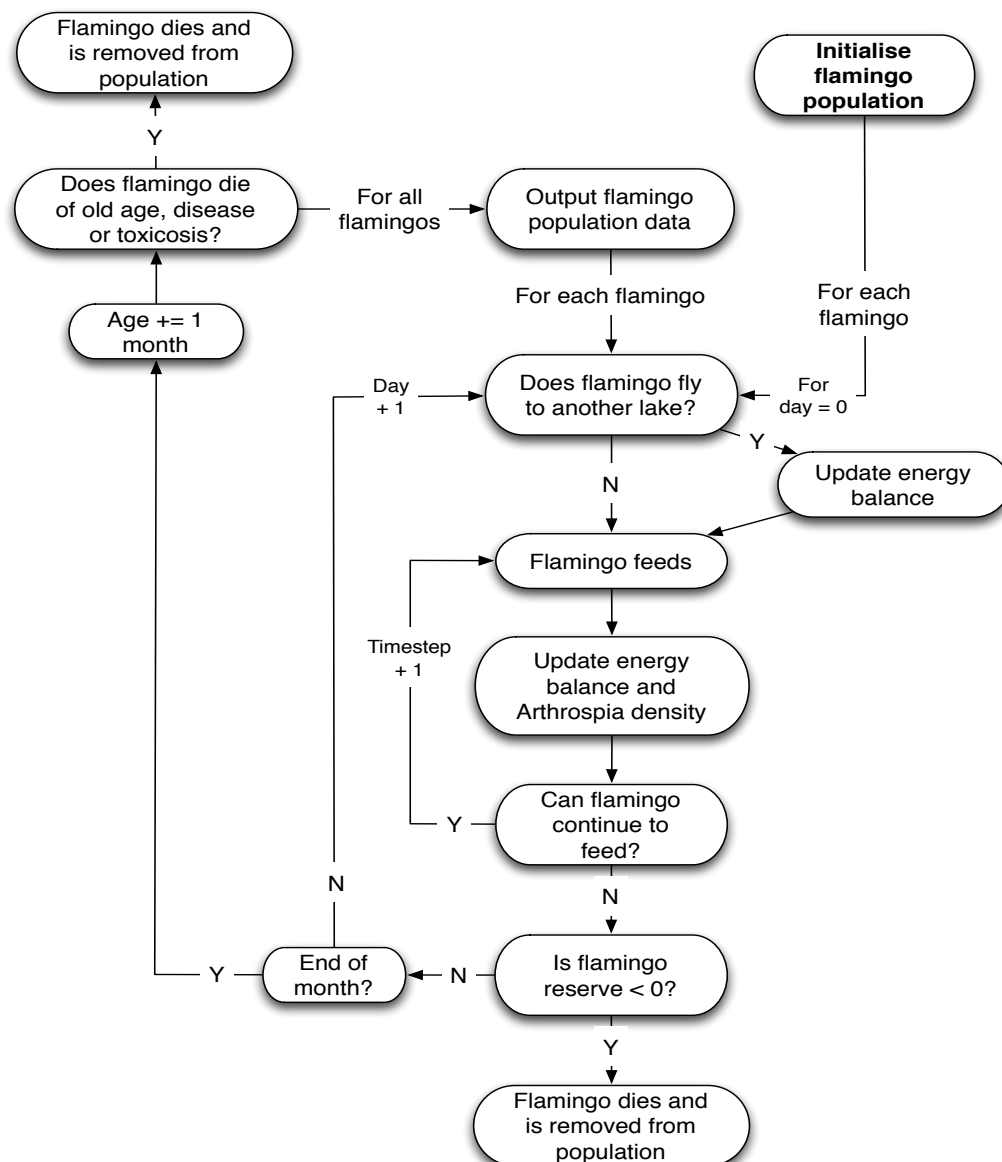


FIGURE 6.8: The flamingo energy balance model.

The main activities flamingos undertake day-to-day can be simplified into three main activities: resting, feeding and flying. These activities each have an associated cost in terms of energy, which if known can be used to calculate the energy budget. The following equations describe these aspects of flamingo energy intake and expenditure. Most activities are described by the Pennycuick and Bartholomew (1973) using Equations 6.2 to 6.7:

When feeding on *Arthrosphaera* lesser flamingos pump water through filters in their bills with their tongues to sieve out *Arthrosphaera* from the lake water.

$$f = vrc \quad (6.2)$$

Where f is the *Arthrosphaera* sieved out of the water in $kg\ s^{-1}$, v is the stroke volume of pump in m^3 , r is the frequency that a flamingo pumps water through its bill (s^{-1}), and c is the density of *Arthrosphaera* in the water in $kg\ m^{-3}$. This is used to calculate the chemical energy, E_{oi} , in J from the food extracted:

$$E_{oi} = eft \quad (6.3)$$

Where e is the food energy content in J , and t is the time in seconds. The energy available for metabolism, E_{av} is:

$$E_{av} = c_{eff}E_{oi} \quad (6.4)$$

Where c_{eff} is the efficiency of conversion of energy from food to energy stored.

The cost of basal metabolism, E_{bmr} is:

$$E_{bmr} = 3.79M^{0.723} \quad (6.5)$$

Where M is the total mass of the flamingo in kg .

The energy used for general daily activity E_{ga} is:

$$E_{ga} = 2.5E_{bmr} \quad (6.6)$$

This allows for day to day activities such as moving around within a lake, preening, drinking etc, but excludes the cost of flight from one lake to another.

The energy balance E_b is therefore:

$$E_b = E_{av} - E_{ga} \quad (6.7)$$

If the energy balance is positive, the flamingo is able to increase its fat reserve. A negative energy balance means that a flamingo is depleting its fat reserves because of low food abundance. The storage of energy in fat reserves is not described by Pennycuick and Bartholomew (1973).

The total mass M_t of a flamingo constitutes of a structural mass M_s and fat reserve mass M_r . The change in fat reserve δM_r is simply calculated:

$$\delta M_r = c_f E_b \quad (6.8)$$

Where c_f is the energy density of fat.

There are three reasons that a flamingo will stop feeding each day in the model. Either the flamingo exceeds the daily energy requirements by a certain proportion, c_A , or they exceed their daily energy requirements and reach the maximum energy reserve store limit, or they have reached the maximum time a flamingo can feed without impinging drastically on other essential activities like resting, drinking, and preening (Pennycuick & Bartholomew, 1973). For a non-breeding flamingo this limit is 18 hours, and for a breeding flamingo 12 hours (Pennycuick & Bartholomew, 1973).

The cost of flight was estimated using the total mass of each flamingo, the flight time t in seconds and the power (P) produced by the flight muscles, which Morris and Askew (2010) found to vary between 40 and 120 $W \ kg^{-1}$ in experiments with cockatiels (see equation 6.9).

$$E_f = PtM \quad (6.9)$$

The flight time is calculated using equation 6.10, where V is the velocity of flight, and distance d is the distance between two lakes.

$$t = d/V \quad (6.10)$$

The distances between the lakes was measured using Google Earth as the distance in a straight line from the centre of one lake to the centre of the next. The distances can be seen in Table 6.5.

If there is no food available a flamingo will have a negative energy balance and fly in search of food at other lakes. However, during months where *Arthrospira* density is low across all of the lakes the entire population would die out unless the flamingos could fall back on diatoms, a low quality secondary food source. When feeding on diatoms the flamingo population has been observed to be distributed across many different lakes (Tuite, 2000). This is due to the lower carrying capacity of lakes when flamingos are

Neighbouring lakes	Distance (m)
Logipi to Bogoria	223,500
Bogoria to Nakuru	63,450
Nakuru to Elmentaita	18,650
Elmentaita to Magadi	157,690
Magadi to Natron	66,000

TABLE 6.5: The distances that flamingos travel flying from one lake to another as they travel along the Great Rift Valley.

feeding on diatoms, since they are a slower growing, less nutritious source of food. The diatom model assumed that flamingos must be evenly distributed between the available lakes in order for the daily energy requirements of the flamingos to be fulfilled. Each lake was given a carrying capacity of one fifth of the flamingo population to encourage flamingos to distribute themselves more evenly between the lakes. A carrying capacity of one sixth would mean each of the six lakes would have to contain one sixth of the flamingo population or large mortalities would occur. This was considered too extreme and would cause unreasonable crashes in flamingo population. When feeding on diatoms if the flock size is equal to or less than one fifth of the total population then the proportion of daily energy requirements that could be met by diatoms was 1.2. If the proportion of the total flamingo population exceeded this limit, then the proportion of daily energy requirements that could be met by diatoms at this lake reduced. This means that flamingos prefer lakes with fewer flamingos during times of low *Arthrospira* density (Table 6.6).

The energy the a flamingo gains when feeding on diatoms E_D is:

$$E_D = c_D E_{ga} T \quad (6.11)$$

Where c_D is the proportion of a flamingos daily energy requirements that can be met by diatoms at this lake (see Table 6.6), E_{ga} is the energy required by a flamingo for daily activity, and T is the time step.

Proportion f of total flamingo population F	Proportion of flamingo daily energy requirements met by diatoms (c_D)
$0 \leq f \leq 0.2$	1.2
$0.2 < f \leq 0.3$	1.0
$0.3 < f \leq 0.4$	0.8
$0.4 < f \leq 0.5$	0.6
$0.5 < f \leq 1.0$	0.4

TABLE 6.6: The diatom model thresholds and proportion of daily energy requirements that can be met by diatoms for a proportion f of total flamingo population F .

6.2.3 Parameters

The values used for the energy budget parameters can be seen in Table 6.7.

Parameter	Value	Units	Reference
Energy density of fat (c_f)	39000	$kJ \ kg^{-1}$	Weathers (1996)
Conversion efficiency (c_{eff})	0.8	-	Pennycuick and Bartholomew (1973)
Cost of flight (E_f)	120	$W \ kg^{-1}$	Morris and Askew (2010)
Flight velocity	18.89	$m \ s^{-1}$	Childress et al. (2004)
<i>Arthrosphaera</i> energy content	2×10^7	$J \ kg^{-1}$	Pennycuick and Bartholomew (1973)
Maximum food consumed as % daily BMR requirement (c_A)	150	%	Free parameter
Maximum time a parent flamingo can feed	12	hours	Pennycuick and Bartholomew (1973)
Maximum time a non-breeding flamingo can feed	18	hours	Pennycuick and Bartholomew (1973)
Structural mass of a flamingo M_s	1.1215	kg	Brown (1973)
Maximum energy reserve size M_r	$0.587 \times M_s$	kg	Ton (2007)
Pump stroke volume	0.5×10^{-6}	m^3	Pennycuick and Bartholomew (1973)
Pump frequency	20	s^{-1}	Pennycuick and Bartholomew (1973)
Pump pressure	25000	Nm^{-3}	Pennycuick and Bartholomew (1973)
Time step (T)	0.0417	days	-

TABLE 6.7: Flamingo energy budget parameters used in the model.

6.2.4 Time steps

Different behaviours and events occur at different time steps in the flamingo behaviour and energy budget models:

- Monthly: New fledglings are added to the model, and age is updated.
- Daily: Flight occurs at the beginning of each day, and the cost of flight is immediately removed from the fat reserve. The energy required for a flamingo to live for the day (Equation 6.6) is subtracted from the fat reserve at the start of each day before it feeds, and the time that a flamingo has been nesting and raising a chick are also incremented daily. The data from the flamingo model is output at the end of each day into a text file.
- Hourly: Feeding on *Arthrosphaera* or diatoms occurs on an hourly time step, so that the impact of flamingos on the growth of *Arthrosphaera* is in sync with NPZF model in Chapter 5. The energy budget of a flamingo is updated after every time step

that it consumes food. This is necessary to allow flamingos to spend more time feeding when energy reserves are low, and less time feeding when there is a high food density or if they are rearing chicks.

The way that the energy budget is updated can also be seen in Figure 6.8.

6.2.5 Data for validation

Flamingo population data: Information about mortality events, breeding events, and the total population and distribution patterns over time are useful for comparing the model output with flamingo behaviour. Some flamingo population data can be found in the literature, and the annual flamingo census in Kenya that began in the early 1990s can also be used. There is little other empirical data available for validation of the flamingo model. However, the dates of breeding events and mortality events that have been documented can be compared with the model output, as well as the decline in overall population size from the 1950s by 21% Simmons (2000). Palaeolimnological techniques can also be used to gain insights into flamingo populations. The $\delta^{15}N$ data (see section 3.5) may be useful as a proxy for flamingo populations, and could help to identify periods when a large congregation of flamingos was present at a particular lake.

1. Flamingo behaviour: Flamingos are known to gather in large flocks when there are high densities of *Arthrospira* at a soda lake and to spread out widely during periods of low food abundance. The real frequency of mortality events and breeding events is unknown as there is no consistent monitoring of flamingo populations. Recorded events can be seen in sections (6.1.1, 6.1.2, and 7.1) of the literature review. Tebbs et al. (2013a) used remotely sensed imagery to identify periods where conditions at Lake Natron may be suitable for breeding by identifying when islands were available within the lake, when lake surface area is between 160 and 725 km^2 . There are descriptions of breeding and display behaviour, and observations of feeding behaviour in the literature. Flamingos also exhibit behaviours common to many prey species, including flocking behaviour, increased vigilance by birds on the edges of the flock, and an increased likelihood of deserting nests for smaller groups. This knowledge will be useful in determining whether the behavioural aspects of the model outputs are realistic, although the conclusion will be somewhat subjective.
2. Flamingo energetics: There has only been one study of the energy budget of the lesser flamingo (Pennycuick & Bartholomew, 1973) which estimates the flow of energy through a flamingo using basic physics principals such as energy conservation and thermodynamics. The series of equations estimates the energy required for a flamingo's 'general activity', which means that different feeding behaviours,

pruning and drinking can be ignored. This paper does not include the energetics of flight, which was estimated using flamingo mass.

3. Energy reserve: The energy reserve size for each flamingo was estimated to reach up to 37% of the total weight of a flamingo based on an observation that flamingos dying of starvation were about 63% of their expected weight (Ton, 2007).
4. Flamingo life-span: The lifespan of a wild flamingo has been roughly estimated to be 50 years. This estimation is based on the low replacement rate of the species and the long lifespan of captive flamingos which have continued to breed successfully at least into their 50's, and the recent recovery of a ring from a dead wild flamingo found at Lake Bogoria in February 2013 which puts the age of that particular flamingo at 51 years.
5. Flamingo movement driver: From the literature review it is clear that lesser flamingo movement is strongly driven by *Arthrosphaera* density, particularly when food abundance suddenly reduces. Pennycuick and Bartholomew (1973) measured the minimum threshold of *Arthrosphaera* required for lesser flamingos to survive. There are also secondary drivers that need to be considered, since lesser flamingos are often seen to depart from lakes with high densities of *Arthrosphaera*. Flamingos have been shown to prefer Lake Nakuru to Lake Bogoria when there are high densities of *Arthrosphaera* at both lakes, which is likely to be a combination of the shallower sandy lake bed (Svengren, 2002), and the milder conditions. The inclination of flamingos to breed and the size of the flock at the location of a flamingo also affect the likelihood of a flamingo to stay or leave its current lake location. There is no evidence that will help to determine precisely when an individual flamingo will fly from one lake to another or which direction it will go. The model can include these behaviours by increasing the probability that a flamingo will decide to move depending on the energy reserves available to it, the number of flamingos nearby and amount of food available.

6.2.6 Assumptions

The assumptions made in the flamingo model:

1. Flamingos die through starvation, or due to old age.
2. Predation is insignificant as a cause of death.
3. Flamingos navigate by following the lakes along the Rift Valley floor, and will always land at each lake along the way to assess food abundance.

4. Flamingos are increasingly likely to search for food elsewhere if *Arthrosipa* is nearing the minimum threshold.
5. Flamingos do not leave the East African Rift Valley in search of food during periods of low food abundance, but subsist on diatoms.
6. Flamingos prefer to be in larger groups.
7. Flamingos cannot breed more than once in a 12 month period, rearing only one chick.

6.2.7 Initial conditions

The flamingo population is of the order of one million birds in all references the literature, and for the population to have a realistic impact on the *Arthrosipa* growth the population modelled needed to be the same order of magnitude. The number of flamingos at the start of the run is set at one million flamingos. In order to reduce the long run time required when the model runs flamingos as individuals, the number of flamingos can be divided into a number of flamingos (N) per ‘group’ (x), so that Nx is equal to one million flamingos. The model therefore calculated the behaviour and energy balance for each group of identical flamingos rather than each individual in each time step.

The minimum threshold that a flamingo can feed at was suggested to be 100 mg L^{-1} dry weight of *Arthrosipa* by Pennycuick and Bartholomew (1973). Although flamingos have been seen to modify their feeding behaviour during lower densities and were seen by Krienitz et al. (2013) to be feeding at concentrations of only 25 mg L^{-1} . An initial value of 100 mg L^{-1} (0.1 kg m^{-3}) was used as the threshold in the model because this was the value predicted by Pennycuick and Bartholomew (1973) flamingo energetics equations that were the basis of this model.

The flamingos in the model are randomly assigned a “structural mass” between 1.0 kg and 1.215 kg . The structural mass is 63% of the mass of a healthy flamingo with full reserves, and the reserve mass is randomly assigned to that flamingo with a value between 0 kg and 0.713 kg , depending on the structural mass of the flamingo. Each flamingo is also assigned a random age between 0 and 50 years, and a random starting location.

The depth and *Arthrosipa* density at each lake visited by flamingos are determined by the hydrological and *Arthrosipa* model outputs.

6.2.8 Results

Each flamingo group undergoes many different interactions in each time step, which increases the runtime of the model. This begins to make a significant impact as the number of simulated groups increases. The model was run for a short period with different sized groups of flamingos using the average monthly rainfall to ensure that stochastic effects could be distinguished from the effects of rainfall variability. Once the effect of group size on the model output was explored, the best compromise between run time and resolution could be found.

The number of agents is equal to the number of groups rather than the total population, where each group contains identical flamingos. The model was run with identical conditions apart from the number of groups, with each configuration repeated five times.

The model was run with 50 groups of 20,000 flamingos, 100 groups of 10,000 flamingos, 1,000 groups of 1,000 flamingos, and 10,000 groups of 100 flamingos. The time it would take to run the model from 1904 to 2012 was estimated at less than one hour for 50 groups of 20,000 flamingos, 100 groups of 10,000 flamingos, and 1,000 groups of 1000 flamingos. The run time increased dramatically for 10,000 groups of 100 flamingos, taking approximately 11 hours for a single full run. After attempting to run the model for 100,000 groups of 10 flamingos it was found to take several minutes to run even a single month, and so running the model at higher resolutions was not practical.

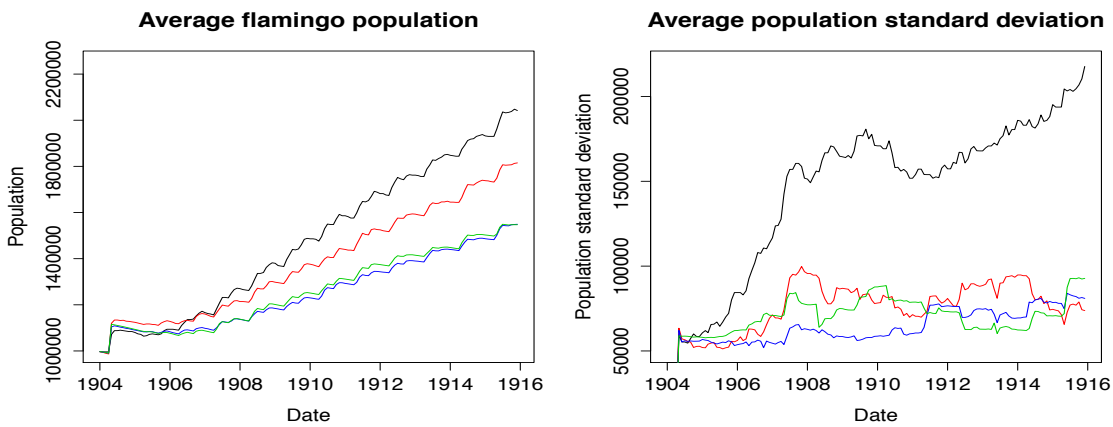


FIGURE 6.9: Population output by ten runs of the model model using average rainfall for 50 groups of 20,000 flamingos (black), 100 groups of 10,000 flamingos (red), 1,000 groups of 1,000 flamingos (blue), and 10,000 groups of 100 flamingos (green). The leftmost graph shows the average population, and the rightmost graph shows the standard deviation of the population over time.

The flamingo population output can be seen in Figure 6.9. The stochastic nature of the rule based flamingo behaviour model causes variation in the overall flamingo population output by this model. A smaller number of agents generally increased variance in the model output, and increased the final total flamingo population.

The problem of small population effects can be avoided by using a smaller group size and larger number of agents. Since 1000 groups of 1000 flamingos produced a similar output to the 10,000 groups of 100 flamingos and was much cheaper computationally, full runs of the model using the normal rainfall data were run using 1000 groups of 1000 flamingos. All subsequent results in this section are averaged from 20 runs of the model using normal rainfall data, and an initial flamingo population of 1000 groups of 1000 flamingos.

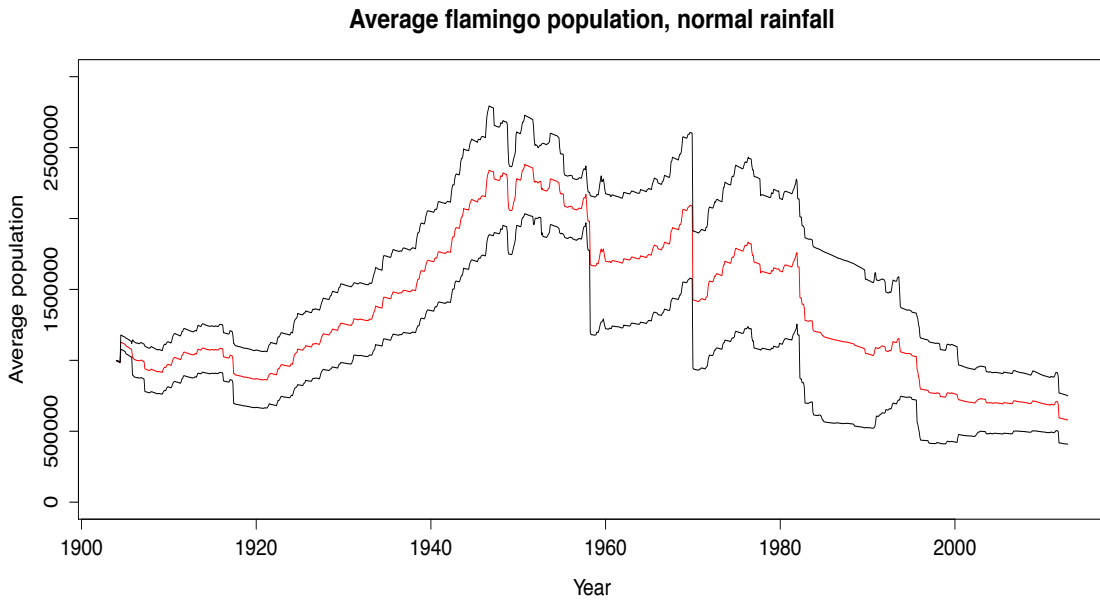


FIGURE 6.10: Average population output by 20 runs (red) and standard deviation (black), of the model using normal rainfall data from 1904 to 2012.

The non-deterministic nature of the flamingo behaviour model allows for different outputs for the same initial conditions. The total flamingo population is clearly affected by the stochasticity of the decisions made by the flamingos in Figure 6.10.

The overall trend in population change is the same for most runs, with a relatively steady increase in flamingo population from 1904 to the late 1940s, peaking in 1950, then a decline punctuated by mortality events. There is significant variation in total population between 1958 and 1990, after which the standard deviation reduces. Population changes often occur at the same point in time. The severity of mortality events and the success of breeding events is likely to be the main cause of the differences in population between runs, since there is an element of randomness in the success of breeding events, and flamingo population distribution is non-deterministic, allowing some groups of flamingos to be more likely than others to survive during periods of low food abundance depending on their lake location and the number of other groups at their location. The population declined from 1.69 million in 1974 to 1.06 million in 1994, a reduction of 38%. This is similar to the 21% decline recorded by Simmons (2000) during this period.

Figure 6.11 shows the average size of breeding events as a percentage of the total population and the standard deviation of each breeding event as a percentage of the number of flamingos breeding. There is a much larger standard deviation associated with larger breeding events, but the percentage standard deviation is low overall (<5%). Large breeding events consisting of more than 20% of the total population occur infrequently. The majority of events include less than 15% of the total flamingo population.

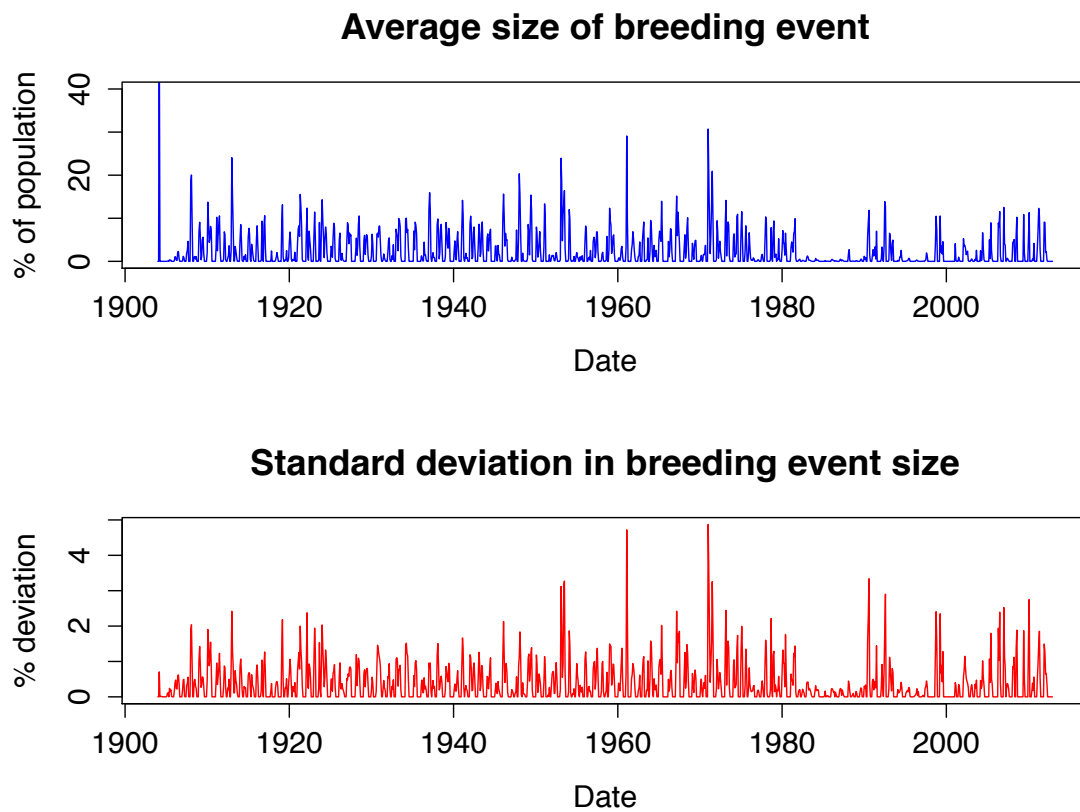


FIGURE 6.11: Average breeding event size as a percentage of the total flamingo population (blue) and the percentage standard deviation of breeding event size (red). The first breeding event is 56% of the total population.

Figure 6.12 shows the number average number of fledgelings output by the model as a percentage of the total population, and the standard deviation of fledgeling number as a percentage of the average fledgeling number. There are larger standard deviations associated with larger numbers of fledgelings, but the standard deviation is low for fledgeling number, with all but one event having a percentage standard deviation of less than 3%.

Figure 6.13 shows the mortality events (where >10,000 flamingos die in a single month) output by the model. The frequency of mortality events increases after 1945. Most mortality events involve less than 20% of the total population, and there is one particularly large mortality event in 1970 (>40% of the total population). The percentage standard

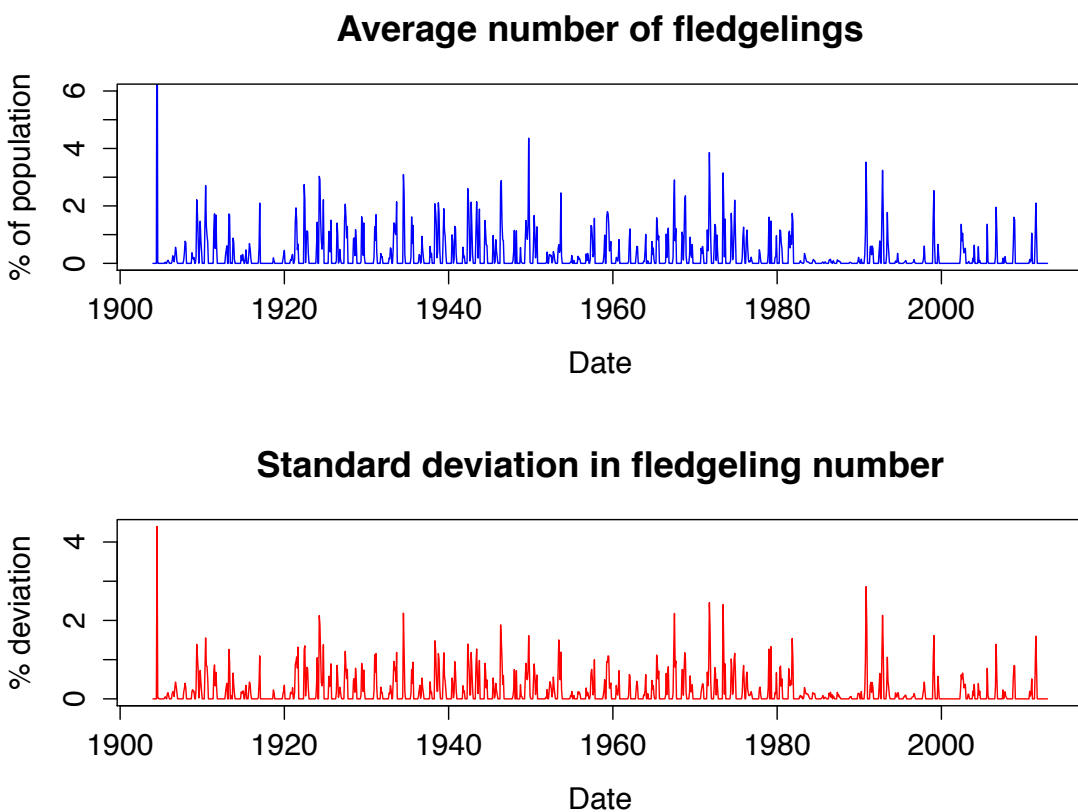


FIGURE 6.12: The average number of fledgelings as a percentage of the total flamingo population and the percentage standard deviation of fledgeling number.

deviation associated with mortality events is larger for larger mortality events, with most having a standard deviation of less than 20%.

Many of these mortality events are associated with relatively fast changes in lake water level in response to high rainfall, such as the 1917 mortality event, or after periods of low rainfall, which is the case in the 1970 mortality event. The largest mortality occurs at the start of 1970 after a period of low food abundance at all lakes apart from Lake Bogoria, which then also experiences a dip in *Arthrosphaera* density. The more efficiently the flamingo population distributes itself after a decline in food abundance between the remaining food resources, the less severe any subsequent mortality event will be.

Figure 6.2.8 shows the percentage flamingo population distribution. The highest proportion of the population is generally found at Lake Bogoria, which is the most reliable *Arthrosphaera* source. The NPZ model output shows that Lake Bogoria has several periods of low food abundance, including 1917, 1961, the late 1970s and the 1980s (see Figure 5.12). During these periods the flamingo population are dispersed evenly across the different lakes to feed on diatoms and less consistent sources of *Arthrosphaera*. This behaviour reflects what is known about the behaviour of flamingos from observations in the field.

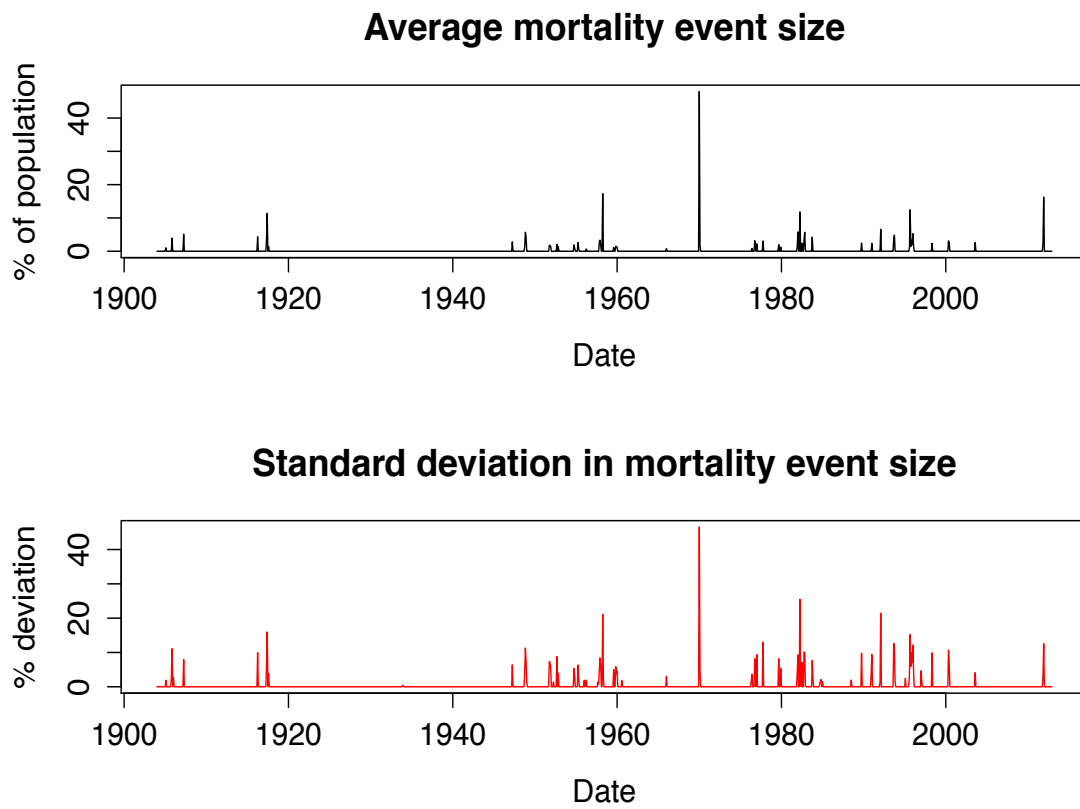


FIGURE 6.13: The average number of mortalities as a percentage of the total flamingo population and the percentage standard deviation of mortality even size.

The flamingo model output is robust, with small standard deviations in average population (12.6%), percentage breeding event size (0.7%), and percentage number of fledgelings (0.5%). The largest standard deviation is in percentage mortality event size (19.3%), which reflects the stochasticity of flamingo distribution in the model caused by the probabilistic nature of flight direction, and is the cause of most of the variance in average population size. The average outputs for breeding, fledgeling and mortality events are well defined peaks in Figures 6.11, 6.12, and 6.13, which shows that these events occur at the same time in each run of the model.

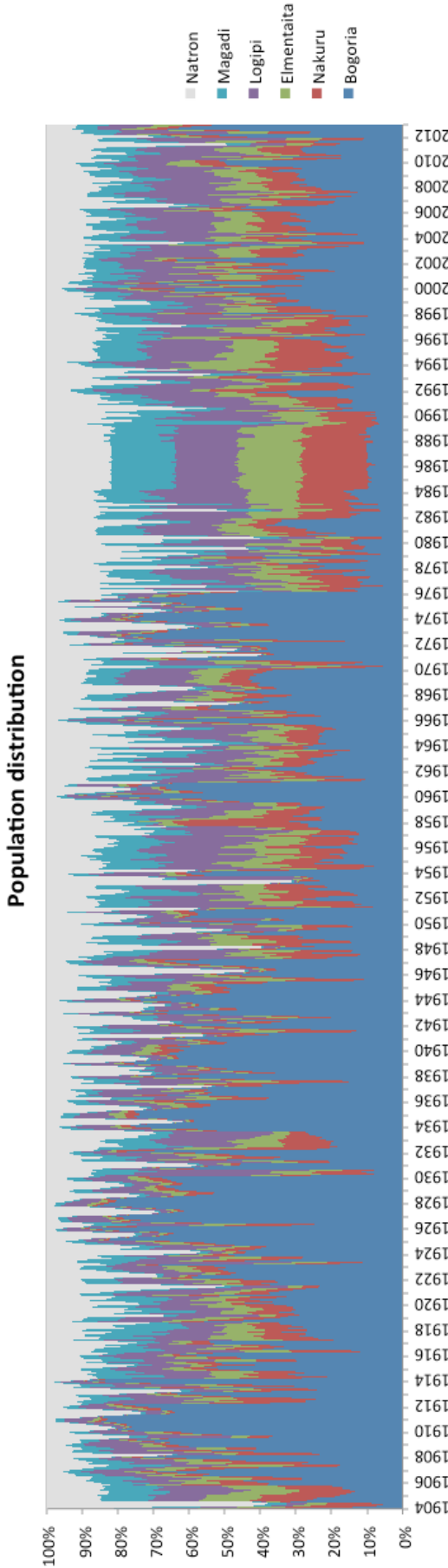


FIGURE 6.14: The flamingo population distribution. It can be seen that there are periods where the flamingo population is concentrated at one or two lakes, usually Lakes Bogoria and Natron, and other periods where the flamingo population is dispersed more evenly between the six lakes.

6.2.9 Sensitivity Analysis

Since there is little data with which to compare the flamingo model output it is challenging to measure the accuracy of the outputs of the flamingo model in a quantitative way. Instead, the sensitivity of the flamingo model was explored by varying the free parameters individually, and evaluating the consequent changes in the model outputs. The flamingo behaviour and energy budget models have a large number of parameters (Tables 6.7 and 6.4), but many are established physical or biological constraints (e.g., flamingo bill pump stroke volume, the energy density of fat, the time taken by a chick to fledge). Rather than vary all of these parameters, it is more useful to explore the model’s “free” parameters, i.e., the ones that are less well specified by empirical data. These are the maximum number of lakes searched per flight (N_L), the minimum fat reserve below which flamingos search for the nearest viable food source (R_v), the minimum fat reserve required before flamingos explore lakes in search of the best quality food source (R_x), the minimum fat reserve required for breeding to occur (R_B), the number of days before a flamingo forgets its previous lake (N_m), and the maximum food consumed as a percentage of its daily BMR requirement (C_A). These parameters were estimated logically, for example, a flamingo with a low fat reserve is unlikely to explore other lakes for a better quality food resource when it can meet its energy requirements at its current lake, whilst a flamingo with a large fat reserve is unlikely to remain at a lake where it has to feed for the maximum time possible in order to meet its basic energy requirements when there might be a better food supply elsewhere which would allow the flamingo to engage in other behaviours such as resting and preening.

To evaluate the impact of varying a free parameter, it was perturbed by plus or minus 10% and ten independent simulation runs were undertaken. For each run, values for the average flamingo population size, smallest and largest population, number of mortality events, size of mortality events, largest mortality event size, and number of breeding events of different sizes were recorded and an average taken for each. Each average was then compared with the corresponding mean value achieved over twenty runs of the simulation using the standard parameter settings. Any deviation between a perturbed run and the standard scenario was judged to be significant if it lay more than two standard deviations from the value recorded under the standard parameter settings. The results can be seen in Table 6.8.

The maximum number of lakes searched per flight (N_L) could only be varied by ± 1 , which is a large perturbation ($\pm 30\%$) which causes some significant deviations from the values output by the model under the standard parameter settings. When flamingos are able to search an extra lake, they are more likely to identify better quality food resources which causes the flamingo population to have a larger fat reserve, which increases the likelihood that each flamingo will survive period of low food abundance, since the size of

mortality events is reduced by 50.9%, causing the average population to be significantly larger (65.4%).

When the number of lakes searched (N_L) is reduced, the flamingo population becomes more vulnerable to localised reduced food abundance, and the number of mortality events increases by 51.2%, although the size of the mortality events is not affected. However, the average population is similar since there is a larger number of small breeding events involving between 10% and 15% of the total population, and a reduction in larger breeding events. It is possible that the reduction in the average size of breeding events occurs since when searching fewer lakes for food, the carrying capacity of each lake is more likely to be exceeded as flamingos distribute themselves less efficiently during times of food stress. As a result there are more regular mortality events, the average fat reserve of the population is likely to be lower, and fewer flamingos are likely to be in breeding condition at any one time.

Changing in the minimum reserve that will cause a flamingo to search for the nearest viable food source (R_v), does not cause any significant change in the output. The minimum fat reserve required for breeding to occur, R_B , does change the overall population size. Reducing the fat reserve required for flamingos to breed increases the number of breeding events involving 10%-15% of the total population by 83.9%, and as a result the average population size is increased. There are also more (+53.5%) mortality events which are smaller in size (-10.4%) as a result, which is to be expected since flamingos that breed with lower fat reserves will be more vulnerable to periods of food stress during or after a breeding event. Reducing R_B therefore reduces the robustness of the flamingo population. Increasing R_B has the opposite effect although the change to overall population is less significant.

(R_x) increases the average population by 27.6%, and reduces the average breeding event size, but increases the number of mortality events by 34.1%. The increase in mortality events is likely to be caused by the flamingos being at lower quality feeding sites.

Increasing the minimum fat reserve required before flamingos explore lakes in search of the best quality food source The ability for a flamingo to remember its previous lake is needed to ensure that flamingos do not search the same lakes repeatedly. If a flamingo remembers its previous lake it will fly away from it in search of food or flamingos. However, if flamingos do not forget the previous lake within one month there are increases in mortality event size and even extinction events. This is because if the flamingos have recently moved as a large flock away from one lake and there is a crash in food abundance, the flamingos are all forced to explore the in the direction away from their previous lake. This prevents the population from spreading out and leads to overgrazing and starvation. When the number of days that a flamingo remembers its previous lake (N_m) was varied by 10% (between 9 and 11 days), it did not cause any significant change in the results.

Perturbed parameter	Average population	Smallest population	Largest population	No. mortality events	Average mortality event size	Largest mortality event size	No. breeding events <10% population	No. breeding events 10-15% population	No. breeding events 15-20% population	No. breeding events >20% population
Standard μ	1,376,356	559,350	2,684,850	12.9	17.2	48.2	166.2	4.3	1.1	1
Standard σ (%)	12.6	23.2	11.6	16.1	19.3	31.5	2.4	28.4	69.8	0
$N_L + 1$	65.4	72.6	51.6	2.3	-50.9	-40.6	-2.4	35.6	-72.7	0
$N_L - 1$	-7.9	-40.6	3.1	51.2	-5.0	-10.8	-3.5	67.8	-54.5	0
$R_v + 10\%$	6.6	-3.7	3.8	1.6	-4.8	-9.7	-0.7	-3.4	-18.2	0
$R_v - 10\%$	-1.3	4.2	-2.4	-2.3	-2.6	-8.9	-2.2	-12.6	0.0	0
$R_B + 10\%$	-36.8	-36.1	-46.2	-44.2	3.3	-29.6	-5.6	-95.4	-100	-100
$R_B - 10\%$	77.9	53.2	90.1	53.5	-10.4	3.0	-15.4	83.9	0.0	20
$R_x + 10\%$	27.6	19.7	41.4	34.1	-0.2	7.9	-12.8	65.5	-36.4	30
$R_x - 10\%$	-1.3	4.2	-2.4	-2.3	-2.6	-8.9	-2.2	-12.6	0.0	0
$N_m + 10\%$	5.3	3.3	0.7	7.8	-8.4	-14.1	-1.5	8.0	-36.4	0
$N_m - 10\%$	4.1	3.3	2.7	1.6	-6.7	-15.2	-2.7	19.5	-54.5	0
$C_A + 10\%$	29.4	23.6	28.6	17.1	-17.3	-8.4	-5.6	12.6	118.2	30
$C_A - 10\%$	-19.7	-27.5	-21.7	-17.1	3.7	-8.8	-1.9	-72.4	0	-100

TABLE 6.8: The sensitivity of the flamingo model was tested by comparing the outputs for perturbations to the free parameters against the standard parameters. The standard deviation σ is a percentage calculated over twenty runs of the model using the standard parameters. All perturbed values are the average of ten runs of the model. The outputs of the perturbed parameters are percentage deviations from the standard parameter means (μ). The values highlighted in red are $> 2\sigma$ away from the mean. N_L is the number of lakes searched per flight. R_v is the minimum reserve that will cause a flamingo to search for the nearest viable food source, R_B is the minimum fat reserve required for breeding to occur, R_x is the minimum fat reserve required before flamingos explore lakes in search of the best quality food source, N_m is the number of days before a flamingo forgets its previous lake, and C_A is the maximum food consumed as % daily BMR requirement.

The maximum food consumed as a percentage of the daily BMR requirement (C_A) has to be greater than 100% to allow a flamingo to replenish its fat reserves. The faster that a flamingo can recover from a period of starvation, the more likely it is to survive future changes in food abundance. Increasing C_A had a more significant affect on overall population, although reducing C_A caused a reduction in the number of breeding events because it takes longer for a flamingo to reach breeding condition after a period of low food abundance.

The sensitivity analysis shows that changes in free parameters by 10% do not alter flamingo behaviour in the model significantly, even when number of lakes searched is changed by 30% the outputs exhibit the same characteristics seen when using standard parameter values, including breeding events and mortality events. The change in the size or frequency of events in response to perturbations in these parameters is logical, and not large enough to cause concern about the sensitivity of these parameters.

Overall, the population output by the model exhibits population breeding events and mortality events without needing to be forced, and exhibits the same overall trend despite the non-deterministic nature of the model. The population fluctuates between 0 and 3 million without dying out which is within realistic population limits. This simple flamingo model can therefore be used as a basis for exploring other hypotheses for population decline to try to understand more about the flamingo population.

Chapter 7

Flamingo hypotheses exploration

In this chapter the model is used to explore some hypotheses about the cause of mortality events and why the population is in decline. There is an overview of the current hypotheses for the causes of mortality events in Section 7.1. The model is then used to explore the hypothesis that disease is a the cause of mortality events in flamingos and the outputs compared to the standard model where starvation and old age are the only causes of death (Section 7.4). Low replacement rate is then explored as a reason for population decline (Section 7.5), and the results discussed in Section 7.6.

7.1 Flamingo mortality events

Mass mortality events at the soda lakes have been recorded since 1974 (Sileo et al., 1979), and there have been many events since that have been witnessed by researchers, recorded in local media and remembered by rural communities. Mortality events can be measured by counting the number of dead flamingos washed up along the shoreline every morning, and calculating the size of the event as a percentage of the total population in the lake. Large mortality events are apparent to observers because flamingo life expectancy is several decades. The extent and frequency of mortality events is not known for certain, since the lakes have not been monitored continuously, and the number of deaths as recorded by the media is likely to be highly subjective. The most significant of these events have occurred at Nakuru and Bogoria, with the first large events recorded in 1993 and 1995 at both Nakuru and Bogoria, which totalled 50-60,000 dead (Kock et al., 1999; Ndetei & Muhandiki, 2005). In 1999-2000 a mortality event occurred at Lake Bogoria, where 200,000 lesser flamingos are estimated to have died, approximately 20% of the birds in the area (Harper et al., 2003). In 2006, 35,000 died at Lake Nakuru (Kihwele et al., 2014).

It is possible that these mortality events are contributing to the overall decline in flamingo population, since lesser flamingos take tens of years to replace themselves. If the lesser flamingo population in East Africa is to be conserved the conditions leading to these mortality events need to be understood. We also need to consider the precise conditions that lead to successful breeding events in order to know if the lesser flamingo population is likely to recover and if the cause of these mortality events can be mitigated.

There have been different suggestions as to the cause of these mortalities, including the accumulation of toxins from heavy metals, pesticides or cyanobacteria (Ballot et al., 2004), tuberculosis, and malnutrition (Vareschi, 1987). Many mortality events have not been linked to any specific cause, and so further investigation is vital for the conservation of the lesser flamingo species.

Heavy metals have been identified in flamingo tissues at Lake Nakuru, which have been attributed to industrial pollution (Nelson et al., 1998), and are suspected by some to be a significant contributor to the flamingo mortalities that have occurred in recent decades (Kock et al., 1999). The significance of heavy metals to flamingo mortality is a subject of debate; Ndetei and Muhandiki (2005) suggest that toxicity from heavy metals is unlikely to be significant compared with other potential causes. Heavy metals are in fact present in all soda lakes frequented by flamingos at the same abundance (Wandiga et al., 1986) except for lakes Magadi and Sonnachi, which have the highest heavy metal concentrations but are visited less often. It has also been found that flamingos in France can tolerate high concentrations of heavy metals (Amiadtriquid et al., 1991).

Tuberculosis has been identified in lesser flamingos in the past. Declines in *Arthospira* abundance and the resulting malnutrition of stranded lesser flamingos has been thought to increase their susceptibility to the disease (Cooper et al., 1975; Sileo et al., 1979). The source of TB in lesser flamingos is unclear since it was not present in populations of poultry on local farms (Ndetei & Muhandiki, 2005).

More recently mortalities in 1994 at lakes Bogoria and Nakuru have also been linked to the production of cyanotoxins (Carmichael, 1997). Cyanotoxins are produced by some species of cyanobacteria, possibly as a defence mechanism against planktivores like the lesser flamingo, or to reduce competition with other cyanobacteria. In the Rift Valley saline-alkaline lakes cyanobacteria species (*Microsyttis*, *Lyngbyia*, *Aphanizomenon*, *Gomphosphaeria*, *Nodularia*, *Oscillatoria*, *Anabaena*, *Nostoc*) were found to produce cyanotoxins under bloom conditions (Dawson, 1997; Meriluoto, 1997). The species *Anabaena* and *Anabaenopsis* have been identified by Ballot et al. (2006), and are known to produce neurotoxins. Microcystins and anatoxin-a have been identified at the hot springs of Lake Bogoria where flamingos wash their feathers and drink (Krienitz et al., 2003). The toxins may be ingested by flamingos at these locations and have been

identified in the intestines of flamingo carcasses and in their droppings (Krienitz et al., 2003).

In 1999 and 2000, deaths occurred in Lake Bogoria when *Microcystis* and *Anabaena* were dominant in the water. High levels were also identified in 2001 which coincided with lower rainfall, and flamingo mortalities continued during this time (Ndetei & Muhandiki, 2005). Another 30,000 lesser flamingo deaths occurred in July 2008 when there was a relatively high abundance of *Anabaenopsis*. These other cyanobacteria species bloom during troughs in *Arthrosphaera* population, but usually at much lower abundances and so food abundance is still lower overall. Another important factor is that *Anabaenopsis* is larger than the excluders in the lesser flamingo filtering mechanism which prevents particles larger than 800 μm reaching the lamellae which are spaced at only 50 μm apart. A species of *Anabaenopsis* was measured by Krienitz and Kotut (2010) at 300-2,000 μm which is too large to be a viable food source for the lesser flamingo. *Anabaenopsis* has also been found to impede the filtering mechanism by blocking some of the excluders in the bill. The deaths in July 2008 are believed to be caused by starvation since no evidence of disease, infection or toxicosis were found (Krienitz & Kotut, 2010). At the mortality event at Lake Bogoria in early 2003, Harper et al. (2003) found that only one in twenty dead birds was 'sick' before it died. The mortalities may have been due to starvation or from being too weak to avoid scavengers.

Without further experiments it is impossible to know for certain whether lesser flamingo mortality events are actually caused by cyanotoxins. It is difficult to know the significance of cyanotoxins to mortality events, and currently the degree to which cyanotoxins have affected lesser flamingos is debated. It is possible that during blooms of toxin producing cyanobacteria the deaths are actually a result of starvation. It would seem illogical that lesser flamingos in East Africa have not evolved to cope with the toxins in their environment, particularly when flamingos in other regions have been found to tolerate toxins (Amiadtrient et al., 1991). It is possible that these toxin producing species are more recent additions to the phytoplankton community structure, or have not previously been present in such large abundances, which may not have given lesser flamingos time to adapt to these changes. If toxins are causing the mortalities, then it is likely to occur when a change in lake water level results in a sudden decline in *Arthrosphaera* and a bloom in toxic cyanobacteria. The other occasion when lesser flamingos would be exposed to increased levels of cyanotoxins is when low precipitation or drought causes the rivers and streams to run dry. This would force the lesser flamingos to wash and drink at the hot springs rather than distributing themselves between the hot springs and the streams or river mouths also feeding the lake.

Initially the primary food source of the lesser flamingo, *Arthrosphaera*, was not considered to produce toxins (Naidu et al., 1999). However, investigations in the last decade have found a strain of *Arthrosphaera* that does produce microcystins and anatoxin-a toxins (Ballot et al., 2004). The production of cyanotoxins is not well understood (Carmichael,

1992), but if toxins are contributing to lesser flamingo deaths it will be useful to know the conditions that trigger their production. The addition of nutrients to lakes from fertilisers are likely to be a cause of cyanobacteria blooms, and may be linked to cyanotoxin production (Matagi, 2004).

It is interesting that the largest known lesser flamingo mortality event, which occurred in 1999-2000, occurred at Lake Bogoria. During this event a large proportion of the total flamingo population of the Rift Valley were at Lake Bogoria, which is the most chemically stable of the soda lakes. If the flamingos are dying at Lake Bogoria in such large numbers due to starvation, all the other shallow lakes must have been unsuitable, causing most of the population to congregate at Lake Bogoria. If the other soda lakes were in a state which could support the lesser flamingos, then it would be unlikely that the whole population at Lake Bogoria died of starvation, and it would be more likely that the deaths were caused by toxicosis or disease.

7.2 Hypotheses

Based on the literature summarised above a series of hypotheses concerning flamingo population decline were formulated. Each of these hypotheses depend on changes in the availability of *Arthrosphaera* or breeding sites in response to lake water level. The hypotheses that were considered were:

1. Mortality events are caused by starvation during periods of low food abundance.
2. Mortality events are caused by disease, which flamingos become increasingly susceptible to during times of stress, i.e., low reserve mass.
3. Mortality events are caused by the accumulation of toxins which flamingos ingest at the hot springs.
4. Mortality events are caused by the accumulation of toxins which flamingos ingest when a bloom of toxic algae occurs.
5. The replacement rate of flamingos is too low to maintain the population.

It is not possible to test all of the different hypotheses using one model. It was considered that to explore the cyano-toxin hypothesis a spatial model would be needed. This increase in model complexity was considered unnecessary since most of the hypotheses could be explored using a simpler, non-spatially explicit model.

The exposure to toxins at the hot springs is also beyond the scope of this model, since there are long dry periods (e.g. between 1910 and 1935) when flamingos would be likely to drink from the hot springs within the constraints of this model. If toxins are naturally present in the hot springs of the soda lakes, and toxins are a cause of

flamingo mortality then flamingos would have to avoid drinking from hot springs and fly to freshwater sources that are not included in this model, such as freshwater Lakes Naivasha and Boringo, in order to avoid extinction. It is possible that either flamingos can tolerate the toxins found in the hot springs, since they have been observed drinking this water when other fresh water inflows were available (pers. obs.), or that the toxin levels are only high periodically as a result of blooms of the bacteria that produce them at the hot springs. After considering these limitations, the model was used to explore the starvation, disease, and low replacement rate hypotheses.

7.3 Starvation

The starvation hypothesis was explored using the ‘vanilla’ version of the model, with no changes made to the flamingo model described in Section 6.2. Death by starvation is already an integral part of this model. Figure 7.1 shows the depletion of flamingo reserve mass for flamingos at the upper and lower limits of structural mass. The mass of each flamingo consists of structural and reserve mass. The reserve mass is the fat reserve which a flamingo relies upon to survive periods of low food abundance. When the reserve mass is depleted the flamingo dies of starvation and is removed from the model population. The largest flamingos can store a maximum of 0.77 kg of fat, and the smallest flamingos can store up to 0.59 kg (Ton, 2007). In Figure 7.1, the depletion of fat reserves over time can be seen by flamingos at the upper and lower mass limit. The reserves of a flamingo can theoretically last up to three months if the only energy expended is for basal metabolic rate. However, in order to perform other activities like preening, washing, drinking and moving around the energy expended is much greater, and so the fat reserve will last between 22 and 26 days. These calculations exclude energy expended if the flamingo were to fly in search of food at other lakes.

A summary of the output from the starvation hypothesis can be seen in Figure 7.2. Figure 7.2 shows the average population, breeding event size, number of fledglings produced, mortality event size and fat reserve. It can be seen that breeding is attempted nearly every year by up to 30% of the flamingo population, although most years breeding events are less than 10% in size. Breeding attempts do not always produce fledglings, and so changing lake water level or lack of food can cause desertion. There are periods e.g. 1917 to 1919, 1983 to 1990, and 1994 to 1997 where there are very few flamingos engaged in breeding activity. Each successful breeding event increases the population by up to 5%, although most breeding events only increase the overall population by up to 2%. The mortality events coincide with low average fat reserves, which reflects low *Arthrosphaera* densities or overgrazing of *Arthrosphaera* or diatoms by flamingos.

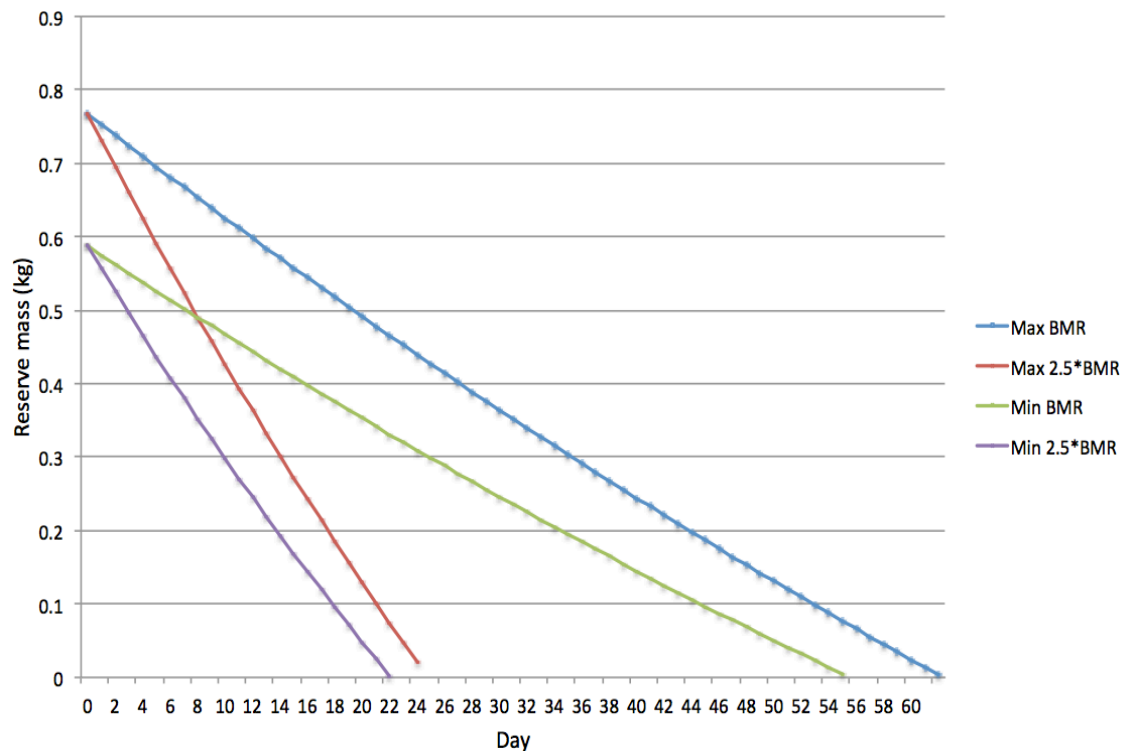


FIGURE 7.1: The mass of flamingo fat reserves over time when there is no food. For the largest modelled flamingos, where the only energy expenditure is basal metabolic rate (BMR) (blue), and for $2.5 * BMR$ (to allow for daily activities) (brown). For the smallest modelled flamingos, where the only energy expended is for BMR (green), and for $2.5 * BMR$ (purple).

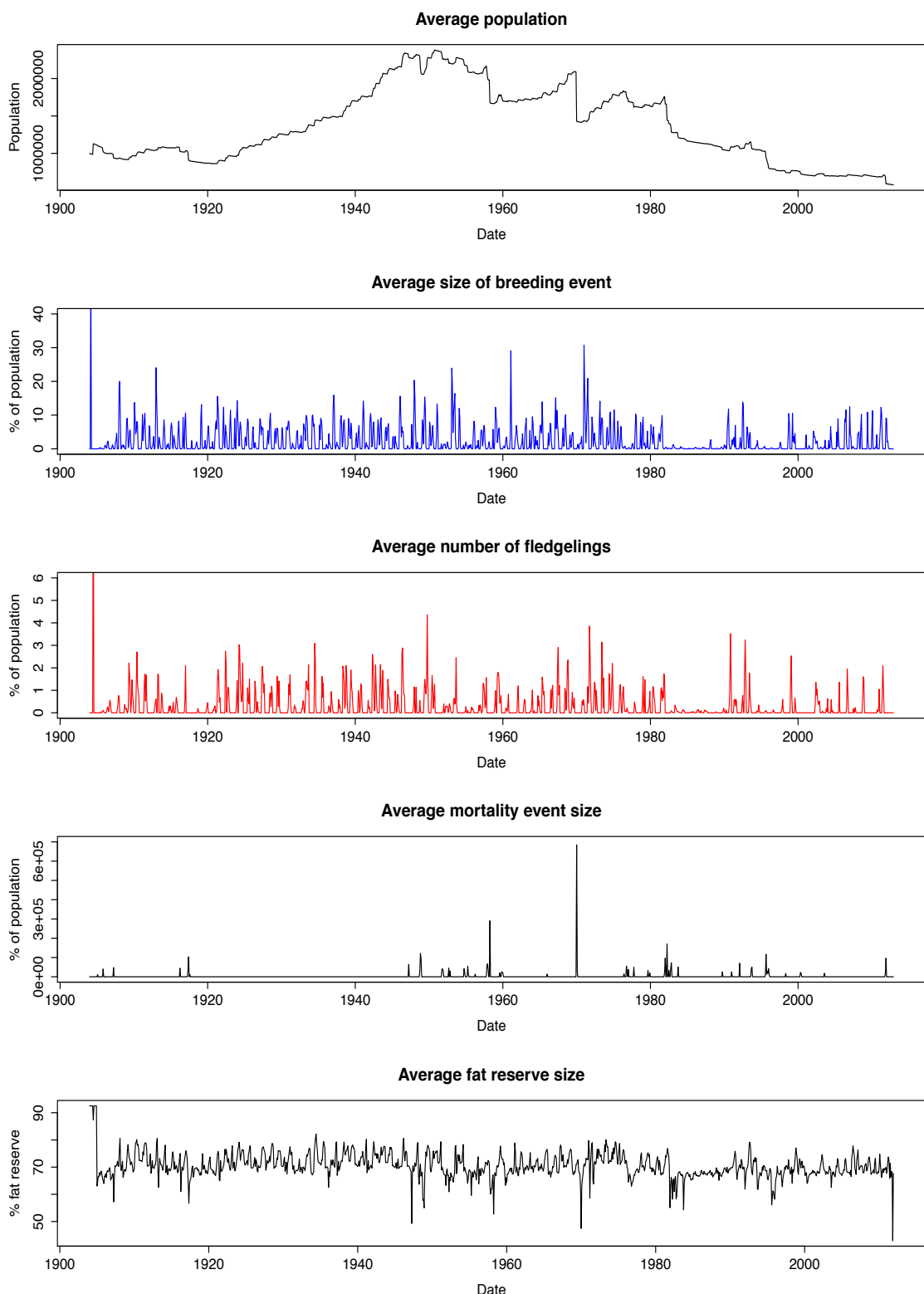


FIGURE 7.2: A summary of the output from the starvation hypothesis where the average standard deviation for total population is 12.6%, 0.7% for average breeding event size, 0.5% for average number of fledgelings, 19.3% for average mortality event size, and 1.76% for average fat reserve size.

7.4 Disease

To explore whether disease could change the pattern of flamingo mortality events, we chose to implement disease as a relatively severe influence on flamingo survival. Disease was implemented by assuming that most flamingos (80%) are carriers of disease, while the remainder (20%) are immune, and that these flamingos become more vulnerable to disease when they are malnourished and under stress due to food shortages. In terms of the model this occurs when flamingos have smaller fat reserves. In the absence of empirical data a vulnerability to disease threshold was set at 30% of the total potential energy reserve for each flamingo. Each day that a flamingo's reserve is below this threshold value, it has a chance to become symptomatic, which means that it starts to exhibit symptoms of the disease and become vulnerable to death. The chance of becoming symptomatic was assumed to increase linearly as fat reserve drops below 30% until it approaches zero, when it will almost certainly become susceptible to disease. Once a flamingo becomes symptomatic, it experiences a risk of dying from disease. The chance of death was chosen to be 5% each day. A flamingo recovers from disease if its reserve mass increased past 30%.

Figure 7.3 shows the average flamingo population output by the disease hypothesis. The disease hypothesis outputs a lower overall population. Figure 7.4 shows the population change alongside the breeding event size, fledgelings produced, the mortality event size and the average fat reserve of the total flamingo population, and Table 7.1 compares starvation and disease outputs. Breeding events are similar to the starvation output hypothesis, with breeding attempted nearly every year, and in small groups. Breeding attempts are not always successful, and so changing lake water level or lack of food can cause desertion.

Flamingos can die of starvation, disease and old age. It is possible for deaths by starvation to occur when flamingo fat reserves drop quickly during low food abundance, because they will have less time to succumb to disease before dying of starvation. Most of the mortality events occur at the same time for the starvation and disease hypotheses output. However, there are more mortality events in the 1980s as a result of disease. This is a result of the low *Arthrosphaera* abundance across the soda lakes during this time, when flamingos have to work harder to find *Arthrosphaera* or diatoms, their fat reserves may dip below the disease susceptibility threshold.

The average fat reserve is 70.16% for the starvation hypothesis, and 71.36% for the disease hypothesis. The starvation and disease outputs are very similar, the only real difference being a lower overall population and slightly higher number of mortality events.

The sensitivity of the model to changes in parameters specific to the disease hypothesis can be seen in Table 7.1. The three parameters include M_D , which is the chance a

symptomatic flamingo will die of disease each day. P_R is the chance that each flamingo will be resistant to disease, and R_V is the fat reserve threshold below which flamingos become symptomatic. None of the perturbed outputs fell outside two standard deviations (σ) of the standard parameter values. Overall population was most sensitive to an increase in the chance that a symptomatic flamingo will die (M_D) which caused a 13.3% reduction of average population, although this was still within one standard deviation of the standard parameter average population.

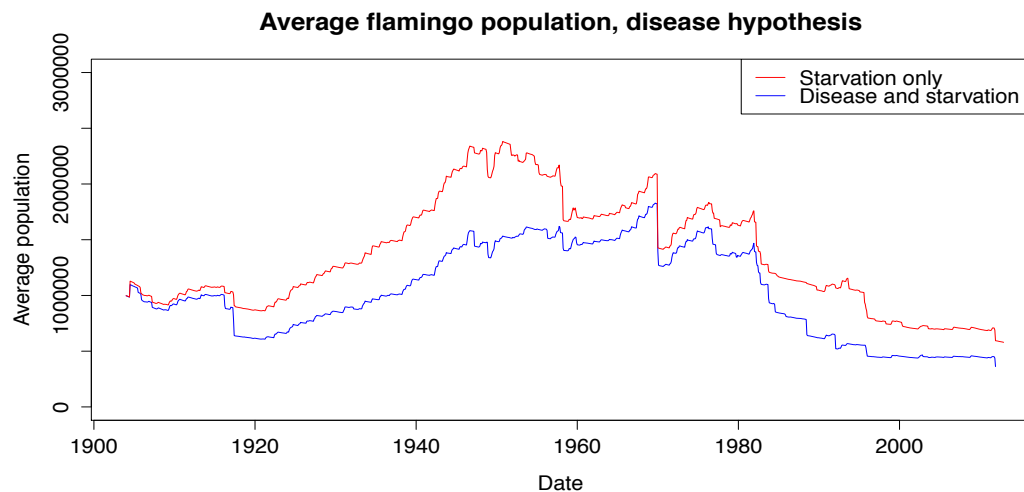


FIGURE 7.3: The average population over ten runs of the disease hypothesis (blue) compared against the average population output by the starvation hypothesis (red).
The average standard deviation for total population is 20.2%.

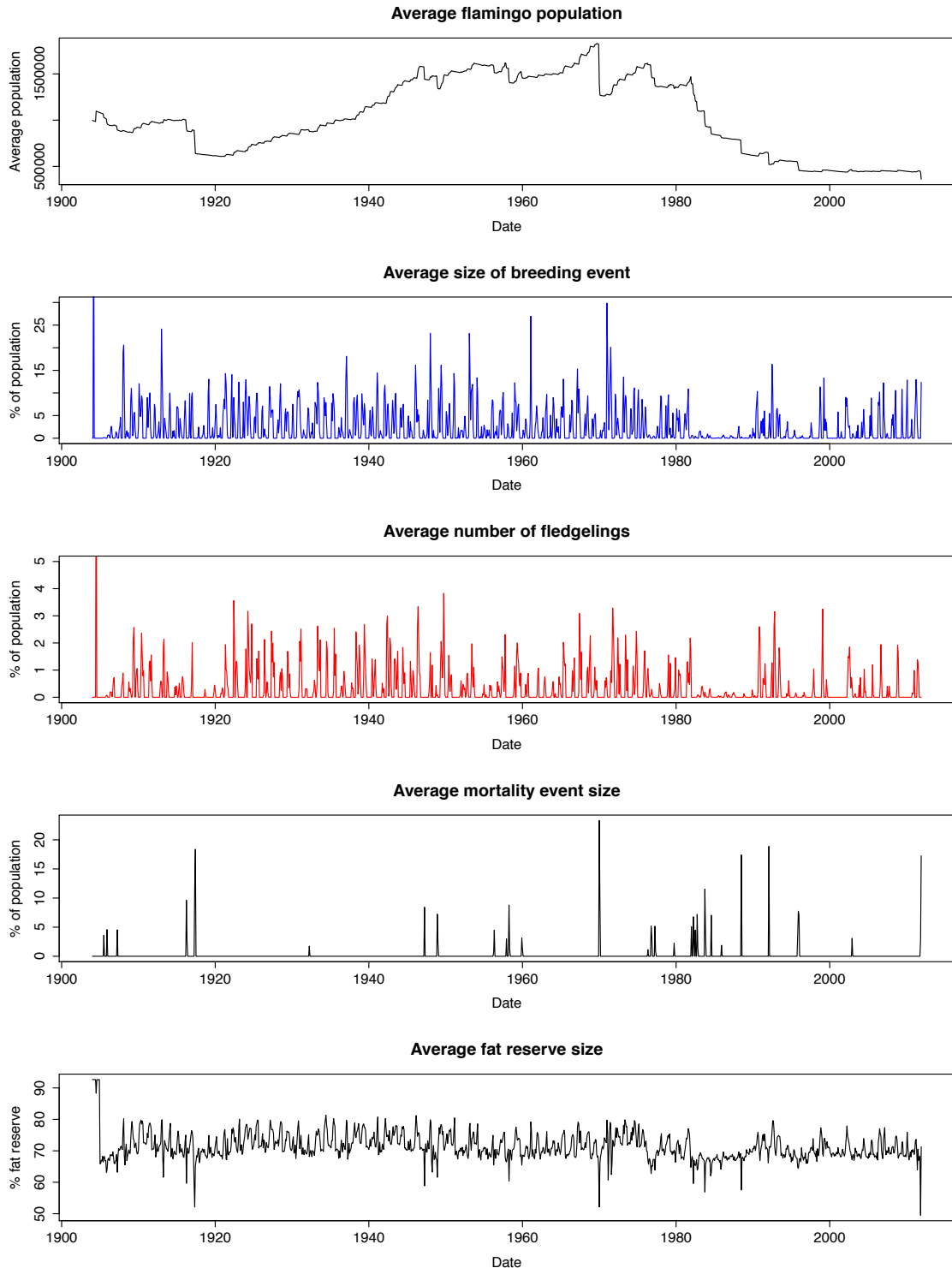


FIGURE 7.4: The average population, breeding event size, number of fledglings and mortality event size averaged over ten runs for the disease hypothesis. The average standard deviation for total population is 20.2%, 4.5% for the average breeding event size, 0.9% for average number of fledglings, 13.7% for average mortality event size, and 1.43% for average fat reserve size.

Parameter	Average population	Smallest population	Largest population	N^0 mortality events	Average mortality event size	Largest mortality event size	N^0 breeding events <10% population	N^0 breeding events 10-15% population	N^0 breeding events 15-20% population	N^0 breeding events >20% population
Starvation	1,376,356	559,350	2,684,850	12.9	17.2	48.2	166.2	4.3	1.1	1
Disease μ	1,024,690	315,400	2,096,800	14.8	17.6	51.5	167.4	5	1.1	1
Disease σ (%)	20.2	22.4	16.3	16.8	13.7	9.5	4.0	31	63.6	0
M_D -10%	3.9	24.6	2.5	6.1	-11.8	-8.2	-0.2	-2	-18.2	0
M_D +10%	-13.3	-1.2	-11.1	-7.4	15.5	-5	0.1	10	-45.5	0
P_R -10%	-0.2	1.3	4.6	8.1	-7.0	5.0	-2	2	9.1	0
P_R +10%	4.6	19.4	3.4	-1.4	-0.4	-3.4	-1.9	-4	27.3	0
R_V -10%	-5.0	6.4	-8.6	-4.1	6.7	-9.3	-0.6	-4	-9.1	0
R_V +10%	-5.7	3.3	-5.3	8.8	-7.2	-7.8	-0.2	-6	-18.2	0

TABLE 7.1: The sensitivity of the model to changes in the disease hypothesis parameters was tested by comparing the outputs for perturbations to the free parameters against the average disease parameters (μ). All perturbation values are the average of ten runs of the model, and are percentage deviations from the final disease parameter means. The standard deviations (σ) of the final disease parameters are compared with the percentage deviation in the outputs of the perturbed parameters. When a flamingo is symptomatic, M_D is the chance the flamingo has of dying of disease each day. P_R is the chance that each flamingo will be resistant to disease, and R_V is the fat reserve threshold below which flamingos becomes symptomatic.

7.5 Low replacement rate

A breeding attempt requires many conditions to be met for nesting to begin. For it to be a success, lake water levels must not allow the breeding islands to be flooded or adjoined to the main-land, and *Arthrospira* must be available throughout the breeding attempt. Figure 5.19 shows the model output for Lake Natron surface area, *Arthrospira* density, and breeding attempts. The lake surface area must be between 160 km^2 and 725 km^2 , and *Arthrospira* density must be greater than 0.1 kg m^{-3} . Both of these fluctuate dramatically, and for a breeding attempt to be successful conditions must remain suitable for a time period of at least three months.

In the model the following rules have to be met for a breeding event to occur:

- A flamingo must be sexually mature, with an age greater than six years (Robinson, pers. comm.).
- A flamingo must have more than 90% reserve mass.
- A flamingo must have engaged in courtship behaviour.
- Breeding islands must be available at Lake Natron.
- A flamingo will desert its nest and young if islands are no longer available, or if its reserve mass drops below 30%.

The limited monitoring of flamingo breeding events makes it difficult to know how frequently large breeding events occur, but the limited data that does exist suggests that there may be a mixture of a few large breeding events, and a higher frequency of small breeding events. To explore this, the minimum breeding colony size was changed to see what impact this had on the model output.

Breeding events usually occurred in the starvation and disease hypotheses in small groups (<10% of the total population), whenever islands were available for breeding. This is in contrast to the observations that are available for breeding events, which suggest that flamingos breed in high numbers, with smaller groups of flamingos considered more prone to nest desertion.

To explore the hypothesis that flamingos usually breed in larger groups, minimum breeding colony sizes were explored. The average population output using different minimum thresholds can be seen in Figure 7.5 and in Table 7.2.

It can be seen that for larger breeding colony sizes, the average population tends to be lower, the number and size of mortality events reduced, and the number of breeding events including 10-15% of the population is increased. These differences became more pronounced for minimum breeding colonies of 100,000 or more, but the trend broke down above minimum colony sizes of 180,000. Extinctions had not occurred in model

runs where minimum breeding colony sizes were less than 180,000, but the population became extinct in one of ten runs with a minimum breeding colony size of 180,000. For minimum colony sizes of 200,000, the flamingo population became unstable, with most runs ending in extinction. These larger breeding colonies often attempted to breed near the end of a period where islands had been available, for the nesting sites to then become unviable, or the breeding colony overgrazed the available *Arthrospira*, and fat reserves began to reduce, forcing flamingos to desert their nests.

When food availability at Lake Natron was forced to higher levels during periods when breeding islands are available for minimum breeding thresholds of 10,000 to 100,000, the population dramatically increased to an average of 6.1 million flamingos, which suggests that low food abundances at Lake Natron is an important factor in the limitation of breeding event success for smaller breeding colonies. However, larger breeding colonies do not breed at the right times to enable breeding to be completed before colonies are flooded or exposed to predators as a result of changing lake water levels.

Figure 7.6 shows that although increasing the minimum breeding sizes make the number of successful breeding events reduce, it does not reduce the frequency of breeding attempts, therefore the success of breeding attempts in this model is reduced by minimum breeding colony sizes above 100,000.

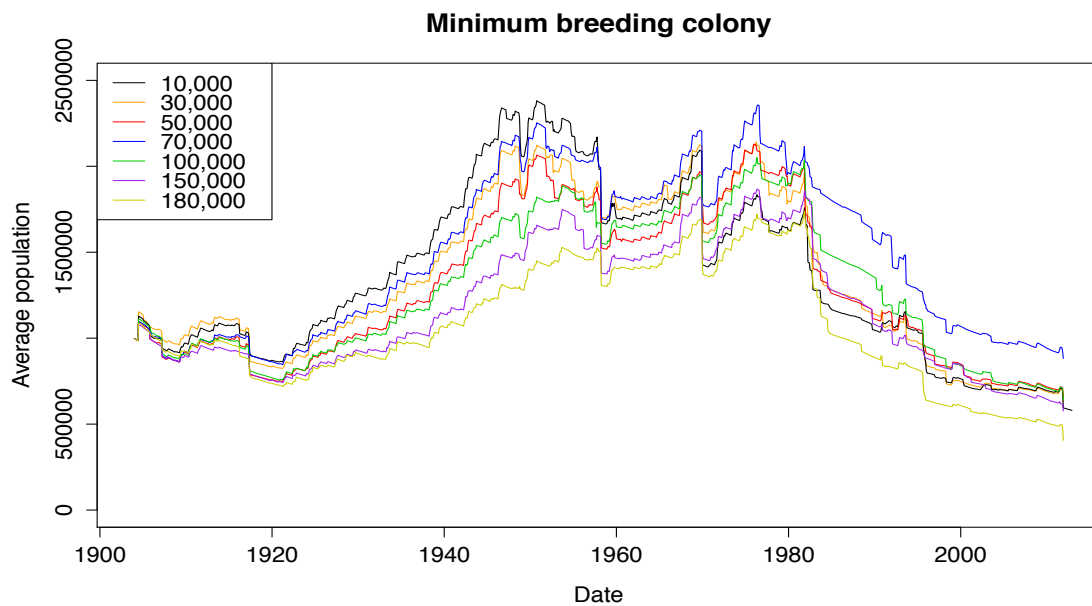


FIGURE 7.5: Average population output by ten runs of the model for minimum breeding colony sizes; 10,000, 30,000, 50,000, 70,000, 100,000, 150,000 and 180,000 flamingos.

Minimum breeding colony size	Average population	Smallest population	Largest population	N^0 mortality events	Average mortality event size	Largest mortality event size	N^0 breeding events <10%	N^0 breeding events 10-15%	N^0 breeding events 15-20%	N^0 breeding events >20%
10,000	1,376,356	559,350	2,684,850	12.9	17.2	48.2	166.2	4.3	1.1	1
30,000	1,348,523	602,600	2,565,000	12.8	16.75	40.82	174.9	5.3	0.5	1
50,000	1,291,729	608,800	2,510,800	12	16.76	42.38	174.1	6.7	0.5	1
70,000	1,485,914	678,000	2,730,500	12.4	13.80	36.20	177	6.3	1	1
100,000	1,288,596	559,100	2,393,300	10.7	16.72	39.70	169.9	9.4	0.9	1
150,000	1,168,993	519,600	2,177,500	10	16.10	33.66	130.7	20.2	2.8	1.2
180,000	1,066,561	405,400	1,926,300	9.8	16.66	37.0	95.3	27	9.2	1.9

TABLE 7.2: The output of the model for an average of ten runs, with different minimum breeding colony sizes.

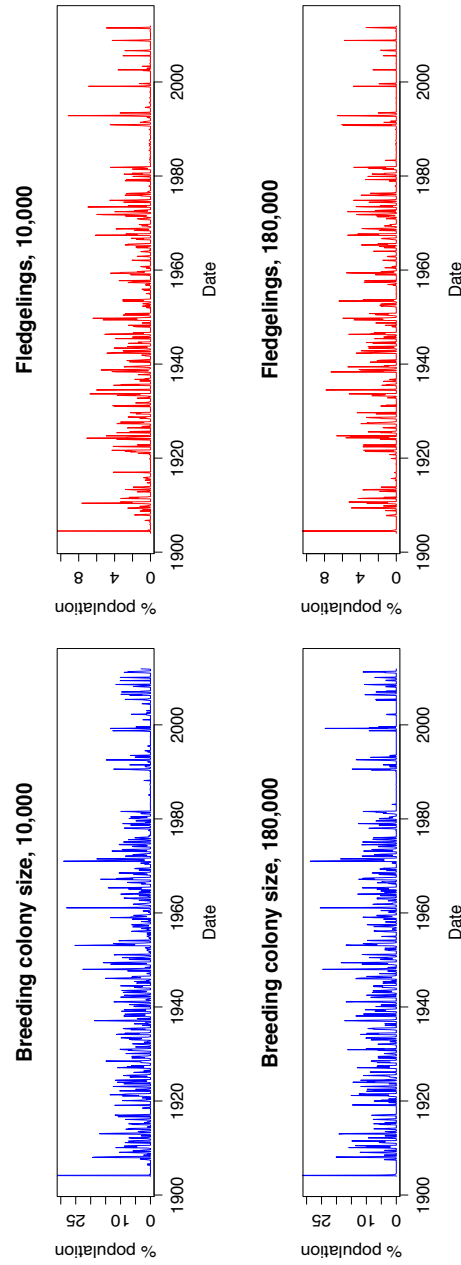


FIGURE 7.6: Average breeding colony sizes and fledgeling numbers output by ten runs of the model for minimum breeding colony sizes; 10,000 and 180,000 flamingos.

There were observed breeding attempts at Lake Natron in 1954, from 1956-1960, 1965-1967, 2002-2004 and 2012 (see Table 6.1). Because breeding occurs so frequently in the model it is not possible to know whether these coincide with breeding attempts by chance. Observed periods of no breeding at Lake Natron are more useful, such as in years 1955, 1961 and 1968, but there are too few data to make any meaningful comparison with the model output. The observational data does suggest that breeding attempts do not occur as often as they do in the model, and that there is some other factor that prevents flamingos from nesting that was not included in the model.

The model output suggests that breeding events occur frequently in smaller groups (<15% of the total population). The accepted theory is that flamingos breed infrequently in large groups which is supported by some observations of smaller breeding events (table 6.1). Monitoring of breeding at Lake Natron has not been continuous, and historic counts of flamingo breeding populations are unlikely to be accurate and more data is needed as well as refinement of the model by further empirical work to help understand how realistic this model output is. The reason that the model struggles to produce large breeding events is likely to be related to the way that *Arthrospira* and diatom abundance is output by the model, since a general NPZ model was applied to six different lakes, and is unlikely to be as realistic as one tailored for each individual lake. Another reason for the absence of larger breeding events also appears to be related to the delay in the establishment of larger breeding colonies which causes them to miss the best conditions at Lake Natron. It appears that simulated flamingos take longer to establish large breeding colonies than real flamingos, which may be caused by the time it takes to organise large flocks that can engage in courtship behaviour in the model. This suggests that there may be other factors or behaviours that encourage flamingos to breed in large groups that have not been considered in the model.

7.6 Discussion

The model was run for starvation, disease, and low replacement rate hypotheses. Death by starvation had to be included in all three since it is a fundamental requirement of the model to allow flamingos to die of starvation.

The population trend is similar for each hypothesis, with no extinctions occurring in runs of the starvation and disease hypotheses, but for the low replacement rate hypothesis extinctions occurred for large breeding colonies of 180,000 and above.

Mortality events occurred at the same time in 20 runs of the standard model. The mortality events can be seen in Table 7.3. Some mortality events occur during a year of high rainfall (1917, 2011), and others occur after periods of below average rainfall and declining lake water level (1948, 1970, 1982). Extreme rainfall events cause a sudden low *Arthrosipa* abundance across the region as a result of quickly increasing water levels and the sudden perturbation to the lake conditions.

During drought periods lake water levels are declining, and low *Arthrosipa* abundance occurs at individual lakes more gradually as the salinity increases beyond the tolerance of *Arthrosipa*.

The reason for other mortality events (e.g. in 1907, 1992, 1995 and 1996) are more difficult to discern, and is more likely to be the result of more subtle changes in lake water level that causes the lake conditions to shift beyond the limits of *Arthrosipa* growth, or overgrazing by lesser flamingos.

Date	Mortality event size (%)	Rainfall or lake water level changes
04/1907	5.1	Rainfall deviation of +12.61%
06/1917	11.4	High rainfall deviation +94%
11/1948	5.7	Preceeded by low rainfall (averaging -12.8%/year) from 1933 to 1946.
04/1958	17.3	Rainfall deviation of +21.75%
01/1970	48.0	Rainfall deviation of +21.87% preceded by 5 years of low rainfall (averaging -25% per year)
01/1982	5.8	+20% rainfall deviation preceded by a period of declining lake water levels.
04/1982	11.8	
11/1982	5.7	
02/1992	6.6	Rainfall deviation of +12%
09/1995	12.4	Rainfall deviation of -21%
01/1996	5.3	Rainfall deviation of -10%
12/2011	16.3	High rainfall deviation (+51%), preceded by high rainfall +71% in 2010.

TABLE 7.3: The average mortality events involving more than 5% of the total flamingo population averaged over 20 runs of the standard model.

Observed flamingo mortality events occurred in 1993, 1995, 1999-2000, 2003, 2006 and 2008. The observed events in 1993, 2000 and 2003 do correspond to smaller mortality events output by the model (4.8%, 3.1% and 2.6% of the total average population respectively), and the 1995 mortality event can be seen in Table 7.3. There are no mortality events in 2006 or 2008 output by the model. This model is a highly simplified model of the system that was expected to exhibit similar emergent properties to the system, not to reproduce real events. However, there is some correspondence between observed mortality events and the model output.

Breeding attempts occurred frequently for low numbers (<15%) of the population) for each hypothesis, even when the minimum threshold for breeding colony size was increased. Not all breeding attempts are successful, with small numbers of fledglings produced every year (increasing total population by <5% on average).

The starvation hypothesis outputs a stable flamingo population that moves between soda lakes in search of food and breeding opportunities, produces breeding events and mortality events without the need to force food abundance conditions. The disease hypothesis does not change the behaviour of the model, apart from to decrease the overall population and slightly increase the number of mortality events.

The exploration of low replacement rate hypothesis as a cause of flamingo population decline found that the success of smaller breeding colonies was determined by the availability of *Arthrosphaera* at Lake Natron during periods when breeding islands are available. Larger breeding colonies (>180,000 flamingos) were limited by the inability to attempt breeding at the right times to enable breeding to be completed before colonies are flooded or exposed to predators as a result of changing lake water levels.

Population decline in the model does occur for short periods as a result of large mortality events during periods of low food abundance, but the population usually recovers in the following decade. There is a longer term decline in population from the early 1980s to 2012 which occurs as a result of a period of infrequent breeding attempts in the 1980s to late 1990s, and although breeding attempts are made in the 2000s the overall population does not begin to recover to previous levels. This suggests that a low replacement rate is the cause of this decline in flamingo population.

Chapter 8

Modelling Discussion

The hydrological, *Arthospira* and flamingo models were constructed separately and then linked together to allow for interactions. Different time steps are used in these models; a daily time step is used in the hydrological model, whilst the NPZF model has an hourly time step. The flamingo model updates some variables each month including flamingo age and number of new fledgelings, other variables are updated daily including flight behaviour and time spent breeding, whilst feeding behaviour is updated hourly in order to allow the NPZ and flamingo models to work together.

The hydrological model made many assumptions and estimations in terms of the way groundwater and runoff behaves. In attempting to model six different lakes and in the absence of river inflow data, and local rainfall records for most locations, it was necessary to make these simplifications. The hydrological model was found to produce stable lake water levels over the last 108 years that fluctuate in response to rainfall. The outputs were compared with the water level data available in the literature, and found to produce very similar modern lake surface area changes, but was less accurate when compared with pre 2000 lake depth data for Lakes Elementaita and Nakuru. Some of the depth data agreed well for short time periods but showed a significant difference in average depth for others, suggesting that attempting to find a single set of parameters to accurately describe catchment processes is not possible. Changes in the lake catchments will occur in response to climate changes. Wetter and drier periods on decadal timescales cause changes in aridity and vegetation cover, which impacts the amount of runoff in a catchment. Human influence, such as deforestation, the increase in intense agriculture, erosion, the abstraction of water from rivers for irrigation and groundwater from wells also impact catchment processes. The Great Rift Valley is geologically very active, and groundwater flows along faults in the rift valley floor. It is possible that changes to groundwater flow can occur in response to tectonic activity such as earthquakes. To account for changing conditions it would be useful to identify different parameters for wet and dry periods to see how this impacts the model output.

Other improvements to the hydrological model that could be made include further refinement of the Lake Bogoria parameters, and improved bathymetry input data to allow the model to run during the high water levels of 1890 to 1910, and especially for the significantly higher water levels between 1700 and 1800. This would allow for the conditions at the current lakes during higher lake water levels, and the affect on the lesser flamingo population to be explored. Bathymetry data could be estimated using elevation data from remote sensing imagery. Lake surface area data needs to be obtained from Landsat images to compare with the model output which would allow for parameterisation of the hydrological model for Lake Magadi. With these improvements it should be possible for the affect of significant increases in lake water levels on the breeding sites of lesser flamingos, and also to explore the possibility that Lakes Magadi and Natron were important feeding lakes for flamingos between 1700 and 1800.

The *Arthrosphaera* (NPZ) model does output the key behaviours that are observed in the soda lakes. Despite the exclusion of other phytoplankton species (which would allow for interactions between phytoplankton such as predation and competition), wind speed and other parameters that may impact primary production, the salinity proxy allowed for rapid fluctuations in *Arthrosphaera* density to be produced. The more stable lakes such as Lake Bogoria were able to support more flamingos, and shallower lakes were generally more variable and with a lower carrying capacity overall. When conditions because fresher zooplankton (Z) began to grow and predated *Arthrosphaera* (P), causing fresher lakes to be less reliable food sources for the lesser flamingos. The NPZ model was modified to incorporate flamingos in an 'NPZF' model. This worked well when flamingo feeding time step and the NPZ model time step were the same. Flamingos were included by consuming *P* and excreting *N* directly back into the lake. The result was to increase the rate of nutrient cycling when flamingos were present in large congregations at a lake. Flamingos could also modify *Arthrosphaera* density, with larger groups abstracting a significant proportion of the daily growth.

Crashes in *Arthrosphaera* at most lakes simply required a rainfall event or drought that would push lake conditions outside of the limits that make it suitable for *Arthrosphaera* growth. This also happened at Lake Bogoria, although less frequently, and so it was not necessary to force crashes on the lake to see what impact crashes would have on the flamingo population.

There have been three observed crashes in *Arthrosphaera* abundance at Lake Bogoria, in 1978, 2001 and 2004. The NPZ model output *Arthrosphaera* crashes at Lake Bogoria in the late 1970s, and around 2004 which occurred at low lake water levels after high rainfall. However, the 2001 crash was not seen in the model output, which occurred when lake water levels were higher. This suggests that the 2001 crash may have been caused by factors not considered by the model or perhaps that Lake Bogoria is more sensitive to changes than the *Arthrosphaera* parameters currently allow. The model was only expected to produce similar behaviours in terms of *Arthrosphaera* abundance change rather than to

produce changes in abundance that occurred at the same time as observed changes. It is therefore more useful to compare frequencies of events rather than directly comparing the time series of the model output with individual empirical data. If these three events were the only crashes in *Arthrosira* that occurred between 1978 and 2004, then there would be one crash expected every 8.7 years. A crash (or die-off) of *Arthrosira* at Lake Bogoria is defined here as a sudden drop in *Arthrosira* density, where density reduces below 0.1 kg m^{-3} . This occurs 12 times in the model output for Lake Bogoria in 108 years, which is an average of once every nine years. Although this is similar to the 8.7 years estimated from current observations, three data points are not enough to make a meaningful comparison with the model output.

The recovery of *Arthrosira* density after a crash is usually very fast compared to the observed data which suggests that the *Arthrosira* growth is not as fast as Kebede (1997) observed in experiments, perhaps due to other factors such as the reduction of light availability after a crash caused by mats of dead *Arthrosira* on the lake surface, or a reduction in oxygen availability resulting from the decomposition of the dead *Arthrosira*.

Many of the parameters required for even the most simple NPZ model had to be taken from a general NPZ model (Fasham et al., 1990) that despite being used in estuarine environments was not ideally suited to hyper-saline conditions. The *Arthrosira* NPZ model could be improved by making the parameters specific to each lake, but despite these general parameter values, the NPZ model output the key behaviours that are observed in the soda lakes, including rapid fluctuations in response to changing lake water levels, and different behaviour output by the NPZ model at each lake.

The flamingo model consisted of the energy budget and the behavioural components. Although this model included many different variables, most could be estimated from the principals of mechanics and energy conservation, and so there only remained a small number of behavioural parameters that had to be estimated. These tended to be thresholds for behaviours, such as ‘minimum reserve threshold before breeding can occur’ and ‘minimum reserve mass before flamingo will search for a larger flock’, which could be roughly estimated using what is known about flamingo behaviour. The flamingo model worked well, allowing flamingos to move between lakes in response to different stimuli and to breed and die of old age or starvation. The population also distributed itself across more lakes to feed on diatoms during times of low *Arthrosira* availability, and would concentrate in high numbers at Lake Bogoria when there were high *Arthrosira* abundances. The total population increased and decreased over time between reasonable limits without dying out for the 108 years considered. Using this model, other hypotheses were explored, including death by disease and low replacement rate.

The model output breeding attempts frequently for low numbers of flamingos (<15% of the population) for each hypothesis, even when the minimum threshold for breeding

colony size was increased. Not all breeding attempts were successful, with small numbers of fledgelings produced nearly every year (increasing total population by <5% on average). This is in contrast to what is widely considered to be true of flamingo breeding events; that they occur infrequently and that larger breeding colonies are more successful. There have been observations of young flamingos at other lakes which suggests that flamingos do also breed in smaller colonies, yet the model output is too extreme to be realistic, suggesting that there is a problem with the model in this respect. The model did not reproduce observed breeding events very well, although there is not much observational data to compare with the model output. There is little known about flamingo breeding events, particularly in relation to the *Arthrospira* availability at Lake Natron. In the model, breeding events were successful if breeding islands and *Arthrospira* were both available for the time it takes to raise a chick, and the population increased dramatically if *Arthrospira* was made available at Lake Natron all times, which suggests that *Arthrospira* availability may be too low in the model, and that *Arthrospira* abundance is the limiting factor in terms of the success of breeding events at Lake Natron. When breeding colonies were restricted to a minimum size >100,000 flamingos the model produced fewer successful breeding events, and imposing minimum breeding colonies of >180,000 caused much larger mortality events that often caused the extinction of the flamingo population. It would be interesting to see whether improved bathymetry data and more lake specific NPZ parameters lead to an improvement of small breeding event success. However, the lack of any large breeding colonies in the model suggests that something has not been considered in the model that is important to the success of larger breeding events.

Between 1953 and 1968, the longest period when flamingo breeding events were monitored, twelve breeding events occurred, which is a frequency of once every 1.25 years. This is half as frequent as breeding attempts in the model output of once every 0.63 years on average, although perhaps surprisingly much more similar than would be expected considering the general consensus that breeding events occur infrequently.

Between 1990 and 2011 there were six mortality events observed at Lake Nakuru and Bogoria, which occurred in 1993, 1995, 1999-2000, 2003, 2006 and 2008. The observed events in 1993, 2000 and 2003 corresponded to smaller mortality events output by the model (4.8%, 3.1% and 2.6% of the total average population respectively), and the 1995 mortality event was more significant at 12.4% of the total population. No mortality events were output in 2006 or 2008. This model is a highly simplified model of the system that was expected to exhibit similar emergent properties to the system, not to reproduce real events. However, it is encouraging to see some correspondence between observed and modelled mortality events.

There have been six observed flamingo mortality events between 1993 and 2012. This is an average frequency once every 3.2 years. The model output an average of 12.9 mortality events between 1904 and 2012, one every 8.37 years. However, the frequency

of mortality events increases in the model after 1945 and again after 1993. There are an average of six mortality events between 1993 and 2012 in the model output, which is the same as the number of observed mortality events.

The number of mortality events was not the same for each run of the standard parameters (an average of 12.9 ± 2.1 mortality events). This variance in the number of mortality events suggests that some mortality events occurred due to regionally low *Arthrosipa* abundance, whilst others were sometimes avoided depending on the behaviour of the flamingo population in response to a reduction in *Arthrosipa* abundance at one or two lakes. In some cases of low local *Arthrosipa* abundance flamingos did not find the best source of food quickly or remained at lakes where the carrying capacity was exceeded by the population attempting to feed on diatoms, which caused a small mortality event that could have been avoided. The disease hypothesis output a higher average number of mortality events than the standard model (14.8 ± 2.5 mortality events), although these included the same mortality events output by starvation alone. The extra mortality events occurred during the 1980s when lake water levels were low and there was no stable source of *Arthrosipa* at any of the six lakes modelled during this period. During this time fat reserves were lower and flamingos became more susceptible to disease. Despite disease being modelled as a relatively strong influence on flamingo survival, the starvation and disease outputs are very similar, which suggests that disease is not an important driver of mortality events.

There is some concern that mortality events could be related to human activity, or as a result of cyanotoxins but the model suggests that mortality events have occurred in the past simply as a consequence of rapid changes in rainfall and the disturbance that this causes to *Arthrosipa* growing in these lakes.

Population decline in the model occurs for short periods as a result of large mortality events during periods of low food abundance, but prior to the 1980s these events do not have a lasting impact on overall population, which recovers in the following decade. There is a longer term decline in population from the early 1980s to 2012 which occurs as a result of a period of infrequent breeding attempts in the 1980s to late 1990s, and although breeding attempts are made in the 2000s the overall population does not begin to recover to previous levels. This suggests that a low replacement rate is the cause of this decline in flamingo population.

The population outputs for the standard flamingo model fluctuated between 550,350 and 2.68 million flamingos, with mortality events occurring as a result of high rainfall, changing lake water levels and low *Arthrosipa* density in the 1980s. The average population was 1.38 million flamingos. The population declined from 1.69 million in 1974 to 1.06 million in 1994, a reduction of 38%. This is similar to the 21% decline recorded by Simmons (2000) during this period, which lends support to ability of the model to simulate overall population changes. The population changes in the model suggest that

21% population decline between 1975 and 1994 (Simmons, 2000) was part of the natural fluctuations in population that occur as a result of irregular breeding and mortality events. Whether flamingo population increases in the next few decades will depend on the availability of food at Lake Natron during breeding events.

The outputs suggested that the simplest model, which only allowed flamingos to die of starvation and old age, exhibited all of the emergent properties that it was hoped would be captured by the model, including mortality events. The occurrence of mortality events when the flamingos are only able to die of starvation or old age suggest that these mortality events are a natural consequence of soda lake dynamics. The non-deterministic nature of flamingo decision making in the model allowed the population to distribute itself differently between lakes in response to a crash in *Arthrosphaera* at one lake, and the choices they made sometimes prevented a mortality event that happened in a different run of the model.

Chapter 9

Synthesis of empirical and modelling work

This chapter brings together the palaeolimnological data and modelling results to see how they can be used to inform each other, and what this can tell us about the effectiveness of using a combined empirical and modelling approach.

Sediment cores from Lakes Bogoria, Elmentaita and Oloidien were used to learn more about the natural variability of these lakes, and the impact this may have on the availability of food for the flamingo population. This was particularly important for Lake Bogoria, since it is considered a stronghold for flamingos during times of low food abundance at other lakes. The palaeolimnological data found that *Arthrosphaera* availability at Lakes Bogoria, Elmentaita and Oloidien has changed significantly on a decadal timescale in response to fluctuations in rainfall. Lake Bogoria was the most productive lake, with the least diverse phytoplankton community, although algae and diatoms do grow in low abundances and can dominate the phytoplankton community for short periods during lower *Arthrosphaera* abundances. Lakes Oloidien and Elmentaita are less productive, with more diverse phytoplankton communities that are only dominated by *Arthrosphaera* during low lake water levels when the lakes become more saline.

The most important data from these cores is the pigment data, which identifies the source of the organic material. It was hoped that the pigment data could be converted into *Arthrosphaera* densities, but this was not possible because pigment preservation is a product of both the phytoplankton composition and preservation conditions. There were some problems where degradation of pigments or low abundances of some pigments meant that some phytoplankton were not detected despite being identified in the lake empirically. The empirical data could therefore not be directly used in the model, although it is still useful to know how variable phytoplankton at Lake Bogoria has been in the past. It was found therefore that empirical data can be used to inform the

model, but that it is not as straight forward as was hoped to reconstruct the precise lake conditions from the fossil material due to differential preservation and degradation.

The model was made to be as simple as possible whilst still capturing the behaviour of the system. To do this it was built in stages, with separate hydrological, NPZ, and flamingo energy budget and behaviour components. Complexity was added when necessary to improve the model, for example, it was found that the model needed to include more lakes and also an alternative food source for lesser flamingos, which was not initially considered. The emergent properties of these soda lake ecosystems were captured using this simple model. Despite the relatively low complexity it was demonstrated that this approach still encounters major challenges. The soda lakes are in remote locations, and by their nature can be difficult to sample. As a result there is very limited data available for some of these lakes. Data limitation is one of the major problems encountered during this project, including difficulties in accessing data held by Kenyan government organisations. The attempt to access river inflow data used by Becht and Harper (2002) and Becht et al. (2006) failed after repeated attempts to contact the Water Research Management Authority in Kenya. The rainfall data from the Kenyan Meteorological Department was only obtained after a period of several months, and the flamingo census data is treated very sensitively by the Nature Kenya, the National Museums of Kenya, and the Kenyan Wildlife Service, making it very difficult to access.

The *Arthospira* density output by the model for Lake Bogoria was compared against the palaeolimnological data in Figures 9.1 and 9.2. Figure 9.1 shows the average density of *Arthospira* output by the NPZ model for different lake depths at Lake Bogoria. Below in Figure 9.2 is a graph showing the geochemistry DCA Axis 1 data, which is used here as a proxy for lake depth, and pigment DCA Axis 2 data, a proxy for cyanobacteria at Lake Bogoria. It is not possible to directly compare depths between these graphs, but the trend at low lake water levels is for lower cyanobacteria densities in both graphs, increasing for intermediate depths and decreasing at high lake water levels, although this decrease is less obvious in the proxy data. Both graphs agree that cyanobacteria usually dominates the phytoplankton community at Lake Bogoria, apart from at very low lake depths, and that at high lake depths cyanobacteria decreases, which we know from the other pigment data occurs as a result of freshening and increased competition from a more diverse phytoplankton community.

Another way to compare the pigment data with the model output is to consider the frequency of potential crashes in *Arthospira* abundance. It was speculated that an *Arthospira* crash occurred in the empirical data where consecutive sediment samples show a significant reduction in myxoxanthophyll concentration. If the younger of two consecutive samples in the south basin core (SB1) at Lake Bogoria contains one third of the previous myxoxanthophyll concentration or less, it could be considered a relatively large reduction in *Arthospira* density and a potential crash. This is because in consecutive samples at Lake Bogoria, the most stable soda lake in this study, changes in

pigment preservation rate as a result of depth changes are likely to be relatively small. There are 17 occasions in the south basin myxoxanthophyll data when this occurs, which is a frequency of once every eight years. Crashes in *Arthrospira* in the model, where density reduces suddenly to below 0.1 kg m^{-3} occurs on average once every nine years. Although speculative, this suggests that there may be some methods for comparing between palaeolimnological data and the model output.

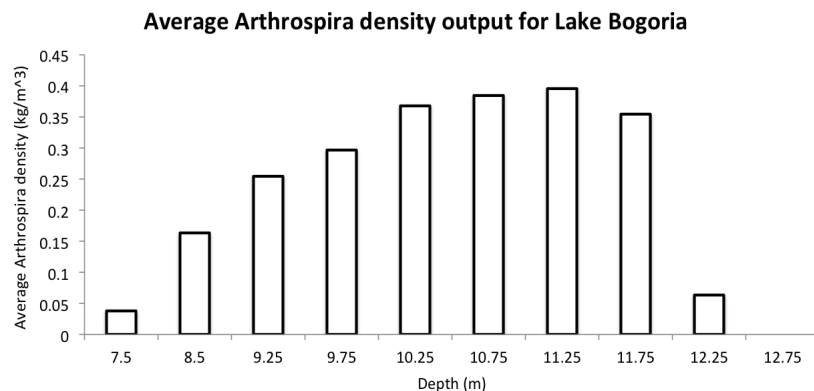


FIGURE 9.1: The average *Arthrospira* density output by the NPZ model for depths of 7-8 m, 8-9 m, 9-9.5 m, 9.5-10 m, 10-10.5 m, 10.5-11 m, 11.5-12 m, and 12.5-13 m.

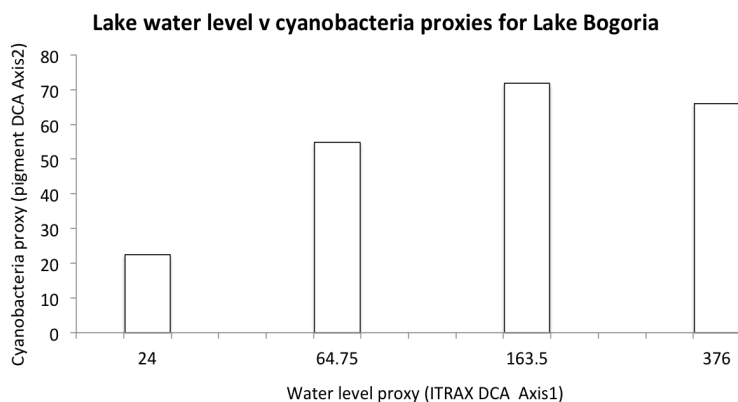


FIGURE 9.2: The average pigment DCA Axis 2 scores, a cyanobacteria proxy (see 3.16), plotted against the geochemistry data DCA Axis 1 score, a proxy for lake depth (see Table 3.5). The Axis 1 scores range from 33 to 410, and the cyanobacteria proxy was averaged for Axis 1 scores of 33-93, 93-226, and 226-410. Higher Axis 1 scores correspond to higher water levels, although the numbers on the x-axis are not proportional to lake depth change.

The variation in $\delta^{15}\text{N}$ values in the sediment suggested that it may be possible to develop $\delta^{15}\text{N}$ as a flamingo proxy. However, with very few observed data of flamingo populations at Lake Bogoria it was not possible to make any meaningful comparison between the data. $\delta^{15}\text{N}$ values were compared against the average modelled flamingo population at Lake Bogoria for the same dates, and the result can be seen in Figure 9.3. There is a negative correlation between $\delta^{15}\text{N}$ and the number of flamingos, which suggests that at low densities of *Arthrospira*, $\delta^{15}\text{N}$ values are relatively high as a result of the much lower

abundance of *Arthrospira*. The variation in *Arthrospira* density is likely to complicate the use of $\delta^{15}\text{N}$ as a flamingo proxy.

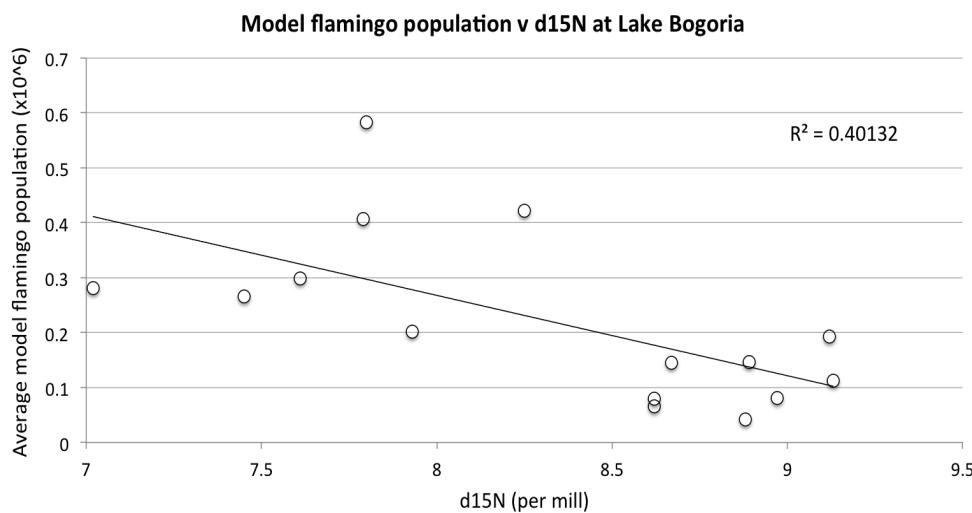


FIGURE 9.3: The average flamingo population output by the model for the standard parameters at Lake Bogoria, averaged over 20 runs of the model, plotted against empirical $\delta^{15}\text{N}$ data from Lake Bogoria. The model flamingo population values corresponding to the dates of each lake sediment sample that has $\delta^{15}\text{N}$ data are plotted here. So each data point effectively represents a particular year.

There are few direct comparisons that can be made directly between the empirical data and model output, because of the difficulty in translating the material preserved in sediment cores into *Arthrospira* densities for lower abundances of *Arthrospira*. This reduces the effectiveness of a combined empirical and modelling approach and leaves a frustrating gap between the model and empirical data. However, the patterns and trends found in the empirical and modelling work can still be compared and used to inform each other.

The model outputs highlighted how little is known about breeding events at Lake Natron, and the conditions that trigger large breeding events. To improve our understanding about breeding events it would be useful to get bathymetry data for Lake Natron, data on *Arthrospira* abundance at Lake Natron and also more information about breeding island surface area from remotely sensed imagery. Cores from the lagoons could also provide useful information about *Arthrospira* abundance, and potentially flamingo populations using the nitrogen isotope ratios.

The empirical work can also be used to inform the development of the model. The pigment data show a large change when lake water levels were higher (up to 12 m higher at Oloidien/Naivasha) between 1890 and 1910, suggesting that Lakes Elementaita and Oloidien were unsuitable feeding sites for flamingos during this time. The Lake Bogoria pigment data showed a freshening of the north basin, with pigment degradation in the south basin making the pigment abundances difficult to discern. However, Lake Bogoria was still very productive during this time, suggesting that there were still high

abundances of cyanobacteria or algae. Observations of the changes at Lake Bogoria after a significant water level increase in July 2012, when the maximum depth was recorded was 11.9 m in the southern basin, suggest that is likely that *Arthrosphaera* may still have been present during high lake water levels between 1890 and 1910. In July 2012 *Arthrosphaera* was in high abundance in the central and southern basins. There was a population of 700,000 flamingos at the lake. These flamingos appeared to be healthy, with many of the adults very pink and performing courtship dances. This suggests that although flamingos cannot feed on *Arthrosphaera* at Lakes Oliden, Nakuru and Elmentaita during high lake water levels, they can feed at Lake Bogoria in the central and southern basins where *Arthrosphaera* still dominates the phytoplankton community. As lake depth continues to increase beyond 11.9 m it is unknown how dominant *Arthrosphaera* will be at Lake Bogoria. The higher $\delta^{15}N$ value at Lake Bogoria in 1895 supports this theory. If Lake Bogoria was the only major feeding lake the flamingo population would be at increased risk of starvation during an *Arthrosphaera* crash, which would cause huge mortality events. However, in January 2012 (during high lake water levels) the large flamingo population at Lake Bogoria left for a few months, possibly due to reduced food availability, and most appeared to have moved to Lake Logipi before slowly moving back to Lake Bogoria in April. Some were also seen at Lake Manyara, a very shallow lake not included in this study. It appears that Lake Logipi is a suitable feeding lake during higher lake water levels, although the flamingos prefer Lake Bogoria when it is available. This availability of other food sources would allow the flamingo population to persist in high numbers between 1890-1910, unless a die off event occurred at both lakes simultaneously.

It is unknown at what depth Lake Bogoria would become fresh enough to allow for a more complex ecosystem where fish and zooplankton may consume phytoplankton at Lake Bogoria, it would become less productive and unsuitable for lesser flamingos. However, if Lakes Bogoria and Baringo continue to increase in depth they will flood the plain between them that was once the Baringo-Bogoria lake bed, and form a new lake which is unlikely to be saline enough for *Arthrosphaera* growth. Lake Baringo is a freshwater lake, with a complex ecosystem including macrophytes, fish, crocodiles and hippos. If these two lakes meet in the next few years it would be very interesting to monitor the changes that occur as the hyper saline Lake Bogoria joins the freshwater Lake Baringo.

This raises questions about how the flamingo population would survive significantly higher lake water levels in East Africa. Verschuren et al. (1999) reconstructed wet and dry periods in East Africa over the past 1100 years by studying the diatoms of a core from Lake Naivasha (Figure 9.4). Figure 9.4 part b shows alternating wet and dry phases, with an overall drier period during the Mediaval Warm Period (1000 to 1270), where salinity at Lake Naivasha increased during low lake water levels of approximately 2m, and was possibly a suitable feeding lake for lesser flamingos. The wetter conditions during the

Little Ice Age (1270 to 1850) is punctuated by drought periods that Verschuren et al. (1999) attribute to peaks in solar radiation. The lake water level fluctuations of the past 100 years are much smaller than the change between 1700 and 1850, where lake depth increased by more than 20 m at Naivasha. During this time Lakes Bogoria and Baringo were probably joined, and the flamingo population is unlikely to have been able to feed at this lake. These wet and dry periods must have significantly affected the lesser flamingo population, at least in terms of population distribution.

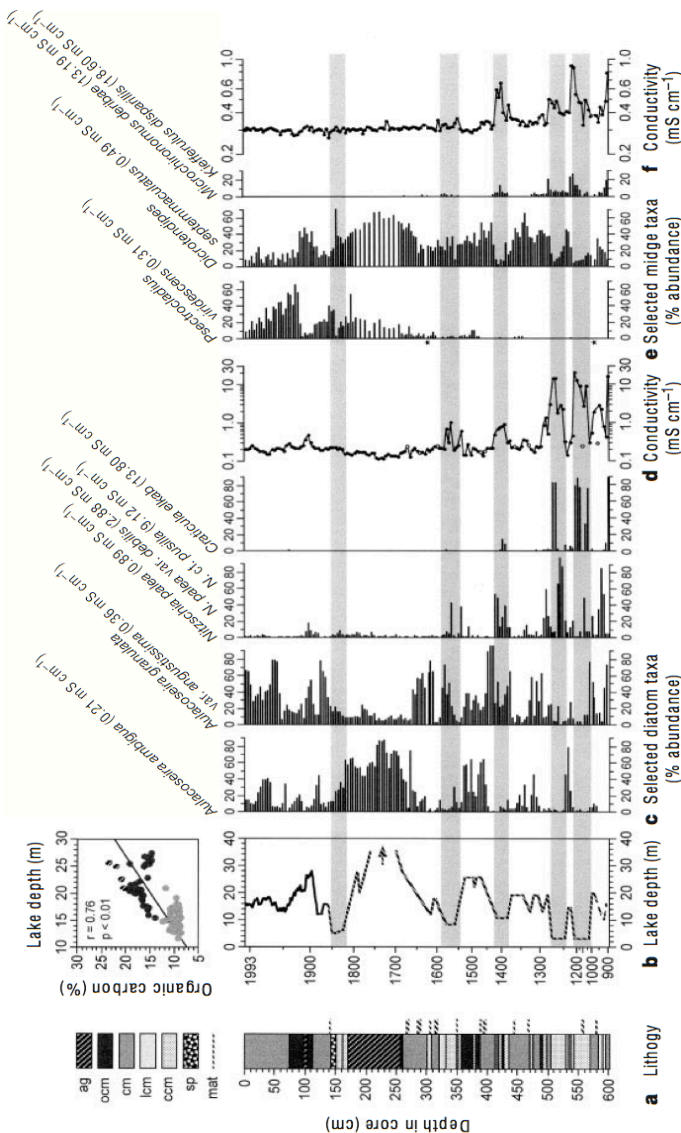


FIGURE 9.4: Lake depth and salinity reconstruction from a Lake Naivasha core by (Verschuren et al., 1999).

If Lake Bogoria became too fresh for *Arthrospira* growth, the flamingos must fall back on lakes that are more saline than Lake Bogoria. Lakes Natron and Magadi may have become fresh enough for *Arthrospira* growth between 1700 and 1850, considering the much higher lake depths in the (Verschuren et al., 1999) data (Figure 9.4). If these lakes were unsuitable the flamingos may have suffered a significant reduction in population,

or would have to search for food outside of the lakes in this study. Data from Lakes Natron and Magadi is essential to help answer this question.

There was a reduction in the total number of flamingos in East Africa to approximately 450,000 flamingos in 1975 (Tuite, 2000). In 1937 and 1961 there was an increase in lesser flamingo population at lakes in Western Uganda that were speculated to have come from the Kenyan and Tanzanian soda lakes (Din & Eltringham, 1976). It may be that the lesser flamingos move to other regions in Africa in order to find food, but there is very limited data about this and requires much more intensive monitoring of flamingo populations using a more frequent flamingo census or tracking larger numbers of them using satellite or cellphone technology.

Regionally higher water levels would also have implications for lesser flamingo breeding. The water level at Lake Natron between 1890 and 1910 were likely to have been too high for islands to be available for breeding. It is possible that the expansion of Lake Natron caused new islands became available that could offer flamingos refuge from predators. One hypothesis is that flamingos did not breed during this time, and survived because they are long lived birds that could have recovered after a 20 year breeding hiatus. Flamingos are known to suffer failed breeding attempts, and it is generally accepted that lesser flamingos can undergo several years without attempting to breed. The model found that the average age of the flamingo population was actually a lot lower than the 50 years that a flamingo can reach in the wild, since to reach old age a flamingo must survive many stressful periods where low food abundance, and potentially disease can cause death. The maximum age of most flamingos in the model population was actually closer to 25 years, and this means that it is unlikely that the flamingo population could survive a 20 year breeding hiatus without undergoing a severe population decline. The decline in flamingo population that concerns conservationists was attributed by the model to the low replacement rate that occurred between 1980 and the late 1990s, which, in the model caused a 38% population decline. The recovery of the flamingo population to the high numbers seen in the 1950's after such a decline between 1890 and 1910 would be very unlikely, unless the total East African flamingo population prior to 1890 was significantly higher than 5 million flamingos (Simmons, 2000).

Lake Magadi is the only lake other than Lake Natron where lesser flamingos have been known to attempt to breed in large numbers. This happened once in 1962 when lake water levels were too high for Lake Natron to be a suitable breeding site, but not high enough for a successful attempt at Lake Magadi (Brown & Root, 1971). It could be that Lake Magadi has been used as a breeding site in the past during significantly higher lake water levels (such as between 1890 and 1910), or simply a desperate measure after the lesser flamingos could not find anywhere suitable at Lake Natron. The other alternative is that flamingos found breeding locations outside of East Africa during very high lake water levels. More research would be required to assess the likelihood that this occurred. To find out more about these lakes as potential breeding locations during

wetter periods, the hydrological model must be improved, and more core data from these lakes, particularly Lakes Magadi and Natron is needed.

To explore past flamingo population size and distribution over the past 1100 years more lakes will need to be included to allow the model to run during periods of low water levels, including freshwater Lakes Naivasha and Boringo. By extending the time period over which flamingos are modelled to include wetter and drier phases in East African climate, insight may be gleaned as to how the lesser flamingo population survived during these more extreme changes.

The attempt to use modelling and empirical data to improve the understanding of a system is not common practice. In this study the soda lakes were considered a good candidate for a combined empirical and modelling approach. It was found that even for a system as simple as the soda lakes where species diversity is relatively low, that there are major challenges in developing models that can be synthesised with empirical data. The most difficult aspects were the amount of data required by the model for hydrological and NPZ models, which require a large number of parameters, and also the difficulty in translating material preserved in sediment cores into *Arthospira* densities for comparison with the model outputs, which reduced the effectiveness of a combined empirical and modelling approach. The challenges that arose for this relatively simple model of a relatively simple system suggest that it will be difficult to combine empirical and modelling approaches for more complex systems. In order to achieve this for other systems, expectations about what the model can achieve need to be changed, since there will be many more parameters, and much more uncertainty. Models are more likely to be useful as a way to inform empirical work rather than forecast future population changes or predict specific events. Rather the expectation should be for more qualitative results and outputs that give insights into the dynamics of these systems.

Despite the challenges that arose in using a combined empirical and modelling approach, this study found that it was possible to develop a model that output general trends and characteristics of the system. The patterns and trends found in the empirical and modelling work could still be compared and used to inform each other, and the model outputs did not only reproduce similar behaviours observed in the soda lake ecosystem, but produced new hypotheses.

Chapter 10

Conclusions

The aim of this project was to investigate the cause of flamingo population changes and the significance of the 21% decline in flamingo population between 1975 and 1994. To do this both palaeolimnological techniques and modelling were used. This approach intended to close the gap between models and empirical data, to try and produce a model that output more realistic behaviour.

The model consisted of a hydrological, NPZ, and flamingo energy budget and behaviour components. A large number of parameters were required for even the simplest models hydrological and NPZ models, and so many assumptions and generalisations were made to fill the gaps in the empirical data. The flamingo model relied more on established physical or biological constraints but some triggers for different behaviours still had to be estimated. The palaeolimnological work gathered data about the changes in lake phytoplankton at Lakes Bogoria, Oloidien and Elmentaita. There was some difficulty in synthesising the modelling and empirical data. However, the empirical and modelling work found that there were similarities in the frequencies of observed breeding, and mortality events with model outputs, as well as the similarity in the trend for cyanobacteria growth at Lake Bogoria, and the similarity between the average population decline between 1974 and 1994 output by the model (38%) with the 21% decline recorded by Simmons (2000), which suggest that the model outputs behaviours that are characteristic of the soda lakes. The empirical and modelling work could also be used to inform each other, and raised questions about the how lesser flamingos survived the more extreme changes in lake water level in the past 1100 years, as well as new hypotheses.

The palaeolimnological data and model output suggests that:

1. *Arthrosphaera* abundance is greatest at intermediate lake water levels (between 10 and 12 m) at Lake Bogoria.
2. *Arthrosphaera* is available at Lakes Oloidien and Elmentaita at low water levels.

3. Nitrogen isotopes have the potential to be used as a flamingo proxy, but further research is needed to test this.

The model outputs suggest that:

1. High rainfall is the cause of the *Arthrosphaera* crashes at Lake Bogoria in 1978 and 2004.
2. Flamingo population is stable, although numbers can fluctuate significantly as a result of irregular mortality and breeding events.
3. The maximum age most flamingos will reach is 25 years.
4. Breeding success and average population size is limited by *Arthrosphaera* availability at Lake Natron.
5. Flamingo mortality events are a natural consequence of changes to *Arthrosphaera* abundance caused by rainfall.
6. Some mortality events can be avoided depending upon the behaviour of the flamingos in response to low *Arthrosphaera* abundance. If the flock distribute themselves efficiently between resources they can sustain the population through periods of low food abundance. However, if too many flamingos attempt to feed on diatoms at the same location they will not be able to support the population and some flamingos will die of starvation.

There is much that can be done to improve the model and further our understanding about how flamingos survive different conditions in the East African Rift Valley lakes. Cores from Lakes Magadi and Natron would help to identify if *Arthrosphaera* grew in these lakes during the higher water levels between 1700 and 1800, whilst cores from Lakes Baringo and Naivasha could tell us whether *Arthrosphaera* could grow in these lakes during very low lake water levels between 1000 and 1300. Remote sensing could be used to improve bathymetry data, lake surface area data, identify large flamingo colonies at Lake Bogoria and potentially breeding colonies at Lake Natron. The hydrological and *Arthrosphaera* models would then need to be re-parameterised and the *Arthrosphaera* model improved to reduce the densities of *Arthrosphaera*, and better represent the growth of *Arthrosphaera* during less saline conditions and after *Arthrosphaera* crashes.

Questions about flamingo behaviour that emerged when building the flamingo model include 'can flamingos see an *Arthrosphaera* bloom from the air?' and 'do flocks of flamingos seen from the air encourage others to land at a lake rather than fly past?'. These questions could be the subject of further empirical work. Tagging flamingos for example would provide information about their movements between lakes, remote sensing could be used to identify periods when flamingos were gathered in large groups, and the potential flamingo proxy investigated in the palaeolimnological research section could all help to identify changes in flamingo population distribution changes.

Even if all of this data could be collected there would still be questions that cannot be answered, particularly flamingo movements that are not driven by large changes in *Arthrospira*. Since flamingos interchange between lakes frequently there must be other drivers of flamingo movements. However, it is likely that more can be learned about the things that cannot be directly measured by using better empirical data in conjunction with the model.

The joint empirical and modelling approach is likely to be more effective when the empirical data required is more easily obtained. The joint approach has allowed for a deeper understanding of the soda lakes and the impact of these dynamic ecosystems on flamingo population than could have been found by an empirical or modelling approach alone, such as the realisation that changes in flamingo population need to be put in context with much longer term changes in climate to fully understand the significance of fluctuations in population in the last 100 years.

Appendix

Average sample depth (cm)	Organic %	Carbonate %	TOC/N
0.5	17.777	3.119	8.279
1.5	16.607	2.638	9.240
2.5	17.379	5.061	
3.5	17.063	3.642	9.954
		4.879	
5.5	17.288	2.474	
6.5	16.762	2.216	9.391
7.5	16.705	2.303	9.851
8.5	15.847	2.376	9.306
9.5	16.235	3.045	9.700
10.5	17.003	4.344	9.100
11.5	14.828	6.706	15.736
12.5	18.176	5.874	9.159
13.5	16.465	3.579	8.964
14.5	15.371	2.871	
15			8.773
15.5	15.478	3.561	
16.5	16.156	2.119	7.718
17.5	15.522	2.582	8.553
18.5	16.190	2.625	8.825
19.5	15.452	2.988	9.080
20.5	15.972	3.040	8.938
21.5	15.951	4.982	9.548
22.5	15.817	3.070	9.915
23.5	14.704	2.849	9.885
24.5	15.413	2.992	9.398
25.5	13.753	2.546	9.728
26.5	14.536	3.118	8.857
27.5	14.013	3.040	8.628
28.5	13.936	2.987	8.702
29.5	14.655	3.866	8.817
30.5	14.598	3.200	9.128
31.5	14.937	2.157	
32.5	14.739	3.374	9.108
33.5	13.111	2.977	9.113
34.5	14.682	3.376	8.906
35.5	13.890	4.165	9.030
36.5	13.314	3.479	9.030

	Average sample depth (cm)	Organic matter (%)	Carbonate (%)
37.5	13.956	3.899	9.472
38.5	13.838	3.399	9.331
39.5	13.252	3.715	9.358
40.5	12.763	3.824	9.215
41.5	13.483	3.473	9.310
42.5	11.698	3.158	9.605
43.5	12.045	2.823	9.733
44.5	11.995	3.060	9.729
45.5	12.722	2.841	9.374
46.5	13.876	3.225	9.805
47.5	13.845	3.528	9.546
48.5	13.088	3.221	10.143
49.5	13.252	3.678	8.704
50.5	15.035	3.692	8.356
51.5	15.715	3.425	8.484
52.5	15.460	4.044	8.423
53.5	15.153	3.471	8.250
54.5	16.585	5.954	9.358
55.5	15.048	3.525	8.052
56.5	15.212	4.088	7.899
57.5	14.973	5.324	9.259
58.5	14.407	4.137	8.394
59.5	13.076	4.721	7.864
60.5	13.339	3.493	8.814
61.5	13.673	3.988	9.357
62.5	12.689	4.600	8.692
63.5	11.876	4.627	7.860
64.5	11.804	4.850	10.114
65.5	13.586	3.511	8.967
66.5	13.045	3.037	8.718
67.5	11.897	3.263	8.150
68.5	12.571	4.565	7.818
69.5	12.993	3.098	8.530
70.5	12.831	3.182	9.030
71.5	13.889	4.891	9.197
72.5	11.802	3.734	8.587
73.5	11.242	3.486	9.360
74.5	11.555	3.447	8.954
75.5	11.655	4.311	8.369
76.5	13.127	3.711	9.420
77.5	12.999	2.915	9.073
78.5	13.370	3.140	9.826
79.5	14.445	3.274	9.467
80.5	13.706	3.605	10.088
81.5	12.672	3.255	9.572

Table 1: LOI and TOC/N data for the north basin of Lake Bogoria (core G1).

Average sample depth (cm)	Organic matter (%)	Carbonate (%)
---------------------------	--------------------	---------------

0.5	24.396	15.917
3.5	22.17	10.346
4.5	21.919	9.38
2.5	22.438	7.303
5.5	21.559	13.799
6.5	22.39	7.04
8.5	21.866	8.437
9.5	21.34	7.575
10.5	23.886	6.127
11.5	21.569	6.547
12.5	21.264	12.134
13.5	25.062	5.468
14.5	22.889	13.419
15.5	19.245	8.073
16.5	25.217	6.044
17.5	19.826	9.555
18.5	20.77	10.405
19.5	23.599	7.903
21.5	21.665	6.87
22.5	21.758	7.741
23.5	21.166	11.416
25.5	20.712	10.792
26.5	21.658	7.841
27.5	21.102	9.282
29.5	20.193	10.693
30.5	20.036	8.852
31.5	21.648	7.614
33.5	19.884	9.475
34.5	19.397	11.203
36.5	17.523	8.576
37.5	17.936	7.362
39.5	20.215	9.427
40.5	18.152	5.953
42.5	16.807	9.289
43.5	16.522	9.343
44.5	18.11	4.511
45.5	15.933	10.03
46.5	18.75	8.417
47.5	18.2	3.93
48.5	16.768	9.1
49.5	16.471	8.236
60.5	18.967	4.227
61.5	15.235	5.076
62.5	13.327	9.085
63.5	16.533	7.749
65.5	10.812	4.742
66.5	13.053	7.028
67.5	16.6	4.74
50.5	13.681	9.25
51.5	15.952	6.827

52.5	13.811	8.395
53.5	17.744	7.671
54.5	17.658	10.722
55.5	17.794	9.179
56.5	20.394	9.088
57.5	19.9	13.293
58.5	16.198	7.446
59.5	19.418	6.235
68.5	15.677	4.938

Table 2: LOI data for the south basin of Lake Bogoria (core SB1).

Sample mid-depth (cm)	Aphani-zophyll	Mxyoxanthophyll a	Myxoxanthophyll	Alloxanthin	Diatoxanthin	Zeaxanthin
0.5	546.86	76.86	102.62	160.51	0	1067.71
1.5	503.45	104.89	151.55	86.98	0	900.37
2.5	358.41	38.66	45.19	48.46	0	600.25
3.5	135.26	23.26	56.23	0	0	269.32
5.5	358.33	82.98	129.92	0	0	590
6.5	214.85	49.61	69.57	0	0	363.08
7.5	344.42	50.29	122.98	0	0	619.32
8.5	346.81	100.2	158	0	0	571.18
9.5	261.09	47.66	109.51	0	0	405.73
10.5	957.37	237.61	372.69	0	0	1404.31
11.5	636.89	102.61	184.43	0	0	1248.16
12.5	429.67	123.85	200.37	0	0	739.76
13.5	212.11	41.04	65.92	0	51.75	355.17
14.5	154.01	36.83	41.75	0	12.72	229.8
15.5	108.45	18.17	32.17	0	23.94	220.12
17.5	219.46	39.69	67.48	0	29.19	385.81
19.5	319.68	65.31	100.03	0	41.95	493.54
21.5	209.84	38.81	65.91	0	23.28	313.88
23.5	161.53	30.41	52.86	0	19.82	270.87
25.5	207.62	33.43	59.37	0	24.41	402.06
27.5	559.64	127.69	190.53	0	0	854.95
28.5	232.22	54.17	61.38	0	0	349.88
30.5	306.04	45.33	66.4	0	0	589.22
32.5	163.72	22.63	42.57	0	15.54	314.27
35.5	189.64	42.87	50.12	0	0	346.29
37.5	96.7	16.15	21.82	0	0	231.69
39.5	329.64	45.88	61.19	0	0	711.74
41.5	50.93	0	13.86	0	0	101.36
43.5	251.21	44.81	68.13	0	0	473.57
45.5	122.01	16.79	26.39	0	0	245.68
47.5	229.6	0	0	0	0	1233.07
49.5	206.96	45.37	89.92	0	0	299.87
51.5	678.73	108.66	152	59.05	0	1199.12
53.5	803.24	231.49	269.13	167.18	122.88	1169.55
55.5	269.99	55.89	79.91	45.01	0	394.82
57.5	531.16	166.56	269.74	0	240.57	857.43
59.5	302.87	59.7	96.08	38.11	120.05	428.76

61.5	209.1	38.95	67.72	28.37	99.05	292.04
63.5	391.06	87.37	121.25	44.94	234.84	527.36
65.5	240.32	65.97	73.71	36.28	222.34	314.37
67.5	304.22	70.58	53.22	101.72	522.85	549.16
69.5	333.93	0	0	303.9	1283.49	901.36
71.5	75.95	0	0	148.78	855.25	231.99
73.5	43.75	0	0	43.75	243.51	67.11
75.5	71.71	0	0	74.47	397.87	240.29
77.5	144.97	32.31	0	119.57	637.25	499.5
79.5	463.17	0	0	359.64	150.34	1166.66

Table 3: Lake Bogoria pigment data (part 1) for the north basin (core G1). Pigment abundances are measured in $nmol\ g^{-1}OM$.

Sample mid depth (cm)	Cantha-xanthin	Chl b	Echinen-one	Chl a	Chl a'	Pheo-phytin b	Pheo-phytin a	β -carotene
0.5	27.39	0	0	345.48	70.58	0	52.93	196.02
1.5	61.97	0	37.5	86.35	22.04	0	43.19	53.55
2.5	79.96	0	41.02	68.81	18.08	0	31.83	35.23
3.5	43.73	0	22.25	34.44	9.65	12.9	25.34	36.52
5.5	49.28	0	31.41	110.61	30.78	0	27.08	114.28
6.5	53.34	0	0	118.57	24.53	18.37	21.59	33.1
7.5	50.03	0	24.54	118.01	36.06	0	42.58	86.47
8.5	25.83	0	0	118.27	36.3	19.83	17.21	51.83
9.5	11.41	0	0	72.71	29.11	13.46	11.04	46.03
10.5	0	0	0	192.1	79.43	20.93	12.9	164
11.5	0	0	0	154.71	124.39	53.92	18.12	100.63
12.5	0	0	0	169.59	125.65	42.26	18.19	87.51
13.5	0	0	0	63.79	64.53	0	0	24.74
14.5	0	0	0	63.19	36.93	14.22	0	12.93
15.5	0	0	0	40.08	32.18	15.09	0	14.63
17.5	0	0	0	30.51	30.77	15.58	0	33.15
19.5	0	0	0	54.55	43.05	21.18	0	32.07
21.5	0	0	0	40.77	32.59	15.03	0	19.25
23.5	0	0	0	29.24	23.52	10.79	0	32.81
25.5	0	0	0	34.23	29.97	14.41	0	34.73
27.5	0	0	0	118.04	58.71	0	9.34	137.23
28.5	0	0	0	36.44	22.73	11.21	0	39.82
30.5	0	0	0	30.85	22.54	11.1	0	35.95
32.5	0	0	0	20.27	21.2	10.96	0	21.19
35.5	0	0	0	24.24	21.34	0	0	29.76
37.5	0	0	0	11.76	6	0	0	20.44
39.5	0	0	0	106.56	34.16	0	0	201.25
41.5	0	0	0	5	4	0	0	13.89
43.5	0	0	0	45.6	21.8	0	0	49.88
45.5	0	0	0	23.84	11.2	0	0	21.16
47.5	242.42	0	198.09	41.74	65.57	71.99	54.04	197.5
49.5	0	0	0	16.42	11.13	0	9.8	35.87
51.5	0	0	0	70.55	32.82	0	17.66	86.84
53.5	42.86	0	25.51	102.18	60.6	33.19	30.2	115.78
55.5	39.35	0	23.03	32.81	35.34	24.45	16.62	53.86

57.5	56.67	0	22.13	67.84	229.65	143.07	45.35	90.38
59.5	0	16.45	0	39.54	240.88	158.14	34.84	43.87
61.5	0	12.09	0	28.17	177.33	110.03	21.81	34.9
63.5	0	21.25	0	55.79	294.02	186.16	18.06	58.93
65.5	0	28.35	0	36.77	333.07	114.08	14.45	15.47
67.5	0	67.8	0	84.39	723.18	616.69	96.83	84.72
69.5	9.62	138.26	0	205.11	1506.51	1169.32	214.22	140.57
71.5	0	132.42	0	69.39	1268.03	892.71	137.05	78.41
73.5	0	35.27	0	25.97	352.69	251.4	44.42	21.35
75.5	0	62.66	0	43.27	659.19	461	88.02	28.53
77.5	0	0	0	80.49	1086.5	623.62	105.13	92.55
79.5	84.2	36.73	50.43	130.51	427.24	299.07	128.75	95.28

Table 4: Lake Bogoria pigment data (part 2) for the north basin (core G1). Pigment abundances are measured in $nmol\ g^{-1}OM$.

Sample mid-depth (cm)	Oscilla-xanthin	Myxo-xanthin	Allox-anthin	Diatox-anthin	Diatox-anthin b	Lutein	Zeax-anthin
0.50	23.55	276.05	664.62	59.28	20.78	n/d	998.18
1.25	0.00	302.94	132.95	78.51	38.81	n/d	1010.14
1.75	32.54	396.99	244.13	111.33	46.09	n/d	987.76
2.25	73.10	939.45	1469.54	590.17	253.12	n/d	3075.58
2.75	46.92	450.92	819.00	1318.56	571.04	434.44	1232.43
3.25	26.17	174.80	594.16	2031.51	919.84	817.74	809.69
3.75	0.00	266.57	776.01	2347.32	1080.06	997.01	1049.65
4.50	0.00	455.49	319.19	848.69	375.12	407.11	1094.39
5.25	20.15	125.53	73.51	206.04	92.56	n/d	500.96
5.75	81.53	1171.14	333.48	322.13	182.54	n/d	2278.80
6.25	94.02	1106.41	581.65	155.86	87.22	n/d	2243.47
6.75	43.40	637.47	523.71	102.18	44.25	n/d	1456.66
7.25	0.00	0.00	0.00	0.00	0.00	n/d	0.00
7.75	0.00	0.00	0.00	0.00	0.00	n/d	0.00
8.25	56.20	776.03	534.50	1717.90	819.10	598.40	1343.26
8.75	0.00	323.53	329.84	1085.74	476.50	429.75	812.23
9.25	145.65	935.45	1065.23	3501.04	1757.70	1287.77	2365.10
9.75	132.18	1410.02	283.25	609.73	273.66	n/d	2255.08
10.25	0.00	241.30	248.28	845.22	388.17	341.70	851.59
10.75	99.92	1586.00	655.83	425.24	252.27	n/d	3361.67
11.25	51.84	632.43	810.81	186.80	81.07	n/d	1731.87
11.75	39.13	541.55	463.14	280.88	129.16	n/d	1339.77
12.25	44.44	668.40	609.59	1095.26	563.18	464.69	1389.29
12.75	25.83	147.18	565.24	1917.77	860.26	738.82	610.99
13.25	0.00	109.47	313.67	1131.01	562.65	566.12	510.55
13.75	21.84	286.82	377.65	1360.94	584.21	562.39	637.38
14.25	38.63	250.94	509.46	1736.24	814.35	683.77	674.39
14.75	34.10	402.51	298.98	1055.08	442.26	311.19	998.23
15.25	36.70	253.14	185.29	550.67	238.38	268.03	659.66
15.75	49.21	1689.85	666.39	773.20	410.54	n/d	6703.06
16.25	0.00	2563.62	607.23	462.34	250.80	n/d	5207.00
16.75	0.00	2237.96	1731.34	883.93	409.80	n/d	4184.49
17.25	0.00	124.06	190.17	180.79	79.47	85.38	430.40

17.75	0.00	309.62	328.72	802.89	376.29	344.40	764.61
18.25	0.00	0.00	0.00	0.00	0.00	0.00	0.00
18.75	0.00	80.12	924.86	3046.82	1732.01	1776.16	862.56
19.25	0.00	11.00	205.11	749.62	328.43	303.18	213.04
19.50	0.00	338.70	1044.32	3022.48	1180.03	1212.39	596.66
20.25	0.00	558.24	3251.40	10557.20	4728.41	4570.51	2803.81
20.75	0.00	362.46	52.10	225.34	113.85	118.54	468.96
21.25	0.00	1002.97	430.65	1019.27	493.63	405.41	1863.90
21.75	0.00	79.63	1.00	27.13	14.21	13.52	119.42
22.25	0.00	1504.00	429.49	340.01	163.32	n/d	2620.30
22.75	0.00	1843.42	467.18	246.73	0.00	n/d	3067.64
23.25	0.00	2234.34	900.35	440.27	191.22	n/d	3880.50
23.75	0.00	1647.83	1221.67	364.80	155.75	n/d	3491.32
24.25	0.00	1150.53	1804.61	524.43	236.42	n/d	3123.00
24.75	0.00	40.00	41.16	16.30	10.86	n/d	81.32
25.25	0.00	443.61	1283.37	2386.49	1356.68	1358.86	1389.24
25.75	0.00	630.34	1467.88	4294.55	1898.92	2196.38	1803.63
26.25	0.00	403.89	365.76	1029.49	425.54	489.94	892.57
26.75	0.00	2744.64	3971.76	9562.03	4668.10	6481.35	4011.95
27.25	0.00	2337.79	9212.94	27237.40	10594.70	15827.40	4923.42
27.75	0.00	197.03	2055.79	8136.69	3908.50	5416.11	2871.46
28.25	0.00	478.39	1804.39	6941.68	3130.10	5916.28	2436.30
28.75	0.00	412.15	736.69	2565.89	1209.85	1470.02	1539.69
29.25	0.00	1361.98	727.17	1493.00	806.96	932.03	2162.78
29.75	0.00	1781.38	656.44	653.44	382.51	n/d	2973.70
30.25	0.00	0.00	0.00	0.00	0.00	0.00	0.00
30.75	0.00	516.60	311.14	338.99	142.99	n/d	1285.43
31.25	0.00	1968.89	1951.50	3966.71	1686.05	1597.99	3990.14
31.75	0.00	1615.13	868.50	1690.73	788.69	783.61	2483.81
32.25	0.00	237.23	303.76	663.13	326.12	297.02	767.83
32.75	0.00	337.23	480.35	1150.98	660.35	522.98	1234.35
33.25	0.00	51.39	71.57	296.60	145.01	134.86	222.11
33.75	0.00	1199.38	1211.07	3859.14	1944.52	3136.27	2673.99
34.25	0.00	155.52	265.11	834.59	394.34	366.76	716.71
34.75	0.00	77.88	166.78	388.52	212.65	209.08	419.27
35.25	0.00	852.04	573.51	223.51	131.91	n/d	2054.80
35.75	0.00	255.40	362.60	68.65	52.89	n/d	1096.25
36.25	0.00	0.00	0.00	0.00	0.00	0.00	0.00
36.75	0.00	157.91	391.59	70.92	32.69	n/d	684.30
37.25	0.00	592.63	678.80	244.08	0.00	366.66	1402.59
37.75	0.00	0.00	0.00	0.00	0.00	0.00	0.00
38.25	0.00	2418.00	2951.05	933.97	0.00	1279.19	4037.04
38.75	0.00	1768.25	3162.19	308.38	207.36	n/d	4014.00
39.25	0.00	0.00	0.00	0.00	0.00	0.00	0.00
39.75	0.00	0.00	0.00	0.00	0.00	0.00	0.00
40.25	0.00	581.83	1094.43	159.74	n/d	n/d	1934.75
40.75	0.00	104.40	158.58	12.00	4.00	n/d	481.59
41.25	0.00	795.22	820.15	218.93	0.00	n/d	2774.40
41.75	0.00	158.02	395.31	26.18	6.54	n/d	983.02
42.25	0.00	38.82	100.46	12.00	4.00	n/d	296.40
42.75	0.00	216.09	500.28	25.24	13.92	n/d	1269.59

67.25	0.00	320.36	765.19	1626.08	2483.92	2676.24	627.86
67.75	0.00	0.00	0.00	0.00	0.00	0.00	0.00
68.50	0.00	515.90	737.15	1265.32	1923.71	2431.63	1686.69
68.25	0.00	0.00	0.00	0.00	0.00	0.00	0.00
68.75	0.00	36.86	13.06	52.90	84.76	155.52	169.22
69.25	0.00	0.00	0.00	0.00	0.00	0.00	0.00
69.75	0.00	0.00	0.00	0.00	0.00	0.00	0.00
70.25	0.00	0.00	0.00	0.00	0.00	0.00	0.00
70.75	0.00	0.00	0.00	0.00	0.00	0.00	0.00
70.50	0.00	0.00	0.00	0.00	0.00	0.00	0.00
71.25	0.00	0.00	0.00	0.00	0.00	0.00	0.00
71.75	0.00	0.00	0.00	0.00	0.00	0.00	0.00
71.50	0.00	0.00	0.00	0.00	0.00	0.00	0.00
72.25	0.00	0.00	0.00	0.00	0.00	0.00	0.00
72.75	0.00	308.72	445.77	837.85	1186.32	1388.01	1271.22
73.25	0.00	423.87	1322.22	3424.29	4906.89	6183.77	2713.18
73.75	0.00	0.00	0.00	0.00	0.00	0.00	0.00
74.25	0.00	570.51	1875.96	4798.37	5276.96	6061.81	2937.86
75.00	0.00	0.00	0.00	0.00	0.00	0.00	0.00
75.25	0.00	0.00	0.00	0.00	0.00	0.00	0.00

Table 5: Lake Bogoria pigment data (part 1) for the south basin (core SB2). Pigment abundances are measured in $nmol\ g^{-1}OM$.

Sample mid-depth (cm)	Canthax-thin	Chl b	Echin-enone	Chl a	Pheophytin b	β - carotene	Pheophytin a
0.50	126.17	0.00	0.00	115.73	70.20	253.98	113.56
1.25	41.25	0.00	0.00	202.96	129.02	363.99	76.51
1.75	42.42	22.35	0.00	268.73	174.21	251.78	87.80
2.25	181.17	145.54	0.00	1159.66	654.50	662.53	307.92
2.75	303.39	290.25	392.54	2982.42	1575.51	312.97	409.97
3.25	13.44	349.13	0.00	2767.68	1660.91	237.34	305.06
3.75	0.00	446.77	0.00	3752.41	1808.26	332.67	352.47
4.50	0.00	204.66	0.00	2084.01	1341.96	243.00	244.62
5.25	0.00	61.28	0.00	660.78	445.70	32.60	87.29
5.75	51.92	60.86	0.00	807.15	470.51	540.33	181.21
6.25	92.88	17.12	0.00	246.63	129.56	954.09	281.27
6.75	85.09	0.00	132.17	140.23	69.93	434.02	102.20
7.25	0.00	0.00	0.00	0.00	0.00	0.00	0.00
7.75	0.00	0.00	0.00	0.00	0.00	0.00	0.00
8.25	19.75	192.09	0.00	2273.53	1829.62	291.46	346.76
8.75	0.00	229.79	0.00	2025.67	1404.09	143.75	279.74
9.25	24.03	510.29	0.00	5204.57	3632.22	22.69	50.69
9.75	0.00	87.44	159.84	999.61	662.38	822.06	248.07
10.25	0.00	240.02	0.00		2106.56	1194.07	231.31
10.75	73.59	85.85	148.23	1125.79	703.53	322.23	218.16
11.25	49.79	21.40	93.13	376.78	239.13	214.72	97.54
11.75	85.82	30.30	113.84	468.63	276.77	131.12	101.26
12.25	307.14	131.04	364.34	1275.82	860.72	286.20	313.97
12.75	19.33	161.90	0.00	1848.24	1241.06	210.91	269.56
13.25	0.00	148.87	0.00	1356.45	1022.89	142.38	190.70

13.75	0.00	143.25	0.00	1525.63	1111.83	205.94	241.51
14.25	0.00	187.19	0.00	1999.22	1141.26	190.01	250.96
14.75	24.83	127.07	87.72	1490.44	995.11	213.42	235.75
15.25	19.52	99.81	0.00	1033.10	324.48	83.43	85.33
15.75	150.94	135.29	213.11	1785.11	922.13	674.75	336.33
16.25	241.81	62.63	26.95	702.84	433.69	549.47	159.11
16.75	543.99	84.11	384.79	595.89	202.59	174.93	82.43
17.25	121.46	28.01	135.08	313.79	216.37	100.71	80.97
17.75	102.24	66.13	128.22	759.79	466.69	396.65	110.32
18.25	0.00	0.00	0.00	0.00	0.00	0.00	0.00
18.75	0.00	490.62	0.00	4080.70	1603.92	304.70	339.62
19.25	8.00	124.14	11.77	1222.69	942.37	106.06	172.73
19.50	15.92	53.10	10.00	213.34	77.61	8.00	10.00
20.25	38.75	489.31	0.00	2321.31	771.45	179.08	122.42
20.75	1.00	24.87	4.00	295.89	191.90	35.84	39.32
21.25	31.99	140.86	0.00	1503.28	850.42	442.05	179.50
21.75	1.00	3.00	1.00	31.77	23.55	5.00	3.00
22.25	40.15	43.80	50.53	468.72	279.03	279.44	60.85
22.75	0.00	13.91	50.73	153.48	89.86	428.95	30.61
23.25	134.62	29.91	145.86	459.58	232.68	426.23	71.50
23.75	0.00	19.53	99.56	301.51	136.25	390.80	48.99
24.25	198.49	36.68	211.63	535.17	241.84	370.55	84.19
24.75	10.00	5.00	12.00	37.33	18.46	10.00	12.00
25.25	267.08	355.58	543.38	3575.14	1810.16	528.39	408.26
25.75	46.64	459.27	39.70	3482.71	1451.12	360.58	251.87
26.25	0.00	196.13	0.00	2025.46	1064.50	212.16	226.12
26.75	634.54	159.70	179.26	982.08	383.66	78.68	44.26
27.25	517.63	1034.69	322.31	2588.88	652.07	177.46	82.43
27.75	26.24	461.41	0.00	1723.82	727.30	154.92	41.75
28.25	0.00	235.86	0.00	863.37	435.69	96.78	42.46
28.75	24.90	267.69	28.00	2228.75	981.03	171.03	174.62
29.25	79.26	174.89	21.00	1599.98	631.32	116.98	106.37
29.75	113.35	65.69	54.43	531.11	213.64	70.84	40.51
30.25	0.00	0.00	0.00	0.00	0.00	0.00	0.00
30.75	240.74	0.00	156.34	321.47	240.73	612.79	92.18
31.25	329.53	409.77	319.87	4412.72	3021.12	1636.32	679.18
31.75	54.94	139.76	161.84	1437.80	887.29	1225.55	120.68
32.25	0.00	72.74	47.17	934.45	650.59	268.47	151.42
32.75	102.39	129.27	36.75	1579.15	1090.18	486.93	237.68
33.25	2.00	25.30	10.00	386.88	303.33	55.74	63.11
33.75	231.69	234.26	102.35	1023.48	325.36	33.87	43.67
34.25	17.41	165.12	0.00	1750.68	1250.62	248.47	272.36
34.75	13.77	59.16	10.00	823.26	568.85	165.27	127.77
35.25	115.97	24.35	98.74	303.23	243.38	360.69	95.28
35.75	97.85	0.00	77.27	119.03	61.28	216.92	68.80
36.25	0.00	0.00	0.00	0.00	0.00	0.00	0.00
36.75	35.31	10.00	54.90	114.93	79.07	371.40	103.59
37.25	88.13	11.87	90.13	96.15	76.56	332.02	57.97
37.75	0.00	0.00	0.00	0.00	0.00	0.00	0.00
38.25	102.20	22.04	308.46	124.10	82.37	253.84	21.66
38.75	230.12	41.68	245.69	292.16	220.20	761.80	425.38

39.25	0.00	0.00	0.00	0.00	0.00	0.00	0.00
39.75	0.00	0.00	0.00	0.00	0.00	0.00	0.00
40.25	259.54	143.97	0.00	33.45	37.83	166.76	124.40
40.75	72.86	1.00	49.33	15.30	19.55	66.97	60.97
41.25	221.13	0.00	134.15	13.27	60.47	144.83	83.57
41.75	118.37	2.00	102.62	44.77	81.55	192.79	172.30
42.25	50.12	2.00	15.00	27.26	29.94	61.97	74.84
42.75	178.63	10.00	150.00	44.68	24.20	346.58	144.19
43.25	1298.06	120.43	1203.82	339.43	258.48	1428.82	823.25
43.75	330.45	20.76	254.20	119.04	121.66	380.66	276.93
44.25	0.00	0.00	0.00	0.00	0.00	0.00	0.00
44.50	5431.56	213.61	2077.43	423.02	187.96	677.86	222.36
45.50	13299.40	366.36	3720.37	571.62	86.78	492.80	51.57
44.75	0.00	0.00	0.00	0.00	0.00	0.00	0.00
45.25	0.00	0.00	0.00	0.00	0.00	0.00	0.00
45.75	2241.96	10.00	419.79	41.90	10.00	254.71	26.34
46.25	448.22	5.00	422.57	35.93	47.52	756.85	133.17
46.75	867.12	35.08	813.33	131.23	123.99	1595.86	569.06
47.25	880.79	10.52	247.79	31.57	10.00	184.92	58.42
47.75	694.03	20.02	699.14	115.47	107.30	1444.19	372.39
48.25	743.81	5.00	795.09	114.76	56.83	1997.50	91.09
48.75	3499.72	44.20	1234.09	77.39	8.84	354.96	14.72
49.25	0.00	0.00	0.00	0.00	0.00	0.00	0.00
49.75	694.86	13.51	632.88	67.82	50.39	826.56	168.21
50.25	0.00	0.00	0.00	0.00	0.00	0.00	0.00
50.75	0.00	0.00	0.00	0.00	0.00	0.00	0.00
51.25	223.38	3.00	249.98	54.53	34.62	578.83	59.67
51.75	0.00	0.00	0.00	0.00	0.00	0.00	0.00
52.25	800.95	40.08	693.48	140.56	52.30	744.97	89.38
52.75	1493.10	0.00	306.72	71.25	15.32	119.41	7.66
53.25	0.00	0.00	0.00	0.00	0.00	0.00	0.00
53.75	0.00	0.00	0.00	0.00	0.00	0.00	0.00
54.25	0.00	0.00	0.00	0.00	0.00	0.00	0.00
54.75	556.88	174.37	836.46	1391.54	494.39	1641.19	104.50
55.25	0.00	0.00	0.00	0.00	0.00	0.00	0.00
55.75	152.90	27.18	501.01	895.34	469.11	1911.07	182.69
56.25	0.00	0.00	0.00	0.00	0.00	0.00	0.00
56.75	183.30	75.71	585.81	752.39	401.42	1334.34	114.36
57.25	66.62	57.36	180.35	712.78	323.33	344.04	69.62
57.75	271.08	214.79	676.85	1956.22	884.01	2438.98	215.56
58.25	52.77	25.90	186.17	328.43	147.88	827.21	51.49
58.75	0.00	0.00	0.00	0.00	0.00	0.00	0.00
59.25	132.83	86.46	476.01	764.90	419.82	1954.67	135.99
59.75	133.78	89.17	470.93	893.48	486.33	2299.44	133.61
60.25	202.95	273.67	785.20	1678.76	568.88	1812.03	131.28
60.75	1118.22	1324.60	3798.50	6419.90	2503.94	10911.60	818.27
61.25	0.00	0.00	0.00	0.00	0.00	0.00	0.00
61.00	0.00	0.00	0.00	0.00	0.00	0.00	0.00
61.75	0.00	0.00	0.00	0.00	0.00	0.00	0.00
62.25	0.00	0.00	0.00	0.00	0.00	0.00	0.00
62.75	256.81	259.19	858.76	1520.96	726.72	3109.07	162.61

63.25	0.00	0.00	0.00	0.00	0.00	0.00	0.00
63.75	2146.69	1074.98	5024.23	4630.16	1905.96	6758.66	535.97
64.25	0.00	0.00	0.00	0.00	0.00	0.00	0.00
64.75	0.00	0.00	0.00	0.00	0.00	0.00	0.00
65.25	144.48	85.47	361.32	500.97	164.40	437.56	19.27
65.75	927.76	568.03	882.17	4447.40	1995.16	823.90	502.95
66.25	3.00	0.00	0.00	4.00	3.00	3.00	1.00
66.75	0.00	0.00	0.00	0.00	0.00	0.00	0.00
67.25	458.77	1258.29	2444.16	903.15	1717.55	1717.55	211.94
67.75	0.00	0.00	0.00	0.00	0.00	0.00	0.00
68.50	749.74	233.96	741.20	613.66	141.10	350.30	24.88
68.25	0.00	0.00	0.00	0.00	0.00	0.00	0.00
68.75	62.95	34.27	209.48	335.78	211.02	1079.46	41.24
69.25	0.00	0.00	0.00	0.00	0.00	0.00	0.00
69.75	0.00	0.00	0.00	0.00	0.00	0.00	0.00
70.25	0.00	0.00	0.00	0.00	0.00	0.00	0.00
70.75	0.00	0.00	0.00	0.00	0.00	0.00	0.00
70.50	0.00	0.00	0.00	0.00	0.00	0.00	0.00
71.25	0.00	0.00	0.00	0.00	0.00	0.00	0.00
71.75	0.00	0.00	0.00	0.00	0.00	0.00	0.00
71.50	0.00	0.00	0.00	0.00	0.00	0.00	0.00
72.25	0.00	0.00	0.00	0.00	0.00	0.00	0.00
72.75	671.11	372.94	1908.09	1756.07	982.02	6114.77	260.95
73.25	606.00	393.34	1416.77	1147.96	362.83	1468.86	67.23
73.75	0.00	0.00	0.00	0.00	0.00	0.00	0.00
74.25	803.89	355.89	1421.81	1043.25	269.01	1103.48	61.30
75.00	0.00	0.00	0.00	0.00	0.00	0.00	0.00
75.25	0.00	0.00	0.00	0.00	0.00	0.00	0.00

Table 6: Lake Bogoria pigment data (part 2) for the south basin (core SB2). Pigment abundances are measured in $nmol\ g^{-1}OM$.

Mid depth	d13C	%C	%N	C/N	%N	d15N(‰)
2.5	-19.2	1.35	0.10	13.3	0.09	8.62
6.5	-19.4	1.49	0.12	12.5	0.11	8.89
7.5	-19.3	1.44	0.11	13.6	0.12	8.67
8.5	-19.1	1.32	0.08	17.3	0.10	8.97
9.5	-18.9	1.29	0.11	12.2	0.09	8.62
10.5	-18.7	1.41	0.13	11.3	0.11	8.88
11.5	-18.4	1.44	0.12	12.5	0.11	9.13
14.5	-18.1	1.23	0.07	17.5	0.10	7.93
19.5	-17.9	1.51	0.10	14.7	0.12	7.79
24.5	-17.7	1.46	0.10	15.1	0.11	7.45
29.5	-17.3	1.37	0.09	15.6	0.09	7.61
33.5	-17.8	1.46	0.10	14.9	0.10	8.25
37.5	-17.8	1.48	0.10	15.4	0.10	7.80
43.5	-18.0	1.33	0.08	17.1	0.10	7.02
59.5	-18.4	1.04	0.06	18.2	0.07	9.12
64.5	-17.5	0.72	0.06	11.5	0.06	8.46
69.5	-18.1	0.77	0.07	11.0	0.06	8.41
75.5	-18.0	0.79	0.07	11.4	0.07	8.05

79.5	-19.1	0.93	0.08	12.3	0.08	8.09
------	-------	------	------	------	------	------

Table 7: Lake Bogoria north basin isotope data.

Mid depth (cm)	SiO ₂ (%)	TiO ₂ (%)	Al ₂ O ₃ (%)	Fe ₂ O ₃ (%)	MnO (%)	MgO (%)	CaO (%)	K ₂ O (%)	Na ₂ O (%)	P ₂ O ₅ (ppm)	Co (ppm)	Cr (ppm)	V (ppm)	Ni (ppm)	Sc (ppm)	Cu (ppm)	Zn (ppm)
7.5	50.33	1.026	16.604	11.299	0.4242	-0.015	2.218	3.593	3.311	0.069	62.4	10.4	34.8	20.4	3.1	20.7	178.6
10.5	51.51	1.051	17.248	12.093	0.4044	-0.178	1.22	3.496	3.248	0.092	63.6	12.3	45.5	17.9	8.6	22.2	184.2
13.5	51.48	1.035	17.266	11.832	0.3668	-0.015	1.202	3.399	3.359	0.077	61	15.9	36.8	17.3	5.3	16.4	188.3
16.5	49.67	1.002	16.425	11.243	0.415	-0.123	2.701	3.419	3.508	0.071	58.2	8.1	32.2	17.4	2.5	21.7	171.4
20.5	51.63	1.022	17.412	12.118	0.2853	-0.462	0.925	3.493	3.792	0.056	61	12.1	41.4	16.3	8	10.2	198.5
24.5	51.49	1.018	17.063	11.855	0.4232	-0.325	1.9	3.544	3.651	0.051	64	14	43.8	20.1	9.1	19.9	196.6
28.5	51.59	1.008	16.862	11.578	0.3585	0.069	1.22	3.482	3.712	0.078	62.2	11.7	41.2	21	15.5	22.5	196.7
32.5	51.10	1.001	16.856	11.38	0.3197	-0.377	1.666	3.515	3.726	0.07	58.9	7.4	36.8	14.7	9.5	17.3	186.8
35.5	52.08	0.996	16.962	11.458	0.3637	-0.265	1.925	3.659	3.778	0.049	60.2	5.3	34.4	17.7	4.7	16.1	191.2
38.5	51.67	1.016	16.656	11.293	0.3796	-0.054	1.994	3.535	3.612	0.069	61.1	11.5	51	20.2	8.4	25.3	203.8
41.5	52.22	0.992	16.445	10.697	0.387	0.007	2.006	3.779	3.777	0.059	54.5	10.8	32.8	17	2.3	17.7	186.2
44.5	53.38	0.99	16.81	10.747	0.3388	-0.258	1.386	3.918	3.982	0.052	54.7	5.5	28.3	16.7	5.3	20.3	199.5
47.5	53.82	0.977	17.005	10.644	0.3214	-0.429	1.391	3.999	3.912	0.046	53.4	6	28.4	13.3	2.9	9.6	192.6
51.5	54.78	0.961	16.793	10.184	0.3019	-0.384	1.042	4.14	3.808	0.048	52	3.5	24.7	11.8	3.7	8.9	192.2
53.5	53.67	0.954	15.919	9.639	0.3394	0.215	1.803	4.087	3.749	0.089	50.1	6.7	29.3	16.3	8.9	16.3	186.3
56.5	52.62	0.912	14.921	8.777	0.3494	0.866	2.814	4.058	3.781	0.141	45.5	4.4	33.2	18.2	8.3	33.5	174.3
59.5	55.07	0.891	14.524	8.862	0.3157	0.872	2.084	3.937	3.998	0.114	46.3	8.1	20.8	18.6	2.2	14.5	178
61.5	54.78	0.873	13.577	8.048	0.2926	0.086	3.186	4.102	4.168	0.127	40.2	2.6	22.4	17	9.5	14	159.8
64.5	54.90	0.873	13.673	7.982	0.2784	-0.173	2.88	4.191	4.352	0.135	40.4	5.4	21.3	18.1	4.9	15.7	160.4
67.5	55.76	0.827	12.893	7.557	0.3069	0.055	3.153	4.132	4.334	0.13	35.8	4.6	17	16.6	7.4	12.6	142.8

TABLE 8: Lake Bogoria bulk XRF data (part 1), for the south basin (core SB1).

Mid depth (cm)	Pb (ppm)	Ba (ppm)	Rb (ppm)	Sr (ppm)	Y (ppm)	Zr (ppm)	Nb (ppm)	Hf (ppm)	La (ppm)	Ce (ppm)	Ga (ppm)	As (ppm)	Br (ppm)	I (ppm)	S (ppm)	Cl (%)
7.5	39.2	281.4	141.6	176.8	53.2	715.4	181	12	218.3	541.6	30.3	4.6	1.2	9.598	0.051	0.053
10.5	40	302.5	143.3	170.7	44.8	783.1	194.7	12.8	230.2	611.5	33.9	4.7	1.7	10.745	0.048	0.076
13.5	29.7	300.3	147.1	209.5	42.2	799.9	204	12.8	236	669.7	33.7	4.6	6	10.449	0.038	0.118
16.5	36.9	292.3	136.5	187.2	56.7	741	180	11.3	217.8	612.7	31.4	4.8	0.6	9.642	0.06	0.096
20.5	29.8	256.5	156.9	108.3	33.8	869	216.8	12.4	145.7	538.4	37.3	6.1	0.9	7.437	0.049	0.12
24.5	42	300.2	156	183.3	49.7	871.8	215.5	12.4	206.4	564.8	36.5	5.4	1.1	10.512	0.035	0.028
28.5	29.1	308.4	154.2	292.7	43.5	805.4	199.2	12.5	336.2	810.8	34.5	5.1	13.2	8.476	0.059	0.058
32.5	30.8	276.7	154.1	151.2	42.2	853.7	208.6	13	165.2	571.3	36.1	6.2	0.5	9.347	0.076	0.12
35.5	36.5	271.5	159.9	127.5	41.5	840.9	207.7	11.6	159.8	492.2	35.2	4.3	1.3	8.222	0.034	0.115
38.5	36.5	264.1	172.1	130.8	49.1	892.8	232.9	11.8	166.9	548.7	38.7	5.2	1.8	11.084	0.049	0.101
41.5	36.1	281.1	162.8	142.5	44	757.7	187.6	10.9	160.7	455.2	36.1	3.9	1.4	8.503	0.05	0.09
44.5	31.3	287.8	178.3	111.7	33.8	809.1	210.7	10.6	134	414.2	37.7	4.4	2	4.926	0.055	0.045
47.5	30.8	265.5	175.8	109.8	30.6	796.9	207.1	10.9	132.3	428.2	36.7	4.2	0.4	11.143	0.037	0.044
51.5	25.8	271	172.7	86.5	27.6	720.6	188.4	10.5	102.4	385.7	34.8	4.2	1	6.867	0.053	0.042
53.5	25.5	294.2	175.2	184	48.9	653.6	171.3	9.6	162.8	416.2	30.5	5.1	2.3	8.642	0.069	0.087
56.5	28.1	305.5	171.9	269.3	70.8	615.7	148	9	180.4	468.1	28.9	6	4.9	11.324	0.068	0.109
59.5	22.9	309.2	188.4	215.2	49.8	588.5	157.7	9.3	179.5	391.6	28.3	7	2.8	6.667	0.077	0.083
61.5	21	367.9	189.1	421.7	91.2	538.4	143.5	7.5	208.1	415	35.2	6.1	1.6	6.817	0.076	0.028
64.5	22.2	363.1	178.2	352.4	86.9	516.7	141.2	7.9	182.6	396.9	35.2	6.3	0.4	7.231	0.09	0.047
67.5	19	363.7	180.2	390.1	91.3	482	130	7.3	163.5	371.1	37.1	6.1	1.3	8.149	0.092	0.07

TABLE 9: Lake Bogoria bulk XRF data (part 2), for the south basin (core SB1).

Average sample depth (cm)	Organic (%)	Carbonate (%)	TOC/N
0.5	31.752	3.037	7.641
1.5	26.759	6.431	6.329
2.5	30.909	4.721	5.656
3.5	36.652	4.219	5.167
4.5	39.448	4.024	7.168
5.5	35.176	4.385	6.519
6.5	30.42	5.943	7.154
7.5	31.152	5.82	5.039
8.5	30.917	6.652	5.343
9.5	31.414	5.459	7.026
10.5	27.572	6.995	7.332
11.5	27.096	7.627	7.48
12.5	26.471	8.125	7.507
13.5	27.028	7.966	7.521
14.5	24.923	7.995	5.813
15.5	24.553	9.509	6.566
16.5	25.465	10.037	6.066
17.5	27.719	9.298	7.9
18.5	26.896	10.907	6.555
19.5	27.356	12.523	8.165
20.5	25.646	12.881	7.724
21.5	25.303	11.608	7.671
22.5	23.606	12.623	6.891
23.5	22.263	12.379	5.916
24.5	24.725	10.615	6.418
25.5	26.347	9.355	7.959
26.5	25.851	11.263	7.973
27.5	27.06	11.764	7.93
28.5	28.393	10.277	7.71
29.5	28.099	10.502	6.858
30.5	29.354	11.232	9.05
31.5	33.493	11.089	8.967
32.5	40.241	8.545	10.536
33.5	42.041	6.114	11.355
34.5	48.361	4.087	10.564
35.5	48.619	2.682	9.356
36.5	48.998	2.836	10.868
37.5	48.492	2.564	11.662
38.5	33.398	4.145	9.139
39.5	17.666	6.445	4.977
40.5	13.795	8.744	4.201
41.5	18.389	8.167	5.544
42.5	17.8	7.078	5.48
43.5	15.248	7.581	5.124
44.5	14.085	8.083	4.532
45.5	15.345	8.305	4.74
46.5	13.127	8.841	4.362
47.5	13.366	10.173	4.903
48.5	15.287	11.55	4.974

Table 10: LOI and TOC/N data for Lake Oloidien (core G7).

Sample mid depth (cm)	Canthaxanthin	Aphanizophyll	Myxoanthophyll	Alloxanthin	Myxoanthophyll b	Diatoxanthin	Lutin-Zeaxanthin
0.5	89.4	0	0	0	0	0	1840.92
1.5	63.79	454.64	142.38	0	83.97	0	2337.57
2.5	56.33	223.86	0	0	0	0	1291.88
8.5	91.27	395.02	0	0	0	0	1939.1
11.5	165.06	33.83	0	0	0	0	4271.73
14.5	134.64	452.39	0	0	0	0	2661.48
17.5	136.91	883.01	0	0	0	106.43	2716.34
20.5	204.46	362.18	0	138.72	0	79.97	2214.99
23.5	225.94	102.68	0	159.77	0	76.09	942.55
26.5	343.09	155.66	0	0	0	0	1216.27
29.5	0	657.62	142.1	0	222.34	100.3	1004.45
32.5	162.38	64.56	0	83.87	0	134.2	2093.68
35.5	87.42	0	0	20.26	0	41.8	691.27
38.5	85.51	0	0	45.75	0	81.4	1211.78
41.5	110.83	55.61	0	0	0	58.39	903.33
44.5	51	31.06	0	12.38	0	42.94	250.4
47.5	150.44	177.95	36.71	125.97	0	132.41	712.83

Table 11: Pigment data (part 1) for Lake Oloidien (core G7). Pigment abundances are measured in $nmol\ g^{-1}OM$.

Sample mid depth (cm)	Chl b	Echinone	Chl a	Chl a2	Pheophytin b	β -carotene	Pheophytin a
0.5	0	47.74	100.14	91.91	35.11	126.14	48.58
1.5	0	0	85.71	119.02	33.2	99.06	30.92
2.5	0	0	63.2	69.31	29.2	70.44	22.98
8.5	0	66.7	173.47	182.73	114.66	298.93	60.12
11.5	9.475	147.37	198.06	162.26	86.26	295.84	61.4
14.5	0	176.66	207.14	134.36	59.21	258.28	58.23
17.5	0	153.04	99.9	93.4	47.81	234.25	44.17
20.5	0	138.57	68.8	97.55	78.33	191.97	63.1
23.5	0	100.38	33.07	61.26	71.71	140.21	46.54
26.5	0	182.43	38.53	73.85	69.61	173.5	52.24
29.5	0	0	47.85	41.12	25.26	121.34	35.89
32.5	0	141.58	0	78.63	80.49	223.61	44.74
35.5	0	70.92	0	35.51	45.69	150.3	25.32
38.5	0	58.44	16.78	42.94	70.82	183.96	42.65
41.5	32.61	47.79	36.32	160.61	130.68	155.69	97.73
44.5	0	32.21	33.44	34.16	43.98	110.22	35.97
47.5	0	75.53	21.81	53.21	60.95	150.17	85.69

Table 12: Pigment data (part 2) for Lake Oloidien (core G7). Pigment abundances are measured in $nmol\ g^{-1}OM$.

Depth	Al	Si	P	S	Cl	Ar	K	Ca	Ti	Cr	Mn
0.5	0.0137	0.024	0.0141	0.016	0.0244	0.031	0.084	1.82	0.027	0.0094	0.15
1.3	0.0078	0.020	0.0113	0.014	0.0065	0.029	0.119	0.82	0.053	0.0035	0.24
2.1	0.0079	0.020	0.0119	0.014	0.0075	0.022	0.108	0.68	0.047	0.0072	0.19
3.0	0.0085	0.017	0.0127	0.014	0.0084	0.033	0.085	0.50	0.035	0.0119	0.15
3.8	0.0079	0.014	0.0123	0.014	0.0084	0.029	0.066	0.32	0.025	0.0118	0.10
4.7	0.0019	0.006	0.0065	0.011	0.0078	0.026	0.050	0.22	0.013	0.0092	0.07
5.5	0.0003	0.002	0.0030	0.008	0.0070	0.023	0.040	0.17	0.012	0.0085	0.05
6.3	0.0055	0.008	0.0090	0.010	0.0075	0.016	0.039	0.10	0.007	0.0066	0.03
7.2	0.0076	0.013	0.0130	0.015	0.0113	0.029	0.056	0.22	0.015	0.0130	0.07
8.0	0.0054	0.010	0.0105	0.013	0.0078	0.021	0.047	0.18	0.012	0.0065	0.05
8.9	0.0062	0.011	0.0108	0.014	0.0085	0.019	0.054	0.24	0.015	0.0069	0.06
9.7	0.0060	0.010	0.0104	0.013	0.0075	0.016	0.049	0.21	0.014	0.0059	0.05
10.5	0.0055	0.010	0.0103	0.012	0.0070	0.014	0.055	0.26	0.016	0.0069	0.06
11.4	0.0070	0.011	0.0113	0.013	0.0069	0.013	0.049	0.18	0.013	0.0079	0.05
12.2	0.0088	0.013	0.0128	0.014	0.0079	0.014	0.052	0.22	0.014	0.0095	0.06
13.1	0.0094	0.013	0.0140	0.016	0.0104	0.020	0.044	0.15	0.010	0.0158	0.05
13.9	0.0099	0.014	0.0151	0.017	0.0119	0.017	0.048	0.16	0.010	0.0106	0.04
14.7	0.0091	0.013	0.0141	0.016	0.0109	0.019	0.050	0.19	0.013	0.0107	0.05
15.6	0.0077	0.012	0.0128	0.015	0.0095	0.022	0.059	0.27	0.020	0.0099	0.06
16.4	0.0104	0.015	0.0149	0.017	0.0117	0.027	0.048	0.14	0.010	0.0149	0.04
17.3	0.0113	0.017	0.0164	0.019	0.0149	0.028	0.050	0.08	0.004	0.0156	0.01
18.1	0.0111	0.015	0.0179	0.021	0.0158	0.042	0.043	0.10	0.005	0.0173	0.03
18.9	0.0079	0.015	0.0166	0.021	0.0165	0.054	0.052	0.29	0.016	0.0194	0.06
19.8	0.0115	0.016	0.0164	0.019	0.0137	0.036	0.055	0.34	0.018	0.0131	0.06
20.6	0.0090	0.016	0.0128	0.016	0.0097	0.030	0.082	0.78	0.033	0.0097	0.12
21.5	0.0093	0.017	0.0129	0.015	0.0086	0.036	0.085	0.79	0.034	0.0101	0.13
22.3	0.0084	0.018	0.0114	0.013	0.0061	0.031	0.096	0.90	0.040	0.0066	0.16
23.1	0.0079	0.015	0.0116	0.013	0.0075	0.025	0.067	0.50	0.025	0.0102	0.13
24.0	0.0027	0.009	0.0070	0.010	0.0059	0.018	0.065	0.55	0.025	0.0066	0.13
24.8	0.0050	0.012	0.0088	0.011	0.0062	0.024	0.066	0.52	0.024	0.0070	0.13
25.7	0.0073	0.015	0.0106	0.013	0.0072	0.032	0.076	0.60	0.027	0.0092	0.14
26.5	0.0065	0.014	0.0100	0.013	0.0070	0.032	0.071	0.55	0.025	0.0078	0.14
27.3	0.0066	0.013	0.0103	0.012	0.0072	0.031	0.062	0.45	0.022	0.0097	0.12
28.2	0.0057	0.011	0.0098	0.013	0.0084	0.028	0.056	0.38	0.019	0.0109	0.11
29.0	0.0067	0.012	0.0114	0.014	0.0088	0.035	0.049	0.31	0.016	0.0142	0.09
29.9	0.0057	0.012	0.0112	0.015	0.0097	0.039	0.058	0.42	0.021	0.0122	0.10
30.7	0.0065	0.013	0.0115	0.015	0.0094	0.040	0.058	0.47	0.023	0.0116	0.11
31.5	0.0061	0.011	0.0111	0.014	0.0092	0.035	0.040	0.26	0.011	0.0127	0.07
32.4	0.0067	0.012	0.0117	0.014	0.0089	0.035	0.048	0.26	0.020	0.0132	0.07
33.2	0.0077	0.014	0.0131	0.015	0.0085	0.035	0.051	0.22	0.023	0.0138	0.06
34.1	0.0045	0.010	0.0103	0.014	0.0088	0.041	0.047	0.16	0.021	0.0137	0.05
34.9	0.0051	0.011	0.0110	0.015	0.0094	0.035	0.046	0.07	0.021	0.0135	0.03
35.7	0.0070	0.013	0.0137	0.016	0.0101	0.046	0.049	0.04	0.024	0.0164	0.04
36.6	0.0080	0.014	0.0144	0.017	0.0106	0.045	0.049	0.04	0.024	0.0188	0.03
37.4	0.0092	0.016	0.0152	0.017	0.0097	0.042	0.058	0.06	0.029	0.0188	0.04
38.3	0.0097	0.018	0.0155	0.016	0.0089	0.032	0.066	0.06	0.032	0.0180	0.05
39.1	0.0101	0.019	0.0144	0.016	0.0082	0.031	0.078	0.12	0.037	0.0163	0.06
39.9	0.0099	0.022	0.0137	0.016	0.0071	0.035	0.119	0.48	0.054	0.0086	0.10
40.8	0.0096	0.027	0.0129	0.014	0.0052	0.041	0.168	0.83	0.075	0.0058	0.20

41.6	0.0095	0.027	0.0126	0.013	0.0052	0.035	0.158	0.82	0.069	0.0062	0.21
42.5	0.0096	0.024	0.0135	0.015	0.0068	0.033	0.137	0.63	0.060	0.0080	0.17
43.3	0.0103	0.026	0.0143	0.015	0.0061	0.038	0.144	0.54	0.060	0.0082	0.17
44.1	0.0126	0.032	0.0148	0.016	0.0056	0.041	0.195	0.63	0.083	0.0083	0.20
45.0	0.0061	0.028	0.0101	0.014	0.0069	0.051	0.202	0.73	0.093	0.0118	0.20
45.8	0.0051	0.024	0.0093	0.014	0.0079	0.051	0.169	0.67	0.078	0.0113	0.18
46.7	0.0055	0.024	0.0088	0.013	0.0066	0.055	0.160	0.66	0.069	0.0112	0.19
47.5	0.0044	0.027	0.0090	0.013	0.0079	0.060	0.191	0.90	0.084	0.0105	0.26
48.3	0.0043	0.027	0.0081	0.013	0.0073	0.066	0.191	1.02	0.083	0.0093	0.28
49.2	0.0043	0.022	0.0080	0.013	0.0065	0.088	0.155	0.88	0.062	0.0054	0.24

Table 13: A summary of the Lake Oloidien ITRAX data (part 1), each element for each sample has been divided by the counts to reduce noise from the uneven core surface.

Depth	Fe	Ni	Cu	Zn	Ga	As	Sr	Zr	Ta	Pb	Th
0.5	1.71	0.081	0.128	0.119	0.084	0.052	0.032	0.07	0.035	0.21	0.28
1.3	3.36	0.026	0.037	0.073	0.026	0.009	0.063	0.19	0.071	0.15	0.19
2.1	3.03	0.033	0.047	0.074	0.032	0.010	0.057	0.18	0.072	0.16	0.20
3.0	2.32	0.035	0.051	0.069	0.028	0.008	0.053	0.16	0.038	0.17	0.20
3.8	1.73	0.045	0.066	0.065	0.037	0.014	0.037	0.11	0.056	0.18	0.22
4.7	1.04	0.024	0.038	0.039	0.016	0.003	0.052	0.12	0.033	0.17	0.19
5.5	0.84	0.008	0.012	0.018	0.003	0.001	0.074	0.15	0.062	0.16	0.16
6.3	0.54	0.014	0.029	0.028	0.016	0.006	0.053	0.10	0.015	0.17	0.19
7.2	1.09	0.040	0.066	0.056	0.038	0.016	0.038	0.11	0.019	0.18	0.22
8.0	1.00	0.012	0.024	0.028	0.009	0.001	0.070	0.17	0.025	0.16	0.17
8.9	1.19	0.012	0.029	0.036	0.012	0.002	0.061	0.17	0.056	0.17	0.18
9.7	1.06	0.014	0.027	0.032	0.011	0.003	0.062	0.17	0.065	0.17	0.18
10.5	1.26	0.014	0.027	0.035	0.012	0.003	0.063	0.18	0.085	0.17	0.18
11.4	1.07	0.016	0.030	0.037	0.013	0.003	0.061	0.17	0.093	0.17	0.19
12.2	1.21	0.036	0.061	0.060	0.039	0.016	0.036	0.14	0.054	0.18	0.22
13.1	0.98	0.052	0.083	0.070	0.049	0.026	0.023	0.12	0.036	0.20	0.24
13.9	0.87	0.027	0.048	0.042	0.024	0.011	0.046	0.14	0.045	0.19	0.21
14.7	1.14	0.034	0.058	0.056	0.036	0.014	0.039	0.12	0.046	0.19	0.21
15.6	1.54	0.031	0.051	0.052	0.031	0.010	0.041	0.12	0.042	0.18	0.21
16.4	0.91	0.055	0.088	0.071	0.052	0.025	0.025	0.09	0.069	0.20	0.24
17.3	0.16	0.053	0.088	0.056	0.053	0.029	0.019	0.06	0.051	0.21	0.25
18.1	0.53	0.044	0.075	0.050	0.036	0.014	0.043	0.11	0.028	0.20	0.23
18.9	1.28	0.046	0.068	0.056	0.034	0.009	0.046	0.13	0.003	0.18	0.21
19.8	1.31	0.042	0.066	0.058	0.038	0.012	0.041	0.14	0.012	0.18	0.21
20.6	2.15	0.040	0.063	0.072	0.040	0.017	0.033	0.15	0.024	0.17	0.22
21.5	2.31	0.045	0.069	0.074	0.043	0.015	0.040	0.16	0.030	0.17	0.22
22.3	2.42	0.040	0.064	0.073	0.040	0.013	0.040	0.17	0.038	0.17	0.21
23.1	1.87	0.045	0.070	0.077	0.042	0.016	0.036	0.16	0.080	0.18	0.22
24.0	1.79	0.021	0.035	0.050	0.019	0.003	0.056	0.18	0.095	0.16	0.20
24.8	1.70	0.032	0.055	0.062	0.031	0.014	0.040	0.15	0.075	0.17	0.21
25.7	1.88	0.039	0.061	0.067	0.039	0.010	0.039	0.15	0.043	0.17	0.22
26.5	1.75	0.038	0.064	0.063	0.036	0.011	0.038	0.13	0.015	0.17	0.21
27.3	1.53	0.038	0.061	0.055	0.035	0.010	0.043	0.13	0.015	0.17	0.21
28.2	1.41	0.036	0.059	0.056	0.032	0.010	0.041	0.13	0.029	0.18	0.21
29.0	1.20	0.040	0.065	0.053	0.035	0.009	0.044	0.14	0.017	0.18	0.21

29.9	1.40	0.032	0.053	0.047	0.024	0.004	0.049	0.15	0.001	0.17	0.20
30.7	1.47	0.034	0.053	0.049	0.026	0.004	0.043	0.14	0.000	0.17	0.20
31.5	1.00	0.039	0.062	0.052	0.032	0.007	0.037	0.11	0.005	0.18	0.21
32.4	1.30	0.038	0.061	0.052	0.030	0.008	0.038	0.09	0.002	0.18	0.21
33.2	1.46	0.046	0.067	0.056	0.036	0.005	0.034	0.08	0.002	0.18	0.21
34.1	1.37	0.032	0.047	0.042	0.020	0.004	0.055	0.08	0.001	0.17	0.19
34.9	1.35	0.033	0.050	0.047	0.023	0.003	0.046	0.07	0.004	0.18	0.19
35.7	1.41	0.039	0.059	0.045	0.025	0.002	0.051	0.07	0.000	0.17	0.19
36.6	1.40	0.048	0.064	0.053	0.031	0.004	0.044	0.06	0.002	0.18	0.20
37.4	1.56	0.049	0.069	0.060	0.032	0.006	0.038	0.05	0.003	0.18	0.20
38.3	1.83	0.054	0.072	0.074	0.040	0.016	0.032	0.04	0.032	0.18	0.22
39.1	2.11	0.049	0.067	0.073	0.036	0.013	0.038	0.05	0.046	0.18	0.21
39.9	3.26	0.039	0.059	0.076	0.034	0.010	0.053	0.09	0.059	0.16	0.20
40.8	4.73	0.032	0.043	0.085	0.031	0.003	0.084	0.16	0.112	0.14	0.19
41.6	4.47	0.035	0.046	0.083	0.034	0.005	0.075	0.16	0.112	0.14	0.20
42.5	3.84	0.039	0.051	0.081	0.033	0.007	0.066	0.13	0.093	0.15	0.20
43.3	3.80	0.041	0.056	0.081	0.037	0.006	0.070	0.11	0.086	0.15	0.20
44.1	5.16	0.039	0.053	0.098	0.035	0.005	0.081	0.12	0.105	0.14	0.19
45.0	5.50	0.048	0.056	0.111	0.039	0.007	0.083	0.12	0.138	0.14	0.19
45.8	4.93	0.046	0.055	0.105	0.038	0.008	0.077	0.12	0.121	0.14	0.20
46.7	4.47	0.038	0.049	0.090	0.032	0.004	0.084	0.13	0.071	0.14	0.19
47.5	5.20	0.041	0.052	0.099	0.035	0.002	0.084	0.15	0.099	0.13	0.19
48.3	5.18	0.035	0.043	0.097	0.028	0.002	0.108	0.18	0.129	0.13	0.18
49.2	4.04	0.013	0.020	0.068	0.009	0.000	0.120	0.23	0.073	0.12	0.16

Table 14: A summary of the Lake Oloidien ITRAX data (part 2), each element for each sample has been divided by the counts to reduce noise from the uneven core surface.

Average sample depth (cm)	Organic %	Carbonate %	TOC/N
0.5	15.331	3.614	8.757
1.5	10.793		8.082
2.5	12.182	3.933	7.847
3.5	11.160		7.881
4.5	11.755		7.649
5.5	11.565	3.943	7.465
6.5	12.152	3.916	7.500
7.5	10.125		7.315
8.5	9.891		7.254
9.5	9.527		7.395
10.5	9.922	4.113	7.378
11.5	10.078		8.676
12.5	9.769		8.145
13.5	10.681		9.256
14.5	10.491		9.566
15.5	8.084		8.372
16.5	7.611		8.853
17.5	6.800		8.748
18.5	7.148		8.470
19.5	7.672	4.840	8.690
20.5	6.988	5.153	8.919

21.5	7.104	4.797	9.979
22.5	7.669	4.823	9.123
23.5	8.377	6.526	8.746
24.5	7.558	5.010	9.463

Table 15: LOI and TOC/N data for core for Lake Elmentaita (core G6).

Sample mid depth (cm)	Fuco-xanthin	Carate-noid x	Aphan-izophyll	Myxoan-thophyll	Allox-anthin	Diatox-anthin	Lutein	Lutin-Zea-xanthin
0.5	168.51	0	155.09	0	193.66	204.48	n/d	2219.4
2.5	204.79	19.6	119.74	0	0	223.04	n/d	1089.26
4.5	100.16	0	0	0	0	102.57	n/d	571.67
5.5	226.98	21.93	165.3	0	0	270.37	n/d	1257.82
6.5	225.48	24.88	115.14	0	0	245.95	n/d	1083.66
7.5	218.77	23.67	128.48	0	0	254.01	n/d	1065.68
8.5	153.92	18.25	85.98	0	0	187.57	n/d	738.18
9.5	115.64	13.92	62.03	0	0	137.3	n/d	543.04
10.5	140.91	19.98	75.77	0	0	186.91	n/d	754.49
11.5	79.22	17.46	40	0	0	140.68	n/d	691.7
12.5	96.5	28.41	61	0	84.14	230.54	n/d	1161.03
13.5	78.31	42.65	65.06	0	0	320.73	n/d	1884.49
15.5	35.29	35.52	0	0	0	108.67	0	1174.57
16.5	25.27	17.39	0	0	0	88.25	n/d	609.63
17.5	44.83	34.75	0	0	0	149.85	n/d	679.59
18.5	34.95	19.53	0	0	0	137.68	0	653.09
19.5	12.28	0	0	0	0	37.68	n/d	177.69
20.5	15.96	0	0	0	0	40.72	0	125.92
21.5	21.2	0	0	0	0	54.95	n/d	179.65
22.5	40.35	22.37	0	0	0	92.49	72.85	275.44
23.5	34	19.25	0	0	0	91.05	n/d	251.61
24.5	21.6	17.25	0	0	0	115.21	75.78	225.04

Table 16: Pigment data (part 1) for Lake Elmentaita (core G6). Pigment abundances are measured in $nmol\ g^{-1}OM$.

Sample mid depth (cm)	Cantha-xanthin	Echin-Chl b	enone	Chl a	Chl a2	Pheo-phytin b	β -carotene	Pheo-phytin a
0.5	117.94	0	118.86	575.12	848.36	131.454	175.65	124.84
2.5	171.01	0	116.13	402.54	1114.19	101.21	187.22	199.88
4.5	85.9	0	54.23	209.71	547.87	44.63	107.59	97.2
5.5	192.38	0	n/d	495.7	908.39	41.05	75.91	86.67
6.5	175.69	0	120.89	385.22	1186.21	97.32	184.83	202.72
7.5	175.29	0	n/d	433.1	919.11	40.22	74.81	91.48
8.5	124.18	0	n/d	365.62	862.41	52.56	97.6	109.41
9.5	91	0	n/d	254.25	601.09	30.36	53.38	68.26
10.5	118.79	0	n/d	297.99	699.15	37.19	66.54	79.24
11.5	104.83	0	n/d	180.11	498.11	33.27	33.82	53.12
12.5	159	13.51	101.01	140.56	731.87	56.1	79.6	87.91
13.5	213.98	29.66	140.88	86.42	738.42	18.89	88.3	121.73
15.5	109.41	29.45	73.07	38.52	538.74	102.82	52.01	85.54

16.5	91.35	22.45	51.26	54.52	586.47	93.24	60.81	85.85
17.5	111.28	34.35	n/d	161.6	865.22	81.65	53.77	87.11
18.5	102.07	31.36	59.37	83.11	688.21	80.03	50.59	82.83
19.5	33.41	0	17.73	16.23	239.95	29.99	15.97	37.4
20.5	33.22	0	22.76	25	206.61	17.47	8	24.11
21.5	43.53	0	37.98	25	354.41	38.36	16.04	53.63
22.5	77.33	0	47.48	23.79	588.24	55.85	22.16	74.41
23.5	72.9	0	39.24	21.86	537.6	48.81	19.6	67.52
24.5	85.24	0	60.94	50	562.86	37.97	0	62.44

Table 17: Pigment data (part 2) for Lake Elmentaita (core G6). Pigment abundances are measured in $nmol\ g^{-1}OM$.

Depth	Al	Si	P	S	Cl	Ar	K	Ca
2.0	0.00879	0.0113	0.0607	0.5097	0.0338	0.1686	0.962	0.231
3.0	0.02255	0.0281	0.0440	0.2040	0.0880	0.1655	0.437	0.099
4.0	0.03421	0.0371	0.0389	0.0628	0.0806	0.0469	0.124	0.018
4.9	0.01506	0.0231	0.0225	0.0363	0.0526	0.0398	0.079	0.068
5.9	0.01777	0.0473	0.0219	0.0291	0.0794	0.0450	0.217	0.424
6.9	0.01731	0.0481	0.0212	0.0272	0.0319	0.0423	0.247	0.482
7.8	0.01887	0.0528	0.0225	0.0273	0.0315	0.0388	0.246	0.491
8.8	0.01922	0.0596	0.0209	0.0265	0.0288	0.0267	0.270	0.547
9.8	0.01557	0.0498	0.0181	0.0239	0.0289	0.0288	0.246	0.497
10.7	0.01708	0.0527	0.0196	0.0247	0.0307	0.0333	0.249	0.503
11.7	0.01598	0.0542	0.0193	0.0259	0.0253	0.0302	0.248	0.493
12.7	0.01707	0.0655	0.0201	0.0266	0.0233	0.0243	0.279	0.569
13.6	0.01702	0.0626	0.0193	0.0257	0.0251	0.0275	0.272	0.554
14.6	0.01696	0.0650	0.0188	0.0259	0.0240	0.0281	0.284	0.575
15.5	0.01732	0.0670	0.0193	0.0253	0.0235	0.0272	0.287	0.579
16.5	0.01714	0.0627	0.0196	0.0256	0.0260	0.0309	0.281	0.563
17.5	0.01619	0.0627	0.0198	0.0262	0.0260	0.0308	0.280	0.560
18.4	0.01523	0.0586	0.0176	0.0239	0.0253	0.0318	0.269	0.535
19.4	0.01554	0.0607	0.0183	0.0241	0.0252	0.0322	0.277	0.549
20.4	0.01602	0.0592	0.0172	0.0236	0.0262	0.0323	0.267	0.536
21.3	0.01552	0.0613	0.0172	0.0238	0.0242	0.0299	0.273	0.552
22.3	0.01543	0.0612	0.0175	0.0235	0.0254	0.0305	0.277	0.564
23.3	0.01543	0.0587	0.0181	0.0246	0.0270	0.0344	0.262	0.533
24.2	0.01669	0.0584	0.0186	0.0253	0.0296	0.0322	0.256	0.510
25.2	0.01605	0.0556	0.0177	0.0252	0.0303	0.0335	0.253	0.504
26.2	0.01561	0.0553	0.0183	0.0275	0.0308	0.0249	0.259	0.455
27.1	0.01737	0.0457	0.0204	0.0272	0.0377	0.0271	0.224	0.381
28.1	0.01715	0.0468	0.0194	0.0266	0.0368	0.0276	0.228	0.393
29.0	0.01668	0.0465	0.0202	0.0288	0.0397	0.0329	0.248	0.417
30.0	0.01723	0.0541	0.0205	0.0288	0.0343	0.0284	0.284	0.470
31.0	0.01632	0.0428	0.0189	0.0259	0.0396	0.0277	0.243	0.410
31.9	0.01728	0.0469	0.0206	0.0292	0.0400	0.0317	0.255	0.417
32.9	0.01715	0.0447	0.0210	0.0290	0.0383	0.0313	0.252	0.411
33.9	0.01693	0.0551	0.0186	0.0289	0.0334	0.0251	0.293	0.466
34.8	0.01705	0.0620	0.0195	0.0300	0.0307	0.0293	0.325	0.499
35.8	0.01775	0.0697	0.0205	0.0323	0.0289	0.0280	0.345	0.525
36.8	0.01652	0.0639	0.0189	0.0311	0.0273	0.0274	0.326	0.511

37.7	0.01784	0.0648	0.0201	0.0302	0.0301	0.0319	0.327	0.500
38.7	0.01799	0.0677	0.0201	0.0318	0.0282	0.0268	0.335	0.516

Table 18: A summary of the Lake Elmentaita ITRAX data (part 1), each element for each sample has been divided by the counts to reduce noise from the uneven core surface.

Depth	Ti	V	Cr	Mn	Fe	Ni	Cu	Zn	Ga
2.0	0.001	0.0069	0.0544	0.048	0.07	0.0023	0.0046	0.0019	0.0015
3.0	0.001	0.0058	0.0533	0.045	0.09	0.0420	0.0495	0.0256	0.0146
4.0	0.003	0.0041	0.0478	0.049	0.11	0.1633	0.2297	0.1543	0.1532
4.9	0.022	0.0009	0.0221	0.043	1.07	0.0572	0.0813	0.0629	0.0480
5.9	0.166	0.0095	0.0196	0.268	8.87	0.0487	0.0372	0.0821	0.0357
6.9	0.186	0.0071	0.0143	0.304	10.45	0.0314	0.0152	0.0801	0.0240
7.8	0.183	0.0051	0.0139	0.302	10.32	0.0317	0.0205	0.0821	0.0282
8.8	0.195	0.0054	0.0133	0.326	10.79	0.0398	0.0252	0.0899	0.0363
9.8	0.181	0.0029	0.0104	0.308	10.28	0.0345	0.0184	0.0834	0.0271
10.7	0.181	0.0035	0.0111	0.301	10.24	0.0361	0.0219	0.0830	0.0296
11.7	0.178	0.0041	0.0140	0.293	10.03	0.0265	0.0104	0.0760	0.0271
12.7	0.200	0.0028	0.0097	0.317	10.66	0.0381	0.0192	0.0850	0.0319
13.6	0.194	0.0020	0.0112	0.317	10.58	0.0392	0.0221	0.0860	0.0363
14.6	0.197	0.0024	0.0124	0.323	10.80	0.0397	0.0218	0.0857	0.0352
15.5	0.197	0.0024	0.0093	0.322	10.80	0.0392	0.0211	0.0866	0.0317
16.5	0.197	0.0032	0.0110	0.326	10.76	0.0426	0.0268	0.0877	0.0369
17.5	0.197	0.0032	0.0097	0.319	10.65	0.0415	0.0247	0.0869	0.0366
18.4	0.190	0.0018	0.0081	0.310	10.42	0.0401	0.0229	0.0851	0.0315
19.4	0.193	0.0027	0.0093	0.312	10.44	0.0344	0.0215	0.0832	0.0331
20.4	0.189	0.0025	0.0107	0.313	10.41	0.0401	0.0260	0.0856	0.0364
21.3	0.191	0.0025	0.0100	0.316	10.53	0.0394	0.0262	0.0906	0.0351
22.3	0.192	0.0018	0.0098	0.323	10.51	0.0395	0.0252	0.0867	0.0344
23.3	0.181	0.0026	0.0107	0.312	10.16	0.0390	0.0267	0.0891	0.0389
24.2	0.184	0.0038	0.0114	0.315	10.07	0.0433	0.0290	0.0883	0.0366
25.2	0.184	0.0050	0.0141	0.319	10.17	0.0442	0.0318	0.0905	0.0394
26.2	0.191	0.0033	0.0133	0.321	10.56	0.0432	0.0180	0.0856	0.0308
27.1	0.177	0.0046	0.0106	0.308	10.27	0.0490	0.0260	0.0901	0.0342
28.1	0.174	0.0049	0.0126	0.309	10.23	0.0502	0.0349	0.0941	0.0402
29.0	0.186	0.0063	0.0121	0.332	11.04	0.0466	0.0276	0.0929	0.0424
30.0	0.199	0.0035	0.0117	0.346	11.52	0.0476	0.0274	0.0938	0.0409
31.0	0.186	0.0050	0.0130	0.334	11.17	0.0502	0.0304	0.0966	0.0397
31.9	0.186	0.0050	0.0117	0.330	11.05	0.0445	0.0278	0.0912	0.0378
32.9	0.186	0.0051	0.0141	0.330	11.10	0.0452	0.0259	0.0987	0.0386
33.9	0.204	0.0041	0.0103	0.345	11.66	0.0438	0.0205	0.0935	0.0368
34.8	0.214	0.0050	0.0114	0.358	12.01	0.0412	0.0197	0.0946	0.0348
35.8	0.223	0.0044	0.0103	0.367	12.35	0.0412	0.0149	0.0923	0.0327
36.8	0.222	0.0037	0.0100	0.362	12.24	0.0407	0.0174	0.0928	0.0352
37.7	0.220	0.0041	0.0121	0.350	11.89	0.0351	0.0154	0.0852	0.0298
38.7	0.228	0.0047	0.0100	0.365	12.30	0.0418	0.0162	0.0895	0.0342

Table 19: A summary of the Lake Elmentaita ITRAX data (part 2), each element for each sample has been divided by the counts to reduce noise from the uneven core surface.

Bibliography

Adeka, J., Strobl, R., & Becht, R. (2008). An Environmental System Analysis of Lake Elementaita, Kenya With Reference To Water Quality. In Sengupta, M., & Dalwani, R. (Eds.), *Proceedings of Taal 2007: The 12th World Lake Conference*, pp. 1365–1372.

Akeley, C. (1912). Flamingos of Lake Hannington, Africa. *American Museum Journal*, 12, 304–308.

Amaral, L., & Meyer, M. (1999). Environmental changes, coextinction, and patterns in the fossil record. *Physical Review Letters*, 82, 652.

Amiadtriquent, C., Pain, D., & Delves, H. (1991). Exposure to trace elements of flamingos living in a biosphere reserve, the Carmague, FranceRepublic of Kenya. Japan Bank for International Cooperation, Tokyo. *Environmental Pollution*, 69, 193–201.

An, L. (2012). Modeling human decisions in coupled human and natural systems: Review of agent-based models. *Ecological Modelling*, 229, 25–36.

Appleby, P. (1978). The calculation of lead-210 dates assuming a constant rate of supply of unsupported ^{210}pb to the sediment. *Catena*, 5(1), 1–8.

Arismendez, S., Kim, H.-C., Brenner, J., & Montagna, P. (2014). Application of watershed analyses and ecosystem modeling to investigate land-water nutrient coupling processes in the Guadalupe Estuary, Texas.. *Ecological Informatics*, 4, 243–253.

Ashfaque, A. (2000). Estimating evaporation from Lake Naivasha Kenya, using remotely sensed Landsat Thematic Mapper (TM) spectral data. *Civil Engineering, The Institution of Engineers, Bangladesh*, 28(2), 189–203.

Ayenew, T., & Becht, R. (2008). Comparative assessment of the water balance and hydrology of selected Ethiopian and Kenyan Rift Lakes. *Lakes and Reservoirs: Research and Management*, 13, 181–196.

Bahr, D., & Bekoff, M. (1999). Predicting flock vigilance from simple passerine interactions: modelling with cellular automata. *Animal Behaviour*, 58, 831–839.

Bajec, L., Zimic, N., & Mraz, M. (2007). The computational beauty of flocking: boids revisited. *Mathematical and Computer Modelling of Dynamical Systems*, 13, 331–347.

Ballot, A., Kotut, K., Novelo, E., & Krienitz, L. (2009). Changes of phytoplankton communities in Lakes Naivasha and Olloidien, examples of degradation and salinization of lakes in the Kenyan Rift Valley. *Hydrobiologia*, 632, 359–363.

Ballot, A., Krienitz, L., Kotut, K., Wiegand, C., Metcalf, J. S., Codd, G. A., & Pflugmacher, S. (2004). Cyanobacteria and cyanobacterial toxins in three alkaline Rift Valley lakes of Kenya-Lakes Bogoria, Nakuru and Elmenteita. *Journal of Plankton Research*, 26(8), 925–935.

Barber-Meyer, S., Kooyman, G., & Ponganis, P. (2007). Estimating the relative abundance of emperor penguins at inaccessible colonies using satellite imagery. *Polar Biology*, 30, 1565–1570.

Bartholomew, G., & Pennycuick, C. (1973). The flamingo and pelican populations of the Rift Valley Lakes in 1968-69. *African Journal of Ecology*, 11(2), 189–198.

Becht, R., & Harper, D. (2002). Towards understanding the human impact upon the hydrology of Lake Naivasha, Kenya. *Hydrobiologia*, 488, 1–11.

Becht, R., Mwango, R., Muno, F., & Amstrong, F. (2006). Groundwater links between Kenya Rift Valley lakes. In *Odada, Eric and Olago, Daniel O. (Ed.) Proceedings of the 11th World Lakes Conference*, Vol. 2, pp. 7–14.

Bengtsson, L., & Enell, M. (1986). *Handbook of Holocene Palaeoecology and Palaeohydrology*, chap. Chemical analysis. No. 423-445. Wiley.

Bennun, L., & Njoroge, P. (1999). Important bird areas in Kenya. Tech. rep., Nature Kenya, Nairobi, Kenya.

Bergner, A., Trauth, M., & Bookhagen, B. (2003). Paleoprecipitation estimates for the Lake Naivasha basin (Kenya) during the last 175 k.y. using a lake-balance model. *Global and Planetary Change*, 36, 117–136.

Blais, J., Kalf, J., Cornet, R., & Evans, R. D. (1995). Evaluation of 210pb dating in lake sediments using stable pb, ambrosia pollen and 137cs. *Journal of Paleolimnology*, 13, 169–178.

Bodin, O., & Saura, S. (2010). Ranking individual habitat patches as connectivity providers: Integrating network analysis and patch removal experiments. *Ecological Modelling*, 221(19), 2393–2405.

Boecklen, W., Yarnes, C., Cook, B., & James, A. (2011). On the Use of Stable Isotopes in Trophic Ecology. *Annual Review of Ecology, Evolution, and Systematics*, 42, 411–440.

Borello, W., Mundi, P., & Liversedge, T. (1998). *Migrating Birds Know No Boundaries*, chap. Movements of Greater and Lesser Flamingos in Southern Africa. Torgos Publications, Israel Ornithology Centre, Tel Aviv, Israel.

Brass, G. (1975). The effect of weathering on the distribution of strontium isotopes in weathering profiles. *Geochimica et Cosmochimica Acta*, 39(12), 1647–1653.

Brown, L. H. (1973). *The Mystery of the Flamingos*. Collins, London.

Brown, L. (1955). The breeding of Lesser and Greater Flamingos in East Africa. *Journal of East African Natural History*, 22(159-162).

Brown, L. (1971a). Flamingo. *World of Birds*, 1(13-18).

Brown, L. (1971b). The flamingos of Lake Nakuru. *New Scientist and Science*, 97–101.

Brown, L., & Root, A. (1971). The breeding behaviour of the lesser flamingo *Phoeniconaias minor*. *Ibis*, 113, 147–172.

Burgis, M., & Symoens, J. (1987). African wetlands and shallow water bodies. Trav doc, ORSTOM, Bondy, France.

Burian, A. (2010). Zooplankton dynamics of two alkaline-saline lakes in the Keyan Rift Valley. Master's thesis, University of Vienna.

Burian, A., Kainz, M., Schagerl, M., & Yasindi, A. (2014). Species-specific separation of lake plankton reveals divergent food assimilation patterns in rotifers. *Freshwater Biology*, 59(6), 1257–1265.

Carmichael, W. W. (1992). Cyanobacteria secondary metabolites: Cyanotoxins. *Journal of Applied Bacteriology*, 72, 445–459.

Carmichael, W. W. (1997). The Cyanotoxins. *Advances in Botanical Research*, 27, 211–256.

Carpenter, S., Elser, M., & Elser, J. (1986). Chlorophyll Production, Degradation, and Sedimentation: Implications for Paleolimnology. *Limnology and Oceanography*, 31(1), 112–124.

Castanier, S., Bernet-Rollande, M., Maurin, A., & Perthuisot, J. (1993). Effects of microbial activity on the hydrochemistry and sedimentology of Lake Logipi, Kenya. *Hydrobiologia*, 267, 99–112.

Chen, J., An, Z., & Head, J. (1999). Variation of rb/sr ratios in the loess-paleosol sequences of central China during the last 130,000 years and their implications for monsoon paleoclimatology. *Quaternary Research*, 51(3), 215–219.

Chen, N., Bianchi, T., McKee, B., & Bland, J. (2001). Historical trends of hypoxia on the Louisiana shelf: applications of pigments as biomarkers. *Organic Geochemistry*, 32, 543–561.

Childress, B., Harper, D., Hughes, B., Bossche, W., Bertold, P., & Querner, U. (2004). Satellite tracking Lesser Flamingo movements in the Rift Valley, East Africa: pilot study report. *Ostrich: Journal of African Ornithology*, 75(1-2), 57–65.

Childress, B., Hughes, B., Harper, D., & van den Bossche, W. (2007). East African flyway and key site network of the Lesser Flamingo (*Phoenicopterus minor*) documented through satellite tracking. *Ostrich*, 78(2), 463–468.

Choong-Jae, K., Yun-Ho, J., & Hee-Mock, O. (2007). Factors Indicating Culture Status During Cultivation of Spirulina (*Arthospira*) *platensis*. *Journal of Microbiology*, 45(2), 122–127.

Cohen, A. (2003). *Paleolimnology: the history and evolution of lake systems*. Oxford University Press, New York.

Cohen, Z. (1997). *Spirulina Platensis Arthospira: Physiology, Cell-Biology And Biotechnology*, chap. The chemicals of Spirulina, pp. 175–204. Taylor & Francis Ltd, London, UK.

Cooper, J. E., Karstad, L., & Broughton, E. (1975). Tuberculosis in lesser flamingos in Kenya. *Journal of Wildlife Diseases*, 11, 32–36.

Croudace, I., & Gilligan, J. (1990). Versatile and accurate trace element determinations in iron-rich and other geological samples using X-ray fluorescence analysis. *X-ray Spectrometry*, 19, 117–123.

Croudace, I., Rindby, A., & Rothwell, R. (2006). *New Techniques in Sediment Core Analysis*, chap. ITRAX: Description and evaluation of a new multi-function X-ray core scanner. London Special Publications.

Daley, R. (1973). Experimental characterization of lacustrine chlorophyll diagenesis 2. Bacterial, viral and herbivore grazing effectserial, viral and herbivore grazing effects. *Archives of Hydrobiology*, 72, 409–439.

Darling, W., Gizaw, B., & Arusei, M. (1996). Lake-groundwater relationships and fluid-rock interaction in the east african rift valley: isotopic evidence. *Journal of African Earth Sciences*, 22(4), 423–431.

Dawson, R. (1997). The toxicology of microcystins. *Toxicon*, 36, 953–962.

Dean, W. (1974). Determination of carbonate and organic matter in calcareous sediments and sedimentary rocks by loss on ignition: comparison with other methods. *Journal of Sedimentary Petrology*, 44, 242–248.

Din, N., & Eltringham, S. (1976). Early records of the lesser flamingo Phoeniconaias minor in western uganda with a note on its present status. *African Journal of Ecology*, 14(2), 171–175.

Donald, C., Gordon, J., William, H., & Sutcliffe, J. (1973). A new dry combustion method for the simultaneous determination of total organic carbon and nitrogen in seawater. *Marine Chemistry*, 1, 231–244.

Dube, A., Jayaraman, G., & Rani, R. (2012). Modelling the effects of variable salinity on the temporal distribution of plankton in shallow coastal lagoons. *Journal of Hydro-environment Research*, 4, 199–209.

Ejrnaes, R. (2000). Can we trust gradients extracted by Detrended Correspondence Analysis?. *Journal of Vegetation Science*, 11(4), 565–572.

Ermentrout, G. B., & Edelstein-Keshet, L. (1993). Cellular Automata Approaches to Biological Modeling. *Journal of Theoretical Biology*, 160, 97–133.

Eugster, H., & Hardie, L. (1978). *Lakes: Chemistry, geology, physics.*, chap. Saline Lakes. Springer, Berlin Heidelberg New York.

Fasham, M., Ducklow, H., & McKelvie, S. (1990). A Nitrogen-based model of plankton dynamics in the oceanic mixed layer. *Journal of Marine Research*, 48, 591–639.

Fleitman, D., Dunbar, R., McCulloch, M., Mudelsee, M., Vuille, M., McClanahan, T., Cole, J., & Eggins, S. (2007). East African soil erosion recorded in a 300 year old coral colony from Kenya. *Geophysical Research Letters*, 34.

Forrester, J. (1971). Counterintuitive behavior of social systems. *Theory and Decision*, 2, 109–140.

Fort, J., Porter, W., & Gremillet, D. (2009). Thermodynamic modelling predicts energetic bottleneck for seabirds wintering in the northwest Atlantic. *The Jounal of Experimental Biology*, 212, 2483–2490.

Fort, J., Porter, W., & Gremillet, D. (2011). Fort 2011 sea bird Phalacrocorax. *Comparative Biochemistry and Physiology Part A: Molecular and Integrative Physiology*, 158, 358–365.

Franks, P. (2002). NPZ Models of Plankton Dynamics: Their Construction, Coupling to Physics, and Application. *Journal of Oceanography*, 58, 379–389.

Gardner, M. (1970). The fantastic combinations of John Conway's new solitaire game "life". *Scientific American*, 223, 120–123.

Gasse, F. (2000). Hydrological changes in the African tropics since the Last Glacial Maximum. *Quaternary Science Reviews*, 19, 189–211.

Gentleman, W. (2002). A chronology of plankton dynamics in silico: how computer models have been used to study marine ecosystems. *Hydrobiologia*, 480, 69–85.

Goldberg, E. (1963). Geochronology with 210pb, radioactive dating.. *International Atomic Energy Agency Journal*, 68, 121–131.

Goldstein, D. (1988). Estimates of daily energy expenditure in birds: The time-energy budget as an integrator of laboratory and field studiesand Field Studies. *Integrative and Comparative Biology*, 28, 829–844.

Grant, W. (2003). *Life Under Extreme Conditions*, chap. Alkaline environments and biodiversity. Eolss Publishers.

Grant, W., Mwatha, W., & Jones, B. (1990). Alkaliphiles: ecology, diversity and applications. *FEMS Microbiology Reviews*, 75(255-270).

Griffin, S., Herzfeld, M., & Hamilton, D. (2001). Modelling the impact of zooplankton grazing on phytoplankton biomass during a dinoflagellate bloom in the Swan River Estuary, Western Australia. *Ecological Engineering*, 16(3), 373–394.

Hansen, M., Potapov, P., Moore, R., Hancher, M., Turubanova, S., Tyukavina, A., Thau, D., Stehman, S., Goetz, S., Loveland, T., Kommareddy, A., Egorov, A., Chini, L., Justice, C., & Townshend, J. R. G. (2013). High-Resolution Global Maps of 21st-Century Forest Cover Change. *Science*, 342(6160), 850–853.

Harper, D., Childress, R., M.M.Harper, Boar, R., Hickley, P., Mills, S., Otieno, N., Drane, T., Vareschi, E., Nasirwa, O., Mwatha, W., Darlington, J., & Escute-Gasulla, X. (2003). Aquatic biodiversity and saline lakes: Lake Bogoria National Reserve, Kenya. *Hydrobiologia*, 500, 259–276.

Hastie, T., & Tibshirani, R. (2009). *Model Assessment and Selection, The Elements of Statistical Learning* (2nd edition). Springer Series in Statistics, New York.

Hertzberg, S., & Liaaen-Jensen, S. (1966). The carotenoids of blue-green algae. i. The caretenoids of Oscillatoria rubescens and an Arthospira sp.. *Phytochemistry*, 5, 557–563.

Hikley, P., Boar, R. R., & Mavuti, K. M. (2003). Bathymetry of Lake Bogoria, Kenya. *Journal of East African Natural History*, 92(1), 107–117.

Hill, M. (1973). Reciprocal averaging: an eigenvector method of ordination. *Journal of Ecology*, 61(1), 237–249.

Hill, M., & Gauch, H. (1980). Detrended correspondance analysis: an improved ordination technique. *Vegetation*, 42, 47–58.

Holmgren, K., & Oberg, H. (2006). Climate change in southern and eastern Africa during the past millennium and its implications for societal development. *Environment, Development and Sustainability*, 8, 185–195.

Hutchinson, L., & Midgely, D. (1978). Modelling the water and salt balance in a shallow lake. *Ecological Modelling*, 4, 211–235.

Jenkin, P. M. (1957). The filter feeding of flamingos (Phoenicopteridae). *Philosophical Transactions of the Royal Society of London. Series B, Biological Sciences*, 240(674), 401–493.

Jenkins, R. (1999). *X-ray Fluorescence Spectrometry* (2nd edition). Wiley, Chichester.

Jimenez, C., Cossio, B., D. Labella, & Niell, F. X. (2003). The Feasibility of industrial production of Spirulina (Arthospira) in Southern Spain. *Aquaculture*, 217, 179–190.

Jørgensen, S., & Bendoricchio, G. (2001). *Fundamentals of Ecological Modelling*. Elsevier.

Junginger, A. (2011). East African Climate Variability on Different Time Scales: The Suguta Valley in the African-Asian Monsoon Domain. Master's thesis, Institut für Erd- und Umweltwissenschaften Mathematisch-Naturwissenschaftliche Fakultät, Universität Potsdam.

Kaggwa, M., Burian, A., Oduor, S., & Schagerl, M. (2012). Ecomorphological variability of Arthospira fusiformis (Cyanoprokaryota) in African soda lakes. *Microbiology-Open*, 3.

Kebede, E. (1997). Response of Spirulina platensis (=Arthospira fusiformis) from Lake Chitu, Ethiopia, to salinity stress from sodium salts. *Journal of Applied Phycology*, 9, 551–558.

Kebede, E., & Ahlgren, G. (1996). Optimum growth conditions and light utilization efficiency of Spirulina platensis (= Arthospira fusiformis) (Cyanophyta) from Lake Chitu, Ethiopia. *Hydrobiologia*, 332, 99–109.

Khal, M. (1975). *Flamingos*, chap. Distribution and numbers - a summary. N. Kear and J. Duplaix-Hall, Berkhamstead, Poyster, UK.

Khedr, A., & El-Dermerdash, M. (1997). Distribution of aquatic plants in relation to environmental factors in the Nile Delta. *Aquatic Botany*, 56(1), 75–86.

Kiage, L. M., & b. Liu, K. (2009). Palynological evidence of vegetation change and land degradation in the Lake Baringo area, Kenya, East Africa during the Late Holocene. *Palaeogeography, Palaeoclimatology, Palaeoecology*, 279, 60–72.

Kiage, L., & Liu, K. (2006). Late Quaternary paleoenvironmental changes in East Africa: a review of multiproxy evidence from palynology, lake sediments, and associated records. *Progress in Physical Geography*, 30(5), 633–658.

Kihwele, E., Lugomela, C., & Howell, L. (2014). Temporal changes in the Lesser Flamingos population (*Phoenicopterus minor*) in relation to phytoplankton abundance in Lake Manyara, Tanzania. *Open Journal of Ecology*, pp. 145–161.

Kock, N., Kock, R., Wambua, J., Kamau, G. J., & Mohan, K. (1999). Mycobacterium avium-related epizootic in free-ranging Lesser Flamingos in Kenya. *Journal of Wildlife Distribution*, 35, 297–300.

Koenig, R. (2006). The pink death: die-offs of the Lesser Flamingo raise concern. *Science*, 313, 1724–1725.

Kooijman, S. (2001). Quantitative aspects of metabolic organisation; a discussion of concepts. *Philosophical Transactions of the Royal Society of Biological Sciences*, 356, 331–349.

Kooijman, S., Sousa, T., Pecquerie, L., Meer, J. V. D., & Jager, T. (2008). From food-dependent statistics to metabolic parameters, a practical guide to the use of dynamic energy budget theory. *Biological Reviews*, 83, 533–552.

Koopmans, M., Köster, J., van Kaam-Peters, H., Kenig, F., Schouten, S., Hartgers, W., de Leeuw, J., & Damsté, J. S. (1996). Diagenetic and catagenetic products of isorenieratene: Molecular indicators for photic zone anoxia. *Geochim Cosmochim Acta*, 60, 4467–4496.

Krienitz, L., Ballot, A., Kotut, K., Wiegad, C., Putz, S., Metcalf, J. S., Codd, G. A., & Pflugmacher, S. (2003). Contribution of hot spring cyanobacteria to the mysterious deaths of Lesser Flamingos at Lake Bogoria, Kenya. *FEMS Microbiology Ecology*, 43, 141–148.

Krienitz, L., Dadheech, P., & Kotut, K. (2013). Mass developments of the cyanobacteria *Anabaenopsis* and *Cyanospira* (Nostocales) in the soda lakes of Kenya: ecological and systematic implications. *Hydrobiologia*, 703, 79–93.

Krienitz, L., & Kotut, K. (2010). Fluctuating algal food populations and the occurrence of lesser flamingos (*Phoeniconaias minor*) in three Kenya Rift Valley Lakes. *Journal of Phycology*, 46, 1088–1096.

Krishnaswami, S., Lal, D., Martin, J., & Maybeck, M. (1971). Geochronology of lake sediments.. *Earth and Planetary Sciences Letters*, 11, 407–414.

Kylander, M., Ampel, L., Wohlfarth, B., & Veres, D. (2011). High Resolution ITRAX Analysis of Les Echets (France) Sedimentary Sequence: Linking Geochemical, Biological and Physical Proxies. *Journal of Quaternary Science*, 26(1), 109–117.

Leavitt, P., Carpenter, S., & Kitchell, J. (1989). Whole-Lake Experiments: The Annual Record of Fossil Pigments and Zooplankton. *Limnology and Oceanography*, 34(4), 1989.

Leavitt, P., & Hodgson (2001). *Tracking Environmental Change Using Lake Sediments*, Vol. 1. Kluwer Academic Publishers.

Leavitt, P., Schindler, D., Paul, A., Hardie, A., & Schindler, D. (1994). Fossil Pigment Records of Phytoplankton in Trout-stocked Alpine Lakes. *Canadian Journal of Fisheries and Aquatic Sciences*, 51, 2411–2423.

Lewontin, R. (1969). The meaning of stability. *Brookhaven Symposia in Biology*, 22, 13–23.

Lotka, A. (1925). *Elements of physical biology*. Williams & Wilkins Company.

Mackereth, F. (1966). Some chemical observations on post-glacial lake sediments. *Philosophical Transactions of the Royal Society of Biological Sciences*, 370, 165–213.

Mackworth-Praed, C., & Grant, C. (1952). *Birds of Eastern and North Eastern Africa*. Longman, London.

Masaya, T. (1975). Spectral analysis of rainfall series in Kenya. In *Working paper no. 211, Nairobi: Institute for Development Studies, University of Nairobi*.

Matagi, S. V. (2004). A biodiversity assessment of the Flamingo Lakes of eastern Africa. *Biodiversity*, 5(1), 13–26.

McCall, G. (1967). Geology of the Nakuru-Thomson's Falls-Lake Hannington area. *Geological Survey Kenya Report*, 78.

McCulloch, G., & Borello, W. (2000). The importance of the Makgadikgadi salt pans in Botswana for flamingos in Africa.. *Waterbirds*, 23 (special publication), 64–68.

McGowan, S. (2007). *Pigment Studies in The Encyclopedia of Quaternary Science*. pages 2062-2074. Elsevier Ltd.

Meinertzhagen, R. (1958). Greater flamingoes in Kenya. *Ibis*, 100.

Melack, J. M. (1976). *Limnology and dynamics of phytoplankton in equatorial African Lakes*. Ph.D. thesis, Duke University, Durham, USA.

Melack, J. M. (1988). Primary producer dynamics associated with evaporative concentration in a shallow, equatorial soda lake (Lake Elmenteita, Kenya). *Hydrobiologia*, 158(1), 1–14.

Meriluoto, J. (1997). Chromatography of microcystins. *Analytica Chimica Acta*, 352, 277–298.

Meyers, P. (1994). Preservation of elemental and isotopic source identification of sedimentary organic matter. *Chemical Geology*, 114, 289–302.

Meyers, P., & Ishiwatari, R. (1993). Lacustrine organic geochemistry—an overview of indicators of organic matter sources and diagenesis in lake sediments. *Organic Chemistry*, 20, 867–900.

Milbrink, G. (1977). On the limnology of two alkaline lakes (Nakuru and Naivasha) in the East Rift Valley System in Kenya. *Internationale Revue der gesamten Hydrobiologie und Hydrographie*, 62, 1–17.

Moore, J., Doney, S., Kleypas, J., Glover, D., & Fung, I. (2002). An intermediate complexity marine ecosystem model for the global domain. *Deep-Sea Research II*, 49, 403–462.

Moreau, J., Mavuti, K., & Daufresne, T. (2001). A Synoptic Ecopath model of biomass flows during two different static ecological situations in Lake Nakuru (Kenya). *Hydrobiologia*, 458, 63–74.

Morris, C., & Askew, G. (2010). Comparison between mechanical power requirements of flight estimated using an aerodynamic model and in vitro muscle performance in the cockatiel (*Nymphicus hollandicus*). *The Journal of Experimental Biology*, 213, 2781–2787.

Murimi, S., Gichuki, F., Mungai, D., Gachene, C., & Thomas, D. (1993). The drying up of East African rift valley lakes in recent times with special reference to Lake Elementeita. Land and water management in Kenya: towards sustainable land use. In *Proceedings of the Fourth National Workshop*, Kikuyu, Kenya.

Murimi, S., & Prasad, H. (2005). Land use changes and hydrological responses in the Lake Nakuru Basin. *Sustainable Management of Headwater Resources Journal*, 155-164.

Murray, A., Martin, R., Johnston, A., & Martin, P. (1987). Analysis for naturally occurring radionuclides at environmental concentrations by gamma spectroscopy. *Journal of Radioanalytical and Nuclear Chemistry*, 115(2), 263–288.

Naidu, K. A., Sarada, R., & et al., G. M. M. (1999). Toxicity assessment of phycocyanin—A blue colorant from blue green bacteria *Spirulina platensis*. *Food Biotechnology*, 13, 51–66.

NASA (2014). Tropical Rainfall Monitoring Mission. Webpage: <http://trmm.gsfc.nasa.gov/>.

Nasirwa, O. (2000). Conservation status of flamingos in Kenya. *Waterbirds*, 23 (special publication), 47–51.

Ndetei, R., & Muhandiki, V. S. (2005). Mortalities of lesser flamingos in Kenyan Rift Valley saline lakes and the implications for sustainable management of the lakes. *Lakes and Reservoirs: Research and Management*, 10, 51–58.

Nelson, Y., Thampy, R., G.K.Motelin, J.A.Raini, DiSante, C., & Lion, L. (1998). Model for trace metal exposure in filter-feeding flamingos at alkaline Rift Valley lakes, Kenya. *Environmental Toxicology and Chemistry*, 17, 2302–2309.

Neuhauser, C., & Pacala, S. (1999). An Explicitly Spatial Version of the Lotka-Volterra Model with Interspecific Competition. *The Annals of Applied Probability*, 9(4), 1226–1259.

Nezen, H., & Arujo, M. (2011). Choice of threshold alters projections of species range shifts under climate chang. *Ecological Modelling*, 18, 3346–3354.

Nicholson, S. (2000). The nature of rainfall variability over Africa on time scales of decades to millenia. *Global and Planetary Change*, 26, 137–158.

Nisbet, R., McCauley, E., & Johnson, L. (2010). Dynamic Energy Budget (DEB) theory and ecology: lessons from Daphnia. *Philosophical Transactions of the Royal Society of Biological Sciences*, 365, 3541–3552.

Nisbet, R., Muller, E., & Lika, K. (2000). From molecules to ecosystems through dynamic energy budget models. *Journal of Animal Ecology*, 69, 913–926.

Norris, D., Arcese, P., Preikshot, D., Bertram, D., & Kyser, T. (2007). Diet reconstruction and historic population dynamics in a threatened seabird. *Journal of Applied Ecology*, 44(4), 875–844.

Nowak, M., & May, R. (1994). Superinfection and the Evolution of Parasite Virulence. *Proceedings of the Royal Biological Sciences Society*, 282(1801).

Nyenzi, B., Kiangi, P., & Rao, N. (1981). Evaporation values in East Africa. *Archives for meteorology, geophysics, and bioclimatology, Series B*, 29, 35–55.

Oduor, S. O., & Schagerl, M. (2007a). Temporal trends of ion contents and nutrients in three Kenyan Rift Valley saline-alkaline lakes and their influence on phytoplankton biomass. *Hydrobiologia*, 584, 59–68.

Oduor, S., & Schagerl, M. (2007b). Phytoplankton primary productivity characteristics in response to photosynthetically active radiation in three Kenyan rift valley saline-alkaline lakes. *Jounal of Plankton Research*, 29(12), 1049–1050.

Ojany, F., & Ogendo, R. (1988). *Kenya, a Study in Physical and Human Geography Longman Kenya*. Longman, Nairobi.

Onyando, J., Mulsila, F., & Awer, M. (2005). The Use Of GIS And Remote Sensing Techniques To Analyse Water Balance Of Lake Bogoria Under Limited Data Conditions. *Journal of Civil Engineering Research and Practice*, 2(1).

Ooyo-Okoth, E., Muchiri, M., Ngugi, C., Njenga, E., Ngure, V., Orina, P., Chemoiwa, E., & Wanjohi, B. (2011). Zooplankton partitioning in a tropical alkaline–saline endorheic Lake Nakuru, Kenya: Spatial and temporal trends in relation to the environment. *Lakes & Reservoirs: Research and Management*, 16, 35–47.

Owino, A., Oyugi, J., Nasirwa, O., & Bennun, L. (2001). Patterns of variation in waterbird numbers on four Rift Valley lakes in Kenya, 1991–1999. *Hydrobiologia*, 458, 45–53.

Pennycuick, C. J., & Bartholomew, G. A. (1973). Energy budget of the lesser flamingo (*Phoeniconaias minor* Geffroy). *East African Wildlife Journal*, 11, 199–207.

Proteau, P., Gerwick, W., Garcia-Pichel, F., & Castenholz, R. (1993). The structure of scytonemin, an ultraviolet sunscreen pigment from the sheaths of cyanobacteria. *Experientia*, 52(12), 1042–1049.

Raini, J. (2006). Long-term trends in water quality, water quantity and biodiversity at Lake Nakuru, Kenya. *Health and Environmental Research Online (HERO)*, 2, 57–62.

Renaut, R., & Tiercelin, J. (1993). Lake Bogoria, Kenya: soda, hot springs and about a million flamingoes. *Geology Today*, 9(2), 56–61.

Reynolds, C. (1987). Flocks, Herds, and Schools: A Distributed Behavioral Model. *Computer Graphics*, 21, 25–34.

Roberts, G. (1997). How many birds does it take to put a flock to flight?. *Animal Behaviour*, 54(6), 1517–1522.

Robins, J. (1978). *Biogeochemistry of Lead in the Environment*, chap. Geochemical and geophysical applications of radioactive lead isotopes., pp. 285–393. Elsevier, North Holland, Amsterdam.

Robinson, V. (2008). Aspects of the feeding ecology of the lesser flamingo (*Phoeniconaias minor*). Master's thesis, Biology, University of Leicester, UK.

Saloniemi, I. (1993). A coevolutionary predator-prey model with quantitative characters. *The American Naturalist*, 141(6), 880–896.

Schagerl, M., & Oduor, S. O. (2008). Phytoplankton community relationship to environmental variables in three Kenyan Rift Valley saline-alkaline lakes. *Marine and Freshwater Research*, 59, 125–136.

Scheffer, M., Carpenter, S., Foley, J., Folke, C., & Walker, B. (2001). Catastrophic shifts in ecosystems. *Nature*, 413, 591–596.

Schneider, E. (1994). Life as a manifestation of the second law of thermodynamics. *Mathematical and Computer Modelling*, 19, 25–48.

Scholl, H. (2001). Agent-based and system dynamics modeling: a call for cross study and joint research. In *HICSS '01 Proceedings of the 34th Annual Hawaii International Conference on System Sciences (HICSS-34)*.

Selous, E. (1931). *Thought-Transference (or What?) in Birds*. Constable Company, London.

Sileo, L., Grootenhuijs, J. G., Tuite, G. H., & Hopcraft, H. D. (1979). Hot spring cyanobacteria to the mysterious deaths of Microbacteriosis in the lesser flamingo of Lake Nakuru, Kenya. *Journal of Wildlife Diseases*, 15, 387–390.

Simmons, R. (2000). Declines and movements of lesser flamingo in Africa. *Waterbirds*, 23 (special publication), 40–46.

Solé, R. V., & Manrubia, S. C. (1996). Extinction and self-organized criticality in a model of large-scale evolution. *Physical Review E*, 54(1), R42.

Someren, U. V. (1922). Notes on the birds of East Africa. *Novitata Zoologie*, 29, 1–246.

Sousa, T., Domingos, T., & Kooijman, S. (2008). From empirical patterns to theory: a formal metabolic theory of life. *Philosophical Transactions of the Royal Society of Biological Sciences*, 363, 2453–2464.

Starfield, A., Farm, B., & Taylor, R. (1989). A rule-based ecological model for the management of an estuarine lake. *Ecological Modelling*, 46, 107–119.

Steele, J. (1974). *The structure of marine ecosystems*. Harvard University Press, Cambridge, Massachusetts.

Steele, J., & Henderson, E. (1992). The role of predation in plankton models. *Journal of Plankton Research*, 14, 157–172.

Steele, J., & Mullin, M. (1977). *The Sea, ideas and observations on progress in the study of the seas*, Vol. 6, chap. Zooplankton Dynamics, pp. 857–890. Wiley-Interscience, New York.

Stoof-Leichsenring, K., Junginger, A., Olaka, L., Tiedmann, R., & Trauth, M. (2011). Environmental variability in Lake Naivasha, Kenya, over the last two centuries. *Journal of Paleolimnology*, 45, 353–367.

Sudhir, P., & Murthay, S. (2004). Effects of salt stress on basic processes of photosynthesis. *Photosynthetica*, 42(4), 481–486.

Svengren, H. (2002). *A Study of the Environmental Conditions in Lake Nakuru, Kenya, Using Isotope Dating and Heavy Metal Analysis of Sediments*. Ph.D. thesis.

Tebbs, E. (2013). *Remote Sensing for the study of Ecohydrology in East African River Basins*. Ph.D. thesis, Physics, Universtiy of Leicester, UK.

Tebbs, E., Remedios, J., Avery, S., & Harper, D. (2013a). Remote sensing the hydrological variability of Tanzania's Lake Natron, a vital Lesser Flamingo breeding site under threat. *Ecohydrology and Hydrobiology*, 13(2), 148–158.

Tebbs, E., Remedios, J., & Harper, D. (2013b). Remote sensing of chlorophyll-a as a measure of cyanobacterial biomass in lake Bogoria, a hypertrophic, saline-alkaline, flamingo lake, using Landsat ETM +. *Remote Sensing of Environment*, pp. 92–106.

Tilman, D., Fargione, J., Wolff, B., D'Antonio, C., Dobson, A., Howarth, R., Schindler, D., Schlesinger, W., Simberloff, D., & Swackhamer, D. (2001). Forecasting Agriculturally Driven Global Environmental Change. *Science*, 292, 281–284.

Totterdel, I. (1993). An Annotated Bibliography of Marine Biological Models. *NATO ASI Series*, 10, 317–339.

Trewavas, E. (1983). Tilapiine Fishes of the genera Sarotherodon, Oreochromis and Danakilia.. Tech. rep., British Museum of Natural History, UK.

Tuite, C. H. (2000). The distribution and density of lesser flamingos in East Africa in relation to food availability and productivity. *Waterbirds*, 23(Special Publication 1), 52–63.

Tuite, C. (1979). Population size, distribution and biomass density of the lesser flamingo in the eastern Rift Valley, 1974–6lley, 1974–6. *Journal of Applied Ecology*, 16, 765–775.

Turner, E., Bruesewitz, D., Mooney, R., Montagna, P., McClelland, J., Sadovski, A., & Buskey, E. (2014). Comparing performance of five nutrient phytoplankton zooplankton (NPZ) models in coastal lagoons. *Ecological Modelling*, 277, 13–26.

Vareschi, E. (1982). The Ecology of Lake Nakuru (Kenya), iii. Abiotic factors and primary production. *Oecologia*, 55, 81–101.

Vareschi, E. (1987). *Saline lake ecosystems*. Springer-Verlag, Berlin.

Vareschi, E., & Jacobs, J. (1985). The ecology of Lake Nakuru VI. Synopsis of production and energy flow. *Oecologia*, 65, 412–424.

Verschuren, D., Cocquyt, C., Tibby, J., Roberts, C., & Leavitt, P. (1999). Long-term dynamics of algal and invertebrate communities in a small, fluctuating tropical soda lake. *Limnology and Oceanography*, 44(5), 1216–1231.

Verschuren, D., Laird, K., & Cumming, B. (2000). Rainfall and drought in equatorial east Africa during the past 1,100 years. *Nature*, 403, 410–414.

Vinebrooke, R., Hall, R., Leavitt, P., & Cumming, B. (1998). Fossil pigments as indicators of phototrophic response to salinity and climatic change in lakes of western Canada. *Journal of Fisheries and Aquatic Sciences*, 55(3).

Vonshak, A. (1997). *Spirulina Platensis Arthospira: Physiology, Cell-Biology And Biotechnology*. Taylor & Francis Ltd, London, UK.

Vonshak, A., Guy, R., & Guy, M. (1988). The response of the filamentous cyanobacterium Spirulina platensis to salt stress. *Archives of Microbiology*, 150(5), 417–420.

Walling, D., Collins, A., & Sichingabula, H. (2003). Using unsupported lead-210 measurements to investigate soil erosion and sediment delivery in a small Zambian catchment. *Geomorphology*, 16, 193–213.

Wandiga, S., Mulepo, J., & Alala, L. (1986). Concentration of heavy metals in water, sediments and plants of Kenyan lakes Prefecture, Japan. WWF-LNCDP (World Wide Fund for Nature-Lake. *Kenya Journal of Science and Technology, Series A*, 89–94.

Wang, R., Dearing, J., Langdon, P., Zhang, E., Yang, X., & Scheffer, V. D. . M. (2012). Lake-sediment-based aquatic-system response variables and historical records of environmental drivers during the period 1883–2009. *Nature*, 492, 419–422.

Weathers, W. (1996). *Avian Energetics and Nutritional Ecology*, chap. Energetics of postnatal growth, pp. 461–496. International Thompson Publishing, New York.

Weltje, G., & Tjallingii, R. (2008). Calibration of XRF core scanners for quantitative geochemical logging of sediment cores: Theory and application. *Earth and Planetary Sciences*, 274, 423–438.

Wersin, P., Hohener, P., Giovanoli, R., & Stumm, W. (1991). Early diagenetic influences on iron transformations in a freshwater lake sediment. *Chemical Geology*, 90, 233–252.

Woodworth, B., Farm, B., Mufungo, C., Borner, M., & Kuwai, J. O. (1997). A photographic census of flamingos in the Rift Valley lakes of Tanzania. *African Journal of Ecology*, 35, 326–334.

Wroblewski, J. (1989). A model of the spring bloom in the North Atlantic and its impact on ocean optics. *Limnology and Oceanography*, 34, 1563–1571.

Yacobi, Y., Eckert, W., Trüper, H., & Berman, T. (1990). High performance liquid chromatography detection of phototrophic bacterial pigments in aquatic environments. *Microbial Ecology*, 19(2), 127–136.

Zengling, M., & Kunshan, G. (2009). Photosynthetically active and UV radiation act in an antagonistic way in regulating buoyancy of *Arthrosphaera (Spirulina) platensis* (cyanobacterium). *Environmental and Experimental Botany*, *66*, 265–269.

Zhang, J., Chen, W., & Zhang, C. (2009). *hetR* and *patS*, two genes necessary for heterocyst pattern formation, are widespread in filamentous nonheterocyst-forming cyanobacteria. *Microbiology*, *155*, 1418–1426.

Zullig, H. (1981). On the Use of Carotenoid Stratigraphy in Lake Sediments for Detecting Past Developments of Phytoplankton. *Limnology and Oceanography*, *26*(5), 970–976.